

## Biomaterial Interfaces Division

Room B117-119 - Session BI2+AS+HC+SS-MoM

### Energy Transfer and Light Induced Phenomena in Biologic Systems

**Moderators:** Morgan Alexander, University of Nottingham, UK, Tobias Weidner, Aarhus University, Denmark

10:40am **BI2+AS+HC+SS-MoM-8 Electrochemically Conducting Lipid Bilayers: Q-Lipid-Containing Membranes Show High in-Plane Conductivity Using a Membrane-on-a-Chip Setup**, U. Ramach, TU Wien, Austria; J. Andersson, IST Austria; Markus Valtiner, TU Wien, Austria

The light-driven reactions of photosynthesis as well as the mitochondrial powersupply are located in specialized membranes containing a high fraction of redox-active lipids. In-plane charge transfer along such cell membranes is recurrently thought to be facilitated by the diffusion of redox lipids and proteins.

Using a membrane on-a-chip setup, we show here that redox-active model membranes can sustain surprisingly high currents (mA) in-plane at distances of 25 nm. We also show the same phenomenon in free-standing monolayers at the air-water interface once the film is compressed such that the distance between redox centers is below 1 nm. Our data suggest that charge transfer within cell walls hosting electron transfer chains could be enabled by the coupling of redox-lipids via simultaneous electron and proton in-plane hopping, similar to conductive polymers. This has major implications for our understanding of the role of lipid membranes, suggesting that Q-lipid-containing membranes may be essential for evolving the complex redox machineries of life.

[1] U. Ramach, J. Andersson, R. Schöfbeck and M. Valtiner, *Iscience* 26 (2), 2023.

11:00am **BI2+AS+HC+SS-MoM-9 Light Responsive Cyclic Peptide Polymer Nanomaterials**, O. Atoyebi, M. Beasley, W. Maza, M. Kolel-Veetil, A. Dunkelberger, Kenan Fears, US Naval Research Laboratory

Cyclic peptides are capable of self-assembling into supramolecular peptide nanostructures, via hydrogen bonding along the backbone of the peptide rings. To improve upon this molecular architecture, we designed and synthesized cyclic peptide polymers by covalently linking the cyclic peptides into a linear polymer chain, and demonstrated the conformation of the polymer chain could be transitioned from an unfolded state into rigid, peptide nanorods by varying solution pH. Here we present an alternate way to control the self-assembly via photo-isomerization. We capitalize on azobenzene's photo-actuable nature using a di-carboxylic acid azobenzene to covalently crosslink the cyclic peptide rings into a linear cyclic peptide polymer via terminal amines present in the ring. Self-assembly of the cyclic peptide nanotube occurs by exposing the polymerized cyclic peptide to ultraviolet radiation causing a trans- to -cis transition of the azobenzene and thus assembling the cyclic peptide nanotube. Furthermore, we fluorescence donor/acceptor pairs can be displayed from these materials, at highly controlled separation distances, to alter the optical response of these materials as a function of polymer conformation.

11:20am **BI2+AS+HC+SS-MoM-10 Programmable Biomimetic Light-Harvesting Systems based on Strong Coupling of Synthetic Peptides and Dye-Functionalised Polymer Brushes to Plasmon Modes**, Graham Leggett, University of Sheffield, UK

Excitation transfer in molecular photonic materials is dominated by incoherent hopping processes; consequently, exciton diffusion lengths are short (~10 nm) placing severe constraints on device design. A grand challenge for the past two decades has been to discover how to achieve efficient long-range transfer of excitation in molecular systems. We have developed a new approach to the design of materials for solar energy capture that combines biomimetic design, inspired by structures used in photosynthesis, with strong light-matter coupling.

Photosynthetic pigment-protein light-harvesting antenna complexes (LHCs) from plants and bacteria are strongly coupled to the localised surface plasmon resonances (LSPRs) in arrays of metal nanostructures leading to the formation of macroscopically extended excited states. Modelling of data indicates that the coupling results from linear combinations of plasmon and exciton states. For example, wild-type and mutant LH1 and LH2 from *Rhodospirillum rubrum* containing different carotenoids yield different coupling energies; the methods of synthetic biology enable strong light-matter coupling to be programmed.

However, proteins are not suitable for putative applications of molecular photonic materials. Instead, we have designed programmable biomimetic pigment-peptide and pigment-polymer antenna complexes, in which surface-grafted peptide and polymer scaffolds organise excitons within localised surface plasmon resonances to achieve strong light-matter coupling. In these systems, delocalised excited states (plexitons) extend across at least 1000s of pigments. In synthetic peptide and protein systems, we find that the plasmon mode couples to states not seen under weak-coupling, providing evidence for the formation of macroscopically-extended excited states that facilitate coherent transfer of excitation across long distances. In pigment-polymer systems, the dye concentration in the film can be increased to ~2M, significantly exceeding the concentration of chlorophyll in biological light-harvesting complexes, by optimisation of the polymer grafting density and the dye-scaffold coupling chemistry. Fitting of spectra for these plexitonic antenna complexes yields Rabi energies up to twice as large as those achieved with biological LHCs. Moreover, synthetic plexitonic antenna complexes display pH- and temperature-responsiveness, enabling active control of strong plasmon-exciton coupling via regulation of the polymer conformation.

These biomimetic quantum-optical brush systems offer great promise for the design of new types of molecular photonic device.

## Chemical Analysis and Imaging of Interfaces Focus Topic

Room A105 - Session CA1+AS+LS+NS+SS+VT-MoM

### Modeling, AI, and Machine Learning Applied to Interfaces

**Moderators:** J. Trey Diulus, NIST, Kateryna Artyushkova, Physical Electronics

8:20am **CA1+AS+LS+NS+SS+VT-MoM-1 Topological and Geometric Descriptors of Complex Self-assembly at Liquid Interfaces**, Aurora Clark, University of Utah

INVITED

Amphiphilic surfactants at liquid/liquid interfaces can form complex self-assembled architectures that underpin interfacial reactivity and transport. This has been demonstrated by surface sensitive spectroscopies and molecular dynamics simulations within the domain of liquid/liquid extraction, which involves solute adsorption, complexation reactions and transport across the phase boundary. Being able to quantify surfactant organization is a significant challenge because the distribution of species is broad and highly heterogeneous. As such, in the analysis of molecular dynamics data, there is significant need to develop descriptors that allow statistical analysis of surface organization. This work presents recent developments based upon geometric measure theory and topological data analysis that are able to identify surface assemblies and their dynamic evolution. These methods are revealing intricate dependencies of surface assembly upon solution composition and the impact this has upon transport mechanisms.

References:

[Kumar, N.; Clark, A. E.](#) Persistent Homology Descriptors for Surface Image Analysis in Complex Chemical Systems, *Journal of Chemical Theory and Computation*, **2023**, In Press. ChemArXiv: <https://doi.org/10.26434/chemrxiv-2023-vwrjx>

Zarayeneh, N.; Kumar, N.; Kalyanaraman, A.; [Clark, A. E.](#) Dynamic Community Detection Decouples Hierarchical Timescale Behavior of Complex Chemical Systems, *Journal of Chemical Theory and Computation*, **2022**, *18*, 7043 – 7051. DOI:10.1021/acs.jctc.2c00454

Kumar, N.; [Clark, A. E.](#) Unexpected Inverse Correlations and Cooperativity in Ion-pair Phase Transfer, *Chemical Science*, **2021**, *12*, 13930-13939. DOI: 10.1039/D1SC04004A

[Liu, Z.; Clark, A. E.](#) An Octanol Hinge Opens the Door to Water Transport, *Chemical Science*, **2021**, *12*, 2294 – 2303. DOI: 10.1039/D0SC04782A.

Alvarado, E.; Liu, Z.; Servis, M. J.; [Krishnamoorthy, B.](#); [Clark, A. E.](#) A Geometric Measure Theory Approach to Identify Complex Structural Features on Soft Matter Surfaces, *Journal of Chemical Theory and Computation*, **2020**, *16*, 4579-4587. DOI: 10.1021/acs.jctc.0c00260,

9:00am **CA1+AS+LS+NS+SS+VT-MoM-3 Machine Learning and the Future of Surface Analysis**, J. Jones, M. Caouette, Kateryna Artyushkova, Physical Electronics

INVITED

Machine learning can potentially revolutionize all areas of material science and engineering, including surface analysis, by automating and accelerating data acquisition and analysis. The application of machine learning and

# Monday Morning, November 6, 2023

artificial intelligence (ML/AI) has been actively evaluated and used in scanning probe microscopic methods<sup>1,2</sup>, while the application of AI in surface analysis methods such as AES, XPS, and TOF-SIMS is in the very early stages.<sup>3</sup> In this talk, I will discuss the potential areas where AI will change how we do surface analysis.

With recent instrumental development yielding improvements in sensitivity and throughput, the data acquisition stage of surface analysis has become much faster than the experimental planning or data analysis stages, which both require significant operator time and human-based decisions. Using a spectrometer still requires a human operator with instrument-specific knowledge and experience in how to operate it. More importantly, the operator uses physical and chemical knowledge to decide on what specific data must be obtained and from which locations on the sample, depending on the analytical question being addressed by the experiment. Experienced scientists make these decisions effortlessly during the experiment, but it is a very challenging task for ML algorithms that rely on training data with explicit descriptors.

Initial AI applications to analytical surface analysis will focus on instrument optimization and performance inherent in the analytical workflow. Unlike acquisition parameters based on chemical or material science requiring broader context, tuning, and standardizing the spectrometer can be easily cast into numerical terms processable by AI.

Machine learning can also be utilized as a live data integrity monitoring service during acquisition, recognizing and rejecting "bad data". Systemically erroneous data caused by charging or sample damage are often not discovered until the experiment is complete and the data analyzed by a human. Catching it automatically during the experiment saves valuable operator and instrument time. Here, I will present an initial application wherein ML was used to identify whether ToF-SIMS spectra were correctly calibrated.

1. S.V. Kalinin, *ACS Nano* 2021, 15, 8, 12604–12627.

2. S.V. Kalinin, arXiv:2304.02048

3. G. Drera *et al* 2020 *Mach. Learn.: Sci. Technol.* 1 015008

9:40am **CA1+AS+LS+NS+SS+VT-MoM-5 Complexity to Clarity: Detecting, Identifying and Analyzing Complex Materials with Machine Learning**, *Paul Pigram, W. Gardner, S. Bamford, D. Winkler, B. Muir, R. Sun, S. Wong*, La Trobe University, Australia

Our ability to analyze and understand any physical, chemical, or biological material relies on accurately determining its structure, characteristics, and responses. Contemporary analytical techniques produce large volumes of data from pointwise sample analyses (one dimensional (1D) data), maps of compositional distributions (two dimensional (2D) data), and depth profiles showing composition throughout a sample volume (three dimensional (3D) data).

Correlative analyses linking data from the same sample, obtained by different analytical techniques or different operating parameters, are becoming critically important. Different analytical perspectives on the same sample enhance the richness and depth of the conclusions that can be drawn from it.

Recent advances in analytical science have resulted in an overwhelming avalanche of data – the “big data” problem. In our lab a single time-of-flight secondary ion mass spectrometry (ToF-SIMS) experiment might collect a map (512 x 512 pixels) with 2000 mass spectral peaks of significant intensity in 2 – 10 minutes. These half a billion data points all have differing degrees of significance.

In many cases, only a small number of peaks, 10 – 200, may be judged to be characteristic of a specific sample, and the rest of the data may be discarded. However, there are significant risks that such analyses are biased, and may miss important but subtle trends.

There is a very substantial knowledge gap in our ability to find and make full use of the information and knowledge contained in large scale data sets. This gap is driving rapid international progress in the application of materials informatics and machine learning to analytical surface science.

This presentation will highlight our work on applying artificial neural network approaches to analysis of a variety of very large hyperspectral data sets to better understand complex materials and their interactions.

## Laboratory-Based Ambient-Pressure X-ray Photoelectron Spectroscopy Focus Topic

Room B116 - Session LX+AS+HC+SS-MoM

### Laboratory-Based AP-XPS: Advances in Instrumentation and Applications

Moderators: Sylwia Ptasińska, University of Notre Dame, Heath Kersell, Oregon State University

8:20am **LX+AS+HC+SS-MoM-1 Instrumentation for Electron Microscopy and Spectroscopy in Plasma Environment**, *Andrei Kolmakov*, NIST-Gaithersburg

INVITED

Plasma-assisted processes are of principal importance for modern semiconductors microfabrication technology, catalysis, environmental remediation, medicine, etc. Understanding the chemical and morphological evolutions of the surfaces and interfaces under a plasma environment requires *operando* metrologies that have a high spatial, temporal, and spectroscopic resolution. Combining the APXPS system with ambient pressure scanning electron microscopy would, in principle, meet these needs. Here we review the status of the field and discuss the prospective designs as well as application examples of ambient pressure scanning electron microscopy and spectroscopy for *in situ* analysis and processing of the surfaces under plasma environments

9:00am **LX+AS+HC+SS-MoM-3 Scienta Omicron HiPPLab - A Lab-based APXPS Instrument for Probing Surface Chemical Reactions**, *Peter Amann*, Scienta Omicron, Germany

Investigating reaction intermediates, oxidation states, solid-liquid interfaces and buried interfaces under near ambient pressure conditions is highly desired in materials science applications. Ambient pressure X-ray photoelectron spectroscopy (APXPS) is a powerful method to investigate the chemical nature of surfaces and interfaces and has undergone a tremendous improvement in the last years. The development of the HiPP analysers allowed to overcome the one bar pressure regime without using pressure separating membranes. [1] [2]

During the past decade, increased attention has been shown to laboratory based APXPS system solutions, which is motivated by the 24/7 access capability and possibility for highly customized sample environments. Drawing on extensive experience in the fields of photoelectron spectroscopy, UHV technology, and system design, Scienta Omicron has designed the HiPPLab as an easy-to-use system that encourages user creativity through flexibility, modularity and an innovate chamber design.[3] It combines a state-of-the-art HiPP analyser with a high flux, variable focus X-ray source. Multiple options complement the HiPPLab offer, including a gas reaction cell, a preparation chamber, laser heating, or options for mass-spectroscopy. Using automated gas-flow controllers, experiments can be conducted in a controlled way. Future upgrade possibilities are given.

The HiPP-3 analyser features a 2D detector allowing for spatial resolved measurements with customer proven results down to 2.8  $\mu\text{m}$  resolution. The swift acceleration mode allows for high electron transmission without applying a sample bias. A sophisticated pre-lens design in which efficient pumping between two close-by apertures is implemented, allows dragging out corrosive gases or moisture, which would otherwise be detrimental to the instrument.

In this presentation, I will give an overview on our APXPS product portfolio focusing on laboratory based solutions and present application examples.

[1] Amann, et al. *Review of Scientific Instruments*, 2019 90(10)

[2] Takagi, et al. X-ray photoelectron spectroscopy under real ambient pressure conditions. *Applied Physics Express*, 2017, 10(7), 8–11.

[3] Scienta Omicron HiPPLab <https://scientaomicron.com/en>

9:20am **LX+AS+HC+SS-MoM-4 Using Microheaters for Time-Resolved APXPS and Correlated ETEM**, *Ashley Head*, Brookhaven National Laboratory; *B. Karagoz*, Diamond Light Source, UK; *J. Carpena-Nuñez*, Air Force Research Laboratory; *D. Zakharov*, Brookhaven National Laboratory; *B. Maruyuma*, Air Force Research Laboratory; *D. Stacchiola*, Brookhaven National Laboratory

With a rise in the number of lab-based APXPS systems, these instruments afford an opportunity to continue the development of multimodal and correlated capabilities for more comprehensive information of reactions at surfaces. Here I will discuss the methods of using an ETEM commercial microheater for collecting APXPS data on the same sample under identical

# Monday Morning, November 6, 2023

conditions. A specialized holder was fabricated to use commercial microheaters on MEMS chips in a lab-based APXPS instrument. The rapid heating of the microheater enables a time-zero for collecting APXPS data with a time resolution of 500 ms. Proof-of-principle measurements following the oxidation and reduction of a Pd film demonstrate correlative experiments with TEM. The specialized holder was fabricated with the possibility of dosing gases locally to the sample surface while confined by a graphene membrane. Using the gas lines, the Pd film was oxidized under a partial pressure of air (~0.4 mbar). Overall, using this microheater in APXPS offers chemical information complementary to structural changes seen in ETEM. The rapid heating enables new opportunities in time-resolution and increased pressure for APXPS experiments.

9:40am **LX+AS+HC+SS-MoM-5 NAP-XPS Instrumentation Came a Long Way - Where Will Applications Lead Us from Here?**, P. Dietrich, F. Mirabella, K. Kunze, O. Schaff, **Andreas Thissen**, SPECS Surface Nano Analysis GmbH, Germany

**INVITED**

Over the last fifty years significant developments have been done in photoelectron spectroscopy instrumentation and thus opened new fields of application. Especially XPS or ESCA developed into the most important standard surface analytical method in many laboratories for surface and materials characterization.

For the last fifteen years XPS under near ambient pressure conditions (NAP-XPS) has gained significant attention. Although invented as a laboratory method it initially started to grow at synchrotrons. The development of more efficient and sensitive electron analyzers and high-brilliance monochromated laboratory X-ray and UV sources running at pressures of up to 100 mbar finally brought it back to the individual laboratories. The reasons are the availability of individual infrastructure for sample preparation and handling, safety regulations and easier access to measurement time on a daily basis. Nowadays the vast majority of instruments worldwide are laboratory-based.

It opened the method XPS to liquids, solid-liquid interfaces, gas-solid-interfaces, gas-liquid-interfaces and many more. The development of instrumentation followed the important applications and besides the "active" components, mainly excitation sources and electron analyzers, a lot of developments have been done in the fields of sample environments, sample handling, system setup and automation and combination with other techniques and even in quantification of data. There are only a few applications left where experiments at synchrotron based beamlines and end stations offer the only solution.

The market driving applications nowadays are catalysis, electrochemistry, behaviour of liquid phases, biological samples and surface chemistry. Along these applications this presentation will show the existing instrumentation, discuss its limits and the perspective for near future developments to further increase the user base of laboratory based NAP-XPS systems to turn it into an integral part of the large routine analysis community.

10:40am **LX+AS+HC+SS-MoM-8 Evolution of Metal-Organic Frameworks in the Presence of a Plasma by AP-XPS and IRRAS**, J. Anibal Boscoboinik, Brookhaven National Laboratory and State University of New York at Stony Brook; M. Ahmad, Stony Brook University/Brookhaven National Laboratory; M. Dorneles de Mello, Brookhaven National Laboratory; D. Lee, Johns Hopkins University; P. Dimitrakellis, University of Delaware; Y. Miao, Johns Hopkins University; W. Zheng, University of Delaware; D. Nykpanchuk, Brookhaven National Laboratory; D. Vlachos, University of Delaware; M. Tsapatsis, Johns Hopkins University

**INVITED**

Zeolitic imidazolate frameworks (ZIF), a class of metal-organic frameworks, are promising materials for various applications, including the separation and trapping of molecules and catalysis. Recent work has shown that exposure to plasma can result in the functionalization of the framework for tailored applications. This talk will report in-situ plasma studies of ZIF-8 as a model system. We will study the framework's evolution in the presence of N<sub>2</sub>, O<sub>2</sub>, and H<sub>2</sub> plasmas by combining lab-based ambient pressure XPS and infrared reflection absorption spectroscopy.

11:20am **LX+AS+HC+SS-MoM-10 Surface Degradation and Passivation in Perovskite Solar Cells**, Wendy Flavell, The University of Manchester, UK

**INVITED**

There is an urgent requirement to make better use of the 120,000 TW of power provided by the Sun, by using it to generate power, or by using its energy directly to make useful chemical feedstocks. Around the world, there is an explosion of research activity in new systems for harvesting solar energy, including solar cells based organometal halide perovskites. Issues of

key importance are the interfacial energy level line-up of the cell components, and the influence of the surface properties of these materials on charge separation in the devices. Indeed, the deployment of perovskites in solar cells is currently limited by their high reactivity and rate of surface oxidation. Thus, a key problem is to develop an understanding of the interface chemistry of solar heterojunctions in order to develop passivation strategies. I show how a combination of techniques including near-ambient pressure photoelectron spectroscopy (NAP-XPS) and hard X-ray photoelectron spectroscopy (HAXPES) may be used to investigate surface ageing and the surface degradation reactions[1-7], chemical composition as a function of depth[4,5], and to develop passivation strategies for perovskite solar cell heterojunctions[2,3,5-7].

## References

1. J C-R Ke, A S Walton, A G Thomas, D J Lewis, *et al.*, *Chem Commun* **53**, 5231 (2017).
2. J C-R Ke, D J Lewis, A S Walton, B F Spencer, *et al.*, *J Mater Chem A*, **6**, 11205 (2018).
3. C-R Ke, D J Lewis, A S Walton, Q Chen, *et al.*, *ACS Applied Energy Materials* **2**, 6012 (2019).
4. B F Spencer, S Maniyarasu, B P Reed, D J H Cant *et al.*, *Applied Surface Science* **541**, 148635 (2021).
5. S Maniyarasu, J C-R Ke, B F Spencer, A S Walton *et al.*, *ACS Applied Energy Materials* **13**, 43573 (2021).
6. S Maniyarasu, B F Spencer, H Mo, A S Walton *et al.*, *J Mater Chem A*, **10**, 18206 (2022).
7. D Zhao, T A Flavell, F Aljuaid, S Edmondson *et al.*, *ACS Applied Materials and Interfaces*, submitted.

## Nanoscale Science and Technology Division Room B113 - Session NS1+2D+BI+SS-MoM

### Combined Nanoscale Microscopy

**Moderators: Adina Luican-Mayer**, University of Ottawa, Canada, **Sergei Kalinin**, Oak Ridge National Laboratory

8:20am **NS1+2D+BI+SS-MoM-1 Combined Metrology at the Nanoscale: Advanced Scanning Probe Microscopy to Evaluate Complex Semiconductors**, **Fernando A. Castro**, National Physical Laboratory, UK

**INVITED**

The performance of semiconductors is strongly affected by spatial variations that can be introduced during manufacturing or due to degradation processes. In addition to the impact of microstructure and defects on electrical and optical properties, complex semiconductors, such as some compound semiconductors, perovskites or 2D materials, can present dynamic changes in properties during operation. Combining metrology methods is critical to better understand and characterise such complex samples as individual methods provide insufficient information. Ideally these combined measurements should be either co-localised or simultaneous in order to reduce uncertainty associated with post process image registration, spatial heterogeneity, or sample contamination. NPL has been developing a suite of spatially resolved measurement methods to understand critical factors that impact semiconductor performance and reliability. In this presentation, we'll focus on nanoscale methods under controlled operational or environmental conditions, including advanced modes of scanning probe microscopy (SPM) such as time-resolved scanning kelvin probe (tr-SKPM) and tip enhanced optical microscopy (TEOS). After introducing the challenges and recent results from the European project PowerELEC, we'll present two examples of how these combined measurements are applied. First, we'll describe the application of SPM to understand degradation mechanisms in state-of-the-art perovskite solar cells (PSCs). Time-resolved SKPM can be used to distinguish the impact of ionic and electronic charges on dynamic processes and in-situ co-localised measurements under controlled environmental conditions can identify nucleation of nanoscale grains on the perovskite film surface at the start of the degradation process, allowing us to link degradation to the local electrostatic environment. The second example will focus on 2D transition metal dichalcogenide (TMD), which present promise for optoelectronic applications but are often limited by Fermi level pinning effects and consequent large contact resistances upon contacting with bulk metal electrodes. A potential solution for near-ideal Schottky-Mott behavior and concomitant barrier height control has been proposed in the literature by

# Monday Morning, November 6, 2023

contacting TMDs and (semi-)metals in van der Waals heterostructures. We will show how combined nanoscale measurements allows to directly access interface parameters relevant to the Schottky–Mott rule on a local scale and how we use SKPM and TEOS measurements under simulated operational conditions (e.g. electrostatic doping induced Fermi levels) to enable decoupling and quantification of contributions from the interface dipole and electrode work function.

9:00am **NS1+2D+BI+SS-MoM-3 Correlated Functional Imaging of Printed and Ferroelectric 2D Devices for Ubiquitous Sensing and Neuromorphic Computing**, *J. Kim, Z. Zhu, T. Chu, H. Choi, M. Moody, Lincoln Lauhon*, Northwestern University

The unique properties of 2D materials stimulate the design of devices that exhibit useful new behaviors. However, the correspondence of expected and actual operating principles of devices cannot always be established from simple analysis of temperature-dependent current-voltage characteristics. As a result, the rational optimization of even simple devices such as thin-film transistors, as well as the successful realization of novel neuromorphic devices, benefits from spatially resolved characterization of nanoscale structure and properties to discern the relative contributions of device geometry and 2D material structure and chemistry to device performance. This talk will describe case studies in which Kelvin probe force microscopy (KPFM) and scanning photocurrent microscopy (SPCM) are used to investigate the operating principles of thin-film transistors (TFTs) and source-gated transistors (SGTs) fabricated from  $\text{MoS}_2$  and  $\text{In}_2\text{Se}_3$ . In the case of n-type semiconducting 2H  $\text{MoS}_2$ , model devices constructed from overlapping exfoliated flakes are analyzed to identify factors limiting the performance of printed thin-film transistors (*ACS Nano* 2023, **17**, 575). KPFM analysis is used to isolate the contact, channel, and junction resistances and calibrate a resistor network model of printed thin films. Simulations of the effective mobility and on-current dependence on flake thickness, size, and degree of overlap suggest that the performance of printed TFTs are limited by resistance arising from unpassivated edge states.

In the second use case, KPFM, SPCM, and piezoresponse force microscopy (PFM) are used to pinpoint the origin of resistance modulation in  $\alpha\text{-In}_2\text{Se}_3$  transistors that exhibit tunable non-volatile channel conductance. Memristive behavior in  $\text{In}_2\text{Se}_3$  TFTs has been attributed to switching of the channel polarization, but the lack of an obvious threshold for switching raises questions about the evolution of domain structure and the contribution of trap states. Furthermore, the presumed modulation of the Schottky barrier has yet to be confirmed experimentally. We address this gap in understanding through correlated PFM, KPFM, and SPCM measurements. We then fabricate  $\text{MoS}_2\text{-In}_2\text{Se}_3$  transistors with a geometry that induces depletion at the source electrode, i.e. a source-gated transistor, and observe non-volatile switching of the low output current. KPFM, SPCM, and finite element simulations are used to confirm source pinch-off and non-volatile multi-level modulation of the effective source resistance. The quantitative correlation of device behaviors with the changes in channel potential at key interfaces usefully constrains the interpretation of the operating principles and builds a foundation for rational design of novel neuromorphic devices and systems.

9:20am **NS1+2D+BI+SS-MoM-4 A Unique New Correlative Microscopy Platform for Combined Nanoscale Microscopy by Combination of AFM and SEM**, *Chris Schwab*, Quantum Design Microscopy GmbH, Germany; *K. Arat*, Quantum Design, Inc.; *H. Alemansour, A. Alipour*, Quantum Design, Inc., Iran (Islamic Republic of); *A. Amann*, Quantum Design, Inc., Germany; *L. Montes*, Quantum Design, Inc., Colombia; *J. Gardiner*, Quantum Design, Inc.; *H. Frerichs, L. Stuehn, S. Seibert*, Quantum Design Microscopy GmbH, Germany; *S. Spagna*, Quantum Design, Inc.

The combination of different analytical methods into one instrument is a powerful technique for the contemporaneous acquisition of complementary information. This is especially true for the in-situ combination of atomic force microscopy (AFM) and scanning electron microscopy (SEM), two of the most powerful microscopy techniques available. This combination gives completely new insights into the nanoscale.

In this work, we introduce a highly integrated new correlative microscopy platform, the FusionScope, that seamlessly combines AFM and SEM within a unified coordinate system. The self-sensing piezoresistive cantilever technology used for the AFM scanner results in a purely electrical measurement of the cantilever deflection signal. This allows for concurrent, correlated acquisition of both SEM and AFM images at the region of interest. In addition, a three-axis sample stage and a trunnion provide

unique experimental capabilities such as profile view – an 80-degree tilt of the combined sample stage and AFM giving full SEM access to the cantilever tip region.

We will present a variety of novel case studies to highlight the advantages of this new tool for interactive, correlative, in-situ nanoscale characterization for different materials and nanostructures. First results will focus on hard-to-reach samples. FusionScope allows for fast and easy identification of the area of interest and precise navigation of the cantilever tip for correlative SEM and AFM measurements. We demonstrate that approach for analysis of blade radius of razor blades and the characterization of lacunae structures on bone surfaces.

In addition, we will present first results for the in-situ characterization of individual nanowires that will be used for energy harvesting applications. The SEM enables the easy location of individual or multiple nanowires, whereas the in-situ AFM allows the characterization of topography, surface roughness, mechanical, and electrical properties of the nanowire.

Based on the broad variety of applications regarding the inspection and process control of different materials and devices, we anticipate that this new inspection tool to be one of the driving characterization tools for correlative SEM and AFM analysis in the future.

9:40am **NS1+2D+BI+SS-MoM-5 Correlative in-Situ Nanoscale Microscopy Using AFM and FIB-SEM for Nanomechanical Property Mapping Throughout a 3D Volume**, *Prabhu Prasad Swain, M. Penedo, N. Hosseini, M. Kangül, S. Andany, N. Asmari, G. Fantner*, Ecole Polytechnique Fédérale de Lausanne (EPFL), Switzerland

In this work, we present results obtained with an atomic force microscope (AFM) integrated in a focused ion beam- scanning electron microscope (FIB-SEM). The FIB-SEM is a powerful instrument, capable of automated structural analysis and prototyping at nanometer resolution, while the AFM is a well-established versatile tool for multiparametric nanoscale characterization. Combining the two techniques allows unprecedented *in-situ* correlative analysis at the nanoscale. Nanoprototyping and enhanced multiparametric analysis can be performed without contamination of the sample or environmental changes between the subsequent processing steps. The power of the combined tool lies in the complementarity of the two techniques. The AFM offers nanomechanical property mapping with electrical and magnetic characterization of the sample, while SEM offers elemental analysis and FIB enables thin slicing of the of the sample for block face imaging. This enables 3D tomographic imaging of complex samples mapping composition and mechanical properties throughout the 3D volume. Controlling both these instruments with open-hardware controller (OHC), allows us to perform automated *in-situ* AFM-FIB-SEM characterization. The setup is aimed to provide true 3D correlative information and mapping, with increased resolution for a larger volume. We will demonstrate the capabilities of correlative AFM/SEM/FIB imaging through a series of correlative experiments on polymers, 2D materials, nanowires and rock sediments.

10:00am **NS1+2D+BI+SS-MoM-6 Anisotropic Friction Effects of Perovskite Nanoplatelets on a vdW Substrate**, *Sidney Cohen, N. Itzhak, I. Rosenhek-Goldian, O. Brontvein, E. Joselevich*, Weizmann Institute of Science, Israel

Interest in 2D materials can be attributed to their unique properties such as electrical, optical, and mechanical characteristics, which can be harnessed in small devices. Assembly of these materials can be challenging. vdW epitaxy is a promising approach, in which nano-sized crystalline structures are grown on a 2D vdW substrate which has minimal interaction energy, resulting in low strain. The epitaxial growth still provides sufficient interaction to favor specific geometries according to lattice directions. In this presentation, the system is  $\text{CsPbBr}_3$  platelets grown on vdW  $\text{ReSe}_2$ . This combination is of fundamental and applied interest due to special optoelectronic properties of these 2D-3D mixed semiconductor systems. The mechanism of the nanoplatelet growth leading to their shape and orientation on the surface remains to be fully revealed. Here, we present tribological studies performed by monitoring the force required to push the platelets along the surface. We observed a significant directional effect expressed in the lateral forces required to slide the platelets along the surface. In particular, forces 4-5 times those required to push rectangular platelets along the  $\text{ReSe}_2$  surface along the long axis were insufficient to move the same platelets along their short axis. STEM images showed that this correlated with commensurability of the two lattice structures. Some of the experiments were performed in an ambient AFM system. Because sliding along the surface can be hindered by atomic steps and defects, unbiased analysis of this effect requires searching for small steps of atomic height along the sliding path. Scanning electron microscopy is a convenient

# Monday Morning, November 6, 2023

way to search for these defects: thus, comparative experiments were performed in-situ in a combined AFM-SEM system. This combination had the additional advantage of allowing rapid overview of the surface to locate regions of interest.

In the process of evaluating the measurements, those performed in vacuum required much higher (by as much as an order of magnitude) forces to support pushing along the surface in comparison with comparable measurements made in the ambient AFM system. These measurements will be presented in the context of the characterization of the 2D substrate and platelet nanostructure as revealed by the two correlative measurement techniques.

## Nanoscale Science and Technology Division Room B113 - Session NS2+2D+BI+EL+SS-MoM

### Chemical Identification with Scanning Probe Microscopy

**Moderators:** Sidney Cohen, Weizmann Institute of Science, Israel, Harald Plank, Graz University of Technology

10:40am **NS2+2D+BI+EL+SS-MoM-8 Nanoscale imaging with photo-induced force microscopy, Eric Potma**, University of California Irvine  
**INVITED**

Imaging with molecular contrast at the nanoscale is important for a myriad of applications, yet it remains a technical challenge. Over the past two decades, various flavors of optical spectroscopy combined with atomic force microscopy have been developed, each offering hope for a more routine nanospectroscopy technology. One of these approaches is photo-induced force microscopy (PiFM), a non-contact scan probe technique that is sensitive to the light-induced polarization in the material. PiFM has been used to generate molecular maps with 5 nm resolution, based on absorption contrast or on contrast derived from nonlinear optical interactions. Nonetheless, questions remain about the origin of the signal, in particular the possible contribution of forces that result from the thermal expansion of the sample. In this presentation, we will discuss various physical mechanisms that contribute to the PiFM signal and highlight several applications that are unique to the PiFM technique.

11:20am **NS2+2D+BI+EL+SS-MoM-10 Near-field Optical Microscopy Imaging and Spectroscopy at 10nm Spatial Resolution, Artem Danilov**, Attocube Systems Inc.

Fourier-transform infrared (FTIR) spectroscopy is an established technique for characterization and recognition of inorganic, organic and biological materials by their far-field absorption spectra in the infrared fingerprint region. However, due to the diffraction limit conventional FTIR spectroscopy is unsuitable for measurements with nanoscale spatial resolution. Scattering-type Scanning Near-field Optical Microscopy (s-SNOM) allows to overcome the diffraction limit of conventional light microscopy or spectroscopy enabling optical measurements at a spatial resolution of 10nm, not only at IR frequencies but also in the whole spectral range from visible to terahertz. s-SNOM employs an externally-illuminated sharp metallic AFM tip to create a nanoscale hot-spot at its apex. The optical tip-sample near-field interaction is determined by the local dielectric properties (refractive index) of the sample and detection of the elastically tip-scattered light yields nanoscale resolved near-field images simultaneous to topography. Use of material-selective frequencies in the mid-IR spectral range can be exploited to fully characterize polymer blends or phase change polymers with nanometer-scale domains. Quantification of free-carrier concentration and carrier mobility in doped semiconductor nanowires, analysis of 2D (graphene) nanostructures, or study phase propagation mechanisms in energy storage materials is achieved by amplitude- and phase-resolved near-field imaging. Furthermore, here we introduce correlative tip-enhanced nanoscopy, enables complete colloidal vibrational analysis of both IR- and Raman-active modes at the same spatial scale. Our instrument allows for a straight-forward implementation of nano-PL measurements using background suppressing provided by the demodulation of detector signal utilized in nano-FTIR detection scheme. Combining Raman, TERS, nano-FTIR and nano-PL measurements in the same instrument significantly reduces the effort of correlating the resulting datasets, enabling complete optical analysis at nanoscale, which has not been possible so far.

11:40am **NS2+2D+BI+EL+SS-MoM-11 Correlative Nanoscale Chemical, Mechanical and Electrical Property Mapping on a Single AFM-IR Platform, C. Li, Martin Wagner, C. Phillips**, Bruker Nano Surfaces Division

Chemical identification on the nanoscale is a long sought after capability from the inception of AFM. AFM-IR has proven to be uniquely successful in achieving this among all other attempts. It uses a mid-IR laser that is focused onto the AFM tip. Light absorption by the sample results in photothermal expansion that causes a detectable cantilever deflection change of the AFM probe. The obtained IR spectra correlate with conventional FTIR spectroscopy but are associated with sub-10nm spatial resolution.

However, a single data set rarely tells the full story and multiplexed analysis is essential to fully understand a material. We use an AFM-IR microscope with image registration and overlay capability to return to the same position on a sample when changing AFM probes, enabling extensive multimodal analysis. Data on a two-component polymer sample PS-LDPE comprising polystyrene and polyethylene reveals nanoIR spectra that correlate well with FTIR, while nanoIR maps at different IR wavenumbers provide the spatial distribution of each component. Further, we show that they are directly correlated at the nanometer level through PeakForce QNM elastic modulus and adhesion maps, as well as work function (surface potential) and dielectric maps with FM-KPFM (frequency-modulated Kelvin probe force microscopy). Many of the properties can be conveniently obtained simultaneously, while others are preferably obtained sequentially in a colocalized manner with the optimal probe choice and parameter settings for each AFM mode. Data on real-world industrial samples is then discussed, e.g. SBR (styrene-butadiene rubber) with carbon-black additives for car tires, exemplifying how ratio-map and multimodal property mapping unravel information not seen through one technique alone. In another use case chemical identification is complemented by nDMA, a mode where viscoelastic nanoscale sample properties are measured that match bulk dynamic mechanical analysis (DMA) data.

## Surface Science Division Room D136 - Session SS1+HC-MoM

### Electrochemistry

**Moderators:** Jan Balajka, TU Wien, Sefik Suzer, Bilkent University, Turkey

8:20am **SS1+HC-MoM-1 Surface Inhomogeneities and Ordering Phenomena of (Pr,Ba)CoO<sub>3-δ</sub> Thin Film Electrocatalysts Induced by High Temperatures and Oxygen Partial Pressures, David Mueller, M. Giesen, T. Duchon, C. Schneider**, Forschungszentrum Jülich GmbH, Germany

Complex transition metal oxides are used ubiquitously in (electro-)catalysis, ternary and quaternary compounds of the perovskite structure showing especial promise for increasing the efficacy of a plethora of redox reactions. The perovskite structure ABO<sub>3</sub> being able to accommodate a huge range of elements on both A- and B-site allows to tune the electronic and physicochemical properties and tailor those towards a certain catalytic application by careful design of the chemistry. This rational design paradigm has led to the identification of simple descriptors that offer structure-property-activity predictions. These descriptors, mostly derived from the electronic states near the Fermi level, can, for example, be elucidated through X-Ray absorption (XAS) or photoemission spectroscopy.<sup>1</sup>

The catalyst surfaces, however, are dynamic in technologically relevant conditions. Design rules thus have to consider structural, chemical and electronic rearrangements at the surface during catalysis or catalyst processing. Adding to this complexity, spatial inhomogeneities may arise from decomposition pathways that are not found in the bulk, and occur on length scales that can not be resolved by standard electrochemical or spectroscopic techniques.

Here, we investigate (Pr,Ba)CoO<sub>3-δ</sub> (PBCO) as a prototypical example material that exhibits both promising catalytic properties towards the oxygen evolution reaction in solid electrochemical cells<sup>2</sup> as well as a rich structural and chemical complexity depending on oxygen content.<sup>3</sup> Exposing epitaxial thin films grown by pulsed laser deposition to elevated temperatures and oxygen partial pressures typically present in operation, we could identify severe chemical rearrangements at the nanoscale using X-Ray absorption photoelectron microscopy (X-PEEM). We employ principal component analysis on the spatially resolved XAS spectra of all constituents to unambiguously identify correlations of chemical and electronic inhomogeneities.<sup>4,5</sup> Even though PBCO has been found to be thermodynamically stable in the cubic phase over a wide range

# Monday Morning, November 6, 2023

temperature and oxygen partial pressures in the bulk, our data suggests a Cahn Hillard type decomposition process confined to the surface after mere hours of exposure. The decomposition products show a considerable lateral inhomogeneity of both A-site chemistry and the electronic structure at the surface, emphasizing that activity descriptors derived from this through spatially averaging techniques have to be heavily scrutinized.

<sup>1</sup>J. Suntivich *et al.*, *Science* **334**, 1383–1385 (2011); <sup>2</sup>A.Grimaud *et al.*, *Nat. Commun.* **4**,2439 (2013); <sup>3</sup>C. Frontera, *Chem. Mater.*, **17**, 5439-5445 (2005); <sup>4</sup>M. Giesen *et al.*, *Thin Solid Films* **665**, 75-84(2018). <sup>5</sup>D. N. Mueller *et al.*, *J. Phys. Chem. C* **125**, 2021, 10043-10050

8:40am **SS1+HC-MoM-2 Understanding the Influence of Electrolyte and the Buried Interface on the Stability of Hybrid Systems: A Spectro-Electrochemical Approach**, **Tom Hauffman**, *N. Madelat, B. Wouters, A. Hubin, H. Terryn*, Vrije Universiteit Brussel, dept. Materials and Chemistry, Belgium

The stability of the interface between (organic) coatings and metal (oxides) is of crucial importance for the durability and efficiency of hybrid structures in numerous applications, e.g. in food packaging, automotive, ... This interface is a challenging zone to analyze: from both sides covered with micro- to millimeter thick layers, surface sensitive spectroscopic techniques cannot unravel its characteristics in a non-destructive way. Moreover, the change of this interface due to environmental influences remains challenging to reveal.

In this work, we propose the use of a combined electrochemical and spectroscopic method: Odd Random Phase Multisine Electrochemical Impedance Spectroscopy in combination with Infrared Spectroscopy in a Kretschmann geometry. This fusion allows to correlate the global electrochemical characteristics of the system – such as water uptake and ion diffusion – with enhanced interfacial information.

The concept of this approach is proven on ultrathin PAA and PMMA layers on aluminium oxide<sup>1</sup>, clearly elucidating the surface sensitivity of the Kretschmann geometry and unravelling the enhanced adhesion effect of water on short time scales.

The combined characterization tool has been employed on “industrial -like” organic coatings on model engineering metals. Here, the influence of water uptake, the possibility to make a distinction between water ingress and water diffusion, the influence of both species on delamination and corrosion and the influence of the tuned buried interface will be presented<sup>2,3,4</sup>.

1. Pletincx S. et al., An in situ spectro-electrochemical monitoring of aqueous effects on polymer/metal oxide interfaces, *Journal of Electroanalytical Chemistry* 848 (2019).
2. Wouters B. et al., Monitoring initial contact of UV-cured organic coatings with aqueous solutions using odd random phase multisine electrochemical impedance spectroscopy, *Corrosion Science* 190 (2021).
3. Madelat N. et al., Differentiating between the diffusion of water and ions from aqueous electrolytes in organic coatings using an integrated spectro-electrochemical approach, *Corrosion Science* 212 (2022).
4. Madelat N. et al., An ORP-EIS approach to distinguish the contribution of the buried interface to the electrochemical behaviour of coated aluminium, *Electrochimica Acta* 455 (2023).

9:00am **SS1+HC-MoM-3 Controlling CO<sub>2</sub> Reduction and Electrocatalysis Reactivity Using Alloy and Polymer-modified Electrodes**, **Andrew Gewirth**, University of Illinois at Urbana Champaign

INVITED

This talk addresses the reactivity associated with CO<sub>2</sub> and nitrate electroreduction. Electrodeposition of metals from plating baths containing 3,5-diamino-1,2,4-triazole (DAT) as an inhibitor yields highly porous materials exhibiting enhanced activity for electrochemical reactions. Electrodeposition of Cu or CuAg and CuSn, alloy films from such plating baths yields high surface area catalysts for the active and selective electroreduction of CO<sub>2</sub> to multi-carbon hydrocarbons and oxygenates. Alloy films containing Sn exhibit the best CO<sub>2</sub> electroreduction performance, with the Faradaic efficiency for C<sub>2</sub>H<sub>4</sub> and C<sub>2</sub>H<sub>5</sub>OH production reaching nearly 60 and 25%, respectively, at a cathode potential of just -0.7 V vs. RHE and a total current density of ~-300 mA/cm<sup>2</sup>. *In-situ* Raman and electroanalysis studies suggest the origin of the high selectivity towards C<sub>2</sub> products to be a combined effect of the enhanced destabilization of the Cu<sub>2</sub>O overlayer and the optimal availability of the CO intermediate due to the Ag or Sn

incorporated in the alloy. Sn-containing films exhibit less Cu<sub>2</sub>O relative to either the Ag-containing or neat Cu films, likely due to the increased oxophilicity of the admixed Sn. A related effect is found for nitrate reduction on alloy-modified Cu electrodes. Modification of the Cu electrode with certain polymers yields substantially enhanced CO<sub>2</sub> reduction reactivity, due in part to control of the Cu<sub>2</sub>O layer and elevated surface pH. Polymer-composite electrodes exhibit enhanced reactivity over a wide range of proton-involved electrochemical reactions. As an example, methanol oxidation reactivity is substantially enhanced with polymer-modified Pt electrodes.

9:40am **SS1+HC-MoM-5 Enhancement of CO<sub>2</sub> Reduction Reaction Activity and Selectivity of Sub-2 nm Ag Electrocatalysts by Electronic Metal-Carbon Interactions**, **Xingyi Deng**, *D. Alfonso, T. Nguyen-Phan, D. Kauffman*, National Energy Technology Laboratory

We show that the activity and selectivity of sub-2 nm Ag electrocatalysts for electrochemical CO<sub>2</sub> to CO conversion is drastically improved by electronic metal-support interactions (EMSI). The EMSIs between Ag and carbon support, created by deposition of Ag onto heavily sputtered, highly oriented pyrolytic graphite (HOPG), were revealed by X-ray photoelectron spectroscopy (XPS), and supported by computational modeling based on density functional theory (DFT). While sub-2 nm Ag electrocatalysts lack of EMSIs showed selectivity (CO Faradaic efficiency FE<sub>CO</sub> < 2%) toward the electrochemical CO<sub>2</sub> reduction reaction (CO<sub>2</sub>RR), similar sized Ag electrocatalysts with EMSIs demonstrated ~100% FE<sub>CO</sub> and more than 15-fold increase of CO turnover frequency (TOF<sub>CO</sub>). Our calculations elucidated that the electronic Ag-C interactions led to a significant charge transfer (1.02 e) from Ag to carbon support and subsequently lowered the potential-limiting step in CO<sub>2</sub>RR by 0.41 eV. Our results provide the direct evidence of improving CO<sub>2</sub>RR performances of electrocatalysts through EMSIs, particularly between metal and carbon. The EMSIs help break the limit of size-dependent CO<sub>2</sub>RR activity in Ag nanoparticles, hinting at a new approach for creating active and selective electrocatalysts.

10:00am **SS1+HC-MoM-6 Super Structure and Surface Reconstructions with High-Energy Surface X-Ray Diffraction**, **Gary Harlow**, University of Oregon; *D. Gajdek*, University of Malmo, Sweden; *G. Abbondanza*, *A. Grespi*, Lund University, Sweden; *H. Wallander*, University of Malmo, Sweden; *A. Larsson*, University of Lund, Sweden; *L. Merte*, University of Malmo, Sweden; *E. Lundgren*, Lund University, Sweden

The performance of an electrocatalyst (its activity, selectivity, and stability) is strongly dependent on the electrode structure and composition, particularly in the near surface region. A successful approach in trying to understand the impact of structure is the use of well-defined model electrodes such as single crystals, to isolate how various changes in structure and composition impact upon the catalyst behavior. Surface x-ray diffraction gives the average surface structure of an isolated facet, whereas real catalysts often contain multiple facets and edge sites. This contribution will discuss the application of high energy surface x-ray scattering to quickly map out large volumes of 3D reciprocal space and then extract crystal truncation rods. These truncation rods can then be used to determine atomic coordinates of surface atoms, in operando.

Examples during methanol oxidation on both Pt(111) and Au(111) surfaces will be presented. As well as measurements on the the stability of ultra-thin Fe oxide layers on Pt(111) after transfer from vacuum to our in situ electrochemical cell.

## Surface Science Division

### Room D136 - Session SS2-MoM

#### Liquid-Solid Interfaces

**Moderators:** Jan Balajka, TU Wien, Sefik Suzer, Bilkent University, Turkey

10:40am **SS2-MoM-8 Local Potential Determinations by XPS Provides the Missing Link about Charge Dynamics of Ionic Liquid Devices**, **Sefik Suzer**, Bilkent University, Chemistry Department, Turkey

Ionic liquid materials show rich dynamic responses on electrified surfaces. A long-standing question is why these materials exhibit very different time responses, ranging from microseconds to several hours, which are attributed to the complex interplay of chemical and physical factors, including steric and molecular interactions. However, experimental observations and theoretical predictions do not always match in IL based devices. Particularly considering the overall electrode capacitance resulting from asymmetric ion size effects, the local voltage levels can show large differences, and drift-diffusion process of ions generally fails to account for

# Monday Morning, November 6, 2023

them. To clarify this point, we have utilized a combination of electrochemical devices with different chemical make-up, geometry and dynamic XPS analysis and modelling, and were able to probe the spatiotemporal voltage profiles directly from the shifts in the binding energy positions of the ionic core levels, within IL based devices. Results from a number of single and mixed ILs, as well as different device geometries will be presented and discussed.

11:00am **SS2-MoM-9 Interactions at the Solid-Liquid Interface of Microcrystalline ZnO and Bacterial Growth Environments**, *Dustin Johnson, J. Reeks, A. Caron, M. Smit*, Texas Christian University; *T. McHenry*, Texas Christian University; *S. McGillivray, Y. Strzhemechny*, Texas Christian University

Despite the prevalence of traditional antibiotics, new threats are posed by bacterial infections due to the rise of antibiotic resistant strains. As such, development of novel antibacterial agents is a critical area of research. In this regard nano- and microscale ZnO have been found to be particularly promising. ZnO at these scales has been shown to exhibit selective toxicity and growth inhibition for a wide range of both Gram-positive and Gram-negative bacteria as well as for microbial strains resistant to traditional antibiotics. The abundance of constituent elements and inexpensive synthesis methods in combination with the aforementioned antimicrobial properties have led ZnO based antibacterial agents to be implemented in biomedical, water treatment, food storage and various other industries. Refinement of current techniques and development of novel bactericidal applications are limited by incomplete descriptions of the fundamental interactions responsible for the observed antibacterial behaviors. In particular, the role and nature of interactions of ZnO with bacterial growth media is not well understood. Herein, we investigate environmental influences relevant to the antibacterial action of ZnO through the interactions with both bacteria and the bacterial environments on the physicochemical and optoelectronic properties of the free crystalline surface of ZnO microparticles (MPs). We expose hydrothermally grown ZnO MPs to phosphate-buffered saline (PBS) media both with and without the presence of Newman strain *Staphylococcus Aureus* (*S. aureus*) bacteria. Surface electronic structure and charge dynamics are probed via both time- and energy-dependent surface photovoltage (SPV) conducted prior to and following biological assays. We observe significant changes in the characteristic timescales under varying conditions, indicating, among other, a possibility of a significant phosphate adsorption at the free crystalline surface. This is further supported by the suppression of spectral signatures of the oxygen-rich defects after exposure to PBS media.

11:20am **SS2-MoM-10 Towards Understanding Interfacial Thermodynamics: Visualizing and Quantifying Competitive Adsorption on Muscovite Mica with AFM**, *Matteo Olgiati, J. Dziadkowiec, A. Celebi, L. Mears, M. Valtiner*, Technische Universität Wien, Austria

Given its peculiar crystal structure and inherent surface charge, the (001) plane of muscovite mica has served as an excellent model system to study the hydration and electric double layer (EDL) forces at solid-liquid interfaces [1]. So far, force spectroscopies, which measure along the direction perpendicular to the surface, as well as molecular dynamics (MD) simulations, have demonstrated a certain ion-specificity towards the strength of hydration forces on mica surfaces [2-5]. These deviations are mainly attributed to the different properties of individual ions (e.g., hydration shell, size, valency, etc.), which ultimately determine their adsorption character on mica, as well as the interfacial hydration structure [5]. Nevertheless, lateral distribution and arrangement of cations adsorbed on mica was experimentally investigated only to a lesser extent [6], although unravelling the ions' organisation directly at the surface is crucial to elucidate the structure and properties of EDLs.

In the present contribution, we discuss how high-resolution atomic force microscopy (AFM) imaging enables us to visualize the lateral distribution of individual mono- and multi-valent ions on the surface of mica. Thanks to this approach, we are able not only to resolve the crystal structure of mica immersed in aqueous solution, but also to transiently picture the population of adsorbed ions from the salt-rich solutions at different concentrations. By using an automated triangulation algorithm, the ion adsorption coverage as a function of concentration can be quantified in a first order approximation. This methodology highlights the possibility to outline a certain competitive behaviour of charged species at the surface. Understanding such competition as a function of type and concentration of ions allows us to unravel the interfacial thermodynamics directly from AFM data, which has been so far mainly exclusive to MD simulations. To further support our findings, we use surface force apparatus and MD simulations to

characterise the structure and mechanical properties of EDLs on mica for different cation species.

## References

- [1] R. M. Pashley, *J. Colloid Interface Sci.* **83**, 2, 531-546 (1981).
- [2] T. Baimpos, B. R. Shrestha, S. Raman and M. Valtiner, *Langmuir* **30**, 4322-4332 (2014).
- [3] Z. Zachariah, R. M. Espinosa-Marzal and M. P. Heuberger, *J. Colloid Interface Sci.* **506**, 263-270(2017).
- [4] I. C. Bourg, S. S. Lee, P. Fenter and C. Tournassat, *J. Phys. Chem.* **C121**, 9402-9412(2017).
- [5] S. R. van Lin, K. K. Grotz, I. Siretanu, N. Schwierz and F. Mugele, *Langmuir* **35**, 5737-5745 (2019).
- [6] M. Ricci, P. Spijker and K. Voitchovsky, *Nat. Commun.* **5**, 4400 (2014).

## Chemical Analysis and Imaging of Interfaces Focus Topic Room A105 - Session CA+AS+LS+NS+SS+VT-MoA

### Environmental and Energy Interfaces

Moderators: Musahid Ahmed, LBNL, Xiao-Ying Yu, Oak Ridge National Laboratory, USA

#### 1:40pm CA+AS+LS+NS+SS+VT-MoA-1 In situ Spectroscopies of Interfacial Reactions and Processes in Batteries, Feng Wang, Argonne National Laboratory

INVITED

The performance and lifetime of batteries, whether they are traditional lithium-ion, solid-state, or other types, strongly depend on the effectiveness and stability of electrochemical interfaces within the devices. To design battery materials and interfaces with desired functionality, it is crucial to have a mechanistic understanding of the interfacial reactions and processes occurring during battery operation. This necessitates developing advanced techniques capable of characterizing local structures and capturing *non-equilibrium* dynamics at electrochemical interfaces, with the relevant spatial, time resolution and chemical sensitivity, both to light elements (H, Li, O) and heavy ones. Herein, we present the development and application of *in situ* spectroscopies specialized for probing interfacial reaction and processes in lithium-ion and solid-state batteries. With specific examples from our recent studies, we will show how to correlate the structure and function of electrochemical interfaces through *in situ* spectroscopy characterization, thereby gaining insights into the design and processing of battery materials, electrolytes and other components. Towards the end of this talk, we will discuss emerging opportunities in data-driven experimentation, analysis, and modeling for closed-loop battery development to accelerate the transition from lab discovery to commercial deployment.

#### 2:20pm CA+AS+LS+NS+SS+VT-MoA-3 Novel Strategies for the Characterization of the Next-Generation Energy Storage Materials by ToF-SIMS: From an in-Situ Exploration to an Operando Measurement, Tangyu Terlier, Q. Ai, S. Sidhik, A. Mohite, J. Lou, Rice University

INVITED

Recently, advances in instrumentation and sample preparation have permitted a rapid development for characterizing a wide range of applications such as next-generation energy storage materials. Developing new materials is one of the most crucial topics for emerging technologies. However, the complexity of these materials in their structures makes them particularly challenging for numerous characterization and analytical techniques. Exploring chemical composition and the potential chemical reactions such as degradation, diffusion, or doping is crucial to understand advanced materials and to transfer the new technologies to the industry. Among the most suitable characterization tool, time-of-flight secondary ion mass spectrometry (ToF-SIMS) is a very sensitive surface analytical technique providing detailed elemental and molecular information about the surface, thin layers, interfaces, and full three-dimensional analysis of the samples.

Thanks to the advances in ToF-SIMS characterization, understanding of the chemical composition and the different components in the complex structures, permit a deeper exploration and a better knowledge in the next-generation energy storage materials such as batteries, perovskites, and 2D materials.

Firstly, we will focus on the characterization of batteries. Initially, we will discuss the sample preparation and our specific setup for transferring the specimens from the inert atmosphere in the glovebox to the ultra-high vacuum chamber of our instrument. We will illustrate the possibility to study the reversibility of the chemical composition between pristine, charged, and discharged batteries using surface mass spectrometry by ToF-SIMS in operando conditions. Then we will compare three methods of cross-sectioning used to identify the interfacial species in a composite cathode.

Secondly, we will show a study of an in-depth distribution of the 3D/2D heterostructures for perovskite solar cells where we have been able to identify individually the 3D and 2D heterostructures along with the depth of the film. Then, we will illustrate the characterization of interdiffusion in quasi-2D perovskite light-emitting diodes as a function of the organic ligand layer inserted into the perovskite crystals.

Finally, we will demonstrate how the retrospective analysis using ToF-SIMS can be very powerful and useful for exploring any single feature in 2D materials. Typically, ToF-SIMS acquisition is recording a full mass range

spectrum per pixel (or voxel), which permits to isolate and to decorrelate specific regions of interest for resolving interfaces, diffusion, and doping in thin 2D structures. We will present how to treat a 3D volume image of a multilayer perovskite device for extracting useful information.

#### 3:00pm CA+AS+LS+NS+SS+VT-MoA-5 Advanced In-Situ and Ex-Situ S/TEM Probing of Interfacial Process in Rechargeable Batteries, Chongmin Wang, Pacific Northwest National Laboratory

In-situ diagnosis appears to be one of the essential methods for gaining insights as how an electrode material failure, therefore feeding back for designing and creating new materials with enhanced battery performances. In this presentation, I will highlight recent progress on ex-situ, in-situ and operando S/TEM for probing into the structural and chemical evolution of interfacial process in energy storage materials. Both ex-situ and In-situ high resolution imaging enables direct observation of structural evolution, phase transformation and their correlation with mass, charge and electron transport, providing insights as how active materials failure during the cyclic charging and discharging of a battery. In perspective, challenges and possible direction for further development of the in-situ S/TEM imaging and spectroscopic methods for energy storage materials and other field will also be discussed. Most importantly, integration of different analytical tools appear to be the key for capturing complementary information.

#### 3:20pm CA+AS+LS+NS+SS+VT-MoA-6 Investigating $sp^2$ and $sp^3$ Carbon Ratios by XPS: A Study of the D-Parameter and a New Second Plasmon Loss (2PL) Parameter, Alvaro Lizarbe, G. Major, B. Clark, Brigham Young University; D. Morgan, Cardiff University, UK; M. Linford, Brigham Young University

The D-parameter provides a useful estimate of the ratio of the  $sp^2$  and  $sp^3$  carbon in a sample. It is the energy difference between the maximum and minimum of the derivative of the C KLL Auger peak. The D-parameter can be an important analytical resource for diamond samples, as the quality of diamond depends on the  $sp^3$  to  $sp^2$  carbon ratio and any lattice impurities. For example, the highly sought after type 2a diamonds, which are colorless and free from impurities, consist almost entirely of  $sp^3$  carbon. According to the universal curve for XPS, electrons with different kinetic energies have different mean free paths. Thus, electrons with different kinetic energies sample materials at different depths. In the case of carbon, the KLL Auger peak comes shallower in a material compared to the C 1s signal, which is a result of electrons with much higher kinetic energies. That is, a limitation of the D-parameter is that it is based on the C KLL Auger peak, found at around 1220 eV, while it is often related to the C 1s peak located at approximately 284.8 eV. Thus, the D-parameter is much more sensitive to adventitious carbon contamination. In an effort to derive a parameter that will be more representative of the amounts of  $sp^2$  and  $sp^3$  carbon in a material, we have examined the plasmon loss peaks of the zero-loss C 1s peak of direct current chemical vapor deposition (DC-CVD) diamonds, carbon nanotubes, and graphitic materials such as HOPG. By analyzing the second plasmon loss signal of the C 1s narrow scan, we obtain a new parameter for analyzing carbonaceous materials: the 2PL parameter. The 2PL parameter is the difference in energy between the second plasmon loss signal and the C 1s peak. We compare the traditional D-parameter with the 2PL parameter for various materials. They correlate quite well. We have also investigated various mathematical methods of deriving the 2PL parameter, including via a weighted average of the second plasmon loss and C 1s signals. Ultimately, because the 2PL parameter involves signals that are closer to the C 1s photoemission binding energy, we believe it may be more representative of the full chemistry of carbonaceous materials.

#### 4:00pm CA+AS+LS+NS+SS+VT-MoA-8 Solid-Liquid Interfaces for Energy-efficient Chemical Separation of Critical Minerals and CO<sub>2</sub> Conversion, Manh-Thuong Nguyen, V. Prabhakaran, D. Heldebrant, G. Johnson, Pacific Northwest National Laboratory

INVITED

Chemical separations consume around 15% of the energy used by industry today. It is thus critical to develop energy- and material-efficient approaches for large-scale separations. In the first part of this presentation, I will illustrate how we employ modified 2-dimensional materials and solvents to separate critical minerals including rare earth elements. Polar functional groups present at the interface of graphene oxide laminate membranes are demonstrated to improve the selectivity of metal cations separated by both adsorption and sieving. Hydrophobic ionic liquid molecules including 1-ethyl-3-methylimidazolium chloride, when used as a minor solvent component, are shown to increase the energy efficiency of the desolvation of aqueous lanthanide cations in electrochemical separations. In the second part, I will present studies exploring the use of functionalized hexagonal boron nitride (h-BN) membranes to separate CO<sub>2</sub>



# Monday Afternoon, November 6, 2023

from multicomponent gas mixtures. Strategies for improving CO<sub>2</sub> separation selectivity and efficiency, such as chemical functionalization and engineering the dimensions of interlayer transport channels, will be discussed. Finally, I will present studies on the electrochemical conversion of CO<sub>2</sub> into value added chemical feedstocks such as methanol on membrane-supported catalysts. Insights into the effects of local structure modification and confinement on catalytic processes will be presented.

4:40pm **CA+AS+LS+NS+SS+VT-MoA-10 Buried Interfaces of Ir Photodetector Devices Analyzed with Lab-Based Xps/Haxpes, Roman Charvier, M. Juhel, STMicroelectronics, France; O. Renault, Univ. Grenoble-Alpes, CEA, Leti, France; A. Valery, D. Guiheux, L. Mohgouk Zouknak, STMicroelectronics, France; B. Domenichini, ICB UMR 6303 CNRS-Université de Bourgogne, France**

The development of new IR photodetectors should respond to challenges in order to reach best performances. A major objective is to understand critical interfaces that play an important role in the final device properties. This work addresses to chemical analysis of molybdenum oxide (MoO<sub>3-x</sub>) used as hole transport material which is deposited between a photosensitive material and top electrode often made of indium-tin oxide (ITO). Such critical interfaces are typically located under 20 to 50 nm under the surface.

In the case of MoO<sub>3-x</sub>, the stoichiometry is generally controlled by X-ray photoelectron spectroscopy (XPS) which is well-known to obtain chemical data close to the material surface (analysis depth < 10 nm). Two methods can be used to analyse deeper buried layers: (i) the use of hard X-rays to perform Hard X-ray PhotoElectron Spectroscopy (HaXPES) and thus generate photoelectrons having a kinetic energy able to go through several tens of nm; (ii) the etching of the surface by means of an Ar<sup>+</sup> beam (having an energy from 0.5 to 3 keV) in order to remove the superficial layers giving access to the underlying layers. In the former case, the analyzed thickness remains far below 100 nm while in the latter case, the chemistry of the surface atoms are often modified by argon ion beam. It is then necessary to mix the two approaches to allow the chemical analysis of buried interfaces. This analysis way is used here to characterize the stoichiometry of MoO<sub>3-x</sub> thin films buried under 50 nm of ITO using chromium K $\alpha$  hard-X-ray from lab-based HaXPES.

5:00pm **CA+AS+LS+NS+SS+VT-MoA-11 Detection and Discrimination of Aquatic Toxins Targeting Voltage Gated Sodium Channels Using Static ToF-SIMS Imaging, Jiyoun Song, K. Engbrecht, J. Mobberley, PNNL**

Neurotoxins from aquatic microorganisms, such as cyanobacteria and algae, have been a public health concern due to their harmful impacts on the nervous systems of animals, including humans. A subset of these neurotoxins, including saxitoxin and brevetoxin, bind to and alter the function of voltage-gated sodium channels, which are essential to generating the cell membrane action potential. Existing detection and categorization methods, such as PCR and antibody-based enzyme-linked immunosorbent assays, are too specific and they require live animals like the mouse bioassay. They also require time-consuming and expensive sample preparation for analysis using LC-MS/MS and HPLC. In this project, we developed a method to detect the activity of the aquatic sodium channel neurotoxins, brevetoxin and saxitoxin, using a cell-based process. We specifically examined the impact of these two neurotoxins on HEK-293 cells, a robust cell line that has been transfected with a voltage-gated sodium channel gene, SCN1A, in order to better study neurotoxins. We cultured a layer of cells onto disinfected silicon chips, exposed the cells to neurotoxins, performed chemical fixation, and then air-dried the chips. We also prepared mock exposed samples where the cells on the silicon chips were not exposed to neurotoxins, but just the solutions each neurotoxin was resuspended in, either a 3mM HCl solution (mock saxitoxin) or a 50:50 ACN: water solution (mock brevetoxin). Control samples, which just exposed cells to cell culture media only, gave us a baseline reference. Dried samples were analyzed with mass spectral imaging using time-of-flight secondary ion mass spectrometry (ToF-SIMS). After collecting a series of spectral data, we utilized an in-house MATLAB tool to run principal component analysis (PCA) as previously described (Yu et al., 2020). Our initial statistical analysis of SIMS spectral data using PCA shows a noticeable difference in peak trends between neurotoxin and mock-exposed cells as well as neurotoxin-exposed and control cells. Our approach utilizes chemical imaging to develop a threat-agnostic model system for detecting and classifying neurotoxin activity. The technology and protocols developed from this work could transition to other rapid cellular assays for pathogenic and chemical threats.

Reference

Monday Afternoon, November 6, 2023

Yu, J., Zhou, Y., Engelhard, M. *et al.* *In situ* molecular imaging of adsorbed protein films in water indicating hydrophobicity and hydrophilicity. *Sci Rep* 10, 3695 (2020). <https://doi.org/10.1038/s41598-020-60428-1>

## Laboratory-Based Ambient-Pressure X-ray Photoelectron Spectroscopy Focus Topic

Room B116 - Session LX+AS+BI+HC+SS+TH-MoA

### Laboratory-Based AP-XPS: Surface Chemistry and Biological/Pharmaceutical Interfaces

Moderators: Gregory Herman, Argonne National Laboratory, Ashley Head, Brookhaven National Laboratory

1:40pm **LX+AS+BI+HC+SS+TH-MoA-1 The Role of Co-Adsorbed Water in Decomposition of Oxygenates, H. Nguyen, K. Chuckwu, Líney Árnadóttir, Oregon State University**

INVITED

The decomposition of oxygenates in the presence of water finds various applications in chemical processes, such as biomass conversion. The presence of co-adsorbates and solvents affects both the reaction rate and selectivity. In this study, we used NAP-XPS and DFT to investigate the decomposition of acetic acid on Pd(111) as a model system for the decomposition of small oxygenates in the absence and presence of water. The decomposition of acetic acid occurs through two main reaction pathways, decarboxylation, and decarbonylation, forming CO<sub>2</sub> or CO, respectively. Our DFT calculations indicate that the two pathways have similar barriers without water. However, in the presence of water, the decarboxylation path becomes. Similarly, our AP-XPS experiments show an increase in the CO<sub>2</sub>/CO ratio as well as a decrease in the CO/acetate-acetic acid and acetic acid/acetate ratios when water is present. The shift in selectivity is not due to a single reaction step, but rather the decreasing barrier in general for OH scissoring and the increasing barrier for C-O scissoring. This shift favors the formation of CO<sub>2</sub>, as demonstrated by our microkinetic model.

2:20pm **LX+AS+BI+HC+SS+TH-MoA-3 Integrating First-principles Modeling and AP-XPS for Understanding Evolving Complex Surface Oxides in Materials for Hydrogen Production and Storage, B. Wood, Tuan Anh Pham, Lawrence Livermore Laboratory**

INVITED

Chemical processes occurring at solid-gas, solid-liquid, and solid-solid interfaces critically determine the performance and durability of hydrogen production and storage technologies. While directly probing behavior of these interfaces under actual operating conditions remains challenging, modern surface science approaches such as ambient-pressure X-ray photoelectron spectroscopy (AP-XPS) can provide insight into the evolution of surface chemistry in approximate environments. However, interpretation of these spectra can be complicated: standards for complex surface chemical moieties are often unavailable, and bulk standards can be unreliable. First-principles computations are emerging as an important companion approach, offering the ability to directly compute spectroscopic fingerprints. This has the advantage of aiding interpretation of the experiments, while simultaneously using the experiment-theory comparison to inform construction of more accurate interface models. In this talk, I will show how computation has been combined with laboratory-based AP-XPS measurements to understand the evolving chemistry of complex native surface oxides. Two examples will be drawn from activities within the U.S. Department of Energy HydroGEN and HyMARC consortia, which focus on renewable hydrogen production and materials-based hydrogen storage, respectively. First, I will discuss the application to surface oxidation of III-V semiconductors for photoelectrochemical hydrogen production, which demonstrates transitions between kinetically and thermodynamically controlled oxidation regimes with implications for device performance. Second, I will also show how the same approach has been applied to understand the rate-determining role of surface oxides in the dehydrogenation performance of NaAlH<sub>4</sub> for solid-state hydrogen storage.

This work was performed under the auspices of the U.S. Department of Energy by Lawrence Livermore National Laboratory under Contract DE-AC52-07NA27344.

# Monday Afternoon, November 6, 2023

3:00pm **LX+AS+BI+HC+SS+TH-MoA-5 Particle Encapsulation on Reducible Oxides Under Near-Ambient Pressures**, F. Kraushofer, M. Krinninger, P. Petzoldt, M. Eder, S. Kaiser, J. Planksky, T. Kratky, S. Günther, M. Tschurl, U. Heiz, F. Esch, **Barbara A. J. Lechner**, TUM, Germany **INVITED**

Catalysts on reducible oxide supports often change their activity significantly at elevated temperatures due to the strong metal-support interaction (SMSI), which induces the formation of an encapsulation layer around the noble metal particles. However, the impact of oxidizing and reducing treatments at elevated pressures on this encapsulation layer remains controversial, partly due to the 'pressure gap' between surface science studies and applied catalysis.

In the present work, we employ near-ambient pressure X-ray photoelectron spectroscopy (NAP-XPS) and scanning tunneling microscopy (NAP-STM) to study the effect of reducing and oxidizing atmospheres on the SMSI-state of well-defined oxide-supported Pt catalysts at pressures from UHV up to 1 mbar. On a TiO<sub>2</sub>(110) support, we can either selectively oxidize the support or both the support and the Pt particles by tuning the O<sub>2</sub> pressure.<sup>[1]</sup> We find that the growth of the encapsulating oxide overlayer is inhibited when Pt is in an oxidic state. Our experiments show that the Pt particles remain embedded in the support once encapsulation has occurred. On Fe<sub>3</sub>O<sub>4</sub>(001), the encapsulation stabilizes small Pt clusters against sintering.<sup>[2]</sup> Moreover, the cluster size and thus footprint lead to a change in diffusivity and can therefore be used to tune the sintering mechanism. Very small clusters of up to 10 atoms even still diffuse intact after encapsulation.

[1] P. Petzoldt, P., M. Eder, S. Mackewicz, M. Blum, T. Kratky, S. Günther, M. Tschurl, U. Heiz, B.A.J. Lechner, Tuning Strong Metal-Support Interaction Kinetics on Pt-Loaded TiO<sub>2</sub> (110) by Choosing the Pressure: A Combined Ultrahigh Vacuum/Near-Ambient Pressure XPS Study, *J. Phys. Chem. C* 126, 16127-16139 (2022).

[2] S. Kaiser, J. Planksky, M. Krinninger, A. Shavorskiy, S. Zhu, U. Heiz, F. Esch, B.A.J. Lechner, Does Cluster Encapsulation Inhibit Sintering? Stabilization of Size-Selected Pt Clusters on Fe<sub>3</sub>O<sub>4</sub>(001) by SMSI, *ACS Catalysis* 13, 6203-6213 (2023).

4:00pm **LX+AS+BI+HC+SS+TH-MoA-8 Applications of NAP XPS in Pharmaceutical Manufacturing: Surface Analysis, Hydrogen Bonds, and Solute-Solvent Interactions**, **Sven Schroeder**, University of Leeds, UK **INVITED**

The availability of laboratory-based NAP XPS creates novel interface research opportunities for scientific disciplines and technology areas that deal with materials incompatible with traditional ultra-high vacuum XPS. This is, for example, the case for many organic and/or pharmaceutical materials and formulations, whose characterization by XPS has hitherto been restricted by their vapour pressures. NAP XPS permits for the first time systematic and detailed analysis of the light element photoemission lines (especially C/N/O 1s) in these materials. In conjunction with elemental analysis by survey XP spectra they provide quantitative information on composition and speciation both in the bulk and at the surfaces of pure organic solids, in their formulations with other components and in solutions. Especially of interest are studies of the solid/liquid interface with water, which is of high relevance for understanding and controlling drug release profiles from tablets. To illustrate these points I will present various examples of research on pharmaceutical materials. Moreover, near-ambient pressure core level spectroscopy turns out to be an extremely powerful probe for the structure and dynamics of hydrogen bonding and proton transfer in materials, both in the solid state and in solutions. NAP XPS measurements provide unique insight into proton dynamics in noncrystalline solids and liquids, where traditional characterisation by crystallography and nuclear magnetic resonance fails or provides ambiguous information on proton locations.

4:40pm **LX+AS+BI+HC+SS+TH-MoA-10 The Change of DNA and Protein Radiation Damage Upon Hydration: In-Situ Observations by Near-Ambient-Pressure XPS**, **Marc Benjamin Hahn**, Bundesanstalt für Materialforschung und -prüfung (BAM), Germany **INVITED**

X-ray photoelectron-spectroscopy (XPS) allows simultaneous irradiation and damage monitoring. Although water radiolysis is essential for radiation damage, all previous XPS studies were performed in vacuum. [1] Here we present near-ambient-pressure XPS experiments to directly measure DNA damage under water atmosphere. They permit in-situ monitoring of the effects of radicals on fully hydrated double-stranded DNA. Our results allow us to distinguish direct damage, by photons and secondary low-energy electrons (LEE), from damage by hydroxyl radicals or hydration induced modifications of damage pathways. The exposure of dry DNA to x-rays leads

to strand-breaks at the sugar-phosphate backbone, while deoxyribose and nucleobases are less affected. In contrast, a strong increase of DNA damage is observed in water, where OH-radicals are produced. In consequence, base damage and base release become predominant, even though the number of strand-breaks increases further. Furthermore, first data about the degradation of single-stranded DNA binding-proteins (G5P / GV5 and hmtSSB) under vacuum and NAP-XPS conditions are presented.

[1] Hahn, M.B., Dietrich, P.M. & Radnik, J. In situ monitoring of the influence of water on DNA radiation damage by near-ambient pressure X-ray photoelectron spectroscopy. *Commun Chem* 4, 50, 1-8 (2021). <https://doi.org/10.1038/s42004-021-00487-1>

## Surface Science Division

### Room D136 - Session SS+AS+TF-MoA

#### Mechanisms at Surfaces and Interfaces

**Moderators: Florencia C. Calaza**, Instituto de Desarrollo Tecnológico para la Industria Química, **Jun Nakamura**, UEC Tokyo

1:40pm **SS+AS+TF-MoA-1 Spin- and Alignment-Controlled O<sub>2</sub> Chemisorption and Catalytic CO Oxidation on Stepped Pt and Pt/Co Alloy Surfaces**, **Mitsunori Kurahashi**, National Institutes for Materials Science, Japan **INVITED**

O<sub>2</sub> chemisorption and catalytic oxidation on Pt and its alloy surfaces have been studied intensively due to the relevance to important processes such as car exhaust gas purification and oxygen reduction reaction (ORR) in fuel cell. Since O<sub>2</sub> is a linear diatomic molecule with an electron spin, the alignment of the O<sub>2</sub> axis relative to the surface local structure is a key to understand the elementary processes of O<sub>2</sub> chemisorption. If the surface is magnetic, the spin correlation between O<sub>2</sub> and the surface also plays an important role. A single spin-rotational state-selected [(J,M)=(2,2)] O<sub>2</sub> beam allows us to investigate the effects of molecular alignment and spin on O<sub>2</sub>/surface interactions [1].

In this talk, I will firstly present the alignment-controlled O<sub>2</sub> chemisorption and CO oxidation on curved Pt(111). The use of a curved crystal surface and a local probe allows us to monitor the step-density dependence in surface properties or reactivity[2,3]. In this study, by scanning the aligned O<sub>2</sub> beam with a dimension of 0.2mmW x 2mm across a curved Pt(111) surface, the step-density and structure dependence in alignment-resolved O<sub>2</sub> chemisorption probability and CO oxidation rate were measured. The results indicate that step affects the reactivity of the neighboring terraces, and that the low temperature CO oxidation rate at step site is much lower than at (111) terrace.

Secondly, I will present the spin-dependent catalytic CO oxidation on Pt/Co/Pt(111). Pt/Co alloy has attracted much attention since it shows a higher ORR activity than pure Pt [4]. The higher reactivity has been attributed to the charge transfer from the subsurface Co to the surface Pt layer while how the spin of the subsurface Co affects the reactivity of the surface Pt remains unclear. Spin-resolved O<sub>2</sub> chemisorption and CO oxidation experiments on a perpendicularly-magnetized Pt/Co(2ML)/Pt(111) film indicate that the O<sub>2</sub> chemisorption probability and the catalytic oxidation rate depend strongly on the spin orientation between O<sub>2</sub> and the Pt surface. The magnitude of the spin orientation dependence was larger than that observed for O<sub>2</sub>/Ni [1,5]. An SPMDS measurement and DFT calculation show that the surface Pt layer is spin-polarized at around E<sub>F</sub>. The present experiments indicate that the catalytic activity of Pt is strongly affected by the magnetism of neighboring atoms.

[1] M. Kurahashi, *Prog. Surf. Sci.*, 91, 29 (2016). [2] A. Walter et al., *Nat. Comm.* 6, 1 (2015); S. Auras, L. Juurlink, *Prog. Surf. Sci.*, 96, 100627 (2021). [3] K. Cao, R. Lent, A. W. Kleyn, M. Kurahashi, and L. B. F. Juurlink, *PNAS* 116, 13862 (2019). [4] V. Stamenkovic et al., *J. Phys. Chem. B*, 106, 11970 (2002). [5] M. Kurahashi, *J. Chem. Phys.*, 157, 124707 (2022).

2:20pm **SS+AS+TF-MoA-3 Atomic-Scale Insights Into the Sintering Resistance and Oxidation of Single-Atom Alloys**, **Audrey Dannar**<sup>1</sup>, Tufts University; **J. Finzel**, University of California, Santa Barbara; **V. Cinar**, **E. Sykes**, Tufts University

Copper-based catalysts are used in a wide range of heterogeneous catalytic processes that can take place in oxidizing environments, where Cu is known to readily oxidize to form CuOx, and reducing environments, where Cu is known to deactivate via sintering. Single-atom alloys (SAAs) are a new type

<sup>1</sup> SSD Morton S. Traum Award Finalist

of catalyst in which isolated atoms of dilute reactive dopants such as Pt and Rh are present in more inert host metals such as Cu. Despite their great promise for hydrogenation and dehydrogenation reactions, there exists limited understanding of these materials under oxidizing conditions. Similarly, SAAs have shown exceptional long-term stability with anecdotal reports of sintering resistance in industrial conditions that are not presently fundamentally understood. This work aims to develop atomic-scale structure-function relationships for Cu-based catalysts that span oxidizing and reducing conditions and understand how single dopant atoms stabilize the undercoordinated Cu atoms responsible for sintering and involved in CuOx formation upon O2 exposure.

First, we used a specialized method for measuring the surface diffusion of metal atoms that leads to sintering with scanning tunneling microscopy (STM) experiments which reveals that single Pt atoms in a Cu(110) surface significantly reduce the rate of Cu atom detachment from undercoordinated surface sites. Thus, the origin of sintering resistance exhibited by SAA is hypothesized to be due to dopant atom stabilization of undercoordinated Cu atoms at the step edge. This is validated by DFT and paired with collaborator work that shows PtCu/SiO2 dilute alloy catalysts are significantly more stable than monometallic Cu/SiO2 in methanol synthesis experiments via EXAFS and TEM.

Next we used STM experiments to elucidate atomic-scale details of the oxidation processes of both PtCu(111) and RhCu(111) SAAs. STM images reveal that on Cu(111), oxidation occurs below Cu step edges, consistent with literature reports. Interestingly, for the RhCu(111) SAA, oxidation occurs both below the step edges and also above, where the Rh atoms are located, but this is not the case for the Pt on PtCu(111). For both Rh and Pt SAAs the oxidation below the step edge is reduced compared to Cu, which we hypothesize is due to the stabilization of Cu step edge atoms, which are required to restructure during CuOx formation below the step. The reduced rates of sintering and oxidation of PtCu SAAs compared to Cu originate from Cu step edge atoms being kinetically stabilized by dilute dopants. Together, these results begin to shed light on the role of single dopant atoms in the mechanisms Cu nanoparticle sintering and Cu oxidation.

**2:40pm SS+AS+TF-MoA-4 Visualization of the Local Dipole Moment at the Si(111)-(2x2) Surface Using DFT Calculations, Akira Sumiyoshi, J. Nakamura, The University of Electro-Communications (UEC Tokyo), Japan**

Understanding the polarization state of a sample is essential in the development of devices and functional materials. Recently, the spatial distribution of the surface polarization has been observed using new microscopy techniques, such as SNDM[1-3]. However, there have yet to be any reports regarding the theoretical simulation of surface polarization. Here, we focused on the dipole moment (DM), an essential aspect of polarization, and developed a method to visualize the distribution of surface DM using theoretical calculations. In this study, we report on the surface DM distribution of Si(111)-(2x2) with the characteristic motif of the Si(111)-(7x7) DAS structure. Furthermore, we confirmed that the surface dipole distribution can be explained consistently with the surface stabilization mechanism.

We defined and calculated the DM using the following formula;

$$\mu_{(x,y,z)} = \int \rho_{(x,y,z)} * (z' - z_0) dz'$$

Here,  $\mu$  is the DM,  $\rho_{(x,y,z)}$  is the total charge density, and  $z_0$  is the origin in the vertical direction. In order to eliminate the effect of the backside surface of the Si(111) slab, we adopted the midpoint of the deepest bulk layer of the slab as the origin and integrated the above formula from  $z_0$  to the vacuum position  $z$  sufficiently far from the topmost surface. The total charge density was calculated using DFT-based first-principles calculations.

Upon optimizing the structure, the restatom was lifted compared to the original bulk position, suggesting the larger orbital electronegativity[4] of the surface orbital of the restatom[5]. This change in orbital electronegativity leads to an electron transfer from the adatom to the restatom, resulting in no surface dangling bond. We calculated the electron localization function (ELF) map and the band diagram to confirm the surface electron transfer. We confirmed the presence of the electron pair on the restatom from ELF. It was revealed that the Si(111)-(2x2) surface has a finite energy gap. As a result, it was clearly shown that the electron transfer occurs from the adatom to the restatom, emptying the dangling bond at the adatom and forming a lone pair at the restatom.

Furthermore, we simulated the surface DM distribution. As a result, an upward DM was observed at the adatom position, which is explained by the

depletion of electrons just above the adatom due to the electron transfer at the surface.

- [1] Yasuo Cho et al., Phys. Rev. Lett. 99, 186101(2007)
- [2] Kohei Yamasue et al., Appl. Phys. Lett. 105, 121601(2014)
- [3] Yasuo Cho, Scanning Nonlinear Dielectric Microscopy, Wood. Pub.(2020)
- [4] Jun Nakamura et al., J. Phys. Soc. Jpn. 66, 1656(1997)
- [5] Akihiro Ohtake, Jun Nakamura et al., Phys. Rev. B 64, 045318(2001)

**3:00pm SS+AS+TF-MoA-5 Mechanism Study of a Chemisorbed O2 Molecule on Ag(110) Induced by High-Order Overtone Excitation Using STM, Minhui Lee, E. Kazuma, The University of Tokyo, Japan; C. Zhang, Tongji University, China; M. Trenary, University of Illinois at Chicago; J. Takeya, The University of Tokyo, Japan; J. Jung, University of Ulsan, Republic of Korea; Y. Kim, The University of Tokyo, Japan**

The dissociation pathway of chemisorbed O2 on Ag(110) was elucidated by single-molecule microscopic and spectroscopic studies using a scanning tunneling microscope (STM). The dissociation reaction was found to be predominantly triggered by inelastically tunneled holes from the STM tip due to the significantly distributed density of states below the Fermi level of the substrate. A combination of action spectroscopy with the STM and density functional theory calculations revealed that the O2 dissociation reaction is caused by direct ladder-climbing excitation of the high-order overtones of the O-O stretching mode arising from anharmonicity enhanced by molecule-surface interactions.

**3:20pm SS+AS+TF-MoA-6 Characterization of Oxygen Evolution from Rh(111), Maxwell Gillum, E. Jamka, F. Lewis, D. Killelea, Loyola University Chicago**

Due to the importance of oxide surfaces in heterogeneously catalyzed reactions, it is critical to gain a fundamental understanding of the reactivity and behavior of oxygen on these transition metal surfaces. In previous studies we have been able to establish that the reactivity and thermodynamic stability of oxygen on Rh(111) relies in part on the concentration of oxygen present in the subsurface. However, more research needs to be conducted in order to gain a better understanding of the relationship between surface reactivity and subsurface concentration. In addition to the techniques used in our previous studies, namely temperature programmed desorption (TPD) and scanning tunneling microscopy (STM), the experiments herein will include simultaneous infrared (IR)/TPD techniques to gain more information on these critical interactions.

**4:00pm SS+AS+TF-MoA-8 Spin-Polarized VLEED from Au(111): Surface Sensitivity of the Scattering Process, Christoph Angrick, A. Reimann, University of Münster, Germany; J. Braun, Ludwig-Maximilians-University of Munich, Germany; M. Donath, University of Münster, Germany**

Low-energy electron diffraction from Au(111) shows the well-known threefold symmetry of the diffracted electron beams despite the sixfold symmetry of the surface layer. This is due to the influence of the second and deeper layers and the probing depth of the electrons. In this work, we investigated Au(111) with spin-polarized very-low-energy electron diffraction (VLEED) [1,2,3] experimentally and theoretically. We monitor the reflected specular beam at a fixed polar angle of incidence of  $\Theta=45^\circ$  while the azimuthal orientation of the crystal is varied. This puts the surface sensitivity of the VLEED scattering process to a test.

Our results show that the electron reflection and the spin-orbit-induced reflection asymmetry along  $\Gamma M$  and  $\Gamma M'$  are equivalent. The observed sixfold symmetry suggests a sensitivity to one atomic layer only. At azimuth angles deviating from the high-symmetry directions  $\Gamma M$  and  $\Gamma M'$ , however, the VLEED signal from Au(111) shows a threefold symmetry. To reveal the origin of this effect, we varied the parameters in the calculation. The results indicate a non-negligible influence of the second atomic layer in the VLEED scattering process.

- [1] Burgbacher et al., Phys. Rev. B **87**, 195411 (2013).
- [2] Thiede et al., Phys. Rev. Applied **1**, 054003 (2014).
- [3] Angrick et al., J. Phys.: Condens. Matter **33**, 115001 (2020).

4:20pm **SS+AS+TF-MoA-9 Unravelling the Chemisorption Mechanism of Epoxy-Amine Coatings on Zr-Based Converted Galvanized Steel by Combined Static XPS/ToF-SIMS Approach**, *Vanina Cristaudo, K. Baert, P. Laha*, Research Group Electrochemical and Surface Engineering (SURF), Vrije Universiteit Brussel, Belgium; *M. Lim, L. Steely, D. Clingerman, E. Brown-Tseng*, Coatings Innovation Center, PPG; *H. Terryn, T. Hauffman*, Research Group Electrochemical and Surface Engineering (SURF), Vrije Universiteit Brussel, Belgium

In the automotive industry, the corrosion protection of hot-dip galvanized (HDG) steel is of primary importance. To this purpose, a Zr oxide-based conversion pre-treatment of the metal surface for passivation and improved adhesion [1], in combination with the application of a polymeric primer coating is often performed. Usually, organic and inorganic additives are used in the acidic conversion bath for a large variety of purposes. For instance, Cu(II) salts are employed to accelerate the deposition of zirconium oxide [1]. Recently, the heterogeneity and multi-metal nature of the resulting surface has been demonstrated in our laboratory [2]. Now, it is of pivotal importance to study the efficiency and durability of such hybrid (hydr)oxide-polymer systems, which depend on the formation and degradation of the chemical bonds at the buried interface.

This work aims at the elucidation of the interfacial interactions established between an epoxy-amine coating and HDG steel [3]. The influences of the Zr-based conversion treatment of the substrate and the use of Cu(II) additive on interfacial bonding will be studied [3]. To this purpose, an amine-functionalized molecule – diethylenetriamine (DETA), a common curing agent – will be adsorbed and used as an indicator of the acid-base properties of the metal oxide surface. The complex multi-metal oxide surface of the Cu-modified Zr-based converted substrate will be decomposed in derivative (simpler) systems, such as pure Zn, Zr, and Cu. The resulting DETA-adsorbed model and multi-metal surfaces will be investigated by X-ray photo-electron spectroscopy (XPS), and by examination of the N 1s peak, the interfacial bond densities will be determined. Time-of-flight secondary ion mass spectrometry (ToF-SIMS) will be performed to discriminate between the different metal oxide contributions present on the substrate surface. Preferential adsorption of the DETA molecule on the zinc atoms is found on converted substrates. SIMS also points out the interfacial bonding with the Cu cationic sites when the copper additive is used, highlighting the extreme usefulness of this analytical technique in the assessment of interfacial interactions of “diluted” adsorption sites.

## References

- [1] I. Milošev, *et al.* Conversion coatings based on zirconium and/or titanium. *J. Electrochem. Soc.* (2018), 165, p.C127.
- [2] V. Cristaudo, *et al.* A combined XPS/ToF-SIMS approach for the 3D compositional characterization of Zr-based conversion of galvanized steel. *Appl. Surf. Sci.* (2021), p.150166.
- [3] V. Cristaudo, *et al.* Unravelling the chemisorption mechanism of epoxy-amine coatings on Zr-based converted galvanized steel by combined static XPS/ToF-SIMS approach. *Appl. Surf. Sci.* (2022), 599, p.153798.

4:40pm **SS+AS+TF-MoA-10 Fermi Surface Emergence and Valence Band Maximum Formation During  $\text{Li}_x\text{CoO}_2$  Insulator-to-Metal Transition**, *Elena Salagre*, Dpto Física Materia Condensada, Universidad Autónoma de Madrid, Spain; *P. Segovia*, Dpto Física Materia Condensada, Universidad Autónoma de Madrid. IFIMAC (Condensed Matter Physics Center), Spain; *M. González-Barrío*, Dpto Física de Materiales, Universidad Complutense de Madrid, Spain; *J. Pearson, I. Takeuchi*, Materials Science and Engineering, Univ. Of Maryland; *E. Fuller, A. Talin*, Sandia National Laboratories; *M. Jugovac, P. Moras*, Istituto di Struttura della Materia, Consiglio Nazionale delle Ricerche, Italy; *A. Mascaraque*, Dto. Física de Materiales, Univ. Complutense de Madrid, Spain; *E. Garcia Michel*, Dto. Física Materia Condensada, Univ. Autonoma de Madrid, IFIMAC (Condensed Matter Physics Center), Spain

Despite the great interest in  $\text{LiCoO}_2$  (LCO) and related materials for their applications in batteries, catalysis and resistive memory devices, uncertainties regarding the valence band structure, charge compensation and the nature of the insulator-to-metal transition (IMT) remain controversial [1][2]. In addition, the use of chemical and electrochemical methods on heterogeneous materials, including cathode binders and solid electrolyte interfaces, pushes research further away from a fundamental understanding of the processes involved in ion deintercalation.

We have developed a surface science-based approach to vary the Li content, based on  $\text{Ne}^+$  sputtering and performed entirely in situ under

ultra-high vacuum (UHV) conditions on epitaxial LCO thin films, without interactions between the material and any electrolyte.

This has allowed us to obtain high-resolution angle-resolved photoemission (ARPES) data of the valence band structure in LCO for a wide range of Li molar fractions, directly observing the IMT at  $x=0.95$  and the regions of phase coexistence and phase dominance. X-ray photoelectron spectroscopy (XPS) and X-ray absorption spectroscopy (XAS) were used to characterize the material during Li deintercalation and to investigate the mechanisms of charge compensation in the absence of electrolyte. Li removal is accompanied by the formation of  $\text{Co}^{4+}$  from the initial  $\text{Co}^{3+}$  in the LCO structure. Oxygen holes were also observed, related to the hybridization of Co 3d and O 2p orbitals. The valence band was interpreted using reported theoretical calculations [3] and limited previous experimental work [4]. We identify the Co 3d  $t_{2g}$  energy levels as those involved in the IMT and locate the valence band maxima (VBM) with a clear 3-fold symmetry and band renormalization, suggesting a Mott character of the transition.

- [1] C. A. Marianetti, G. Kotliar, y G. Ceder, «A first-order Mott transition in  $\text{Li}_x\text{CoO}_2$ », *Nat. Mater.*, vol. 3, n.º 9, pp. 627-631, 2004
- [2] A. Milewska *et al.*, «The nature of the nonmetal-metal transition in  $\text{Li}_x\text{CoO}_2$  oxide», *en Solid State Ionics*, Elsevier, 2014, pp. 110-118
- [3] S. K. Radha, W. R. L. Lambrecht, B. Cunningham, M. Grüning, D. Pashov, y M. Van Schilfgaarde, «Optical response and band structure of  $\text{LiCoO}_2$  including electron-hole interaction effects», *Phys. Rev. B*, vol. 104, n.º 11, p. 115120, 2021
- [4] Y. Okamoto *et al.*, «Electronic structure and polar catastrophe at the surface of  $\text{Li}_x\text{CoO}_2$  studied by angle-resolved photoemission spectroscopy», *Phys. Rev. B*, vol. 96, n.º 12, p. 125147, 2017

5:00pm **SS+AS+TF-MoA-11 Nanoscale Hydrogen Detection Using Time-of-Flight Secondary Ion Mass Spectrometry**, *B. Paudel, J. Dhas, M. Choi, Y. Du, Zihua Zhu*, Pacific Northwest National Laboratory

Hydrogen in materials attracts tremendous interest as its incorporation leads to significant alterations in structure, composition, and chemistry, which in turn impacts functional properties. Additionally, it has been integral to nuclear fusion reactors and is regarded as the major source of clean energy. However, nanoscale manipulation and characterization of hydrogen in materials are challenging as only a selected few analytical technique can readily detect hydrogen, among which time-of-flight secondary ion mass spectrometry (ToF-SIMS) is a unique and powerful technique due to its excellent detection limit along with decent spatial and depth resolutions. In our lab, ToF-SIMS has been used for hydrogen detection for more than 15 years, and it became more and more important in the last several years. In this presentation, we will discuss, using selected examples, how the detection and quantification of hydrogen in materials by ToF-SIMS has been utilized to reveal the hydrogenation/protonation-induced novel functional states in different classes of materials along with some tricks on sample preparation, optimized experimental conditions to achieve reasonable detection limits of hydrogen, and future prospects. We emphasize the unique capabilities of ToF-SIMS which can potentially unlock new functional states and answer some outstanding scientific questions in materials science.

## Chemical Analysis and Imaging of Interfaces Focus Topic Room A105 - Session CA+AS+LS+LX+MN+SE+SS-TuM

### Novel Developments and Applications of Interfacial Analysis

**Moderators:** **Andrei Kolmakov**, National Institute of Standards and Technology (NIST); **Slavomir Nemsak**, Advanced Light Source, Lawrence Berkeley National Laboratory

8:00am **CA+AS+LS+LX+MN+SE+SS-TuM-1 Hypervelocity Nanoprojectile Impacts on Graphene, Graphene-Solid/Liquid Interphases: From Mechanisms of Interaction/Ejection to Practical Applications, Dmitriy Verkhoturov**, Texas A&M University; *S. Lee*, Mayo Clinic; *M. Eller*, California State University Northridge; *M. Goluński, S. Hrabar*, Jagiellonian University, Poland; *S. Verkhoturov*, Texas A&M University; *Z. Postawa*, Jagiellonian University, Poland; *A. Kolmakov*, National Institute for Science and Technology (NIST); *A. Revzin*, Mayo Clinic; *E. Schweikert*, Texas A&M University

**INVITED**

Presented here are the experiment and theory on processes accompanying the impacts of  $C_{60}$  and  $Au_{400}$  projectiles ( $\sim 1$  keV/atom) on graphene/matter interphases. A variety of targets were used: a) free standing graphene, b) molecules and extracellular vesicles (EVs) deposited on free standing graphene, c) interphases graphene-solids/liquids, d) EVs deposited on functionalized monocrystals.

Two custom-built Cluster ToF secondary ion mass spectrometry (SIMS) devices with similar parameters were used. The experiments were run in the event-by-event bombardment/detection mode where the regime of bombardment is super-static<sup>1</sup>. The analyzed surfaces were bombarded at the rate of  $\sim 1000$  impacts/sec with  $1-6 \times 10^6$  impacts collected on a surface area of 50-500  $\mu m$  in diameter. This regime allows acquisition of individual mass spectra for each impact, thus allowing the comparison of experimental data with MD simulations at the level of single projectile impacts. The method allows detection of ejecta in reflection (3D case) and transmission (2D case) directions.

The mechanisms of ejection from 2D and 3D materials (including graphene-solid/liquid interphase) are different. For example, in the case of  $C_{60}$  impacts on a molecular layer deposited on graphene (2D case) the mechanism of ejection is described with the "trampoline" model<sup>2</sup>. For the 3D case of graphene-solid/liquid interphase, graphene suppresses the ejection of molecules. The compression of matter in the excitation volume around the impact is not sufficient to destroy the graphene<sup>3</sup>.

Our method allows to test individual nano-objects. A biological example is EVs. There were anchored on functionalized Si and graphene substrates, with the EVs labeled with antibodies carrying lanthanide tags (Ab@Ln) for normal hepatic and liver cancer markers. Up to four Ab@Ln tags could be detected simultaneously, enabling analysis of population heterogeneity with single EV resolution and to distinguish between normal and cancer EVs based on surface marker expression. Using co-localization of cancer biomarkers, it is possible to find small subpopulation of EVs originating from cancerous cells potentially allowing for early cancer detection. The sensitivity of the method can be increased several folds via transmission configuration where ejecta are emitted and detected in the forward direction. In this case nano-objects, such as EVs, are anchored on graphene oxide, a 2D material.

<sup>1</sup>S.V. Verkhoturov et al. J. Chem. Phys. 150 (2019)

<sup>2</sup>R.D. Rickman et al. Phys. Rev. Lett. 92, 047601 (2004)

<sup>3</sup>D.S. Verkhoturov et al. Biointerphases 11, 02A324 (2016)

Acknowledgements: NSF Grant CHE-1308312, NIH Grant R01 GM123757-01,

Polish National Science Center 2019/33/B/ST4/01778, PLGrid Infrastructure Grant

8:40am **CA+AS+LS+LX+MN+SE+SS-TuM-3 Applying *in Situ* Bias During TOF-SIMS Analysis to Investigate Ion Migration in Perovskite Devices, Steven Harvey**, National Renewable Energy Laboratory; *I. Gould*, University of Colorado, Boulder; *D. Morales, M. McGehee*, University of Colorado Boulder; *A. Palmstrom*, National Renewable Energy Laboratory

Metal Halide Perovskite Photovoltaics have the potential to be a game-changing technology in photovoltaics, with low cost solution processing inherent to the technology and a rapid progress in device efficiency and stability. Understanding ion migration in these materials has led to

improvements in both efficiency and reliability, and further understanding of these phenomena is of great importance.

Time of flight secondary ion mass spectrometry is well suited to provide unique insight for this class of materials, as it can reveal the distribution of both the organic and inorganic components of a device stack (both through the depth as well as laterally with 2-D and 3-D imaging). We will briefly cover our past work on technique development for this class of materials, before presenting new work where an *in situ* electrical bias was placed on a perovskite device while under investigation with TOF-SIMS. This was completed with simple commercial off the shelf components in an ION-TOF TOF-SIMS V instrument and could be easily implemented on other instruments. A device stack of glass / ITO / Me-4PACz / DMA0.1FA0.6Cs0.3Pb(I0.8Br0.2)3 / LiF (1 nm) / C60 (30 nm) / SnOx (15 nm)/Au (20 nm) was used for this study. An electrical bias was applied between the top gold contact and the bottom ITO contact during TOF-SIMS measurements. By applying a +0.75V and -0.75V forward and reverse bias to the device, a driving force for negatively charged halide ions is created to migrate towards the back or front of the device, respectively. The *in-situ* data shows the halide ion migration towards the back ITO contact after the forward bias is applied. The negative bias was then applied and the halide ions migrate back towards the front of the device and return to the original unbiased state. In both cases the formamidinium and lead traces do not show similar migration, showing only the charged species in the device are affected by the bias. The results show a framework that can be used for further study. Potential complications with the analysis of this type of data will be discussed.

9:00am **CA+AS+LS+LX+MN+SE+SS-TuM-4 Oxidation of a Single Fe Nanoparticle at the Nanoscale and Real-Time by Operando Atom Probe, Sten V. Lambeets**, Pacific Northwest National Laboratory; *N. Cardwell, I. Onyango*, Washington State University; *T. Visart de Bocarmé*, Université libre de Bruxelles, Belgium; *J. McEwen*, Washington State University; *D. Perea*, Pacific Northwest National Laboratory

Physics governing surface chemical reactions and interfaces involved in heterogeneous catalysts fundamentally depends on the synergistic interactions between reactive gases and specific surface structures. Surface science techniques are continuously evolving to help bridge knowledge gaps between fundamental research and real-world applications. In the past decade, an increasing number of analytical techniques successfully achieved their evolution towards an *in situ* and operando version of themselves, and recently such approaches are being developed for atom probe microscopy (APM) techniques. In this work, we will present the recent advances in the conversion of Atom Probe Tomography (APT) to study surface dynamics of  $O_2/Fe$  using two different APM techniques and modifications: Field Ion Microscopy (FIM), and Operando Atom Probe (OAP).

APM techniques are capable of imaging the apex of sharp needles with nanometric lateral resolution, which can be seen as model nanoparticles. FIM is used to image such needles with atomic resolution and to identify the crystal orientation along with the local surface reaction dynamics during oxygen interaction with Fe. The resulting FIM image corresponds to a stereographical projection of the apex and allows the identification of the crystal orientations with atomic resolution. Regular APT, from which the OAP derives, relies on the thermally assisted field evaporation of positively charged ions from a needle shaped specimen. In regular use, the APT is performed in an Ultra High Vacuum ( $<10^{-11}$  mbar) while the sample is cooled at 50K. The OAP modification consists of performing the atom probe analysis in the presence of reactive gas at 300 K.

Once the FIM characterization is complete the sample is maintained at 300K before starting APT analysis and introducing  $1.1 \times 10^{-7}$  mbar of pure  $O_2$ . As soon as the  $O_2$  is introduced, we can measure the surface formation of Fe oxides by monitoring the local concentration of  $Fe_2O^{+}$  ion species extracted from the surface over time. We can track the local concentration over the different surface regions in real time. We observe the progressive surface oxidation starting from open facets structures, such as Fe{222} and Fe{112}, towards the central Fe(011) and the Fe{024} which show significantly higher resistance toward oxidation. The combination of the different concentrations allows us to reconstruct the full movie of the surface oxidation in real-time. However, since the measurements are

# Tuesday Morning, November 7, 2023

performed in the presence of very strong electric fields ( $>10$  V/nm), it is necessary to discuss the potential influences of it on the system as well.

## 9:20am CA+AS+LS+LX+MN+SE+SS-TuM-5 Reporting Interfaces: Unconventional Excitation of Interfaces Enables Exquisite Gas Sensing Toward Our Sustainable Future, Radislav Potyrailo, GE Research INVITED

As our society is developing solutions for more sustainable types of energy, the need for reliable, yet affordable tools for monitoring of emissions of greenhouse and other gases in urban and industrial environments is a substantial undertaking for two main reasons. First, to achieve a desired accuracy, existing gas monitoring solutions in complex backgrounds utilize traditional analytical instruments. While their mathematical design principles provide needed independent response outputs, their hardware design principles do not allow cost-effective ubiquitous implementations. Second, all gas sensors based on interface-driven interactions between gases of interest and sensing materials are single-output devices. By their original design principles from early last century, these sensors operate well only when levels of interfering gases are low. Once levels of interfering gases increase, existing sensors lose their accuracy because of competing interactions between the sensor interface and numerous interfering gases versus a gas of interest.

In this talk, we will present gas sensors that we built following mathematics of traditional analytical instruments but with our own different types of independent variables for detection of multiple gases with enhanced accuracy and stability. These sensors are multivariable gas sensors where independent response outputs are provided by our unconventional methodologies of excitation of interfaces between a sensing material and different ambient gases. We will show that our approach results in a reliable differentiation of one or more analyte gases in complex backgrounds of interfering gases with an individual multivariable gas sensor. This exquisite (i.e., accurate and reliable) gas sensing provides an affordable technical solution for monitoring of emissions of greenhouse and other gases in urban and industrial environments. Such technical solution is mathematically not feasible using conventional single-output sensor designs. We will also show that such multivariable gas sensors have the ability for self-correction for sensor drift. Our approach for the multi-gas detection and drift self-correction should allow implementations of gas sensors in diverse applications that cannot afford weekly, monthly, or quarterly periodic maintenance, typical of traditional analytical instruments.

## 11:00am CA+AS+LS+LX+MN+SE+SS-TuM-10 A "Simple" Approach to Combine Electrochemistry and Operando Near Ambient Pressure XPS Studies, F. Mirabella, Paul Dietrich, A. Thissen, SPECS Surface Nano Analysis GmbH, Germany INVITED

Electrochemical water splitting is an environmentally friendly technology to store renewable energy in the form of chemical fuels. Among the Earth-abundant, first-row transition metal-based catalysts, Ni and Fe oxides have shown promising performances as effective and low-cost catalysts of the oxygen evolution reaction (OER) in alkaline media. Notably, their structure evolves under oxygen evolution operating conditions with respect to the as-prepared catalysts but these changes and consequently the active sites have not been identified yet due to the difficulties associated with surface analysis measurement under working conditions (*operando*).

In this presentation, we will demonstrate the enormous potential of laboratory NAP-XPS for investigations of solid-liquid interfaces in electrochemical systems at elevated pressures ( $\leq 25$  mbar), also illustrating the ease of use of this specific setup. We will show a versatile three-electrodes electrochemical setup that allows for operando studies of solid-electrolyte interfaces, i.e., of nickel oxide foils as cathode for OER in alkaline environment as a simple laboratory NAP XPS experiment.

## 11:40am CA+AS+LS+LX+MN+SE+SS-TuM-12 Recent Developments in Probing Buried Interfaces Using Standing-Wave Photoelectron Spectroscopy, Slavomir Nemsak, Lawrence Berkeley Lab

Standing-wave photoelectron spectroscopy of multi-layer structures proved to be a very powerful technique for probing solid/solid, but also solid/liquid and solid/gas interfaces. Its superior depth selectivity and non-destructive nature were crucial to answer key questions in problems spread over several scientific fields, such as emergent phenomena at complex oxide interfaces [1], artificial multiferroics [2], adsorption mechanisms in liquids [3], corrosion [4], and electrocatalysis [5]. These achievements were only possible thanks to innovative approaches both in experiments and

analyses, including development of X-ray optical simulations package [6] and its coupling with the black-box optimizer [7]. In this talk I will introduce novel tools and approaches for standing-wave experiments and I will highlight some of the recent applications [8,9,10].

- [1] S. Nemsak et al., *Physical Review B* **93** (24), 245103 (2016).
- [2] H. P. Martins et al., *arXiv preprint arXiv:2012.07993*.
- [3] S. Nemsak et al., *Nature Communications* **5**, 5441 (2014).
- [4] O. Karslioglu et al., *Faraday Discussions* **180**, 35 (2015).
- [5] C. Baeumer et al., *Nature Materials* **20**, 674 (2021).
- [6] S.-H. Yang et al., *Journal of Applied Physics* **113**, 073513 (2013).
- [7] O. Karslioglu et al., *Journal of Electron Spectroscopy and Related Phenomena* **230**, 10 (2019).
- [8] M. Scardamaglia, et al., *Journal of Electron Spectroscopy and Related Phenomena* **262**, 147281 (2023).
- [9] G. Conti et al., *Journal of Micro/Nanopatterning, Materials, and Metrology* **20**, 034603 (2021).
- [10] H.P. Martins et al., *Journal of Physics D: Applied Physics* **56**, 464002 (2021).

## 12:00pm CA+AS+LS+LX+MN+SE+SS-TuM-13 The Influence of Surface Structure and Electrostatics on Measuring Unoccupied Electronic States via Low Energy Inverse Photoemission Spectroscopy (LEIPS), James Johns, Physical Electronics USA

A material's energetic distribution of electronic states near the Fermi level is a key physical property for determining how it behaves in electronic, chemical, and optical applications. Photoemission has long been the gold standard for measuring the occupied electronic states below the Fermi level and is one of the most common surface science techniques worldwide. Inverse photoemission (IPES), the related process whereby an electron is absorbed at the surface and a photon is emitted, is similarly a very powerful tool for measuring the unoccupied electronic states. Unfortunately, the intrinsically lower rate for IPES and technical hurdles related to relevant photodetectors has historically necessitated the use of electron sources with sufficient energy to damage all but the most chemically robust surfaces.

The availability of narrow bandpass optical filters at UV photon energies between 3.5 and 6 eV over the past decade have enabled the development and commercialization of Low Energy Inverse Photoemission Spectroscopy (LEIPS)<sup>1,2</sup>. Efficient detection of low energy UV photons (lower than traditional IPES at 9-10 eV) enables the use of low energy electrons (below 5 eV) which avoid damaging sensitive materials including organics. This key innovation has revitalized interest in IPES because the technique can now be applied to molecular materials and interfaces relevant to wide range of applications e.g. batteries, photovoltaics, organic semiconductors and OLEDs, chemical sensors. Furthermore, optical UV filters also improve the energy resolution, further enhancing the appeal of LEIPS over traditional IPES.

Like any surface science technique, the quality of LEIPS data depends on both the instrumentation and sample preparation. Here, I will discuss the material requirements and limitations for successful LEIPS measurements, several of which differ from more common techniques such as XPS, SPM, or electron microscopy. I will also present LEIPS data from taken at the interface between two metals and explain those results using calculated trajectories of the electron beam. Finally, I will illustrate a key difference between LEIPS, which probes the true unoccupied electronic density of states, and optical methods, such as optical spectroscopy or EELS which measure the joint density of states, by presenting LEIPS spectra of an excitonic 2D material.

<sup>1</sup> Yoshida, H; "Near-ultraviolet inverse photoemission spectroscopy using ultra-low energy electrons" *Chem. Phys. Lett.* **539-540**, 180-185, (2012)

<sup>2</sup> Lida, S.; Terashima, M; Mamiya, K; Chang, H. Y.; Sasaki, S; Ono, A; Kimoto, T; Miyayama, T; "Characterization of cathode-electrolyte interface in all-solid-state batteries using TOF-SIMS, XPS, and UPS/LEIPS" *J. Vac. Sci. & Tech. B*, **39**, 044001, (2021)

## Nanoscale Science and Technology Division Room B113 - Session NS+2D+EM+MN+SS-TuM

### Scanning Probe Microscopy

**Moderators:** **Aubrey Hanbicki**, Laboratory for Physical Sciences, **Fernando Castro**, National Physical Laboratory, U.K.

8:00am **NS+2D+EM+MN+SS-TuM-1 AVS Medard W. Welch Award Talk: Microscopy is All You Need: The Rise of Autonomous Science, Sergei Kalinin<sup>1</sup>**, University of Tennessee Knoxville **INVITED**

Making microscopes automated and autonomous is a North Star goal for areas ranging from physics and chemistry to biology and materials science – with the dream applications of discovering structure-property relationships, exploring physics of nanoscale systems, and building matter on nanometer and atomic scales. Over the last several years, increasing attention has been attracted to the use of AI interacting with physical system as a part of active learning – including materials discovery and optimization, chemical synthesis, and physical measurements. For these active learning problems, microscopy arguably represents an ideal model application combining aspects of materials discovery via observation and spectroscopy, physical learning with relatively shallow priors and small number of exogenous variables, and synthesis via controlled interventions. I introduce the concept of the reward-driven experimental workflow planning and discuss how these workflows can be implemented via domain-specific hyper languages. The applications of classical deep learning methods in streaming image analysis are strongly affected by the out of distribution drift effects, and the approaches to minimize though are discussed. The real-time image analysis allows spectroscopic experiments at the predefined features of interest and atomic manipulation and modification with preset policies. I further illustrate ML methods for autonomous discovery, where the microstructural elements maximizing physical response of interest are discovered. Complementarily, I illustrate the development of the autonomous physical discovery in microscopy via the combination of the structured Gaussian process and reinforcement learning, the approach we refer to as hypothesis learning. Here, this approach is used to learn the domain growth laws on a fully autonomous microscope. The future potential of Bayesian active learning for autonomous microscopes is discussed. These concepts and methods can be extended from microscopy to other areas of automated experiment.

8:40am **NS+2D+EM+MN+SS-TuM-3 Dielectric Constant Measurement Sensitivity in Electrostatic Force and Force Gradient Microscopy-Based Modes, Gheorghe Stan**, National Institute of Standards and Technology (NIST); **C. Ciobanu**, Colorado School of Mines

Understanding of the nanoscale electrostatic interaction between a conductive atomic force microscopy (AFM) probe and a dielectric film is central to the operation of various nanoscale dielectric microscopies and determination of dielectric properties of the film. There is no simple analytical description of the electrostatic interaction generated in the confined probe-sample geometry of neither the static nor dynamic AFM modes used for dielectric measurements. An accurate description of the involved physics is obtained only by means of a finite element analysis modeling of the system. However, the alternative of using numerical analysis is not very popular being slower and requiring relatively high computation resources. In this work we revised the contributions from different parts of the AFM probe to the probe-sample capacitance by both analytical and numerical methods. We tried to reconcile the two approaches and observed the differences as a function of geometry and material parameters. Under various noise levels, the efficiency of an analytical model was tested against finite element analysis that captures in detail the electrostatic interaction in AFM-based dielectric measurements. The investigation was performed in both spectroscopic force-distance curves and constant height scans with measurements for the deflection and frequency of the AFM probe. The obtained measurement sensitivities are relevant in selecting the optimal scanning mode and its operational parameters for given film thicknesses and dielectric constants but are also showing the critical role of the numerical analysis to the correct interpretation of the measurements.

9:00am **NS+2D+EM+MN+SS-TuM-4 Measuring and Understanding the Nanomechanical Properties of Halide Perovskites and Their Correlation to Structure, I. Rosenhek-Goldian**, Dept. of Chemical Research Support, Weizmann Inst. of Science, Israel; **I. Buchine, N. Prathibha Jasti**, Bar-Ilan Inst. for Adv. Mater. and Nanotechnol & Dept. of Chem. Bar-Ilan Univ., Israel; **D. Ceratti**, Dept. of Mol. Chem. & Materials Science, Weizmann Inst. of Science, Israel & CNRS, UMR 9006, IPVF, Institut Photovoltaïque d'Île-de-France; **S. Kumar**, Bar-Ilan Inst. for Adv. Mater. and Nanotechnol & Dept. of Chem. Bar-Ilan Univ. Ramat Gan Israel. & Dept. of Mol. Chem. & Materials Science, Weizmann Inst. of Science, Israel; **D. Cahen**, Bar-Ilan Inst. for Adv. Mater. and Nanotechnol & Dept. of Chem. Bar-Ilan Univ. & Dept. of Mol. Chem. & Materials Science, Weizmann Inst. of Science, Israel; **Sidney R. Cohen**, Dept. of Chemical Research Support, Weizmann Inst. of Science., Israel

Halide perovskites, HaP, and especially Pb-based ones exhibit a plethora of remarkable properties. Of these, their photovoltaic properties are the most widely studied due to the proven potential these materials hold for significant technological impact. In addition to photoresponse, this material class is characterized by interesting physical properties, of which mechanical properties enjoy special attention, not only because of potential use in flexible devices, but also from a fundamental science point of view. The mechanical response can shed light on the materials' behavior including dynamic processes and strain-related effects on optoelectronic behavior.

In the context of these studies, particular emphasis has been placed on environmental factors which can alter, especially degrade, material functionality and device performance. Exposure to humidity, light, and oxygen rank prominently amongst these factors.

In this study we measure the humidity influence on the mechanical properties, i.e., elastic modulus (E) and hardness (H), for two series of lead halide perovskite single crystals, varying either by cation or by anion type. Our conclusions are based on comparing results obtained from several different nano-indentation techniques, which separate surface modulus from that of the bulk, and probe different manifestations of the hardness. These studies reveal the different crystalline parameters governing influence of humidity on the mechanics at the surface and in the bulk.

An atypical inverse correlation between E and H was measured (as seen in the supplementary figure a). Furthermore, humidity influenced these two properties in opposite fashion – humidity exposure led to lower H, but to higher E (supplementary figure b). This trend is opposite to that found in most materials where hydration lowers both E and H. We suggest a link between dynamic disorder, self-healing, and the intriguing relation between E and H.

9:20am **NS+2D+EM+MN+SS-TuM-5 3D Nanoprinting of Advanced AFM Nano-Probes, Harald Plank, M. Brugger-Hatzl, R. Winkler, L. Seewald**, Graz University of Technology, Austria

The demand for correlative microscopy is still increasing, as it enables a superior ensemble of information by using various methods to combine individual strengths. The highest level of that approach are hybrid microscopes, which enable individual characterization at the very same spot in a consecutive or even parallel way. With that, however, comes the demand of a conflict-free integration of different microscopes, which require a radical redesign of the instrumentation. A major step in that direction is a recently introduced dual system called FUSIONScope, which is a deeply integrated scanning electron microscopy (SEM) and atomic force microscopy (AFM) solution. While the former enables high-resolution guidance towards the region of interest, the latter complements SEM capabilities by true quantitative 3D surface information, which together exploit their full potential by the possibility to precisely land the AFM tip on highly exposed regions. Even more importantly, advanced AFM modes such as conductive AFM (CAFM), magnetic force microscopy (MFM), electrostatic / Kelvin force microscopy (EFM/KFM), scanning thermal microscopy (SthM) or mechanical mapping, provide functional information beyond SEM capabilities. For that, special nano-probes are required, which typically achieve their intended functionality by additional thin film coatings, which contains two main disadvantages. First, they increase the apex radii and limit the lateral resolution, which is in conflict with the still decreasing feature sizes. Secondly, coatings are prone to delamination during operation, which affects resolution, lateral correlation and reliability. Therefore, to exploit the full potential of advanced AFM modes, it is of great interest to develop new approaches for the fabrication of functional nano-probes. Following that motivation, we joined forces with industry and apply the additive direct-write technology focused electron beam induced

<sup>1</sup> Medard W. Welch Award Winner  
Tuesday Morning, November 7, 2023

# Tuesday Morning, November 7, 2023

deposition (FEBID) for the development of novel 3D nano-probe concepts with industrial relevance. In this contribution, we briefly discuss the 3D nano-printing process and then go through a variety of advanced, FEBID-based tip concepts for CAFM, EFM, MFM and SThM. The joint element for all probes is the coating-free character, which eliminates the aforementioned risks during operation. Additionally, the apex regions are routinely in the sub-10 nm regime, which allows for high-resolution imaging. Aside of comparisons to traditionally used nano-probes, which reveal the superior performance of FEBID-based nano-tips, we discuss on currently ongoing research towards multi-functional AFM tips, based on FEBIDs flexibility.

11:00am **NS+2D+EM+MN+SS-TuM-10 Chemical, Mechanical, and Morphological Evolution of Nanostructures on the Surfaces of Asphalt Binders**, *L. Lyu, J. Pei*, Chang'an University, China; *E. Fini*, Arizona State University; *L. Poulidakos*, EMPA (Swiss Federal Laboratories for Materials Science and Technology), Switzerland; *Nancy Burnham*, Worcester Polytechnic Institute

Bitumen (asphalt binder) holds roads together. It is a complex, dynamic, nanostructured material that comes from the bottom of an oil refinery stack—a non-renewable resource. It ages, and it ages more quickly under the influence of heat and light. Can additives made from waste materials increase the longevity of bitumen, and thus roads?

In this study, atomic force microscopy (topography, phase imaging, PF-QNM) and its combination with infrared spectroscopy (AFM-IR) were used to explore the chemical, mechanical, and morphological evolution of the surface of bitumen without and with additives. Aging is assumed to begin at the surface.

Samples of bitumen were made with and without introducing bio-modified rubber additives. Each sample was exposed to several thermal and UV aging protocols. Evolution of surface under aging was studied. Depending on the additive and type of aging (thermal, UV, or combined), the nanostructures changed their chemistry, mechanical properties, and size. Furthermore, the matrices and phases immediately surrounding the nanostructures evolved differently upon aging than the included nanodomains. In general, carbonyl and sulfoxide IR bands became more prevalent, the samples became stiffer and less adhesive, and the phase immediately surrounding the nanostructures became smaller. One additive made from two different waste materials was found to enhance the stability of the surfaces.

By understanding the evolution of asphalt binders and which additives promote their stability, longer lasting roads might be designed and built, thereby lowering the need for a non-renewable resource.

11:20am **NS+2D+EM+MN+SS-TuM-11 Identifying Potential Carbon Sources for Direct Carbon Material Production by AI Assisted HR-AFM**, *Percy Zahl*, Brookhaven National Laboratory; *Y. Zhang*, ExxonMobil Technology and Engineering Company; *S. Arias*, Brookhaven National Laboratory

High-resolution Atomic Force Microscopy (HR-AFM) has proven to be a valuable and uniquely advantageous tool for studying complex mixtures such as petroleum, biofuels/chemicals, and environmental or extraterrestrial samples. However, the full potential of these challenging and time-consuming experiments has not yet been fully realized. To overcome these bottlenecks and enable further research into solutions for the energy transition and environmental sustainability, automated HR-AFM in conjunction with machine learning and artificial intelligence will be crucial [1].

In this study, we focus on identifying potential carbon sources suitable for more direct carbon material production by analyzing various pitch fractions based on their solubility in toluene. Specifically, we present the first comprehensive AI-assisted study of hydrocarbon fractions derived from petroleum and coal tar pitch, using and refining our previously introduced "Automated HR-AFM" tools. We explored four classes derived from Petroleum Pitch (PP) and Coal Pitch Tar (CPT), separated into toluene soluble (TS) and toluene insoluble (TI) fractions. Our analysis revealed differences in the structural characteristics of the molecules, which we binned based on the number of aromatic rings.

(Please see also the in our supplemental document included figures 1 and 2)

Overall, our results demonstrate the potential of automated HR-AFM and AI-assisted analysis for understanding complex mixtures and identifying potential carbon sources for direct carbon material production. This work represents an important step towards more sustainable and environmentally-friendly energy solutions.

Reference:

[1] Yunlong Zhang, *Energy & Fuels* 35(18), 14422 (2021)

11:40am **NS+2D+EM+MN+SS-TuM-12 Automated Microscopy for Physics Discovery: From High-Throughput to Hypothesis Learning-Driven Experimentation**, *Yongtao Liu, R. Vasudevan, M. Ziatdinov, S. Kalinin*, Oak Ridge National Laboratory

In this work, we explore the ferroelectric polarization switching in relation to the applied pulse bias including bias voltage and time in scanning probe microscopy (SPM). We perform two types of automated and autonomous experiments. First, we conduct automated high-throughput experimentation to gain a comprehensive understanding of the relationship between pulse biases and ferroelectric domain growth. Second, we employ an autonomous experimentation driven by machine learning (ML) algorithm to optimize experimental conditions based on real-time experiment results.

SPM has proven to be a powerful tool for manipulating and visualizing ferroelectric domains at the nanoscale. Investigations of ferroelectric domain size and stability can advance our knowledge of ferroelectrics application in memory devices, such as operating time, retention time, and bit size. However, conventional SPM measurements have been time-intensive and dependent on experienced researchers to perform repetitive tasks and make real-time decisions regarding measurement parameters. For example, researchers determine and manually tune the parameters for next iteration of experiment according to the previous results. Here, we perform automated and autonomous experiments in SPM to explore the mechanism of ferroelectric polarization. The first experiment is a high-throughput experiment of applying various bias pulse conditions to write ferroelectric domains followed by imaging domain structure using piezoresponse force microscopy. In this automated experiment, we systematically adapt the bias pulse parameters to gain a comprehensive understanding of their relationship with the resulting domain structures. We discovered different polarization states that show up upon different bias conditions. In the second experiment, we implement a hypothesis active learning (HypoAL) algorithm based on structured Gaussian process to control the SPM for ferroelectric domain writing. The HypoAL analyzes the relationship between the bias pulse conditions and the written domain size in real-time experiments, and determines the bias pulse parameters for the next iteration. The goal of HypoAL is to establish the best physical hypothesis for the material's behaviour within the smallest number of experiment step. The HypoAL identifies that the domain growth in a BaTiO<sub>3</sub> film is governed by kinetic control. The approaches developed here have the potential to be extended to other experiments beyond SPM in the future to accelerate the discovery of new materials and advances in physics.

## Surface Science Division

### Room D136 - Session SS+2D+AS+HC-TuM

#### Oxide and Chalcogenide Surfaces and Interfaces

**Moderators:** *Rachael Farber*, University of Kansas, *Gareth Parkinson*, TU Wien

8:00am **SS+2D+AS+HC-TuM-1 ViPerLEED: LEED- $I(V)$  Made Easy**, *Alexander Michael Imre*<sup>1</sup>, TU Wien, Austria; *F. Kraushofer*, TU Munich, Germany; *T. Kijblinger, L. Hammer*, Friedrich-Alexander-University Erlangen-Nürnberg (FAU), Germany; *M. Schmid, U. Diebold, M. Riva*, TU Wien, Austria

Most surface science laboratories are equipped with a low-energy electron diffraction (LEED) setup. LEED patterns provide quick, qualitative insight into surface structure and ordering. However, the diffracted electron beams contain a large amount of additional structural information which is often ignored. By studying the diffraction intensities as a function of incident electron energy [LEED- $I(V)$ ], it is possible to quantitatively compare experimentally observed surfaces with structural models.

Despite the clear need for such a direct experiment-to-theory comparison, LEED- $I(V)$  is only routinely used by few specialized groups. A main obstacle for widespread adoption is that existing solutions for LEED- $I(V)$  analysis and simulation are time-consuming and hard to use for scientists who are not already experts in the field.

To resolve this issue, we have developed the Vienna Package for Erlangen LEED (ViPerLEED) – a package of three independent but complementary

<sup>1</sup> SSD Morton S. Traum Award Finalist



# Tuesday Morning, November 7, 2023

tools for easy LEED- $I(V)$  acquisition and analysis. All parts of ViPERLEED will be released as open source at the time of publishing:

1. **Electronics:** We provide schematics and control software for electronics, which allows users to easily and cheaply upgrade most existing LEED setups for acquiring high-quality LEED- $I(V)$  data. These ViPERLEED electronics are based on an Arduino microcontroller and can be home-built from off-the-shelf components. The associated control software synchronizes with the camera and automates the experiment.
2. **Spot-tracker:** ViPERLEED provides a plugin for the public-domain image processing program ImageJ, for spot tracking and extraction of LEED- $I(V)$  spectra from series of raw diffraction images. The automatically extracted  $I(V)$  curves can be used for further analysis or as a fingerprint of the surface surface. The plugin package also provides user-friendly options for examination, selection and smoothing of the  $I(V)$  data.
3. **Simulation software:** For structure analysis, we introduce a Python package for calculation of LEED- $I(V)$  spectra and structure optimization. This software is based on the established TensErLEED package and extends its functionality while still making it easy for new users to get started with the technique. It uses standard file formats for the surface structure, provides automated symmetry detection, and requires just a handful of parameters for running a structure determination.

8:20am **SS+2D+AS+HC-TuM-2 Quasicrystal-like Ordering of the  $\text{La}_{0.8}\text{Sr}_{0.2}\text{MnO}_3(001)$  Surface**, Erik Rheinfrank, G. Franceschi, L. Lezuo, M. Schmid, U. Diebold, M. Riva, TU Wien, Austria

Lanthanum-strontium manganite ( $\text{La}_{0.8}\text{Sr}_{0.2}\text{MnO}_3$ , LSMO) is a perovskite oxide used as a cathode material in solid oxide fuel cells, which convert chemical energy to electrical energy. To gain deeper insights into the reaction mechanisms, it is important to understand the structure of the surface at the atomic scale. To this end, we grow atomically flat single-crystalline LSMO thin films on Nb-doped  $\text{SrTiO}_3$  (STO) substrates via pulsed laser deposition (PLD). Previously, this has been achieved for the (110) orientation.<sup>[1,2]</sup> Here, we use a similar approach on the (001) surface that is commonly used for oxide-based electronics and spintronics. The as-grown films have a  $\text{MnO}_x$  terminated surface that shows a 4-fold symmetric structure in low-energy electron diffraction (LEED), best explained by a set of four basis vectors reminiscent of quasicrystals. Scanning tunnelling microscopy (STM) and Q+ non-contact atomic force microscopy (nc-AFM) reveal an aperiodic arrangement of tiles with rotation angles of  $\pm 26.6^\circ$  and  $90 \pm 26.6^\circ$ , and a Fourier transform consistent with the LEED pattern. As for quasicrystals, the surface has a sharp diffraction pattern despite the lack of translational symmetry.

[1] Franceschi *et al.*, J. Mater. Chem. A, 2020, **8**, 22947-22961

[2] Franceschi *et al.*, Phys. Rev. Materials, 2021, **5**, L092401

8:40am **SS+2D+AS+HC-TuM-3 AVS Graduate Research Awardee Talk: The Selective Blocking of Potentially Catalytically-Active Sites on Surface-Supported Iron Oxide Catalysts**, Dairong Liu<sup>1,2</sup>, N. Jiang, University of Illinois - Chicago

The extensive research on ultrathin ferrous oxide (FeO) islands and films over the last few decades has significantly contributed to the understanding of their structural and catalytic properties. One important aspect that has been investigated is the surface properties of ultrathin FeO islands, particularly the role played by the edges of these islands in catalytic reactions, such as CO oxidation. So far, two different types of edge, Fe-terminated edge and O-terminated edge, have been identified in the well-growth FeO island. However, despite this significant progress, the local chemical properties of these two types of edges, including their metal affinity, have remained largely unexplored. Here, we used scanning tunneling microscopy (STM) to study the interaction of Pd and Pt with FeO grown on Au(111). Different Fe affinities for Pd and Pt are demonstrated by the preferential growth of Pd on the Fe-terminated edge and Pt on the O-terminated edge of FeO nanoislands, resulting in selectively blocked FeO edges. In addition to revealing the different metal affinities of FeO edges, our results provide new insights into the edge reactivity of FeO/Au(111) and suggest an approach for controlling the selectivity of FeO catalysts. By comparing the behavior of different edges in the catalysis reaction, the

catalytic activity of these edges can be studied solely, thereby sheds light into the future modification of ferrous-based catalysts.

9:00am **SS+2D+AS+HC-TuM-4 Unraveling Surface Structures of Ga-Promoted Transition Metal Catalysts in  $\text{CO}_2$  Hydrogenation**, Si Woo Lee, S. Shaikhutdinov, B. Roldan Cuenya, Fritz Haber Institute of the Max Planck Society, Germany

Gallium-containing alloys with transition metals (TM) have recently been reported to be reactive in the selective hydrogenation of  $\text{CO}_2$  for methanol synthesis. However, a full understanding of the Ga-promoted catalysts is still missing due to the lack of information about the surface structures formed under reaction conditions. In this respect, studies using surface-sensitive techniques applied to well-defined model systems can provide key information to elucidate the reaction mechanism and provide the basis for the rational design of Ga-promoted catalysts.

In this work, we employed *in-situ* Near Ambient Pressure Scanning Tunneling Microscopy (NAP-STM) and X-ray Photoelectron Spectroscopy (NAP-XPS), which make it possible to study surfaces in the reaction conditions, for monitoring the structural and chemical evolution of the Ga-covered Cu surfaces in the  $\text{CO}_2$  hydrogenation reaction. NAP-STM images recorded in the reaction mixture revealed temperature- and pressure-dependent de-alloying of the initially formed, well-ordered ( $\sqrt{3} \times \sqrt{3}$ ) $R30^\circ$ -Cu(111) surface alloy and the formation of Ga-oxide islands embedded into the Cu(111) surface, exposing  $\text{GaO}_x/\text{Cu}(111)$  interfacial sites. Notably, in our atomically-resolved STM image of Ga-oxide/Cu(111), it is clearly observed that Ga-oxide grows into an ultrathin oxide layer form with ( $4\sqrt{3} \times 4\sqrt{3}$ ) $R30^\circ$  superstructure. From NAP-XPS studies on Ga/Cu(111) in the presence of  $\text{CO}_2$  and  $\text{H}_2$ , the formation of formate was observed, and this reaction intermediate was eventually transformed into methoxy at elevated temperatures, representing the final surface-bound intermediate for methanol synthesis. In contrast to Ga-containing Cu catalyst, on the other hand, there was no reaction intermediate at high temperature on the Ga-free Cu(111) surface, demonstrating that further reactions do not occur anymore from chemisorbed  $\text{CO}_2^{\delta-}$  on Cu surface alone. Therefore, the  $\text{GaO}_x/\text{Cu}$  interface formed under reaction conditions may expose catalytically active sites never considered for this reaction before. We believe that our experimental results shed light on the complex surface structure of Ga-containing catalytic systems, which is only possible to obtain using state-of-the-art experimental techniques under reaction conditions. Only by establishing the atomic structure of the Ga-oxide layer(s) and its interface to the transition metal under working conditions can one bring insight into the reaction mechanism of this methanol synthesis catalyst.

9:20am **SS+2D+AS+HC-TuM-5 Ultrathin Metal Oxide, Nitride and Sulfide Films: Bringing the Well-Known Compounds to a Unit-Cell Thickness**, Mikołaj Lewandowski, NanoBioMedical Centre, Adam Mickiewicz University in Poznań, Poland

INVITED

Bringing the well-known materials from bulk size to a unit-cell thickness may significantly influence their structure and physicochemical properties. As an example, ultrathin (< 1-nanometer-thick) films of metal/non-metal compounds, such as metal oxides, nitrides or sulfides epitaxially grown on single-crystal supports, are characterized by unique electronic, catalytic and magnetic properties not observed for their bulk counterparts. Such films also exhibit superior structural flexibility, undergoing phase transitions upon exposure to external factors (such as reactive gases or high temperatures) [1,2]. All this makes them promising candidates for applications in various technological fields, including nanoelectronics, spintronics and heterogeneous catalysis.

Within the lecture, I will address the growth, structure and properties of ultrathin metal oxide, nitride and sulfide films, with compounds of iron as exemplary cases. The scanning tunneling microscopy and spectroscopy (STM/STS), low energy electron diffraction (LEED), X-ray photoelectron spectroscopy (XPS), low energy electron microscopy (LEEM) and density functional theory (DFT) results – obtained by my group and our collaborators – provide universal guidelines for designing ultrathin films with desired structure and properties [1–3].

[1] Y. Wang, G. Carraro, H. Dawczak-Dębicki, K. Synoradzki, L. Savio, M. Lewandowski, Applied Surface Science 528 (2020) 146032.

[2] N. Michalak, T. Ossowski, Z. Miłosz, M. J. Prieto, Y. Wang, M. Werwiński, V. Babacic, F. Genuzio, L. Vattuone, A. Kiejna, Th. Schmidt, M. Lewandowski, Advanced Materials Interfaces 9 (2022) 2200222.

<sup>1</sup> AVS Graduate Research Awardee

<sup>2</sup> SSD Morton S. Traum Award Finalist

# Tuesday Morning, November 7, 2023

[3] P. Wojciechowski, W. Andrzejewska, M.V. Dobrotvorska, Y. Wang, Z. Miłosz, T. Ossowski, M. Lewandowski, submitted (2023).

The author acknowledges financial support from the National Science Centre of Poland (through SONATA 3 2012/05/D/ST3/02855, PRELUDIUM 11 2016/21/N/ST4/00302 and M-ERA.NET 2 2020/02/Y/ST5/00086 projects), as well as the Foundation for Polish Science (First TEAM/2016-2/14 (POIR.04.04.00-00-28CE/16-00) project co-financed by the European Union under the European Regional Development Fund).

**11:00am SS+2D+AS+HC-TuM-10 Optimized Infrared Reflection Absorption Spectroscopy for Metal Oxides: Overcoming Challenges of Low Reflectivity and Sub-Monolayer Coverage, Jiri Pavelec, D. Rath, M. Schmid, U. Diebold, G. Parkinson, Vienna University of Technology, Austria**

Infrared reflection absorption spectroscopy (IRAS) is a wide-spread technique in heterogeneous catalysis, and it is an ideal tool for the comparison of real and model catalysts [1]. Most surface science groups perform IRAS studies either directly on metal single crystals, or on (ultra-)thin metal oxide films grown on such samples [2]. Achieving high-quality data from metal-oxide single crystal surfaces is difficult because their low reflectivity necessitates averaging many individual measurements with long acquisition times [3]. The goal of this work was to develop an IRAS setup for studying the adsorption of molecules on model "single-atom" catalysts. Here, the low reflectivity of oxide support is exacerbated by the sub-monolayer coverage of adsorbates on single adatoms. In the contribution, I will present the novel IRAS system we have developed to overcome these two challenges.

The main improvements over commonly-used setups are a high numerical aperture, an optimized optical path, control of the incidence angle range, and high mechanical stability. The high numerical aperture of the optical system leads to an increase in the amount of light reflected from a small single crystal sample. This is achieved by placing both the illumination and collector mirrors inside the UHV chamber close to the sample. To minimize the loss of signal, optimization of the optical path was performed using a ray tracing program. The other limit is the small area on the sample that is covered with adsorbates: in our setup, a molecular beam delivers adsorbates with a spot diameter of 3.5 mm [4]. Infrared light is reflected only from this area.

The reflectivity and absorbance of non-metallic samples varies strongly with incidence angle, and can even change a sign, leading to cancellation. The optimum angle ranges are different for every material. As our setup has a large range of incident angles, we can use this to our advantage: Using two adjustable aperture plates, we can vary the minimum and maximum incidence angle from 49° to 85° to maximize the signal for each single crystal sample. Angle control also allows us to optimize the signal for both p-polarized and s-polarized light independently.

We successfully executed and compared D<sub>2</sub>O and CO absorbance measurements on a rutile TiO<sub>2</sub>(110) surface, and our results agree with the established literature [3]. By properly selecting the incidence angle range, we achieved a signal-to-noise ratio of ~16 for 1 ML CO adsorbed on TiO<sub>2</sub> with only 150 seconds of measurement time.

- [1] F. Zaera, Chem. Soc. Rev., 43, 2014  
[2] J. Libuda et al., J. Chem. Phys., 114, 10, 2001  
[3] N. G. Petrik et al., The Journal of Physical Chemistry C, 126 (51), 2022  
[4] J. Pavelec et al., J. Chem. Phys., 146, 2017

**11:20am SS+2D+AS+HC-TuM-11 VO Cluster-Stabilized H<sub>2</sub>O Adsorption on a TiO<sub>2</sub> (110) Surface at Room Temperature, Xiao Tong, Brookhaven National Laboratory**

We probe the adsorption of molecular H<sub>2</sub>O on a TiO<sub>2</sub> (110)-(1 × 1) surface decorated with isolated VO clusters using ultrahigh-vacuum scanning tunneling microscopy (UHV-STM) and temperature-programmed desorption (TPD). Our STM images show that preadsorbed VO clusters on the TiO<sub>2</sub> (110)-(1 × 1) surface induce the adsorption of H<sub>2</sub>O molecules at room temperature (RT). The adsorbed H<sub>2</sub>O molecules form strings of beads of H<sub>2</sub>O dimers bound to the 5-fold coordinated Ti atom (5c-Ti) rows and are anchored by VO. This RT adsorption is completely reversible and is unique to the VO-decorated TiO<sub>2</sub> surface. TPD spectra reveal two new desorption states for VO stabilized H<sub>2</sub>O at 395 and 445 K, which is in sharp contrast to the desorption of water due to recombination of hydroxyl groups at 490 K from clean TiO<sub>2</sub>(110)-(1 × 1) surfaces. Density functional theory (DFT) calculations show that the binding energy of molecular H<sub>2</sub>O to the VO clusters on the TiO<sub>2</sub> (110)-(1 × 1) surface is higher than binding to the bare surface by 0.42 eV, and the resulting H<sub>2</sub>O-VO-TiO<sub>2</sub> (110) complex provides the anchor point for adsorption of the string of beads of H<sub>2</sub>O dimers.

**11:40am SS+2D+AS+HC-TuM-12 Synthesis and Multimodal Characterization of Thin-Film Oxides, Dario Stacchiola, Brookhaven National Laboratory**

Thin films of metal oxides exhibit a variety of unique physical and chemical properties leading to broad applications in optics, microelectronics, optoelectronics, superconducting circuits, gas sensors, thermal catalysis, electrocatalysis, and solar energy harvesting. Many metal oxides can form stoichiometric and non-stoichiometric alloys and compounds with each other, commonly known as complex metal oxides. Alloy and compound formation, including growth and process conditions, offer great flexibility for manipulating the lattice, atomic scale structure motifs, and electronic structure to realize desired properties. In order to exploit this potential, knowledge about fundamental processes and atomic level structural information is required. We present here the synthesis and multimodal characterization of mixed-oxide films based on silica and titania, from single layers to complex metal oxides.

1. "Deciphering phase evolution in complex metal oxide thin films via high-throughput materials synthesis and characterization", Nanotechnology 34, 125701 (2023)
2. "Resolving the evolution of atomic layer deposited thin film growth by continuous in situ X-ray absorption spectroscopy", Chem. Mat. 33, 1740-1751 (2021)
3. "First-Principles Study of Interface Structures and Charge Rearrangement at the Aluminosilicate / Ru(0001) Heterojunction" J. Phys. Chem. C 123, 7731-7739 (2019)

**12:00pm SS+2D+AS+HC-TuM-13 Atomic Structure of Reconstructed Al<sub>2</sub>O<sub>3</sub>(0001) Surface, J. Hütner, A. Conti, TU Wien, Austria; D. Kugler, CEITEC, Czechia; F. Mittendorfer, U. Diebold, M. Schmid, Jan Balajka, TU Wien, Austria**

Corundum α-Al<sub>2</sub>O<sub>3</sub> is an important ceramic widely used in electronics, optical applications, or as catalyst support. Despite its importance, the atomic structure of the most stable (0001) termination has not been conclusively determined. Detailed studies of Al<sub>2</sub>O<sub>3</sub> surfaces have been stymied by its insulating nature, preventing the use of many surface science methods.

Structural models based on surface X-ray diffraction (SXRD) [1], and atomic force microscopy (AFM) [2], concluded the (√31 × √31)R±9°-reconstructed Al<sub>2</sub>O<sub>3</sub>(0001) surface formed upon high-temperature annealing is terminated by one or two layers of metallic Al strained to lattice-match the oxide substrate.

We imaged the reconstructed Al<sub>2</sub>O<sub>3</sub>(0001) surface with noncontact AFM (nc-AFM) using specifically functionalized tips for chemically-sensitive contrast. In particular, CuO<sub>x</sub> terminated tips [3], enabled us to directly identify oxygen and aluminum atoms in the topmost layer.

With the aid of *ab-initio* calculations, we propose a structural model of the (√31 × √31)R±9°-reconstructed Al<sub>2</sub>O<sub>3</sub>(0001) surface consistent with atomically resolved nc-AFM images and area-averaging spectroscopic data. Unlike prior models, the surface does not contain a metallic Al layer but consists of oxygen and aluminum atoms arranged in similar structural units as reported in thin AlO<sub>x</sub> films [4,5].

- [1] G. Renaud, et al., Phys. Rev. Lett. **73**, 13 (1994)  
[2] J. V. Lauritsen, et al., Phys. Rev. Lett. **103**, 076103 (2009)  
[3] B. Shulze Lammers, et al., Nanoscale **13**, 13617 (2021)  
[4] G. Kresse, et al., Science **308**, 1440 (2005)  
[5] M. Schmid, et al., Phys. Rev. Lett. **99**, 196104 (2007)

## Theory for Surface Processes and Spectroscopies Focus Topic

### Room B116 - Session TH1+AS+SS-TuM

#### Introduction and Core-Level Spectroscopies I

**Moderators: Gianfranco Pacchioni, Università degli Studi di Milano-Bicocca, John Rehr, University of Washington**

**8:00am TH1+AS+SS-TuM-1 X-Ray Photoelectron Spectroscopy as a Useful Tool to Study Surfaces and Model Systems for Heterogeneous Catalysts, Hans-Joachim Freund, Fritz-Haber-Institut der Max-Planck-Gesellschaft, Germany**

**INVITED**

After a brief introduction into the concepts of photoemission, including multielectron excitations, and a discussion of ways how to extract

information on the chemical state of atoms in the non-ionized ground state from the chemical shift in XPS spectra, as well as from the evaluation of the so-called Auger parameter, we present several examples on how appropriate theoretical calculations may be crucial to properly interpret the spectra in terms of initial and final state effects. Four studies on systems representing model systems for heterogeneous catalysts are discussed. The first two refer to simple thin film oxide systems of MgO(100)/Ag(100) supported on metal single crystals. We interpret line widths in terms of vibrational excitations, depending on the thickness of the oxide film, and compare surface core level chemical shifts with those in the bulk, and discuss the differences on the basis of ab-initio cluster calculations. The third example refers to chemical shifts of metal/(Pd) atoms adsorbed on bilayer silica films on Ru(0001), and illustrates the use of the Auger parameter to extract initial state chemical shifts. The last example deals with CeO<sub>2</sub>(111) surfaces and exemplifies the influence of open shell on the complexity of core level spectra.

**8:40am TH1+AS+SS-TuM-3 X-Ray Absorption and Emission Spectroscopy of Actinide Materials: Electronic Structure Questions from the Experimental Viewpoint, Bianca Schacherl, Karlsruhe Institute of Technology (KIT), Institute for Nuclear Waste Disposal (INE), Germany**  
**INVITED**

Understanding the electronic structure of one of the most complex element groups in the periodic table, the actinides, has been topic of extensive research in the last decades.

Spectroscopic tools for these investigations are provided by X-ray absorption spectra. Especially the An M<sub>4,5</sub>-edge high-resolution X-ray absorption and emission spectroscopy has proven to be a powerful tool for electronic structure investigations.<sup>1,2</sup>

In this talk it will be demonstrated how newly revealed spectral features can be used for in-depth analyses of the actinide-ligand chemical bond. For model systems, one focus will lie on how the spectra change upon changes in the electronic structure of the actinide compound. It will be highlighted how several theoretical methods can give a valuable input to understand the origin of the spectral features.<sup>3-7</sup>

*This work is supported by the ERC Consolidator Grant "The Actinide Bond" (N°101003292) under the European Union's Horizon 2020 research and innovation program. The Institute for Beam Physics and Technology (IBPT), KIT is acknowledged for the operation of the storage ring, the Karlsruhe Research Accelerator (KARA).*

(1) Vitova, T.; Pidchenko, I.; Fellhauer, D.; Bagus, P. S.; Joly, Y.; Průbmann, T.; Bahl, S.; Gonzalez-Robles, E.; Rothe, J.; Altmaier, M.; Denecke, M. A.; Geckeis, H. *Nat. Commun.* **2017**, *8* (May), 1–9.

(2) Vitova, T.; Pidchenko, I.; Fellhauer, D.; Průbmann, T.; Bahl, S.; Dardenne, K.; Yokosawa, T.; Schimmelpfennig, B.; Altmaier, M.; Denecke, M.; Rothe, J.; Geckeis, H. *Chem. Commun.* **2018**, *54* (91), 12824–12827.

(3) Polly, R.; Schacherl, B.; Rothe, J.; Vitova, T. *Inorg. Chem.* **2021**, *60* (24), 18764–18776.

(4) Bagus, P. S.; Schacherl, B.; Vitova, T. *Inorg. Chem.* **2021**, *60* (21), 16090–16102.

(5) Schacherl, B.; Trumm, M.; Beck, A.; Vitova, T. **2024**, *submitted*.

(6) Schacherl, B.; Bowes, E.; Adelman, S. L.; Dardenne, K.; DiMucci, I.; Kozimor, S. A.; Long, B. N.; Müller, N.; Pace, K.; Pruessmann, T.; Rothe, J.; Xu, L.; Kasper, J. M.; Batista, E. R.; Yang, P.; Vitova, T. **2023**, *submitted*.

(7) Schacherl, B.; Tagliavini, M.; Popa, K.; Beck, A.; Walter, O.; Pruessmann, T.; Vollmer, C.; Kaufmann, H.; Mazzanti, M.; Haverkort, M.; Vitova, T. **2023**, *submitted*.

**9:20am TH1+AS+SS-TuM-5 Towards New Spectroscopic Tools for Detection of Bonding Properties in Radiopharmaceuticals: Application on La Used as a Homolog of Ac, Tonya Vitova, Karlsruhe Institute of Technology (KIT), Institute for Nuclear Waste Disposal, Germany; B. Schacherl, H. Ramanantoanina, Karlsruhe Institute of Technology (KIT), Institute for Nuclear Waste Disposal (INE), Germany; M. Benesova, German Cancer Research Center, Im Neuenheimer Feld 280, 69120 Heidelberg, Germany; J. Göttlicher, Karlsruhe Institute of Technology, Institute for Photon Science and Synchrotron Radiation (IPS), P.O. Box 3640, D-76021 Karlsruhe, Germany; R. Steininger, Karlsruhe Institute of Technology, Institute for Photon Science and Synchrotron Radiation (IPS), Germany; M. Haverkort, Heidelberg University, Institute for Theoretical Physics, P.O. Box 105760, 69047 Heidelberg, Germany; A. Kovac, European Commission, Joint Research Centre Karlsruhe, P.O. Box 2340, 76125 Karlsruhe, Germany**

In recent years the use of radiopharmaceuticals based on alpha-particle emitting radionuclides has seen a considerable growth. In pre-clinical research and first clinical trials targeted alpha therapy has shown great potential. However, there are still many challenges in this field, one being the need for tight chelating of the alpha-emitting radionuclides and their daughters. We aim to understand relations between bonding properties and bond stability of such compounds.

High-energy resolution X-ray absorption near edge structure (HR-XANES) spectroscopy is a valuable tool for the electronic structure study of actinides and lanthanides.<sup>1-2</sup> Here we employ it first to probe the bonding properties of La, a homolog of Ac, with different ligands in discussion as nuclide binding site in radiopharmaceuticals for targeted alpha treatment.

[La(H<sub>2</sub>O)<sub>9</sub>]<sup>3+</sup>, [La(TRIS)(H<sub>2</sub>O)<sub>6</sub>]<sup>3+</sup>, [La(TRIS)<sub>2</sub>(H<sub>2</sub>O)<sub>3</sub>]<sup>3+</sup> (buffer media), [La(DOTA)(H<sub>2</sub>O)]<sup>2+</sup>, [La(MACROPA)]<sup>1+</sup> and [La(PSMA-617)(H<sub>2</sub>O)] have been prepared and characterized. We measured La L<sub>2</sub>-edge HR-XANES spectra at the Synchrotron Laboratory for Environmental Studies (SUL-X) beamline and La L<sub>3</sub>-edge extended X-ray absorption fine structure spectroscopy (EXAFS) at the INE-Beamline at the KIT Light Source. Additionally, density functional theory (DFT) and FDMNES calculations were performed to compute the spectra. Bonding interactions were evaluated using natural orbitals for chemical valence (NOCV) and quantum theory of atoms in molecules (QTAIM) which describes the topology (i.e., shape and magnitude) of the electron density between two bonded atoms.

Several tools (spectroscopic and theoretical) to determine the covalency of the La-ligand bond were developed. One example of this measure can be the comparison of position and shape of the pre- and main absorption edges. EXAFS and HR-XANES analysis gave insights into the coordination environment. With QTAIM bond analysis the covalent from the ionic part of the bonding was differentiated. Combined these results are the first steps towards developing new spectroscopic tools that will help understand the electronic structure and the bonding and will potentially help designing new chelating ligands for use in radiopharmaceuticals for targeted alpha therapy.

References

1. T. Pruessmann et al., *J Synchrotron Radiat* **2022**,*29*, 53-66.

2. T. Vitova et al., *Commun Chem* **2022**, *5* (1).

**9:40am TH1+AS+SS-TuM-6 Potential Energy Curves of Core-Excited States and Vibrational Broadening of X-Ray Adsorption Spectra of Uranyl, Robert Polly, Karlsruhe Institute of Technology (KIT), Germany; P. Bagus, University of North Texas**

It is well known that vibrational excitations lead to an observable broadening of the features in the X-Ray Photoelectron Spectroscopy, XPS, in ionic compounds. This broadening is described as a Franck-Condon, FC, broadening since it arises because there is a change in the equilibrium geometry of the ionized system from that in the initial, ground, state of the system. Studies have shown how the FC broadening is sensitive to coordination to the ionized atom [1] and to the covalent character of the cation – anion interaction [2]. For Uranyl UO<sub>2</sub><sup>2+</sup> the different potential energy curves of the relevant core-excited states of the U M<sub>4,5</sub>-edge manifold differ significantly and cause different broadenings for the three peaks which characterize the U M<sub>4,5</sub>-edge X-Ray Adsorption Near Edge Spectroscopy, XANES. Thus, FC broadening effects affect the features as they do for XPS. This should be of particular importance in determining the resolution possible with High-Resolution XANES, HR-XANES [3-4]. However, to our knowledge, the possibility of different FC broadening in XANES or HR-XANES has not been considered previously and theoretical modeling of the spectra has used the same geometry for the initial and excited

# Tuesday Morning, November 7, 2023

configurations [4-5]. In the present work, we examine vibrational excitations for the representative case of uranyl,  $\text{UO}_2^{2+}$ . The U  $M_{4,5}$ -edge HR-XANES spectra reveal three distinct peaks which are assigned to excitations into different 5f valence orbitals. The corresponding core-excited states differ significantly depending on the 5f valence orbital occupation and so does the FC broadening. Based on rigorous *ab initio* calculations of the wavefunctions, WFs, for the  $M_4$  and  $M_5$ -edge XANES, we show that there are considerable changes in the geometry and we provide reliable estimates of the FC broadening due to these geometry changes. We also explain the linear behavior of the observed peak splittings with the internuclear distance, but we can not confirm a relation of the peak splittings with the covalence of the Uranium-Oxygen bond lengths.

[1] C. J. Nelin *et al.*, *Angew. Chem. Int. Ed.*, 2011, **50**, 10174-10177.

[2] P. S. Bagus and C. J. Nelin, "Computation of Vibrational Excitations in XPS Spectroscopy", in *Rare Earth Elements and Actinides: Progress in Computational Science Applications*, edited by D. A. Penchoff, et al. (American Chemical Society, 2021), Vol. 1388, p. 181.

[3] T. Vitova *et al.*, *Nat. Commun.*, 2017, **8**, 16053.

[4] R. Polly *et al.*, *Inorg. Chem.*, 2021, **60**, 18764-18776.

[5] P. S. Bagus *et al.*, *Inorg. Chem.*, 2021, **60**, 16090.

## Theory for Surface Processes and Spectroscopies Focus Topic

### Room B116 - Session TH2+AS+SS-TuM

#### Core-Level Spectroscopies II

**Moderators:** Ria Broer, University of Groningen, Bianca Schacherl, Karlsruhe Institute of Technology

11:00am **TH2+AS+SS-TuM-10 Cumulant Green's Function Approaches for Satellites and Multiplets in X-Ray Spectra**, *John J. Rehr*, Dept of Physics, University of Washington; *J. Kas*, Department of Physics, University of Washington

**INVITED**

The treatment of electronic correlations in open-shell systems is one of the most challenging problems in atomic, molecular, and condensed matter physics. Their importance is particularly evident in x-ray spectra, where the single particle theory breaks down and many-body effects such as satellites and atomic multiplet effects are observed. Conventional approximations are only partly successful. Ligand-field multiplet theory and dynamical mean field theory can describe intra-atomic correlation effects well but typically ignore long range correlation effects. The real-time cumulant Green's function method can describe shake-up effects well [1] but ignores multiplets. We have found, however, that separating the dynamic Coulomb interactions into local and longer-range parts with *ab initio* parameters yields a combined multiplet-plus-cumulant approach that can account for both local atomic multiplets and satellite excitations [2]. The approach is illustrated for transition metal oxides and explains the multiplet peaks, charge-transfer satellites, and distributed background features observed in XPS experiment. In an alternative approach for molecular systems, we have found that a real-time equation of motion coupled-cluster (RT-EOM-CC) cumulant approach can also describe both correlation effects at the CCSD level and intrinsic losses in x-ray spectra, including orthogonality corrections that enhance XAS at the edge [3]. Comparisons with other approaches [4] are also discussed.

[1] Strengths of plasmon satellites in XPS: Real-time cumulant approach: J. J. Rehr and J. J. Kas, *J. Vac. Sci. Technol. A* **39**, 060401 (2021).

[2] *Ab Initio* Multiplet-Plus-Cumulant Approach for Correlation Effects in X-Ray Photoelectron Spectroscopy, J. J. Kas, J. J. Rehr, and T. P. Devereaux, *Phys. Rev. Lett.* **128**, 216401 (2022).

[3] Equation of motion coupled-cluster cumulant approach for intrinsic losses in x-ray spectra, J. Chem. Phys. J.J. Rehr, F.D. Vila, J.J. Kas, N.Y. Hirshberg, K. Kowalski, and B. Peng **152**, 174113 (2020).

[4] Analysis of the Fe 2p XPS for hematite  $\text{Fe}_2\text{O}_3$ : Consequences of covalent bonding and orbital splittings on multiplet splittings, P.S. Bagus, C. J. Nelin, C. R. Brundle, N. Lahiri, E. S. Ilton, and K. M. Rosso, *J. Chem. Phys.* **152**, 014704 (2020).

11:40am **TH2+AS+SS-TuM-12 Understanding Multiplets in the XPS of Transition Metal Oxides: Experiment and Theory and the Effects on Quantitation Procedures**, *Christopher Richard Brundle*, C. R. Brundle and Associates; *B. Christ*, XPS library; *P. Bagus*, Center for Advanced Scientific Computing and Modeling (CASCAM) Department of Chemistry University of North Texas

**INVITED**

Atoms with open valence shells suffer splitting to their XPS core-levels owing to the different spin-spin coupling possibility between the remaining unpaired core electron and the electrons in the open shell (1). This results in a spectrum with two components of unequal intensity, separated by an *ev* or two. Gupta and Sen (2) expanded the multiplet splitting theory to include spin-orbit coupling (angular momentum coupling), providing highly cited predictions for the 2p spectra of TM cations (eg  $\text{Ni}^{2+}$ ). Bagus, et al (3), and others, using rigorous *ab initio* MO calculations on clusters, have expanded theory further to allow XPS predictions for solid TM compounds (eg  $\text{Ni}^{2+}$  in  $\text{NiO}$ ,  $\text{Fe}^{3+}$  in  $\text{Fe}_2\text{O}_3$ ) which include both ligand field and bonding effects. Finally, they included shake-up effects (excitation of valence electrons in addition to core level ionization), which can substantially alter the distribution of intensities across the complete core-level spectrum, for example Ni 2p for  $\text{NiO}$  (4). This progression in the understanding of the origin of the features of TM core-level spectra is discussed, as is also the effects on requirements for providing quantitation of TM compounds using core level intensity ratios or peak fitting. Comparison is then made to alternative theory approaches to modeling the spectra, such as the freely available semi-empirical charge transfer method, CTM4XAS, (5), and the many-body cumulative theory of Rehr and Kass (6). We examine how these agree/differ in the interpretation/understanding of the XPS features, usefulness in ascribing chemical states, and quantitation aspects.

1. C. S. Fadley, D. A. Shirley, A. J. Freeman, P. S. Bagus, and J. V. Mallow, *Phys. Rev. Lett.*, 1969, **23**, 1397-1401.
2. R. P. Gupta and S. K. Sen, *Phys. Rev. B*, 1974, **10**, 71-77; P. Gupta and S. K. Sen, *Phys. Rev. B*, 1975, **12**, 15-19.
3. P. S. Bagus, C. J. Nelin, C. R. Brundle, B. V. Crist, N. Lahiri, and K. M. Rosso, *Phys. Chem. Chem. Phys.*, 2022, **24**, 4562-4575.
4. P. S. Bagus, C. J. Nelin, C. R. Brundle, B. V. Crist, E. S. Ilton, N. Lahiri, and K. M. Rosso, *Inorganic Chemistry*, 2022, **61**, 18077
5. F. De Groot and A. Kotani, *Core level spectroscopy of solids*. CRC Press, Boca Raton, 2008.
6. J. J. Kas, J. J. Rehr and T. P. Devereaux, *Phys. Rev. Lett.* 2022, **128**, 216401

## Quantum Science and Technology Mini-Symposium Room B110-112 - Session QS+SS-TuA

### The Quantum Metrology Revolution

Moderators: Luxherta Buzi, IBM, Petra Reinke, University of Virginia

2:20pm **QS+SS-TuA-1 Quantum Sensing Enabled by Spin Qubits in Diamond**, Fedor Jelezko, Institute of Quantum Optics, Ulm University, Germany

INVITED

Synthetic diamond has recently emerged as a candidate material for a range of quantum-based applications including quantum information processing and quantum sensing. In this presentation we will show how single nitrogen-vacancy (NV) colour centres can be created with a few nanometers accuracy and coherent dipole-dipole coupling was employed to generate their entanglement. Single NV centers and clusters of entangled spins created close to the diamond surface can be employed as nanoscale sensors of electric and magnetic fields. We will show nanoscale NMR enabled by single NV centers and discuss sensitivity and spectral resolution limits of nanoscale NMR. We will also discuss applications of NV centres for hyperpolarization of nuclear spins and application of optical spin polarization in MRI.

3:00pm **QS+SS-TuA-3 Tunneling Andreev Reflection - New Quantitative Microscopy of Superconductors with Atomic Resolution**, W. Ko, University of Tennessee Knoxville; S. Song, J. Yan, Oak Ridge National Laboratory; C. Lane, Los Alamos National Laboratory; J. Lado, Aalto University, Finland; Petro Maksymovych, Oak Ridge National Laboratory

Andreev reflection is an established method to probe the existence of superconductivity, and, crucially, the symmetry of the superconducting order parameter. In its conventional implementation of the point contact Andreev reflection (PCAR), the technique relies on so-called directional contacts, which inject quasiparticles into superconductors with well-defined momentum. However, good momentum resolution requires a trade-off for essentially no spatial resolution, which has limited the applicability of PCAR to atomic-scale properties of superconductors, including inhomogeneities and interfaces.

In this talk, we will present our latest developments in Tunneling Andreev Reflection - a new experimental approach which we recently introduced to quantify Andreev reflection through atomic-scale tunnel junction [1]. Similar to PCAR, TAR exhibits direct sensitivity to the superconducting order parameter in both conventional and unconventional superconductors [2]. Recently, we used TAR to unambiguously confirm the sign-changing order parameter in paradigmatic FeSe, and further revealed suppression of superconductivity along the nematic twin boundaries above 1.2 K [2]. Locally suppressed superconductivity, in turn, explains the peculiar vortex templating effect exerted by twin boundaries - essentially causing recrystallization of the vortex glass phase [3]. However, due to atomic-spatial resolution TAR lacks momentum resolution - the opposite of PCAR. Therefore, the measurements, observables and their interpretation are fundamentally distinct from PCAR as well. We will discuss our present understanding of this technique, relevant methods of data analysis needed to reveal Andreev signal, and specific effects of band structure on TAR. These effects are crucially important for robust characterization of unconventional superconductivity, while also enabling TAR to complement tunneling spectroscopy and quasiparticle imaging in search for exotic quantum materials. Research sponsored by Division of Materials Science and Engineering, Basic Energy Sciences, Office of Science, US Department of Energy. SPM experiments were carried out as part of a user project at the Center for Nanophase Materials Sciences, Oak Ridge National Laboratory, a US Department of Energy Office of Science User Facility.

1. W. Ko, J. Lado, P. Maksymovych, *Nano Lett.* 22 (2022) 4042.
2. W. Ko, S. Y. Song, J. Lado, P. Maksymovych, arXiv:2303.05301 [https://arxiv.org/abs/2303.05301].
3. S. Y. Song, C. Hua, L. Bell, W. Ko, H. Fangohr, J. Yan, G. B. Halász, E. F. Dumitrescu, B. J. Lawrie, P. Maksymovych, *Nano Lett.* 23(2023)2822.

3:20pm **QS+SS-TuA-4 Patterned-Stress-Induced Compositional Manipulation of Epitaxially Grown Semiconductors for Quantum Applications**, Leonid Miroshnik, University of New Mexico; B. Rummel, Sandia National Laboratories; M. Patriotis, University of New Mexico; A. Li, T. Sinno, University of Pennsylvania; M. Henry, Sandia National Laboratories; G. Balakrishnan, S. Han, University of New Mexico

We have previously demonstrated compositional patterning of epitaxially grown compound semiconductors, using lithographically patterned nanoscale pillars as a mechanical press.<sup>1-3</sup> The elastically introduced strain from the press, at elevated temperatures, steers large atoms out of the compressed region of compound semiconductors (e.g., indium in InGaAs) to form quantum confined structures. This approach allows forming quantum structures at desired locations in an addressable manner. In this work, we describe a new approach to introduce a patterned stress field to semiconductor films, using Surface Acoustic Waves (SAW) generated by Interdigitated transducers (IDTs). We fabricate SAW devices on GaAs(100) substrate and demonstrate that we can image standing surface acoustic waves using 2D Raman spectroscopy as well as atomic force microscopy.<sup>4</sup> The magnitude of these waves, upon optimization of SAW devices<sup>5</sup>, reaches greater than 5 nm, introducing 100s of MPa stress. We will share the stress characterization and optimization approach in this presentation and assess the likelihood of using the stress field to induce compositional patterning.

This material is based upon work supported by the National Science Foundation under Grant No. DMR-1809095

1. S. Ghosh, D. Kaiser, J. Bonilla, T. Sinno, and S. M. Han, "Stress-Directed Compositional Patterning of SiGe Substrates for Lateral Quantum Barrier Manipulation," *Applied Physics Letters* 107, 072106-1:5 (2015)
2. D. Kaiser, S. Ghosh, S. M. Han, and T. Sinno, "Modeling and simulation of compositional engineering in SiGe films using patterned stress fields," *Molecular Systems Design and Engineering* 1, 74-85 (2016)
3. D. Kaiser, S. Ghosh, S. M. Han, and T. Sinno, "Multiscale Modeling of Stress-Mediated Compositional Patterning in SiGe Substrates," *High Purity and High Mobility Semiconductors* 75, 129-141 (2016)
4. B. D. Rummel, L. Miroshnik, M. Patriotis, A. Li, T. R. Sinno, M. D. Henry, G. Balakrishnan, and S. M. Han, "Imaging of surface acoustic waves on GaAs using 2D confocal Raman microscopy and atomic force microscopy," *Applied Physics Letters* 118, 031602-1:6 (2021) <https://doi.org/10.1063/5.0034572>.
5. B. D. Rummel, L. Miroshnik, A. B. Li, G. D. Heilman, G. Balakrishnan, T. Sinno, and S. M. Han, "Exploring electromechanical utility of GaAs interdigitated transducers; using finite-element-method-based parametric analysis and experimental comparison," *Journal of Vacuum Science & Technology B* 41, 013203-1:8 (2023) <https://doi.org/10.1116/6.0002169>.

4:20pm **QS+SS-TuA-7 Atomic Tunneling Defects in Superconducting Quantum Circuits: Origins and Remedies**, Jürgen Lisenfeld, Karlsruhe Institute of Technology (KIT), Germany

INVITED

Parasitic two-level systems formed by defects in the materials of superconducting qubits are a major source of decoherence. I will review the defects' origins, and discuss possible ways to mitigate their detrimental impacts. A focus will be set on recent experiments in Karlsruhe, where we develop novel methods to in-situ control defect properties by applied mechanical strain and electric fields. E-field tuning of defects provides a possibility to mitigate energy loss of qubits due to resonant defects. It also allows us to identify the locations of defects in a given quantum circuit which helps to guide the way towards better qubit fabrication.

5:00pm **QS+SS-TuA-9 Mechanistic Investigations of Superconducting Film Growth: Substrate-Mediated Sn Diffusion on a Niobium Oxide**, Sarah Willson, University of Chicago; R. Farber, University of Kansas; S. Sibener, University of Chicago

Niobium is the highest temperature elemental superconductor, making it the standard material for superconducting radiofrequency (SRF) cavities in next-generation linear accelerators. These facilities require cryogenic operating temperatures (< 4 K) to limit the formation of superconductivity-quenching hot spots in the near-surface region of the cavity. Widespread efforts are underway to increase the accelerating fields and reduce the cryogenic burden by improving SRF surfaces.

A promising solution is to coat the Nb SRF surface with a Nb<sub>3</sub>Sn thin film via Sn vapor deposition. The higher critical temperature and critical field makes Nb<sub>3</sub>Sn an ideal candidate for capping Nb surfaces. However, the persistence of defects, stoichiometric inhomogeneities, and excessive surface

# Tuesday Afternoon, November 7, 2023

roughness in formed these Nb<sub>3</sub>Sn films nucleate quenching sites – limiting the SRF performance.

As part of a widespread interdisciplinary effort to optimize SRF accelerating capabilities, this work aims to develop a comprehensive growth model for pristine Nb<sub>3</sub>Sn films. We aim to understand the interplay between the underlying Nb oxide morphology, Sn coverage, and Nb deposition temperature on Sn wettability and Nb<sub>3</sub>Sn growth mechanisms. Alloy films are grown on single crystal and polycrystalline Nb surfaces terminated with a diverse range of morphologies and analyzed using both *in situ* and *ex situ* techniques.

Characterization of initial Sn/Nb<sub>x</sub>O<sub>y</sub> phases provide insight towards the dynamic and reactive interface that templates Nb<sub>3</sub>Sn films. Complementary experiments of Nb<sub>3</sub>Sn films grown at higher Sn coverages further illustrate how the diverse underlying Nb oxide surface morphologies impact the quality, and ultimately the accelerating performance, of these SRF surfaces.

**5:20pm QS+SS-TuA-10 Revealing Pairing Symmetry of Superconductors by Tunneling Andreev Reflection, Wonhee Ko**, University of Tennessee, Knoxville; *S. Song, J. Yan*, Oak Ridge National Laboratory; *J. Lado*, Aalto University, Finland; *P. Maksymovych*, Oak Ridge National Laboratory

Andreev reflection (AR) is an electronic transport process at the junction of a normal metal and a superconductor, where the electrons in the normal metal transform to the Cooper pairs by retroreflecting holes and conducts current across the junction. The process is highly sensitive to the superconducting order parameters and functions as a tool to directly probe the superconductivity. Based on AR, we developed a new technique, tunneling Andreev reflection (TAR), by applying AR to the tunnel junction in scanning tunneling microscope (STM) [1,2]. Specifically, we precisely tune the STM tip-sample distance to systematically study the AR as a function of the tunneling barrier height. Since the AR is a higher order tunneling process compared to the normal electron tunneling, the relative decay rate of the tunneling conductance increases inside the superconducting gap, whose specific shape depends on the nature of the superconductivity [3]. By comparing the decay rate spectra with the theoretical calculations, we identify the pairing symmetry of various kinds of superconductors, from conventional s-wave ones to the unconventional high-T<sub>c</sub> ones such as iron-based or cuprate superconductors.

This research was performed at the Center for Nanophase Materials Sciences which is a DOE Office of Science User Facility.

[1] W. Ko, E. Dumitrescu, and P. Maksymovych, *Phys. Rev. Res.* **3** 033248 (2021)

[2] W. Ko, J. L. Lado, and P. Maksymovych, *Nano Lett.* **22** 4042 (2022)

[3] W. Ko, S. Y. Song, J. Yan, J. L. Lado, and P. Maksymovych, *arXiv:2303.05301*

**5:40pm QS+SS-TuA-11 Single-nm-Resolution Gate Fabrication for Top-Gated Quantum Dot Qubits, J. Owen, Joshua Ballard, E. Fuchs, J. Randall**, Zyvex Labs; *F. Beaudoin*, Nanoacademic Technologies, Canada; *A. Sigillito*, U. Pennsylvania

Top gated semiconductor quantum dot qubits represent an attractive path to quantum computing. However, variations in the physical dimensions of the top gates create significant variations in the electrostatic confinement and therefore the energy levels in the qubit. The variation in gate dimensions complicates the design of multi qubit systems and the required tuning of the biases on the gates for multiple qubits is so complex that machine learning is employed.

Multiple modeling runs of a generic top gated multi-qubit system carried out with the spin-qubit computer-aided design tool QTCAD has found that a variation in the gate dimensions of ~2 nm causes a factor of 2 change in the tunneling rates, or a factor of 4 in the Exchange Interaction strength. This level of precision is not achievable using e-beam lithography where the proximity can cause an increase in the written feature width by 15 nm compared to the pattern.

We describe an alternative path which uses Atomic Precision Lithography[1] to create far more precise gates. Two methods to transfer the pattern into the gate structures are described; either saturate the patterns with dopant precursors to make dopant-based gate structures or growing area-selective etch mask material. The former will preserve the precision, but is less compatible with CMOS processes. Otherwise, area-selective atomic layer deposition and reactive ion etching can be used to make nanoimprint templates[2]. The accuracy of templates thus produced, and the precision

of Jet and Flash Nanoimprint lithography will produce far more uniform top gates with a scalable manufacturing technique.

1. Bussmann, E.; Butera, R. E.; Owen, J. H. G.; Randall, J. N.; Rinaldi, S. M.; Baczewski, A. D.; Misra, S. Atomic – Precision Advanced Manufacturing for Si Quantum Computing. *MRS Bull.* **2021**, *46*, 1–9.

2. Ballard, J.; McDonnell, S.; Dick, D.; Owen, J.; Mordi, G.; Azcatl, A.; Campbell, P.; Chabal, Y.; Randall, J.; Wallace, R., Patterned atomic layer deposition on scanning tunneling microscope constructed templates. *Technical Proceedings of the 2013 NSTI Nanotechnology Conference and Expo, NSTI-Nanotech 2013* **2013**, *2*, 481-484.

**6:00pm QS+SS-TuA-12 The Changing Role of National Metrology Institute with Quantum-Based Standards and the Nist on a Chip Program, Jay Hendricks, B. Goldstein**, NIST

This oral presentation covers a bit of metrology history of how we got to where we are today and gives a forward-looking vision for the future of measurement science. The role of NIST as a National Metrology institute (NMI) is briefly described considering the world-wide redefinition of units that occurred on May 20<sup>th</sup>, 2019. The re-definition of units is now aligned with physical constants of nature and fundamental physics which opens new realization routes with quantum-based sensors and standards. The NIST on a Chip program (NOAC) is briefly introduced in this context. The re-definition of the SI units enables new ways to realize the units for the pascal and the kelvin. These quantum-based systems; however exciting, do raise new challenges and several important questions: Can these new realizations enable the size and scale of the realization to be miniaturized to the point where it can be imbedded into everyday products? What will be the role of metrology institutes in the is new ecosystem of metrology and measurement? What will be the NMI role for quality systems and measurement assurance for these new quantum-based systems? This talk will begin to explore these important philosophical questions.

## Surface Science Division

### Room D136 - Session SS+HC-TuA

#### Photochemistry

**Moderators: Erik Jensen**, University of Northern British Columbia, **Ahmad Nawaz**, Hebrew University of Jerusalem

**2:20pm SS+HC-TuA-1 Pt Nanoclusters on GaN Nanowires for Solar-Assisted Seawater Hydrogen Evolution, Victor Batista, W. Dong, Y. Xiao, K. Yang, Z. Ye, P. Zhou, I. Navid, Z. Mi**, Yale University

**INVITED**  
Seawater electrolysis provides a viable method to produce clean hydrogen fuel. To date, however, the realization of high-performance photocathodes for seawater hydrogen evolution reaction has remained challenging. Here, we introduce n+p Si photocathodes with dramatically improved activity and stability for hydrogen evolution reaction in seawater, modified by Pt nanoclusters anchored on GaN nanowires (Fig 1). We find that Pt-Ga sites at the Pt/ GaN interface promote the dissociation of water molecules and spilling H\* over to neighboring Pt atoms for efficient H<sub>2</sub> production. Pt/GaN/Si photocathodes achieve a current density of -10 mA/cm<sup>2</sup> at 0.15 and 0.39 V vs. RHE and high applied bias photon-to-current efficiency of 1.7% and 7.9% in seawater (pH = 8.2) and phosphate-buffered seawater (pH = 7.4), respectively. We further demonstrate a record-high photocurrent density of ~169 mA/cm<sup>2</sup> under concentrated solar light (9 suns). Moreover, Pt/GaN/Si can continuously produce H<sub>2</sub> even under dark conditions by simply switching the electrical contact. This work provides valuable guidelines to design an efficient, stable, and energy- saving electrode for H<sub>2</sub> generation by seawater splitting.

**3:00pm SS+HC-TuA-3 Photoreactivity of Single Micro-Sized TiO<sub>2</sub> Crystals, H. Zhu, W. Lu, K. Park, Zhenrong Zhang**, Baylor University

Understanding the reactivity of TiO<sub>2</sub> particles with different polymorphs and morphologies is important for many photocatalytic applications. Here, the reactivity of individual anatase TiO<sub>2</sub> microcrystals with a large percentage of (001) facet was monitored and studied using operando photoluminescence microscopy. The photoreduction of resazurin on anatase microcrystals shows that the photoreduction rate on each microcrystal was different although the microcrystals had comparable sizes and exposed the same facets. The reaction rate changes from no reactivity to higher than that of the anatase (001) bulk single crystal. The reaction rate of the anatase microcrystals depends on the morphology and the structure of each particle. The reactivities of the microcrystals with mixed

anatase-rutile phases and after the anatase-to-rutile phase transformation have also been monitored.

**3:20pm SS+HC-TuA-4 Electron Induced Photochemistry of Nitrous Oxide-Water Co-Adsorbed Film (N<sub>2</sub>O@H<sub>2</sub>O) as a Model Study of Astrochemistry in the Interstellar Medium, Ahmad Nawaz**, The Hebrew University of Jerusalem, Israel

The desorption kinetics of N<sub>2</sub>O@H<sub>2</sub>O film deposited on a Ru (0001) surface under ultra-high vacuum (UHV) environment (2x10<sup>-10</sup> Torr) has been investigated as a model study for electrons-induced reactivity that takes place in the interstellar medium, using temperature-programmed desorption (TPD) measurements, at substrate temperature of 35K. The TPD spectra of all the prominent product masses were well detected by the QMS, employing a 3D-TPD analysis. The N<sub>2</sub>O molecules, embedded within ASW as the host matrix, decompose upon exposure to electrons at kinetic energies of 10eV and 50 eV. This leads to the formation of new molecular products at m/z values of 28 (N<sub>2</sub>) and 30 (NO) as the primary products. Typical TPD spectra of the parent N<sub>2</sub>O molecules, while embedded in ASW layer (15 ML) are shown in Figure 1a and product formation is shown in Figure 1b. Here, the primary N<sub>2</sub>O TPD peaks appear at ~82K, while some of these molecules are trapped within the water film and desorb together with the main ASW film at ~160K.

**4:20pm SS+HC-TuA-7 Structure and Chemistry of Aqueous Oxide Interfaces from Molecular Simulations, A. Selloni, A. Raman**, Princeton University; **Marcos Calegari Andrade**, Lawrence Livermore National Laboratory; **B. Wen**, Henan University, China **INVITED**

Photo-electrocatalysis involving complex oxide-water interfaces is a highly promising technology for the sustainable production of fuels. However, probing these complex interfaces and gaining atomistic insights is still very challenging for current experimental methods, and is often only possible through accurate computational simulations. In this talk I will discuss some of our recent work on the application of ab-initio based molecular simulations to understand the structure and dynamics of interfacial water on photoelectrochemically relevant oxide surfaces. Specific topics will include proton transfer at the aqueous TiO<sub>2</sub> and IrO<sub>2</sub> interfaces and the influence of surface atomic structure on the water dissociation fraction and hydroxyl lifetimes at the interface.

**5:00pm SS+HC-TuA-9 Photodissociation of an Adsorbate via Coadsorbed Photon Absorption: Electronic Energy Transfer in Heterogeneous Molecular Thin Films, Erik Jensen**, University of Northern B.C., Canada

The photophysics of many small aromatics and related molecular systems has been studied intensely and widely for many years, both in understanding the molecular origins of natural phenomenon such as photosynthesis, as well as in areas of technological interest. Although the UV photosensitization of CH<sub>3</sub>I dissociation in gas-phase mixtures with benzene was noted many years ago<sup>[1]</sup>, we can find no subsequent examples of studies of the photochemical dynamics of this process. We have studied a set of thin film molecular systems on a metal substrate using UHV surface science techniques and time-of-flight spectroscopy on neutral photofragments.

In the present work, we have studied the dynamics of the near-UV photodissociation of CH<sub>3</sub>I adsorbed on thin films (1–10ML) of benzene<sup>[2]</sup> and a variety of fluorinated benzenes grown on a Cu(100) substrate. Using polarized 248nm light, we find that the kinetic energies of the CH<sub>3</sub> photofragments point to significantly altered CH<sub>3</sub>I dissociation dynamics when adsorbed on C<sub>6</sub>H<sub>6</sub>, C<sub>6</sub>H<sub>5</sub>F and C<sub>6</sub>H<sub>4</sub>F<sub>2</sub> thin films, with progressive changes in the observed dynamics as higher fluorobenzenes are used (up to C<sub>6</sub>F<sub>6</sub>). The altered CH<sub>3</sub>I photodissociation dynamics and coincidentally increased effective photodissociation cross sections are ascribed to a new pathway with initial photoabsorption in the aromatic thin film, and the excitation energy being efficiently transported to the CH<sub>3</sub>I adsorbed on top. There is evidence that excitons in the aromatic thin film play a significant role in the transport and transfer of the electronic excitation to the CH<sub>3</sub>I top layer.

## References

- [1] Dubois, J.T. and Noyes Jr., W.A., *Photochemical Studies XLVI: Photosensitization by Benzene and Pyridine Vapours*, J. Chem. Phys. **19**, 1512 (1951).
- [2] Jensen, E.T., *Contrasting Mechanisms for Photodissociation of Methyl Halides Adsorbed on Thin Films of C<sub>6</sub>H<sub>6</sub> and C<sub>6</sub>F<sub>6</sub>*. Phys. Chem. Chem. Phys.

**5:20pm SS+HC-TuA-10 UV-Induced Oxidation of Aluminum, Robert Berg, C. Tarrío, T. Lucatorto**, National Institute of Standards and Technology (NIST); **F. Eparvier, A. Jones**, Laboratory for Atmospheric and Space Physics

Aluminum oxide films are usually grown on aluminum metal by anodization in a liquid electrolyte (thick films) or heating in the presence of oxygen gas (thin films). A third way is to expose the aluminum to ultraviolet radiation (UV) in the presence of water vapor. We devised a model of such oxidation that combined descriptions of photoemission from the Al metal, electron-phonon scattering in the oxide, Al<sup>3+</sup> ion transport in the oxide, and the adsorption and ionization of H<sub>2</sub>O on the oxide surface. It also accounted for UV-induced desorption of H<sub>2</sub>O and the effect of the Al<sup>3+</sup> ion flux on the surface reactions.

The model's five free parameters were fit to our measurements of UV-induced oxidation of aluminum. The UV, which was produced by filtering synchrotron radiation, comprised wavelengths from 150 nm to 480 nm, and the H<sub>2</sub>O pressure was varied between 3 × 10<sup>-8</sup> mbar and 1 × 10<sup>-4</sup> mbar. Exposures lasted from 3 hours to 20 days. An exposure with oxygen instead of water caused oxidation consistent with the background H<sub>2</sub>O pressure; the oxygen caused no additional oxidation.

The parameter values fitted to our measurements allowed us to describe the oxidation of aluminum membranes that were used to filter extreme UV wavelengths on the Solar Dynamics Observatory, a sun-observing satellite. This new understanding will help prevent similar problems on future satellites. These results are the first experimental confirmation of a model of UV-induced oxidation.

**5:40pm SS+HC-TuA-11 Self-Induced and Progressive Photo-Oxidation of Organophosphonic Acid Grafted Titanium Dioxide, Nick Gys**, Vrije Universiteit Brussel, Belgium; **B. Pawlak**, Hasselt University, Belgium; **K. Marcoen**, Vrije Universiteit Brussel, Belgium; **G. Reekmans**, Hasselt University, Belgium; **L. Fernandez Velasco**, Royal Military Academy, Belgium; **R. An**, University of Antwerp, Belgium; **K. Wyns**, Flemish Institute for Technological Research, Belgium; **K. Baert**, Vrije Universiteit Brussel, Belgium; **K. Zhang, L. Lufungula**, University of Antwerp, Belgium; **A. Piras**, Hasselt University, Namur University, Belgium; **L. Siemons**, University of Antwerp, Belgium; **B. Michiels**, Flemish Institute for Technological Research, Belgium; **S. Van Doorslaer, F. Blockhuys**, University of Antwerp, Belgium; **T. Hauffman**, Vrije Universiteit Brussel, Belgium; **P. Adriaensens**, Hasselt University, Belgium; **S. Mullens**, Flemish Institute for Technological Research, Belgium; **V. Meynen**, University of Antwerp, Belgium

The introduction of organic molecules onto the surface of metal oxides through surface grafting provides the ability to tailor the surface properties towards an increased specificity and control of interactions. In the field of hybrid organic-inorganic materials, organophosphonic acid (PA) grafted metal oxides are becoming increasingly more prominent given their versatility in surface tuning and their specific merits in applications ranging from supported metal catalysis<sup>[1]</sup>, hybrid (photo)-electric devices<sup>[2]</sup>, biosensing<sup>[3]</sup> and sorption and separation processes.<sup>[4]</sup> While synthesis-properties-performance correlations are being studied for organophosphonic acid grafted TiO<sub>2</sub>, their stability and the impact of exposure conditions on possible changes in the interfacial surface chemistry remain unexplored. In addition, a differentiation in the stability of the organic group (carbon chain) and the M-O-P bonds is missing. In this study<sup>[5]</sup>, the impact of different ageing conditions on the evolution of the surface properties of propyl- and 3-aminopropylphosphonic acid grafted mesoporous TiO<sub>2</sub> over a period of 2 years is reported, using solid-state <sup>31</sup>P and <sup>13</sup>C NMR, ToF-SIMS, EPR and XPS as main techniques. In humid conditions under ambient light exposure, PA grafted TiO<sub>2</sub> surfaces initiate and facilitate photo-induced oxidative reactions, resulting in the formation of phosphate species and degradation of the grafted organic group with a loss of carbon content ranging from 40 to 60 wt%. Since exposure under dry air does not result in ageing phenomena, humidity and more specifically, the interactions of adsorbed water with the grafted surface, play a fundamental role in the ageing process. By revealing the underlying ageing mechanism, solutions were provided to prevent degradation. This work creates critical awareness in the research community working on hybrid titania materials and other possible photo-active materials to evaluate changes in photo-activity and stability after surface grafting.

1. F. Forato et al., Chem. - A Eur. J. **24**, 2457–2465 (2018).
2. H. Chen, W. Zhang, M. Li, G. He, X. Guo, Chem. Rev. **120**, 2879–2949 (2020).

# Tuesday Afternoon, November 7, 2023

3. N. Riboni et al., RSC Adv. 11, 11256–11265 (2021).
4. G. A. Seisenbaeva et al., RSC Adv. 5, 24575–24585 (2015).
5. N. Gys et al., Chempluschem. 88 (2023), doi:10.1002/cplu.202200441.

6:00pm **SS+HC-TuA-12 "Laser-XPS" invented 1989 in Japan, Patented 1997, B. Vincent Crist**, XPS Library

In 1989, a novel technique, Laser-XPS, was developed. Laser-XPS uses XPS to probe the core level surface chemical physics of various solid state materials while the materials are held in an ultra-high vacuum (UHV) chamber and irradiated with CW tunable organic dye or argon ion lasers. These two tunable CW lasers provide energy in the 1.9-3.5 eV range (655-351 nm, 44-81 Kcal/mol) with power levels ranging from 100-1,000 mW. A dynamic mode of operation uses XPS to directly measure the electronic nature of the photo-excited states, the photo-thermal effects, and the lifetimes of the associated initial and final states produced by the tunable CW laser irradiation. Several reversible phenomena, which are wavelength or power level dependent, were observed via the dynamic mode. These phenomena include: energy shifts in XPS signals, changes in XPS peak widths, charge control quality, and phosphorescence during XPS. A sequential mode of operation makes it possible to study the non-reversible effects of irradiating materials under UHV conditions with CW lasers. Non-reversible phenomena observed via the sequential mode include: surface chemical reactions, elimination of adventitious carbon contamination, elimination of oxygen species associated with the presence of water, hydroxides, or carbonates, color changes, outgassing, and melting. The initially expected energy shifting of a specific XPS signal within a complex spectrum of XPS signals from very similar chemical species due to narrow, selective photo-excitation of specific valence bands, was, however, not realized in this preliminary study.



# Wednesday Morning, November 8, 2023

## Applied Surface Science Division

Room B117-119 - Session

AS+2D+CA+EL+EM+MS+NS+SE+SS+TF-WeM

### Multi-Modal & Multi-Dimensional Analysis

**Moderators:** Gustavo Trindade, National Physical Laboratory, UK, Paul Mack, Thermo Fisher Scientific, UK, Tim Nunney, Thermo Fisher Scientific, UK

8:00am AS+2D+CA+EL+EM+MS+NS+SE+SS+TF-WeM-1 **Growth and Characterization of Large-Area 2D Materials**, Glenn Jernigan, US Naval Research Laboratory **INVITED**

Nothing could be more coupled than Growth and Characterization. When two dimensional (2D) materials appeared on the radar of the scientific community (with the amazing properties of graphene), it was immediately obvious that large area samples would be needed. Exfoliating flakes was insufficient for the demands of scientific studies, in addition to not being viable should a commercial application be developed. Thus, the search began for growth methods to produce large-area 2D materials for large scale testing and development.

The Naval Research Laboratory has, over the past 15 years, pursued research programs in producing large areas of graphene, transition metal dichalcogenides (TMDs), boron nitride (BN), and other 2D materials. In every one of those programs, they began with surface analysis of composition, chemistry, and morphology of the grown films. The uniquely sensitive nature of x-ray and ultraviolet photoelectron spectroscopy (XPS and UPS) and scanning tunneling and atomic force microscopy (STM and AFM) to 2D materials was necessary to measure the electrical, chemical, and physical properties obtained in the large area films and to understand what was observed in the exfoliated flakes. The production of large areas allowed "mass-scale" optical and electrical characterization, which then became a feedback loop in the search for new and interesting properties and relevant applications. In this presentation, I will show how we developed large-area graphene, by both epitaxial growth and chemical vapor deposition methods, TMDs, and other 2D materials for characterization and device utilization.

8:40am AS+2D+CA+EL+EM+MS+NS+SE+SS+TF-WeM-3 **Using a Correlative Approach with XPS & SEM to Measure Functionalized Fabrics for Antimicrobial Applications**, Tim Nunney, H. Tseng, Thermo Fisher Scientific, UK; D. Marković, M. Radetić, University of Belgrade, Serbia

Medical textiles are an indispensable component for a wide range of hygienic and healthcare products, such as disposable surgical gowns and masks, or personal protection equipment, with opportunities to provide further protection by engineering textiles with suitable medical finishing. While antibiotics are considered a viable option for their efficiency in treating bacterial infections, their abuse can result in adverse effects, e.g., bacteria resistance. Nanocomposites have emerged as a promising alternative to antibiotics, as the large surface-to-volume ratio and high activity helps attain the targeted antimicrobial efficiency by using tiny amounts of nanocomposites, and their biocompatibility and scalability are particularly advantageous for medical applications [1]. Thus, developing processing methods to integrate nanocomposites in the fabrics is essential for exploiting their properties for medical textiles.

In this study, polypropylene fabrics, alginate and copper oxides, were selected to develop novel antimicrobial nanocomposites based on various surface treatments, i.e. corona discharge and alginate impregnation, which led to improved fabrics hydrophilicity with functional groups introduced as binding sites for Cu(II), a precursor that formed Cu nanoparticles when reacted with reducing agents, i.e. NaBH<sub>4</sub> and ascorbic acid. The composition of the fabrics after being treated with corona discharge and impregnation observed by XPS indicates the materials formed mainly consisted of C and O, attributed to the presence of a thin, hydrophilic layer and alginate, respectively, consistent with depth profiling measurements. Following Cu reduction, XPS mapping of the fabrics finds that, reacting with ascorbic acid resulted in formation of nanocomposites containing a mixture of Cu and Cu (II) oxides across the surface, which could be visualised by using SEM in the same locations. Excellent anti-microbial activity against Gram-negative bacteria *E. coli*, Grampositive bacteria *S. aureus* and yeast *C. albicans* was observed for the treated fabrics[2]. This result not only demonstrates a cleaner, and healthier approach for developing novel nanocomposites, but more importantly highlights the role of surface

techniques in uncovering challenges in designing and engineering functional textiles.

References:

[1] D. Marković, J. Ašanin, T. Nunney, Ž. Radovanović, M. Radoičić, M. Mitrić, D. Mišić, M. Radetić, *Fibers. Polym.*, 20, 2317–2325 (2019)

[2] D. Marković, H.-H. Tseng, T. Nunney, M. Radoičić, T. Ilic-Tomic, M. Radetić, *Appl. Surf. Sci.*, 527, 146829, (2020)

9:00am AS+2D+CA+EL+EM+MS+NS+SE+SS+TF-WeM-4 **Multi-Modal Analysis in Photoelectron Spectroscopy: From High-Resolution Imaging to Operando Experiments**, Olivier Renault, CEA-Leti, France; A. Benayad, CEA, France; N. Gauthier, CEA-Leti, France; R. Charvier, ST Microelectronics, France; E. Martinez, CEA-Leti, France

Over the past years, the field of surface and interface analysis has been greatly expanded by new developments made possible by lab-scale instruments enabling higher excitation energies. These new developments are directly serving technological advances especially in the area of technologies in renewable energies and nanoelectronics, which are addressing more and more complex system requiring to go beyond traditional ways of characterizing surfaces and interfaces. Different dimensions are to be explored in multi-modal surface analysis : the depth dimension, the lateral dimension, and the dynamic dimension.

After a short review of some of the achievements towards enhancing the depth dimension by lab-scale hard X-ray photoelectron spectroscopy (HAXPES) and the lateral dimension using X-ray PEEM, we will present different application cases of *operando* HAXPES. Here, the material is analyzed as being part of a device operated *in situ* during the experiment, in conditions that are as close as possible to the final applications and where the interfaces can be studied in dynamic conditions. We will first review some results of *operando* HAXPES on resistive memories obtained with synchrotron radiation [1, 2] before presenting various lab-scale experiments [3, 4] and the current limitations to such approaches.

[1]B. Meunier, E. Martinez, O. Renault et al. *J. Appl. Phys.* **126**, 225302 (2019).

[2]B. Meunier, E. Martinez, O. Renault et al., *ACS Appl. Electron. Mater.* **3** (12), 5555–5562 (2021).

[3]O. Renault et al., *Faraday Disc.* **236**, 288-310 (2022).

[4]A. Benayad et al., *J. Phys. Chem. A* 2021, 125, 4, 1069-81.

9:20am AS+2D+CA+EL+EM+MS+NS+SE+SS+TF-WeM-5 **Multi-Modal Analyses of Ultrasonic-Spray-Deposited Ultrathin Organic Bathocuproine Films**, J. Chen, Juliet Risner-Jamtgaard, T. Colburn, A. Vaillionis, A. Barnum, M. Golding, Stanford University; K. Artyushkova, Physical Electronics; R. Dauskardt, Stanford University

Bathocuproine (BCP) is a small organic molecule that is typically used as an ultrathin hole blocking interlayer (< 10 nm thickness) in organic solar cells and perovskite solar cells. The film is typically deposited via low-throughput vacuum thermal evaporation with an *in-situ* Quartz Crystal Monitor to measure film thickness. Open-air ultrasonic spray deposition for low-cost and large-scale deposition is an attractive alternative method for solution processing of BCP films, but the process lacks a comparable *in-situ* metrology. Given that the BCP film is transparent to visible light and ultrathin, it is important to utilize a multi-modal approach to evaluate optoelectronic and physical properties of the sprayed film.

A suite of characterization techniques that span a range of equipment complexity, measurement time, and measurement sensitivity are used to analyze the BCP films. We begin by demonstrating the limitations of the singular ellipsometry model<sup>1</sup> for BCP found in literature and motivate a need to rely on other techniques. Multi-modal analyses including X-Ray Reflectivity, Angle-Resolved X-ray Photon Spectroscopy (AR-XPS), Auger Spectroscopy, Scanning Electron Microscopy, and Transmission Electron Microscopy with EELS are then performed on the sprayed BCP film. The advantages and disadvantages of each characterization technique are compared and discussed. We conclude that AR-XPS provides the most distinctive determination of individual layer thicknesses for a sample architecture consisting of silicon substrate/native SiO<sub>2</sub>/BCP across the applicable range of AR-XPS from ~ 1-10 nm.

# Wednesday Morning, November 8, 2023

<sup>[1]</sup>Liu, Z.T., *et al.* The characterization of the optical functions of BCP and CBP thin films by spectroscopic ellipsometry. *Synthetic Materials*. 150(2):159-163. (2005)

9:40am **AS+2D+CA+EL+EM+MS+NS+SE+SS+TF-WeM-6 Combinatorial Synthesis and High-Throughput Characterization of Pt-Au Thin Films Fabricated by Confocal Magnetron Sputter Deposition, David Adams, R. Kothari, M. Kalaswad, C. Sobczak, J. Custer, S. Addamane, M. Jain, E. Fowler, F. DelRio, M. Rodriguez, R. Dingreville, B. Boyce, Sandia National Laboratories**

A few binary metal alloys are predicted to form thermally stable, compositionally segregated structures owing to the thermodynamic preference for minority species to collect and remain at grain boundaries established within the solid. (J.R. Trelewicz *et al.*, PRB, 2009) When produced as a nanocrystalline thin film, these stable structures afford the potential to maintain excellent mechanical properties (e.g., high hardness) even after annealing to elevated temperature. Indeed, several systems, including Pt<sub>9</sub>Au<sub>1</sub> thin films, are reported to develop thermally-stabilized, hard, nanocrystalline structures attributed to solute segregation at grain boundaries. (P. Lu *et al.*, *Materialia*, 2019)

Future studies that seek optimal stoichiometry and/or preferred synthesis processes require access to a wide range of composition as well as an ability to vary key deposition parameters. Toward this end, our team reports on the challenges and the benefits of combinatorial synthesis for expediting the discovery of improved binary metal thin films. Our study utilized confocal sputter deposition wherein Pt and Au targets were individually sputtered via pulsed DC magnetron methods. Substrates (150 mm diameter wafers) were fixed in order to gain access to a wide compositional range for each deposition. The sputter power and cathode tilt orientation were then varied in subsequent depositions to access the nearly full binary metal compositional range. The binary collision Monte Carlo program SiMTra (D. Depla *et al.*, *Thin Solid Films* 2012), which simulates the transport of sputtered atoms within the process gas, helped guide the selection of these process parameters in order to achieve compositional goals in relatively few depositions. Notably, the binary compositions predicted by SiMTra closely matched (within a few molar %) the measured compositions determined by Wavelength Dispersive Spectroscopy completed in 112 different areas across each wafer. The various combinatorial Pt-Au films were further characterized by high-throughput Atomic Force Microscopy, automated X-ray Diffraction, fast X-ray Reflectivity, mapping four-point probe sheet resistance, and automated nanoindentation. These studies reveal how hardness, modulus, film density, crystal texture, and resistivity of combinatorial films varied with composition as well as the atomistics of film deposition. Attempts to correlate key film characteristics with the kinetic energies and incident angles of arriving metal species (estimated by SiMTra) are discussed with a goal of improving fabrication processes.

Sandia National Laboratories is managed and operated by NTESS under DOE NNSA contract DE-NA0003525.

11:00am **AS+2D+CA+EL+EM+MS+NS+SE+SS+TF-WeM-10 Optical and X-Ray Characterization and Metrology of Si/Si(1-x)Ge(x) Nanoscale Superlattice Film Stacks and Structures, Alain Diebold, SUNY Polytechnic Institute INVITED**

As traditional scaling of transistors comes to end, transistor channels and capacitors are being stacked to form new 3D transistor and memory devices. Many of these devices are fabricated using films stacks consisting of multiple Si/Si(1-x)Ge<sub>x</sub> layers known as superlattices which must be fabricated with near atomic precision. In this talk, we discuss how Optical and X-Ray methods are used to measure the feature shape and dimensions of these structures. The use of X-Ray methods such as  $\omega$ -2 $\theta$  scans and reciprocal space maps provide layer thickness and stress characterization. We will use simulations to show how a buried layer with a different thickness or Ge concentration alters the data. Recent electron microscopy studies have quantified the stress at the interfaces of these superlattices. We will also discuss how Mueller Matrix spectroscopic ellipsometry (MMSE) based scatterometry is used to measure feature shape and dimension for the nanowire/nanosheet structures used to fabricate nanosheet transistors and eventually 3D DRAM. The starting point for optical scatterometry is determining the optical properties of stressed pseudomorphic Si(1-x)Ge<sub>x</sub>. MMSE can be extended into the infra-red and into the EUV. In addition, small angle X-Ray scattering has been adapted into a method known as CDSAXS which can be used to characterize these structures. This talk will be an overview of these methods.

11:40am **AS+2D+CA+EL+EM+MS+NS+SE+SS+TF-WeM-12 Non-Destructive Depth Differentiated Analysis of Surfaces Using Ion Scattering Spectroscopy (ISS), XPS and HAXPES, Paul Mack, Thermo Fisher Scientific, UK**

Recently there has been renewed interest in probing deeper into surfaces using HAXPES in addition to the more surface sensitive (soft X-ray) XPS. On modern XPS systems, with high sensitivity, the total sampling depth may be somewhere between 10nm and 15nm but HAXPES enables the analyst to look deeper, without having to destructively sputter the surface with ions. For a complementary, more comprehensive analysis, XPS and HAXPES can be combined with Ion Scattering Spectroscopy (ISS). ISS is far more surface sensitive than XPS, typically being thought of as a technique to analyse the top monolayer of a sample for elemental information.

In this work, the combination of XPS, HAXPES and ISS on a single tool has been used to give a non-destructive depth differentiated analysis of a range of samples, including a perovskite and an industrially relevant material containing multiple transition metals. The combination of all three techniques provides insight into the depth distributions of elements and chemical states, from the top monolayer to beyond 20nm into the surface.

12:00pm **AS+2D+CA+EL+EM+MS+NS+SE+SS+TF-WeM-13 Towards Measurement of Molecular Shapes Using OrbiSIMS, Gustavo F. Trindade, J. Vorng, A. Eyres, I. Gilmore, National Physical Laboratory, UK**

An OrbiSIMS [1] instrument features a dual analyser configuration with a time-of-flight (ToF) mass spectrometer (MS) and an Orbitrap™ MS, which confer advantages of speed and high-performance mass spectrometry, respectively. The ability to combine the MS performance usually found in a state-of-the-art proteomics and metabolomics MS with 3D imaging at the microscale and from nanolayers of <10 nm of material has proved popular in a broad field of application from organic electronics to drug discovery. For secondary ions to be efficiently transferred to the Orbitrap analyser, the sample is biased by a target voltage  $V_T$  necessary to match the acceptance window of the Orbitrap. Furthermore, the ions kinetic energy from the SIMS collision process must be reduced. Therefore, in the OrbiSIMS, a transfer system with helium gas at a pressure  $P_{He}$  slows the ions and reduces their kinetic energy distribution through inelastic collisions with gas atoms. Usually, an Orbitrap is used with an ambient pressure ion source and so here an extra gas flow of nitrogen is introduced that leads to an increase of pressure  $P_{N_2}$  to compensate.

We conducted a systematic assessment of  $V_T$  and  $P_{He}$  and  $P_{N_2}$  on the transmitted secondary ion intensities [2] and revealed a complex behaviour, indicating the possibility for additional separation of ions based on their shape, stability, and kinetics of formation. We showed that the  $V_T$  for maximum transmission of secondary ions will not be the same for all molecules of the same material and that sometimes multiple maxima exist. Here, we present recent progress towards the understanding of these phenomena and how we are leveraging it to measure molecular shape by using reference trisaccharides raffinose, maltotriose and melizitose [3].

[1] M. K. Passarelli *et al.*, "The 3D OrbiSIMS—label-free metabolic imaging with subcellular lateral resolution and high mass-resolving power," *Nat. Methods*, no. november, p. nmeth.4504, 2017, doi: 10.1038/nmeth.4504.

[2] L. Matjacic *et al.*, "OrbiSIMS metrology part I: Optimisation of the target potential and collision cell pressure," *Surf. Interface Anal.*, no. November 2021, pp. 1–10, 2021, doi: 10.1002/sia.7058.

[3] G.F. Trindade *et al.*, In preparation.

# Wednesday Morning, November 8, 2023

## Fundamental Discoveries in Heterogeneous Catalysis Focus

### Topic

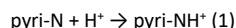
### Room B113 - Session HC+SS-WeM

### Origins of Single Atom Catalysis

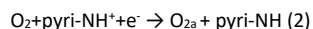
**Moderators:** Rachael Farber, University of Kansas, Gareth Parkinson, TU Wien

8:00am **HC+SS-WeM-1 Role of Pyridinic Nitrogen in the Mechanism of the Oxygen Reduction Reaction on Carbon Electrocatalysts**, *Kotaro Takeyasu*, University of Tsukuba, Japan; *S. Singh*, Shiv Nadar University, India; *K. Homma*, *K. Hayashida*, University of Tsukuba, Japan; *S. Ito*, *T. Morinaga*, National Institute of Technology, Tsukuba College, Japan; *Y. Endo*, *M. Furukawa*, University of Tsukuba, Japan; *T. Mori*, National Institute for Materials Sciences (NIMS), Japan; *H. Ogasawara*, SLAC National Laboratory; *J. Nakamura*, International Institute for Carbon-Neutral Energy Research, Kyushu University, Japan

Nitrogen doped carbon catalysts are promising Pt-free catalysts for the oxygen reduction reaction (ORR) in polymer electrolyte fuel cells owing to the high durability and the high activity in alkaline media. The primary active site in N-doped carbon catalysts is the pyridinic nitrogen (pyri-N), which is bound to two carbon atoms with negative charge.[1] However, a large barrier of N-doped carbon catalysts for the commercial usage is the decreased activity in acidic media. Hence, we investigated this deactivation phenomenon to widen the applicability of N-doped carbon catalysts. In acidic media, the protonation of pyri-N (pyri-NH<sup>+</sup>) occurs as the first step owing to the basicity of pyri-N.



As the following process, we have demonstrated the electrochemical reduction of pyri-NH<sup>+</sup> coupled with thermal O<sub>2</sub> adsorption on carbon atoms near pyri-NH<sup>+</sup> using model catalysts:



In this reaction, the thermal adsorption of O<sub>2</sub> let the electrochemical reduction of pyri-NH<sup>+</sup> to pyri-NH thermodynamically favorable due to the adsorption energy of O<sub>2</sub>. Although the formation of pyri-NH<sup>+</sup> is a cause of the decrease in ORR activity, but pyri-NH<sup>+</sup> itself is essential for the formation of pyri-NH and the adsorption of O<sub>2</sub>. A key point is that a doped electron into π\* orbital of π-conjugative system near pyri-NH promotes the adsorption of O<sub>2</sub>. However, the hydration of pyri-NH<sup>+</sup> forming pyri-NH<sup>+</sup> · (H<sub>2</sub>O)<sub>n</sub> causes a lower shift in the redox potential and consequently, Eq. 2 becomes the rate-determining step (RDS). Therefore, we consider that the hydration of pyri-NH<sup>+</sup> is the main cause of the decrease in ORR activity in acid electrolytes.[2] Thus, we hypothesize an enhanced ORR activity by the introduction of hydrophobicity in the vicinity of pyri-NH<sup>+</sup>, suppressing the extent of hydration.

Introducing the hydrophobic cavity prevented the hydration of pyri-NH<sup>+</sup> but inhibited the proton transport. We then increased proton conductivity in the hydrophobic cavity by introducing SiO<sub>2</sub> particles coated with ionic liquid polymer/Nafion® which kept the high onset potentials with an increased current density even in acidic media.[3]

### References

- [1] D. Guo, J. Nakamura et al., *Science*, 2016, 351, 361-365.
- [2] K. Takeyasu, J. Nakamura et al., *Angew. Chem. Int. Ed.* 60, 5121 (2021).
- [3] S. K. Singh, K. Takeyasu, J. Nakamura et al., *Angew. Chem. Int. Ed.* 61, e202212506 (2022).

8:20am **HC+SS-WeM-2 Atomic-Level Studies of Mono-Carbonly and Gem-Dicarbonyl Formation on Rh-Decorated Fe<sub>3</sub>O<sub>4</sub>(001)**, *Panukorn Sombut*, *C. Wang*, *L. Puntischer*, *M. Meier*, *J. Pavelec*, *Z. Jakub*, *M. Schmid*, *U. Diebold*, TU Wien, Austria; *C. Franchini*, University of Vienna, Austria; *G. Parkinson*, TU Wien, Austria

Understanding the interaction between reactant molecules and “single atom” active sites is important for comprehending the evolution of single-atom catalysts in reactive atmospheres. Here, we study how Fe<sub>3</sub>O<sub>4</sub>(001)-

supported<sup>1</sup> Rh<sub>1</sub> monomers and Rh<sub>2</sub> dimer species interact with CO using density functional theory (DFT), combined with temperature-programmed desorption, x-ray photoelectron spectroscopy, and in-situ scanning tunneling microscopy techniques. Our results show that stable Rh<sub>1</sub>(CO)<sub>1</sub> monocarbonyls are the exclusive product of CO adsorption at both 2-fold and 5-fold coordinated Rh<sub>1</sub> sites, but the different coordination environment leads to different adsorption energies. The DFT calculations reveal that the Rh<sub>1</sub>(CO)<sub>1</sub> formed at the 5-fold coordinated Rh<sub>1</sub> site adopts an octahedral structure, while the Rh<sub>1</sub>(CO)<sub>1</sub> formed at the 2-fold coordinated Rh<sub>1</sub> site forms an additional bond to a subsurface oxygen atom of the support, leading to a pseudo-square planar structure. The direct addition of a second CO molecule to Rh<sub>1</sub>(CO)<sub>2</sub> at the 2-fold coordinated Rh<sub>1</sub> site to form a Rh<sub>1</sub>(CO)<sub>2</sub> gem-dicarbonyl is energetically favorable according to DFT; however, this process is not observed in experiments under UHV conditions. Instead, we observe the formation of limited Rh<sub>2</sub>(CO)<sub>2</sub> exclusively via the CO-induced breakup of Rh<sub>2</sub> dimers, in agreement with DFT results, which suggest an unstable Rh<sub>2</sub>(CO)<sub>3</sub> intermediate.

1. Blum, R. *et al.* Subsurface cation vacancy stabilization of the magnetite (001) surface. *Science* **346**, 1215–1218 (2014).

8:40am **HC+SS-WeM-3 A Few Questions About Single Atom Catalysts: When Theory Helps**, *Gianfranco Pacchioni*, University of Milano-Bicocca, Italy **INVITED**

In the past, single atom catalysts (SACs) could not be clearly visualized and characterized due to the limitations associated with instrumental resolution. Today this is a new frontier in heterogeneous catalysis due to the high activity and selectivity of SACs for various catalytic reactions. This has opened various questions for theory. One is where are the atoms and what is the stability of SACs in working conditions. In order to address these questions, we will discuss the nature of isolated metal species deposited on oxide surfaces (TiO<sub>2</sub> and ZrO<sub>2</sub> in particular). These systems have been characterized experimentally using high-resolution scanning transmission electron microscopy (STEM), Fourier transform infrared spectroscopy (FTIR), and temperature programmed desorption (TPD) spectra of adsorbed CO probe molecules. Combining these data with extensive Density Functional Theory (DFT) calculations one can provide an unambiguous identification of the stable single-atom species present on these supports and of their dynamic behavior.

The other question that can be addressed by theory is the prediction of the behavior of SACs in electrocatalytic processes such as the oxygen reduction (ORR), the oxygen evolution (OER) and the hydrogen evolution (HER) reactions. In this context we assist to a rapidly growing number of DFT studies and of proposals of universal descriptors that should provide a guide to the experimentalist for the synthesis of new catalysts, in particular related to graphene-based SACs. We will critically analyze some of the current problems connected with these DFT predictions: accuracy of the calculations, neglect of important contributions in the models used, physical meaning of the proposed descriptors, inaccurate data sets used to train machine learning algorithms, not to mention some severe problems of reproducibility. It follows that the “rational design” of a catalyst based on some of the proposed universal descriptors or on the DFT screening of large number of structures should be considered with some caution.

9:20am **HC+SS-WeM-5 A Multi-Technique Study Of Ethylene and H<sub>2</sub> Adsorption on Rh<sub>1</sub>/Fe<sub>3</sub>O<sub>4</sub>**, *Gareth Parkinson*, *C. Wang*, *P. Sombut*, *L. Puntischer*, TU Wien, Austria

The hydroformylation of alkenes has emerged as one of the most interesting applications of “single-atom” catalysis. Nevertheless, there have been relatively few fundamental studies into how the reactants (CO, alkene, and H<sub>2</sub>) bind at the active site. In this talk I will show STM, XPS, TPD and DFT results to illustrate how C<sub>2</sub>H<sub>4</sub> and H<sub>2</sub> interact with a Rh<sub>1</sub>/Fe<sub>3</sub>O<sub>4</sub>(001) model catalyst. Ethylene binds strongly at the Rh<sub>1</sub> sites, but there is very little evidence for the formation of di-ethylene species under UHV conditions. H<sub>2</sub> adsorbs as a dihydride at the Rh<sub>1</sub> sites, and desorbs close to room temperature in TPD experiments without spilling over onto the oxide support. Evidence for the co-adsorption of the different reactants will be discussed in the context of the hydroformylation reaction.

9:40am **HC+SS-WeM-6 Remote Activation of H–H bonds by Platinum in Single-Atom Alloy Catalysts**, *Francisco Zaera*, University of California Riverside

With heterogeneous catalysts, chemical promotion takes place at their surfaces. Even in the case of single-atom alloys (SAA), where a reactive

# Wednesday Morning, November 8, 2023

metal is atomically dispersed in small quantities within the main host, it is assumed that both elements are exposed and available to bond with the reactants. Here we show, on the basis of *in situ* x-ray absorption spectroscopy data, that the Pt atoms in Cu-Pt SAA catalysts are located at the inner interface between the metal nanoparticles and the silica support instead. Kinetic experiments indicated that these catalysts still display better selectivity for the hydrogenation of unsaturated aldehydes to unsaturated alcohols than the pure metals. Quantum mechanics calculations not only corroborated the particular stability of Pt at the metal-support interface, but also explained the catalytic performance improvement as due to a remote lowering of the activation barrier for the scission of the H-H bond in molecular hydrogen at Cu sites by the internal Pt atoms.

11:00am **HC+SS-WeM-10 Electrifying Industrial Chemistry at the Molecular Level: Controlling the Electrocatalytic Transformation of Alcohols and Alkanes to Valuable Products, Marcel Schreier, University of Wisconsin-Madison** **INVITED**

Producing fuels and chemicals using renewable electricity holds the promise to enable a truly sustainable circular economy based on sustainably produced carriers of electrical energy and sustainably produced chemicals. To date, the vast majority of electrocatalytic reactions are limited to the transformation of small inorganic molecules such as CO<sub>2</sub>, H<sub>2</sub>O, N<sub>2</sub>, as well as the oxidation and reduction of alcohols. However, comprehensive electrification of the chemical industry will require electrocatalytic reactions that can promote the transformations of C(sp<sup>3</sup>)-H and C(sp<sup>3</sup>)-C(sp<sup>3</sup>) bonds, which are central to today's industry.

In this presentation, I will show how fundamental understanding of the interfacial processes occurring in electrocatalytic reactions can be exploited to expand the reaction scope of electrocatalysis to the transformation of complex substrates involving the controlled activation of C-H and C-C bonds. In a first step, I will show how this approach allows us to transform ethanol to ethylene oxide, an important plastic precursor. Subsequently, I will discuss methods to electrocatalytically transform inert alkanes such as methane and ethane at room temperature.

11:40am **HC+SS-WeM-12 Probing Elementary Steps and Catalyst Structure Evolution: Insights into Formic Acid Conversion on Rh/Fe<sub>3</sub>O<sub>4</sub>(001) Model Catalysts, Zdenek Dohnalek, Pacific Northwest National Laboratory**

Single-atom catalysis represents an exciting area of research due to the potential to qualitatively transform the activity and selectivity of supported metal catalysts. However, our fundamental understanding of their stability under reaction conditions is limited. To address this gap, we employed scanning tunneling microscopy (STM), X-ray photoelectron spectroscopy (XPS), and temperature programmed desorption (TPD). We prepared well-characterized model Rh/Fe<sub>3</sub>O<sub>4</sub>(001) catalysts with distinct types of Rh single-atom sites. In model catalytic studies, we investigated the effect of reactants on the structure and activity of such Rh/Fe<sub>3</sub>O<sub>4</sub>(001) catalysts. Formic acid, which deprotonates to surface formate and hydroxyl species, is employed as a model to follow the fate of dehydration and dehydrogenation reaction channels. We demonstrate that small amounts of Rh adatoms induce a shift from the dehydration pathway yielding CO on bare Fe<sub>3</sub>O<sub>4</sub>(001) to dehydrogenation yielding CO<sub>2</sub> on Rh<sub>ad</sub>-Fe<sub>3</sub>O<sub>4</sub>(001). Multiple turnovers are achieved on each Rh<sub>ad</sub> during the single TPD sweep. As Rh adatoms are highly unstable, we further studied the Rh stabilized in octahedral iron sites within the Fe<sub>3</sub>O<sub>4</sub>(001) surfaces that are stable on high surface area Rh/Fe<sub>3</sub>O<sub>4</sub> catalysts. A similar shift from dehydration to dehydrogenation is observed, but much higher coverages of Rh are required. We showed that adsorbed species transiently destabilize Rh<sub>oct</sub> and lead to the formation of Rh<sub>ad</sub>, which is only present during the reaction. Independent studies of hydroxylated surfaces reveal that surface OHs are responsible for the Rh<sub>oct</sub> destabilization and conversion to active Rh<sub>ad</sub> species. Studies of elementary reaction steps and catalyst dynamics on well-defined model systems are critical for the future design of catalysts with maximum activity and selectivity.

12:00pm **HC+SS-WeM-13 Hydrogen and Hydrocarbon Reactions on Single-Atom RhCu(100), Laurin Joseph, M. Powers, J. Rosenstein, A. Utz, Tufts University**

A class of catalysts called single-atom alloys allow for the combination of a more reactive, more expensive dopant metal dispersed within a less active, more selective, and cheaper base metal. These catalysts have been well characterized and studied using techniques such as temperature programmed desorption (TPD), scanning tunneling microscopy (STM), and reflection absorption infrared spectroscopy (RAIRS). However, the detailed,

molecular-level bond activation energetics and kinetics have not yet been experimentally interrogated for high-barrier reactions on these catalysts—a region where more efficient catalysts are most sorely needed.

We will present recent results that first characterize the dissociation and spillover of H resulting from both atomic and molecular H<sub>2</sub> adsorption on base Cu(100) and RhCu(100) single atom alloy, and then describe results from energy resolved molecular beam studies of CH<sub>4</sub> dissociation that quantify reaction probability as a function of energy distribution among reactant and surface degrees of freedom. We expect these studies will reveal new insights into the molecular mechanism for an important class of heterogeneously catalyzed reactions and provide new benchmarks for computational studies of single atom catalysts.

## Surface Science Division

### Room D136 - Session SS+2D+AS+HC-WeM

#### Surface Science of 2D Materials

**Moderators: Irene Groot, Leiden University, The Netherlands, Bo-Hong Liu, National Synchrotron Radiation Research Center**

8:00am **SS+2D+AS+HC-WeM-1 Heterogeneous Photocatalysis: Alcohols on Bare and Metal-loaded TiO<sub>2</sub>(110) and Fe<sub>2</sub>O<sub>3</sub>(012), Moritz Eder, TU Wien, Austria; P. Petzoldt, M. Tschurl, Technical University of Munich, Germany; J. Pavelec, M. Schmid, U. Diebold, TU Wien, Austria; U. Heiz, Technical University of Munich, Germany; G. Parkinson, TU Wien, Austria**

We investigated the (photo)chemistry of alcohols on TiO<sub>2</sub>(110) and Fe<sub>2</sub>O<sub>3</sub>(012) in ultra-high vacuum. Our studies focused on the role of the metal co-catalyst in the photocatalytic reaction by comparing the reactivity of bare and metal-loaded surfaces. We show that photocatalytic reactions are not merely a couple of redox reactions, but an interplay of thermal and photon-driven surface reactions.

Our results demonstrated that the co-catalyst plays a crucial role in the outcome of the reaction. On TiO<sub>2</sub>(110), alcohols are oxidized to the aldehyde/ketone and hydrogen surface species upon illumination. The hydrogen surface species were thermally converted to H<sub>2</sub> by the co-catalyst, allowing for a steady-state photocatalytic conversion of alcohols and the continuous production of molecular hydrogen. Using mass spectrometry, we determined turnover frequencies and rate constants. The identification of surface mechanisms on Fe<sub>2</sub>O<sub>3</sub> is less advanced, but there seem to be strong parallels in the photochemistry.

Our studies shed light on the fundamental processes involved in photocatalytic reactions on metal-loaded surfaces and contribute to the development of sustainable energy technologies.

8:20am **SS+2D+AS+HC-WeM-2 Factors Governing the Reactivities of Transition Metal Carbides at Vapor/Solid and Liquid/Solid Interfaces, S. Alhowity, A. Ganesan, M. Gharraee, O. Omolere, Qasim Adesope, K. Balogun, P. Chukwunonye, F. D'Souza, T. Cundari, J. Kelber, University of North Texas**

Transition metal carbides are of broad interest for both heterogeneous and electro-catalysis. However, fundamental understanding of chemical factors governing reactivities and selectivities at the vapor/solid and liquid/solid interfaces remain sparse. Herein, *in situ* XPS results, electrochemical measurements, and DFT-based calculations are presented regarding the reactivities of NbC and TaC in the presence of O<sub>2</sub> vapor, and reactivity in solution towards the reduction of N<sub>2</sub> to NH<sub>3</sub>. NbC and TaC films were prepared by DC magnetron sputtering deposition, then exposed to O<sub>2</sub> vapor at room temperature, and analyzed by *in situ* XPS without exposure to ambient. Similarly prepared samples were also analyzed by *ex situ* XRD. These data show that, although Nb and Ta have similar oxophilicities, (a) deposited NbC films contain significant amounts of Nb oxide phases throughout the film, whereas TaC films deposited under similar conditions do not, and (b) the exposure of NbC films to O<sub>2</sub> at 300 K results in significant Nb oxide formation, but that TaC films remain inert towards O<sub>2</sub> under these conditions. DFT calculations indicate that this significant reactivity difference towards O<sub>2</sub> is due in large part to the greater Ta-C bond

# Wednesday Morning, November 8, 2023

strength compared to Nb-C, and in part due to the relative energetic stabilities of the corresponding oxides. Electrochemical studies show that ambient-exposed NbC, with a Nb<sub>2</sub>O<sub>5</sub> surface layer, becomes reactive towards N<sub>2</sub> reduction to NH<sub>3</sub> under acidic conditions, but only after etching in NaOH to remove the surface oxide layer. Additionally, chronoamperometric data indicate that this reactive NbC surface is eventually modified under electrochemical conditions and becomes relatively inert towards N<sub>2</sub> reduction with time. Experiments involving *in situ* sample transfer between UHV and electrochemistry environments demonstrate that electrochemically active NbC surfaces in solution comprise Nb sub-oxide surface layers, in line with previous studies showing that effective NRR catalysts contain surface transition metal ions in intermediate oxidation states, supporting both N<sub>2</sub> lone pair attraction and pi-backbonding to bind and activate the NN triple bond.

**Acknowledgement** This work was supported in part by the UNT College of Science through COS grants 1600089 and RSG-2023-002 and in part by the NSF under grant no. DMR 2112864.

8:40am **SS+2D+AS+HC-WeM-3 Tunable Interfacial Electrochemistry at Moiré Material Interfaces, D. Kwabena Bediako**, University of California at Berkeley **INVITED**

At electrode–electrolyte interfaces, crystallographic defects are frequently implicated as active sites that mediate interfacial electron transfer (ET) by introducing high densities of localized electronic states (DOS). However, conventional defects can be challenging to deterministically synthesize and control at an atomic level, challenging the direct study of how electronic localization impacts interfacial reactivity. Azimuthal misalignment of atomically thin layers produces moiré superlattices and alters the electronic band structure, in a manner that is systematically dependent on the interlayer twist angle. Using van der Waals nanofabrication of two-dimensional heterostructures, scanning electrochemical cell microscopy measurements, and four-dimensional scanning transmission electron microscopy, we report a strong twist angle dependence of heterogeneous charge transfer kinetics at twisted bilayer and trilayer graphene electrodes with the greatest enhancement observed near the ‘magic angles’. These effects are driven by the angle-dependent engineering of moiré flat bands that dictate the electron transfer processes with the solution-phase redox couple, and the structure of the relaxed moiré superlattice. Moiré superlattices therefore serve as an unparalleled platform for systematically interrogating and exploiting the dependence of interfacial ET on local electronic structure.

9:20am **SS+2D+AS+HC-WeM-5 Growth of Ultrathin Silica Films on Pt(111) and Rh(111): Influence of Intermixing with the Support, Matthias Krinninger**, Technical University of Munich, Germany; *F. Kraushofer*, Technical University of Munich, Austria; *N. Refvik*, University of Alberta, Canada; *F. Esch*, Technical University of Munich, Germany; *B. Lechner*, Technical University of Munich, Austria

Silica is a widely used catalyst support material for clusters and nanoparticles. Understanding the relationship between these clusters and the support is challenging, however, because SiO<sub>2</sub> is insulating, and in most applications not crystalline which drastically limits the use of experimental techniques to those that work on insulating samples and are not diffraction-based. Several previous studies have investigated ultrathin, quasi-2D silica films on a variety of metal supports [1], which can then be measured by scanning tunneling microscopy (STM), XPS and most other surface science methods. Previous work on Pt(111) did not result in closed films, which was attributed to lattice mismatch [2]. We show that closed films can in fact be grown on Pt(111) when silica is deposited in excess, likely due to formation of a platinum silicide layer with slightly expanded lattice constant at the interface. We also report results of film growth on Rh(111), which is a near-perfect match to the lattice constant of freestanding SiO<sub>2</sub> films as calculated by theory. However, no high-quality films were achieved on Rh due to thermodynamic competition with a silicide.

References:

- [1] C. Büchner, M. Heyde, Two-dimensional silica opens new perspectives, *Prog. Surf. Sci.*, 92 (2017) 341-374.
- [2] X. Yu, B. Yang, J. A. Boscoboinik, S. Shaikhutdinov, and H.-J. Freund, *Appl. Phys. Lett.* 100 (2012), 151608.

9:40am **SS+2D+AS+HC-WeM-6 CO<sub>2</sub> Adsorption on Graphitic-Like Bilayer ZnO Film Studied by NAP-XPS, Bo-Hong Liu, S. Cheng**, National Synchrotron Radiation Research Center, Taiwan

CO<sub>2</sub> activation is a fundamental process in heterogeneous catalysis. ZnO-based catalyst has been extensively used in commercial methanol synthesis from CO<sub>2</sub> gas and the reverse water gas shift reaction. The adsorption behavior of CO<sub>2</sub> on the catalyst surface is pivotal to the reactivity. Whereas ZnO(0001)-Zn physisorbed or weakly chemisorbed CO<sub>2</sub>,<sup>1</sup> strong chemisorption of the molecule happens on non-polar surfaces, such as ZnO(10-10), resulting in a tridentate carbonate.<sup>2</sup> In Operando TEM investigation during methanol synthesis shows that ZnO single atomic layer stacks distortedly around Cu nanoparticles via strong metal-support interaction. The lack of interlayer ordering between the layers suggests a weak interlayer interaction; therefore, each layer resembles a free-standing sheet.<sup>3</sup> DFT modeling concluded that free-standing ZnO(0001) layer adopts a graphitic-like co-planar structure. The co-planar feature was verified experimentally for the bi-layer ZnO(0001) supported on Ag(111) and Au(111).<sup>4</sup> On Au(111) substrate, TPD shows that CO<sub>2</sub> adsorbs on the low coordinate sites at the layer edges.<sup>5</sup> In the present study, we investigate the CO<sub>2</sub> adsorption on bi-layer ZnO/Ag(111) film using NAP-XPS to extend the pressure condition towards reality. We found a more considerable CO<sub>2</sub> chemisorption at elevated pressure. The presentation will also address how the surface hydroxyl group influences CO<sub>2</sub> adsorption.

1. Wang, J.;Hokkanen, B.; Burghaus, U., Adsorption of CO<sub>2</sub> on pristine Zn–ZnO (0 0 1) and defected Zn–ZnO (0 0 1): A thermal desorption spectroscopy study. *Surf. Sci.* **2005**,577 (2-3), 158-166.
2. Schott, V.;Oberhofer, H.; Birkner, A.;Xu, M.;Wang, Y.;Muhler, M.;Reuter, K.; Wöll, C., Chemical activity of thin oxide layers: strong interactions with the support yield a new thin-film phase of ZnO. *Angewandte Chemie International Edition* **2013**,52 (45), 11925-11929.
3. Lunkenbein, T.;Schumann, J.;Behrens, M.;Schlögl, R.; Willinger, M. G., Formation of a ZnO overlayer in industrial Cu/ZnO/Al<sub>2</sub>O<sub>3</sub> catalysts induced by strong metal–support interactions. *Angewandte Chemie* **2015**,127 (15), 4627-4631.
4. Tusche, C.;Meyerheim, H.; Kirschner, J., Observation of depolarized ZnO (0001) monolayers: formation of unreconstructed planar sheets. *Phys. Rev. Lett.* **2007**,99 (2), 026102.
5. Deng, X.;Sorescu, D. C.; Lee, J., Enhanced adsorption of CO<sub>2</sub> at steps of ultrathin ZnO: the importance of Zn–O geometry and coordination. *Phys. Chem. Chem. Phys.* **2017**,19 (7), 5296-5303.

11:00am **SS+2D+AS+HC-WeM-10 Investigation of Nitride Spintronic and Kagome-Structured Intermetallic Topological Materials Using Molecular Beam Epitaxy and Scanning Tunneling Microscopy, Arthur R. Smith**, Ohio University Physics and Astronomy Department

Owing to the overwhelming interest in topological [1] and spintronic materials [2], it is imperative to investigate these down to the atomic scale for their possible use in advanced devices. Many promising properties discovered among nitride materials, such as chemical stability and wide band gaps [3], may be combined with the equally promising aspects of topological materials, such as the topological Hall and Nernst effects [4]. Very recent work illustrates that spin-polarized scanning tunneling microscopy is a powerful tool for exploring topological band-structured Kagome antiferromagnets [5]. In our current work, we investigate both nitride material systems grown using molecular beam epitaxy as well as the growth of topological systems such as Kagome antiferromagnetic materials. Ongoing work in our group encompasses the investigation of Mn<sub>3</sub>Sn, FeSn, CrSn, Mn<sub>3</sub>Ga, and as a spintronic and topological nitride, Mn<sub>3</sub>GaN. These materials are grown in combined UHV MBE and scanning tunneling microscopy chamber systems in which the grown samples are first fabricated using MBE and after that investigated for their structural, electronic, and magnetic properties including using STM and tunneling spectroscopy. Our goal is also to investigate these materials using spin-polarized STM as a function of temperature and applied magnetic field. Our current results show that these materials can be fabricated effectively using molecular beam epitaxy and investigated using various *in-situ* techniques such as reflection high energy electron diffraction and STM. Results from multiple on-going investigations will be presented with a birds-eye view of the progress. Especially to be presented will be STM and STS results in these Kagome systems grown using MBE.

# Wednesday Morning, November 8, 2023

This work is supported by the U.S. Department of Energy, Office of Basic Energy Sciences, Division of Materials Sciences and Engineering under Award No. DE-FG02-06ER46317.

- [1] P. Liu *et al.*, "Topological nanomaterials," *Nat. Rev. Mater.* **4**, 479 (2019).
- [2] A. Hirohata *et al.*, "Review on spintronics: Principles and device applications," *Journal of Magnetism and Magnetic Materials* **509**, 166711 (2020).
- [3] M. Xu *et al.*, "A review of ultrawide bandgap materials: properties, synthesis and devices," *Oxford Open Materials Science* **2**(1), itac004 (2022).
- [4] S. Roychowdhury *et al.*, "Giant Topological Hall Effect in the Noncollinear Phase of Two-Dimensional Antiferromagnetic Topological Insulator MnBi<sub>4</sub>Te<sub>7</sub>," *Chemistry of Materials* **33**, 8343 (2021).
- [5] H. Li *et al.*, "Spin-polarized imaging of the antiferromagnetic structure and field-tunable bound states in kagome magnet FeSn," *Scientific Reports* **12**, 14525 (2022).

11:20am **SS+2D+AS+HC-WeM-11 Molecular Beam Epitaxial Growth and Investigations of FeSn on LaAlO<sub>3</sub>**, Tyler Erickson, S. Upadhyay, H. Hall, D. Ingram, S. Kaya, A. Smith, Ohio University

Kagome antiferromagnetic and ferromagnetic materials provide an interesting avenue for research through the investigation of frustrated magnetism, band topology and electronic correlations [1-4]. FeSn is a layer-wise antiferromagnetic Kagome structured material with characteristic dispersion-less flat bands and Dirac cones at the Brillouin zone boundaries. Li *et al.* have presented exciting spin-polarized scanning tunneling microscopy results revealing surface electronic and magnetic properties of *in-situ* cleaved bulk FeSn [1]. Zhang *et al.* reported strain engineering of FeSn on SrTiO<sub>3</sub> (111) with precise control of the stanene layers [2]. Kawakami *et al.* reported Fe<sub>3</sub>Sn<sub>2</sub> growth on Pt buffer layers on top of Al<sub>2</sub>O<sub>3</sub> and studied various topological phenomena of this topological Kagome material [3,4]. Bhattarai *et al.* studied the magnetotransport properties of FeSn grown on silicon substrates [5]. Here, we study the growth of FeSn directly on LaAlO<sub>3</sub> and report the successful growth of high-quality crystalline thin-films of FeSn. Reflection high-energy electron diffraction and x-ray diffraction are used to discover the *in-plane* and *out-of-plane* lattice constants, while atomic force microscopy and Rutherford backscattering provide topographical and stoichiometric characterization. Preliminary results indicate *in-plane* and *out-of-plane* lattice constants of 5.290 Å and 4.56 Å compared to the expected results of 5.297 Å and 4.481 Å, respectively. Besides discussing the thin film FeSn growth results, we also plan to present scanning tunneling microscopy results on the MBE-grown surfaces.

This work is supported by the U.S. Department of Energy, Office of Basic Energy Sciences, Division of Materials Sciences and Engineering under Award No. DE-FG02-06ER46317.

- [1] H. Li *et al.*, *Scientific Reports*, 12 14525 (2022)
- [2] H. Zhang *et al.*, *Nano Lett.* **23**, 239 – 2404 (2023)
- [3] I. Lyalin *et al.*, *Nano Lett.* **21**, 6975 – 6982 (2021)
- [4] S. Cheng *et al.*, *APL Mater.* **10**, 061112 (2022)
- [5] N. Bhattarai *et al.*, *Phys. Status Solidi A*, **220**: 2200677 (2023)

11:40am **SS+2D+AS+HC-WeM-12 AVS Graduate Research Awardee Talk: Molecular Beam Epitaxial Growth, Structural Properties, and Surface Studies of *a*-Plane-Oriented Mn<sub>3</sub>Sn on *c*-Plane Al<sub>2</sub>O<sub>3</sub>**, Sneha Upadhyay<sup>1</sup>, T. Erickson, Ohio University; J. Hernandez, Universidad Autonoma de Puebla, Mexico; H. Hall, K. Sun, Ohio University; G. Cocolezzi, Universidad Autonoma de Puebla, Mexico; N. Takeuchi, Universidad Nacional Autonoma de Mexico, Mexico; A. Smith, Ohio University

Recently, Chen *et al.* reported the observation of tunneling magnetoresistance in an all-antiferromagnetic tunnel junction consisting of Mn<sub>3</sub>Sn/MgO/Mn<sub>3</sub>Sn.<sup>1</sup> Furthermore, Bangar *et al.* demonstrated a technique for engineering the spin Hall conductivity of Mn<sub>3</sub>Sn films by changing the Mn: Sn composition.<sup>2</sup> These works show the potential of studying this Kagome antiferromagnetic material and the importance of being able to grow smooth films. This work uses molecular beam epitaxy to investigate

the growth of Mn<sub>3</sub>Sn (11 $\bar{2}$ 0) on Al<sub>2</sub>O<sub>3</sub> (0001). The growth is monitored *in-situ* using reflection high energy electron diffraction and measured *ex-situ* using X-ray diffraction, Rutherford backscattering, and atomic force microscopy. In our previous work, we carried out a single-step growth at 450°C, which resulted in a crystalline but discontinuous *a*-plane-oriented (~43% 11 $\bar{2}$ 0) Mn<sub>3</sub>Sn film with a mix of other orientations including 0002.<sup>3</sup> Leading from this work, changes were made to the growth recipe, which involved carrying out a two-step growth procedure at room temperature, resulting in a contiguous, epitaxial Mn<sub>3</sub>Sn film with up to ~82% 11 $\bar{2}$ 0-orientation. We are also exploring the effect of varying the Mn: Sn flux ratio and the film thicknesses (in the range of 5 – 200 nm) on the film crystallinity and orientation. We observe that varying the Mn: Sn flux ratio leads to a change in the RHEED patterns from pointy to streaky, and the XRD shows that the 11 $\bar{2}$ 0 peak can be varied between ~82% to ~38% of all the peaks' total intensity. We also plan to present the first results on ultra-high vacuum scanning tunneling microscopy imaging of the (11 $\bar{2}$ 0) Mn<sub>3</sub>Sn surface.

## Acknowledgments:

The authors acknowledge support from the U.S. Department of Energy, Office of Basic Energy Sciences, Division of Materials Sciences and Engineering under Award No. DE-FG02-06ER46317. The authors would like to thank Dr. Eric Stinoff and his students for back-coating the sapphire (0001) substrates.

<sup>1</sup> X. Chen *et al.*, "Octupole-driven magnetoresistance in an antiferromagnetic tunnel junction." *Nature* **613**, 490 (2023).

<sup>2</sup> H. Bangar *et al.*, "Large Spin Hall Conductivity in Epitaxial thin films of Kagome Antiferromagnet Mn<sub>3</sub>Sn at room temperature", *Adv. Quantum Technol.* **6**, 2200115 (2023).

<sup>3</sup> S. Upadhyay *et al.*, "Molecular beam epitaxy and crystal structure of majority *a*-plane oriented and substrate strained Mn<sub>3</sub>Sn thin films grown directly on sapphire (0001)", *Journal of Vacuum Science and Technology A*, to be published (2023).

## Thin Film Division

### Room A105 - Session TF2+AP+SE+SS-WeM

#### Controlling Microstructure and Accessing Non-Equilibrium Phases in Thin Films

Moderators: Robert Grubbs, IMEC Belgium, Richard Vanfleet, Brigham Young University

11:00am **TF2+AP+SE+SS-WeM-10 Stabilizing Polar Polymorphs of Scandium Ferrite for Photovoltaics**, M. Frye, Lauren Garten, Georgia Institute of Technology

INVITED

Metastability is no longer synonymous with unstable or unattainable, but further work is needed to enable the next generation of electronics and photovoltaics. In this talk I will discuss the development of a stabilization route for the P63cm phase of ScFeO<sub>3</sub> through precursor control and interface engineering. The P63cm phase has potential for lead-free piezoelectric, photo-ferroic, and ferroelectric applications. Unfortunately, this phase is in competition with four other known polymorphs that are similar in structure and energy and there is not a well matched epitaxial substrate. So we took a different approach by controlling the atomic layering of the precursor structure and the deposition timing to stabilize the P63cm phase under conditions that previously lead to the ground state. The film structure is verified by transmission electronic microscopy and x-ray diffraction. Ab initio calculations confirm that layered growth stabilizes the metastable phase and highlights the importance of the variable oxidation state of iron, the high activation energy against diffusion, and the surface termination of the substrate in designing a stabilization approach. This work highlights routes to access similar polymorphs on an array of different substrates, opening up new materials and new device architectures.

11:40am **TF2+AP+SE+SS-WeM-12 The Role of Thermal Vibrational Disorder in the Structural Phase Transition of VO<sub>2</sub> Probed by Raman Spectroscopy**, Aminat Oyiza Suleiman, Institut National de la Recherche Scientifique, Canada; S. Mansouri, Institut National de la Recherche Scientifique, Canada; N. Émond, Massachusetts Institute of Technology, Canada; T. Bégin, J. Margot, Université de Montréal, Canada; C. Mohamed, National de la Recherche Scientifique, Canada

Vanadium dioxide (VO<sub>2</sub>) is a typical correlated electron material which exhibits a first-order metal-insulator transition (MIT) at a near-room temperature of about 340 K. Upon heating, VO<sub>2</sub> switches from an insulating

<sup>1</sup> AVS Graduate Research Awardee

# Wednesday Morning, November 8, 2023

monoclinic phase (M1 or M2) to a metallic tetragonal rutile phase (R). The mechanism behind the MIT in VO<sub>2</sub> is still controversial: Is it a structure driven Peierls transition mechanism or a Mott transition where strong electron-electron correlations drive charge localization and collapse the lattice symmetry? By directly comparing the electrical and lattice-dynamic properties of VO<sub>2</sub>, useful information about the MIT/SPT in VO<sub>2</sub> can be obtained.

Herein, we therefore present a detailed Raman study of undoped (M1) and Cr-doped (M2) VO<sub>2</sub> thin films as a function of temperature. The studied VO<sub>2</sub> films with different thicknesses are deposited on c- and r-sapphire substrates. While their structural properties and morphology are examined by XRD and AFM techniques, respectively, Raman measurements are correlated to four-point probe resistivity measurements, giving an insight into the coupling between VO<sub>2</sub> structural phase (SP) and MI transitions. By distinctively combining the Raman data with information from reported EXAFS data, a relationship between the Raman intensities and the mean Debye-Waller factors ( $\sigma^2$ : the mean-square relative displacements) is established. The temperature dependence of the vanadium dimers Waller factor ( $\sigma_R^2(V-V)$ ), as calculated from the Raman intensity, was found to follow the temperature profile of the  $\sigma_{EXAFS}^2(V-V)$  obtained from the reported EXAFS data. These findings provide an evidence on the critical role of the thermal vibrational disorder in VO<sub>2</sub> phase transitions, demonstrating that by correlating Raman data with EXAFS analysis, both lattice and electronic structural dynamics can be probed.

12:00pm **TF2+AP+SE+SS-WeM-13 Interplay of Lattice Distortion and Electronic Structure in Metastable Brookite TiO<sub>2</sub>**, *Pritha Biswas*, Oregon State University; *M. Choi, K. Koirala, M. Bowden, L. Strange*, Pacific Northwest National Laboratory; *H. Zhou*, Argonne National Laboratory; *J. Tate*, Oregon State University; *Y. Du, T. Kaspar, D. Li, P. Sushko*, Pacific Northwest National Laboratory

Controlling the coupling between lattice distortions and electronic properties is one of the promising routes toward enhancing the performance of materials used in energy technologies, such as photocatalysis, photovoltaics, and energy storage. Oxide semiconductors that exhibit polymorphism represent a convenient class of systems to study this coupling by investigating the effect of external stimuli on transition pathways between polymorphs. Among the oxide semiconductors, earth-abundant TiO<sub>2</sub> exists in several polymorphic forms, including rutile, anatase, and brookite, with distinctly different structural symmetries. Compared to the common rutile and anatase polymorphs, metastable brookite TiO<sub>2</sub> is the least studied one due to the difficulties associated with its synthesis in a phase pure form. At the same time, mechanisms of its transformation to the more stable anatase and rutile polymorphs are promising to provide a rich insight into the relationships between the character of the lattice deformations, defect content, and electronic structure. We have developed a recipe for phase selective TiO<sub>2</sub> polymorph formation, where tuning of oxygen vacancy concentration drives the crystallization of amorphous TiO<sub>2</sub> thin films towards a specific polymorphic structure. In this study, thermal treatment was used to control the evolution of as-deposited, sputtered amorphous TiO<sub>2</sub> thin films towards the brookite lattice. The crystallinity and phase purity of the resulting structures were investigated by lab-based grazing incidence XRD, synchrotron XRD, and transmission electron microscopy. The dependence of structural variations present in the sample on the details of the annealing treatments was evaluated using Rietveld refinement analysis. X-ray photoelectron spectroscopy (XPS), confocal Raman spectroscopy, and high-resolution transmission electron microscopy (HRTEM) were used to understand the effect of local deformation on the electronic structure of brookite. We found a correlation between the degree of lattice parameter deviation, shifts of the Raman vibrational modes, and the position of the brookite valence band. The effect of these lattice distortions at the atomic scale on the photocatalytic activity of brookite will be discussed.

# Wednesday Afternoon, November 8, 2023

## Applied Surface Science Division

Room B117-119 - Session AS+CA+EL+EM+SE+SS+TF-WeA

### Quantitative Surface Analysis I

**Moderators:** David Cant, National Physical Laboratory, UK, Peter Cumpson, University of New South Wales, Christopher Moffitt, Kratos Analytical Inc, Lev Gelb, University of Texas at Dallas

2:20pm AS+CA+EL+EM+SE+SS+TF-WeA-1 Status of Efforts to Upgrade the Quality of Surface Analysis Data in the Literature, Donald Baer, Pacific Northwest National Laboratory

Multiple efforts are being undertaken to address a growing presence of faulty surface analysis data and/or analyses appearing in the literature. Issues include bad data, incorrect analysis, and highly incomplete reporting of instrument and analysis parameters. This talk describes the status of four efforts to address some of the issues. Recognition of this problem within the surface analysis community has increased with an understanding that both inexperienced users and increased use of surface analysis methods outside the surface analysis community contribute to the problem. The current efforts build upon decades of development and efforts by standards committees, excellent books and journal publications, websites, short courses, and other efforts. A collection of guides, protocols and tutorials addressing reproducibility issues with a significant focus on XPS was published in JVSTA in 2020/21. A second collection, *Reproducibility Challenges and Solutions II*, with a more general focus on Surface and Interface Analysis was initiated in 2022 and is being finalized. The second collection addresses several techniques, including SIMS, SPM, and UPS, and includes topics such as theoretical modeling and machine learning in data analysis. A second effort focuses on a part of the community less interested in general understanding but needs to answer specific surface analysis questions. A new type of paper called Notes and Insights is being published in the journal Surface and Interface Analysis with the objective to provide incremental bits of useful information of importance to non-expert analysts. Two additional activities are underway to assist with reporting issues. Examination of papers in multiple journals found that instrument and analysis related information needed to assess or reproduce data is often incomplete or absent. To assist authors in reporting instrument parameters, papers describing in some detail related families of commercial instruments are being prepared for Surface Science Spectra. These papers describe the instrument, major components, geometry and provide example data related to common data collection modes. Authors will be able to reference these papers and identify specific modes of instrument operation used in their research. Another parameter reporting activity concerns sample handling before analysis. ISO Technical Committee 201 is developing a series of documents (ISO 20579 parts 1 to 4) on what needs to be reported regarding sample handling, storage, processing, and mounting for analysis. These standards describe what needs to be reported and contain informative annexes that provide information regarding the needs and challenges to proper sample handling to produce reliable useful surface analysis data.

2:40pm AS+CA+EL+EM+SE+SS+TF-WeA-2 The behavior of the Shirley background of the Ti 2p spectra across the Ti 1s edge, Dulce Maria Guzman Bucio, CINVESTAV-Unidad Queretaro, Mexico; D. Cabrera German, Universidad de Sonora, Mexico; O. Cortazar Martinez, J. Raboño Borbolla, CINVESTAV-Unidad Queretaro, Mexico; M. Vazquez Lepe, Universidad de Guadalajara, Mexico; C. Weiland, J. Woicik, National Institute of Standards and Technology; A. Herrera Gomez, CINVESTAV-Unidad Queretaro, Mexico  
A wide variety of photoemission spectra display a step-shaped background, called the Shirley-type background, which should be accounted for in the total background signal for reliably assessing chemical composition. However, it cannot be modeled with any method based on extrinsic processes like the inelastic dispersion of the photoelectrons (e.g., Tougaard-type backgrounds). Although its physical origin is still unknown, experimental data suggest that the Shirley-type background is due to phenomena occurring inside the atom [1,2]. To gain insights into those phenomena, we studied the behavior of the Shirley-type background for the Ti 2p photoemission spectra.

In this work, Ti 2p photoemission spectra were acquired with Synchrotron light (at Beamline 7-2 at the Brookhaven National Laboratory) from a clean metallic titanium film (sputtered on a Si (100) substrate) capped with an

ultra-thin aluminum layer. The spectra were collected with 44 excitation energies around the Ti 1s edge. By simultaneously fitting Ti 2p photoemission spectra obtained with excitation energies higher than the Ti 1s edge, we robustly determined the peak structure of the Ti 2p spectra. Outstandingly, the parameter of the Shirley-type background associated with the Ti 2p peak structure is modulated as the photon energy crosses the Ti 1s edge. The relation of this phenomenon with the physical origin of the Shirley background will be discussed. The KVL<sub>2,3</sub> Auger peaks—which overlap with the Ti 2p peaks—do not have a step-shaped background for most of the excitation energies.

Acknowledgments:

Use of the Brookhaven National Laboratory is supported by the U.S. Department of Energy's (DOE) Office of Science.

This work was partially financed by CONACyT Project Fronteras 58518, Mexico.

References:

- [1] A. Herrera-Gomez, D. Cabrera-German, A. Dutoi, M. Vazquez-Lepe, S. Aguirre-Tostado, P. Pianetta, D. Nordlund, O. Cortazar-Martinez, A. Torres-Ochoa, O. Ceballos-Sanchez, L. Gomez-Muñoz, Intensity modulation of the Shirley background of the Cr 3p spectra with photon energies around the Cr 2p edge, Surf. Interface Anal. 50 (2018) 246–252. <https://doi.org/10.1002/sia.6364>.
- [2] A. Herrera-Gomez, Interchannel Coupling with Valence Band Losses as the physical origin of the Shirley background in photoemission spectra (Old title: The unresolved physical origin of the Shirley background in photoemission spectra), Queretaro, 2015. <http://www.qro.cinvestav.mx/%0A~aherrera/reportesInternos/unknownOri ginShirley.pdf>.

3:00pm AS+CA+EL+EM+SE+SS+TF-WeA-3 Chemical Analysis of Multilayer System by Photoemission: The Binding Energy Reference Challenge, Thierry Conard, A. Vanleenhove, IMEC Belgium; D. Desta, H. Boyen, University of Hasselt, Belgium

XPS is a well-established technique used for non-destructive analysis of the chemical composition of thin layers and interfaces. It is most commonly performed using Al K $\alpha$  radiation (1486.6 eV), which limits the analysis to the top 5-10nm. The recently developed laboratory-based hard X-ray photoelectron spectrometers (HAXPES) provide new analysis options. They enable the analysis of thicker film structures and interfaces buried down to 20-50 nm depending on the photon energy and facilitate the analysis of fragile buried layers without ion-induced chemical damage.

Increasing the number of analyzed (insulating) layers enhances the risk of significant vertical differential charging and makes the repeatability of binding energy determination more challenging. While charging has to be taken into account for XPS, the analysis of most XPS spectra is quite straightforward as long as the surface charge is stable and the lateral distribution of surface charge is uniform within the area of analysis. For HAXPES however vertical charge distribution comes into the game for a large group of structures whose development can benefit from HAXPES analysis. Vertical charge build-up can be complex, especially if examined structures exist of multiple layers and hence multiple interfaces, containing a large variety of materials. But even in 'simple' non-conducting one-layer structures a vertical charge gradient builds up when exposed to X-rays and small changes in the parameters of standard surface charge neutralization techniques - as the use of e-beam flood guns - can influence the nature of the charge gradient.

In this work, we will examine the influence of measurement conditions in single and multiple layers systems relevant to the microelectronic industry on the determination of precise binding energies.

HAXPES spectra of technologically relevant samples will be discussed to demonstrate the challenge of determining exact binding energy values. The set of examined samples comprises oxide layers Si samples and metal/high-k/Si stacks including high-k materials as HfO<sub>2</sub> and Al<sub>2</sub>O<sub>3</sub>. The surface potential will be precisely set and monitored in situ by depositing a metallic layer (such as Ag) on top of the stack and applying an external potential instead of using an electron neutralization source. All experiments are performed in a PHI Quantex system and/or a Scienta Omicron HAXPES Lab, both equipped with two monochromatic X-ray sources: an Al K $\alpha$  (1486.6 eV) and a Cr K $\alpha$  (5414.8 eV - Quantex) or Ga K $\alpha$  (9252.1 eV - HAXPES lab) X-ray source.



# Wednesday Afternoon, November 8, 2023

3:20pm **AS+CA+EL+EM+SE+SS+TF-WeA-4 Where Are We on the Road-Map to Artificially Intelligent Interpretation of X-ray Photoelectron Spectra?**, C. Moffitt, Kratos Analytical Inc; A. Roberts, J. Counsell, C. Blomfield, Kevin Good, K. Macak, Kratos Analytical Limited, UK

Robust peak identification is crucial for accurate sample analysis using X-ray photoemission spectroscopy (XPS). Automation of peak ID enhances this process by minimizing user error and bias. Current acquisition software offers improved computer-derived peak identification from unknown samples, instilling confidence in the correct identification of elements. Moreover, this forms the foundation for an automated sample analysis workflow known as Data-dependent Analysis (DDA). DDA involves identifying peaks in a survey spectrum and subsequently acquiring high-resolution spectra from major components. A recent User survey revealed that a significant majority of users rely on the large area survey acquisition mode as a starting point for analysis.

To provide a metric for confidence in the DDA process, existing spectral analysis data, which includes the element composition information, is used to generate reference spectra for testing purposes. These reference spectra serve as the basis dataset against which the performance of the automated analysis algorithm can be evaluated. By comparing the results of the algorithm with the reference spectra, statistical parameters can be calculated to assess the algorithm's precision, sensitivity, specificity, and accuracy in identifying elements of unknown spectra.

For experienced analysts, DDA serves as a time-saving acquisition method, while for inexperienced analysts, it provides assurance in accurate peak identification and appropriate high-resolution spectra acquisition. Here we highlight current status of automated XPS data acquisition in relationship to the 'expert system', championed in the early 2000's and full AI interpretation of XPS spectra of the future.

4:20pm **AS+CA+EL+EM+SE+SS+TF-WeA-7 Thin Film Analysis by XPS: Quantitative Analyses Using Physics-Based and Machine-Learning Approaches**, Lev Gelb, N. Castanheira, A. Walker, University of Texas at Dallas

We present progress towards quantitative analysis of XPS data using both model-based "fitting" approaches and machine learning methods. Two separate applications are considered.

The first concerns the simultaneous extraction of both compositional profiles and sputtering parameters from XPS sputter depth-profiles of multilayer films. Depth-profile data are routinely processed to provide "fractional composition vs ion dose" profiles, but such analyses typically assume the sample is homogeneous in the probed region, which is not true near interfaces, and cannot precisely convert between units of ion dose and depth without extensive calibration data. Our approach is to first construct analytical models for both the sample structure and for the sputtering process, and then to determine the model parameters (layer thicknesses, interfacial widths, material removal rates, etc.) that are most likely given the observed apparent fractional composition profiles. This is done numerically, by iteratively comparing simulated and observed apparent composition profiles. The only additional required inputs are the inelastic mean free paths for each tracked peak in each material present. The efficacy of this approach is demonstrated using both synthetic and experimental data sets, and various model improvements (sputter-induced mixing, *in situ* chemical reactions) are discussed.

The second application concerns the application of machine-learning tools to remove the inelastic scattering background from XPS spectra in order that accurate peak areas can be obtained. Our approach here is to generate a training data set which consists of a thousands of simulated XPS spectra with and without inelastic scattering included. This is accomplished using the SESSA software package[1]. This data set is then used to train a neural network algorithm to output a "no-background" spectrum from an input "with-background" spectrum; this output spectrum can then be used to compute peak areas for compositional analysis. The training set generation methodology and network structure are discussed, and application of the tool to both simulated and experimental spectra is demonstrated.

[1] Werner, W., Smekal, W., Powell, C. and Gorham, J. (2021), *Simulation of Electron Spectra for Surface Analysis (SESSA) Version 2.2 User's Guide*, Natl Std. Ref. Data Series (NIST NSRDS), <https://doi.org/10.6028/NIST.NSRDS.100-2021>.

4:40pm **AS+CA+EL+EM+SE+SS+TF-WeA-8 Room Temperature Ionic Liquids as Reference Materials for Photoelectron Spectrometers**, Benjamin Reed, National Physical Laboratory, U.K.; J. Radnik, BAM Berlin, Germany, UK; A. Shard, National Physical Laboratory, U.K.

Room-temperature ionic liquids (RTILs) are materials consisting of organic salts that are liquid below temperatures of 100°C and are used in several fields including electrochemistry,<sup>1</sup> pharmaceuticals, and medicine.<sup>2</sup> RTILs have several notable properties that make them ideal for X-ray photoelectron spectroscopy (XPS) analysis. They have an extremely low vapor pressure and high surface tension, and so can be analysed using conventional XPS under ultrahigh vacuum without the need for near-ambient pressure instrumentation. Also, when deposited in a recessed sample holder, the meniscus of an RTIL will be perfectly flat meaning that there are no contributions from sample topographic effects. Finally, and most importantly, they are highly homogeneous and have well-defined stoichiometries.<sup>3</sup>

These properties make RTILs potential reference materials for validating the intensity calibration of a photoelectron spectrometer. RTILs with non-coordinating bistriflimide (NTf<sub>2</sub>) anions (e.g. PMIM<sup>+</sup>NTf<sub>2</sub><sup>-</sup>) or dimethyl phosphate (DMP) anions (e.g. MMIM<sup>+</sup>DMP<sup>-</sup>) are such candidates, with core levels up to ~800 eV binding energy, making them apt for verifying the quantification of light elements, especially for organic materials.<sup>4,5</sup>

To accurately determine peak areas, however, requires the principal and secondary photoelectron signals to be deconvolved. Previous attempts by multiple laboratories using different quantification methods give a mean atomic composition within 1 at.% of the known stoichiometry, but some individual elements (such as fluorine) exhibit differences greater than 1 at.% because the elastic and inelastic secondaries are not suitably deconvolved. Attention must be paid to the energy loss function that defines the inelastic background over the full energy range of an XPS spectrum so that a suitable Tougaard background subtraction can be applied.<sup>6</sup> Here we present a study on several RTILs and discuss how they may be used to validate an XPS intensity calibration and provide confidence in measurements to XPS instrument operators.

<sup>1</sup>M. Armand, F. Endres, D. R. MacFarlane et al., *Nat. Mater.* **8**, 621 (2009).

<sup>2</sup>K. S. Egorova, E. G. Gordeev, and V. P. Ananikov, *Chem. Rev.* **117**, 7132 (2017).

<sup>3</sup>E. F. Smith, I. J. Villar Garcia, D. Briggs et al., *Chem. Commun.* **45**, 5633 (2005).

<sup>4</sup>B.P. Reed, J. Radnik, and A.G. Shard, *Surf. Sci. Spectra* **29**, 014001 (2022).

<sup>5</sup>X. Knigge and J. Radnik, *Surf. Sci. Spectra* **30**, 014006 (2023).

<sup>6</sup>M. P. Seah, I. S. Gilmore, and S. J. Spencer, *Surf. Sci.* **461**, 1 (2000).

5:00pm **AS+CA+EL+EM+SE+SS+TF-WeA-9 Fractional Coverage Analysis of Monolayers with XPS and Non-Destructive Depth-Profiling with Combined Soft and Hard X-Rays**, Norbert Biderman, K. Artyushkova, D. Watson, Physical Electronics USA

X-ray photoelectron spectroscopy (XPS) is a well-established technique for non-destructive analysis of the chemical composition of thin layers and interfaces. Angle-resolved XPS (AR-XPS) has been used to determine composition of depth profiles and layer thicknesses, traditionally with Al K $\alpha$  (1486.6 eV) X-ray beams for depths up to 5-10 nm below the surface. In recent years, new AR-XPS capabilities have been added to Physical Electronics XPS scanning microprobe instruments including Cr K $\alpha$  (5414.8 eV) hard X-ray photoelectron spectroscopy (HAXPES) that can probe buried interfaces up to 15-30 nm below the surface. Coinciding with the HAXPES development, the StrataPHI analysis software was developed to reconstruct quantitative, non-destructive XPS/HAXPES depth profiles from angle-dependent and single-angle photoelectron spectra.

In this talk, we will show that the StrataPHI software has been further developed to combine Al K $\alpha$  and Cr K $\alpha$  XPS and HAXPES data within a single depth profile to enhance extracted analytical information from various depths below the surface. We will explore the method of the combined technique as well as its application to multilayered thin film samples. The updated StrataPHI software also includes a fractional coverage analysis mode, relevant in situations where ultra-thin films exist as discrete islands – commonly observed in early thin-film deposition stages on the substrate rather than as a continuous, uniform film. A model system of discrete molybdenum sulfide (MoS<sub>2</sub>) monolayer triangles deposited on SiO<sub>2</sub>/Si substrate will be discussed.

# Wednesday Afternoon, November 8, 2023

Such added StrataPHI capabilities allow for scientists and engineers in metrology and research & development to analyze multi-layered thin films and ultra-thin films rapidly and non-destructively without potentially damaging ion beam sputtering that might otherwise be required to depth-profile or sputter-clean adventitious contamination off the surface.

5:20pm **AS+CA+EL+EM+SE+SS+TF-WeA-10 Reassessing the Reduction of Ceria in X-Ray Photoelectron Spectroscopy**, *David Morgan*, Cardiff University, UK

Given its excellent redox abilities, the use of cerium dioxide ( $\text{CeO}_2$ , ceria) and related materials in catalysis is widespread [1]. This  $\text{Ce}^{3+}/\text{Ce}^{4+}$  redox shuffle allows for great catalytic ability and a method of correlation of catalytic activity to the state of ceria [2–4]. Given that catalysis is a surface mediated process, XPS is critical in the analysis of pre- and post-mortem materials.

Over the years there has been debate on the degree of reduction of  $\text{CeO}_2$  during XPS analysis. Therefore, in continuation of our work on understanding the reduction of materials in modern spectrometers [5], we have investigated different cerium oxide preparations and shown that not only is the rate of reduction dependent on instrument type and experimental configuration (and hence appropriate analysis protocols should be implemented), but is also related to the morphology of the cerium which may, at least in part, account for the discrepancies in the degree of reduction in the literature. It is postulated that reduction rates could be used to indicate likely ceria morphology where other analysis is unavailable.

## References

[1] Catalysis By Ceria And Related Materials, 2nd Edition.; Trovarelli, A., Fornasiero, P., Eds.; Imperial College Press: London, 2013.

[2] Smith, L. R.; Sainna, M. A.; Douthwaite, M.; Davies, T. E.; Dummer, N. F.; Willock, D. J.; Knight, D. W.; Catlow, C. R. A.; Taylor, S. H.; Hutchings, G. J. "Gas Phase Glycerol Valorization over Ceria Nanostructures with Well-Defined Morphologies". *ACS Catal*, 2021, 11 (8), 4893–4907.

[3] Qiao, Z.-A.; Wu, Z.; Dai, S. "Shape-Controlled Ceria-Based Nanostructures for Catalysis Applications". *ChemSusChem*, 2013, 6 (10), 1821–1833.

[4] Ziemba, M.; Schilling, C.; Ganduglia-Pirovano, M. V.; Hess, C. "Toward an Atomic-Level Understanding of Ceria-Based Catalysts: When Experiment and Theory Go Hand in Hand". *Acc Chem Res*, 2021, 54 (13), 2884–2893.

[5] Morgan, D. J. "XPS Insights: Sample Degradation in X-ray Photoelectron Spectroscopy". *Surface and Interface Analysis*, 2023. (In Press)

## Acknowledgements

This work acknowledges the EPSRC National Facility for XPS ('HarwellXPS'), operated by Cardiff University and UCL, under contract No. PR16195, and C.M.A. Parlett and X. Zhou for provision of nanostructured ceria materials.

5:40pm **AS+CA+EL+EM+SE+SS+TF-WeA-11 Using High Sensitivity – Low Energy Ion Scattering Spectroscopy (LEIS) to Unravel the Complex Nature of High Entropy Alloys**, *Matthias Kogler*, *C. Pichler*, Centre for Electrochemistry and Surface Technology (CEST GmbH), Austria; *M. Valtiner*, Vienna University of Technology, Austria

Complex metallic materials such as Multi-Principal Alloys (MPEAs) and High Entropy Alloys (HEAs) have emerged as a promising class of materials given their unique inherent characteristics. Excellent mechanical, thermal, and corrosion properties allow for a broad spectrum of applications. However, due to the multi-element nature of these alloys, characterisation of the composition and microstructure proves to be a challenging task.

Especially with regard to corrosion-protective passivation films, the complex correlations with the corrosion behaviour are fully unclear to date, and require an in-depth atomic level characterisation and rationalisation. However, the precise layer by layer structure of such passive films is particularly demanding to assess, since traditional techniques such as XPS (X-ray photoelectron spectroscopy) or AES (Auger electron spectroscopy) have analysis penetration depths of several nanometres and cannot reach

atomic layer resolution. However, to fully understand and quantify the passivation layer structure, such an atomic layer resolution of the surface region is necessary, due to the complexity of HEAs.

In order to obtain an exact understanding of the atomistic mechanism at the monoatomic layer level, High-Sensitivity - Low Energy Ion Scattering Spectroscopy (HS-LEIS), was applied, which provides the required monolayer sensitive resolution to study the passivation layers of such complex multi-component alloys. The unique surface sensitivity combined with the implementation of in-situ treatment methods enabled the real-time study of oxide layer growth, as well as the analysis of temperature-dependent changes in the elemental surface composition. Due to the high resolution achieved by static and dynamic sputter depth profile modes, we could determine the exact composition of the HEA passivation layer with resolution on atomic monolayer scale.

The findings provide the potential to significantly advance the current understanding of the passivation behaviour of MPEAs and HEAs, and the development of novel metallic materials with superior properties. Valuable insights for understanding the material characteristics for those highly advanced materials could thereby be generated.

## Fundamental Discoveries in Heterogeneous Catalysis Focus Topic

### Room B113 - Session HC+SS-WeA

#### Advances in Complex Catalytic Systems

**Moderators:** *Zdenek Dohnalek*, Pacific Northwest National Laboratory, *Dan Killelea*, Loyola University Chicago

2:20pm **HC+SS-WeA-1 Computational Studies of Selective Reduction Reactions on Metal and Metal Compounds Electrocatalysts**, *J.R. Schmidt*, UW Madison

Understanding and controlling the factors that govern selectivity in electrocatalysis is key to enabling a wide range of electrochemical transformations. I will highlight efforts from two ongoing collaborative studies, focusing on the selective 2e<sup>-</sup> reduction of oxygen to hydrogen peroxide over a series of transition metal dichalcogenides; and the selective reduction of highly functionalized biomass molecules using traditional metallic electrocatalysts. In both cases, I will demonstrate how emerging computational electrocatalysis approaches yield a rich picture for the factors that govern catalytic selectivity in these systems. In addition, I will briefly discuss recent work focused on increasing the long-term stability of these electrocatalysts, opening the doors to potential commercial applications.

3:00pm **HC+SS-WeA-3 Metal Atom Chemical Potential: A Key Descriptor for Predicting Particle Size Effects on Catalyst Performance, and How to Estimate It**, *Charles T. Campbell*, *K. Zhao*, *N. Janulaitis*, University of Washington

Many important catalysts and electrocatalysts for energy and environmental technologies involve late transition metal nanoparticles dispersed across the surface of some oxide or carbon support. The activity and long-term stability of these materials depend strongly on particle size below 7 nm, and, in this size range, upon the composition and atomic-level structure of the support surface. We show here that the chemical potential of the metal atoms in such supported catalysts provides a convenient descriptor of their performance as heterogeneous catalysts that captures many of the effects of particle size, metal-metal alloying and support on catalyst performance. Based on microcalorimetric measurements of metal adsorption energies, the metal chemical potential is shown to be predictable as a function of metal particle size and the adhesion energy of the particle to the support. For oxide supports, this adhesion energy correlates predictably with metal oxophilicity, as we defined based on heats of oxide formation from gaseous metal atoms. For carbon supports, this adhesion energy correlates predictably with metal carbophilicity, as we defined based on DFT estimates of C atom adsorption energies. These correlations provide predictions of metal chemical potential that can enable catalyst design.

Work supported by DOE-OBES under Grant Number DE-FG02-96ER14630.

3:20pm **HC+SS-WeA-4 Size-Dependent Properties of Cobalt Nanoclusters on CeO<sub>2</sub>(111)**, *M. Rahman*, Louisiana State University; *T. Ara*, University of Wyoming; *Ye Xu*, Louisiana State University; *J. Zhou*, University of Wyoming  
Cobalt is a versatile catalytic metal. It has been used to catalyze many reactions of technological importance, including Fischer-Tropsch synthesis,

# Wednesday Afternoon, November 8, 2023

reforming, and ammonia synthesis, where oxidic Co and metallic Co lead to different catalytic pathways. Meanwhile, ceria offers a desirable set of properties as catalyst support, including the abilities to stabilize nanoclusters, undergo redox interaction with metals, and enhance oxygen availability. Nanoparticles of Co supported on ceria have therefore been the mainstay of many heterogeneous catalysis studies. We have carried out an investigation of Co nanoclusters supported on stoichiometric CeO<sub>2</sub>(111) using computational modeling and scanning tunneling microscopy (STM). Various sizes up to ca. 20 Co atoms have been optimized using a minima hopping algorithm combined with density functional theory (DFT) calculations, which identifies many compact, symmetric structures as minimum-energy for the sizes that are considered. Theory predicts that in this size regime, the Co clusters prefer to be notably wider than they are high. A significant fraction of the Co atoms in each cluster are oxidized, and most of those are located on the periphery between the clusters and ceria. Co atoms that are not directly in contact with the surface are effectively screened and remain neutral. The large aspect ratios and high fractions of oxidic Co in small clusters at low Co metal coverages are corroborated by STM studies of Co deposited on CeO<sub>2</sub>(111) thin film surfaces at ambient temperature. Our findings shed light on atomic-level characteristics of Co nanoclusters on ceria that are relevant to catalytic applications.

**4:20pm HC+SS-WeA-7 on-Surface Synthesis of Porous Planar-Carbon-Lattices: Fundamental Properties and Applications, Abner de Siervo, Institute of Physics Gleb Wataghin, University of Campinas (UNICAMP), Brazil** **INVITED**

Materials science in the nanoscale domain has become a reality for several applications, from integrated circuits, sensors, catalysts, medicines, and data-storage devices, among others [1]. We achieved the ability to understand materials and, more importantly, command the materials' properties at the atomic level using precise synthesis and growth methods. Therefore, during the last decades, enormous efforts have been made to develop new processes for the fabrication, characterization, and manipulation of materials in complex nanoarchitectures with atomic precision, making it possible to express emergent new chemical, electronic, photonic, magnetic, and structural properties. On-surface synthesis becomes a powerful bottom-up technique to fabricate such nanostructures using organic and organometallic precursors as molecular building blocks [2]. In this talk, I will present some strategies we have adopted to produce planar carbon lattices nanostructures, for example, porous nanoribbons and nanomembranes [3-5]. For a complete understanding of the atomic and electronic properties of the materials, we have combined scanning tunneling microscopy and spectroscopy (STM/STS), X-ray photoelectron spectroscopy (XPS), and numerical simulations based on density functional theory (DFT) calculations.

Acknowledgments:

FAPESP, CNPq, and CAPES from Brazil have financially supported this work.

References:

[1] G Ali Mansoori and TA Fauzi Soelaiman. Nanotechnology—An introduction for the standards community. ASTM International, 2005.

2005.

[2] Johannes V. Barth. Annual Review of Physical Chemistry, 58(1):375–407,

2007.

[3] Alisson Ceccatto dos Santos, et al., Chemistry of Materials 32 (5), 2114-2122 (2020).

[4] Nataly Herrera-Reinoza, et al., Chemistry of Materials 33, 2871-2882 (2021).

[5] Alisson Ceccatto dos Santos, et al., J. Phys. Chem. C 125, 31, 17164–17173 (2021).

**5:00pm HC+SS-WeA-9 2D Surface Optical Reflectance for Surface Studies in Harsh Environments, A. Larsson, Lund University, Sweden; S. Pfaff, Sandia National Laboratories; L. Rämisch, S. Gericke, A. Grespi, J. Zetterberg, Edvin Lundgren, Lund University, Sweden**

During recent years, 2D Surface Optical Reflectance (2D-SOR) [1,2] microscopy [3] has emerged as a valuable surface characterization tool for model catalysts or electrodes [4] when performing operando investigations in harsh environments. In particular, 2D-SOR microscopy is favorably used as a complementary technique to other photon-in-photon-out techniques which do not carry direct information on the surface 2D morphology. In this presentation we will present the development and examples of 2D-SOR instrumentation and investigations from single and poly-crystalline samples in combination with Planar Laser Induced Fluorescence (PLIF) [2, 3], High Energy Surface X-Ray Diffraction (HESXRD) [5,6,7] and Polarization Modulation-Infrared Reflection Absorption Spectroscopy (PM-IRRAS) [8] coupled to Mass Spectrometry (MS) and Cyclic Voltammetry (CV) in thermal catalysis, electrocatalysis and corrosion. Illustrating examples of the versatility of the technique will be shown including reflectance changes during the thermal CO oxidation over Pd(100) and Pd polycrystalline surfaces. We show that reflectance changes during the reaction can be associated with the formation of thin Pd oxides by the combination of 2D-SOR and Surface X-Ray Diffraction (SXRD). The combined measurements demonstrate a sensitivity of 2D-SOR to the formation of a 2-3 Å thin Pd oxide film. During Cyclic Voltammetry (CV) in an acidic electrolyte using a Au(111) surface as an electrode, we show that the differential of the change in 2D-SOR reflectance correlate to various current features in the CV curve. This observation can be used to differentiate current features in the CV curve from a polycrystalline Au surface, demonstrating that the different grains contribute to the current at different potentials due to the different surface orientations. Finally, we show that 2D-SOR is a cheap and useful technique to investigate the corrosion of applied materials such as duplex stainless steels and Ni alloys.

[1] W. G. Onderwaater et al Rev. Sci. Instrum., **88** (2017) 023704.

[2] J. Zhou et al, J. Phys. Chem. C **121** (2017) 23511.

[3] S. Pfaff et al, ACS Appl. Mater. Interfaces **13** (2021) 19530.

[4] W. Linpe, et al, Rev. Sci. Instrum., **91** (2020) 044101.

[5] S. Pfaff, et al Rev. Sci. Instrum. **90** (2019) 033703.

[6] S. Albertin, et al, J. Phys. D: Appl. Phys. **53** (2020) 224001.

[7] W. Linpé, et al J. Electrochem. Soc. **168** (2021) 096511.

[8] L. Rämisch et al, Appl. Surf. Sci. **578** (2022) 152048

**5:20pm HC+SS-WeA-10 Interrogating Reactive Sites with Intrinsic Kinetics Over Well-Defined Supported Pt Nanoparticles, T. Kim, C. O'Connor, Christian Reece, Harvard University**

The chemical industry is the primary consumer of energy and fossil fuels in the industrial sector and relies almost entirely on complex heterogeneous catalytic systems. Yet our ability to employ these systems far outweighs our understanding. While a detailed understanding of heterogeneous catalysts does exist for model systems (e.g., 2D single crystals) at ultra-high vacuum, our understanding of applied catalytic materials (e.g., metal nanoparticles deposited on a metal oxide support) under reaction conditions is still lacking. Herein we utilize the Temporal Analysis of Products (TAP) technique to precisely resolve the intrinsic kinetics of CO oxidation of size selected 2nm Pt nanoparticles supported on SiO<sub>2</sub>. Using Diffuse Reflectance Infrared Fourier Transform Spectroscopy (DRIFTS) we identify multiple types of well-coordinated, undercoordinated, and bridge-bound CO sites exist on the Pt nanoparticles. However, through a combination of isotopic labelling and microkinetic modelling, we find that only two pathways for CO oxidation exist over the catalyst surface under the entire range of reaction conditions studied: a fast and a slow pathway. The fast pathway follows typical catalytic behaviour and shows a strong temperature dependence and a linear dependence on CO coverage, but the slow pathway is independent of both temperature and CO coverage which is unexpected for a slow catalytic process. This study demonstrates the importance of being able to precisely resolve kinetics over applied catalytic materials using techniques such as TAP. Further, it also hints that under reaction conditions the highly dynamic nature of catalytic surfaces implies that our classical understanding of structure-activity-relationships may not hold as strong as originally hoped.

**5:40pm HC+SS-WeA-11 The Effects of Catalytic Cluster Size on Catalysis and Electrocatalysis, Scott Anderson, University of Utah** **INVITED**

Supported sub-nano clusters are potentially a metals-efficient approach to catalysis, where all the expensive catalytic atoms (Pt, Pd, etc.) are exposed

# Wednesday Afternoon, November 8, 2023

in the surface layer. In addition, because the properties of small clusters are highly size dependent, varying the cluster size provides a parameter that can be used to tune activity and selectivity. The problem with small clusters is that they tend to sinter and poison easily, and much of our work is in developing approaches to stabilize the supported clusters under thermal or electro-catalytic conditions.

Deposition of mass-selected clusters in UHV is used to prepare model catalysts and electrocatalysts with catalytic centers that all start out being the same size. We have developed an in-vacuum ALD-like self-limiting reaction approach to dope or alloy the clusters with elements like B, Sn, or Ge, with the goal of stabilizing the clusters against both poisoning and sintering. Two types of catalysis experiments will be described.

Gas-surface catalysis is studied in the UHV system by mass spectrometric methods, but we also have new microreactor system that allows clusters deposited on alumina or silica surfaces to be exposed to reactant flows at pressures up to 1 atm, with mass spectrometric product detection. This part of the talk will focus on using Ge doping to stabilize small Pt clusters against deactivation by both carbon deposition (coking) and sintering at temperatures up to 700 K. To goal is to make stable and selective alkane dehydrogenation and cracking catalysts.

Electrocatalysis is studied either *in situ*, using an electrochemical cell housed in an antechamber to the UHV system, or in conventional benchtop electrochemical cells. The *in situ* experiments allow us to study aqueous electrochemistry with minimal air exposure, while the *ex situ* setups allow more elaborate types of electrochemical measurements. Results for the hydrogen evolution reaction (HER), oxygen evolution reaction (ORR), and alcohol electro-oxidation will be presented for catalytic Pt<sub>n</sub> clusters deposited on indium tin oxide (ITO), fluorine tin oxide (FTO), and graphite (HOPG). For ITO/FTO, electrodes were prepared by soft landing the clusters. For HOPG, the effects of deposition energy on electrocatalytic activity and stability, and on physical properties measured by XPS and ISS will be discussed.

## Surface Science Division

### Room D136 - Session SS-WeA

#### A Special Session Honoring Wilson Ho: 25 Years of Single-Molecule Vibrational Spectroscopy and Microscopy

Moderators: Xi Chen, Tsinghua University, Xiaohui Qiu, Nanocenter

#### 2:20pm SS-WeA-1 Development of Single-Molecule Spectroscopy Inspired by STM-IETS, Yousoo Kim, RIKEN, Japan INVITED

The scanning tunneling microscope (STM) is a versatile and powerful tool for investigating and controlling the chemistry of individual molecules on solid surfaces, mainly due to its extremely high spatial resolution. Using tunneling electrons from an STM tip, it is possible to excite various quantum states of single molecules on a surface, providing insights into the mechanisms of surface chemical reactions. Inspired by the pioneering work of Wilson Ho's group on single-molecule vibrational spectroscopy by inelastic electron tunneling spectroscopy combined with STM, we have been able to establish a dynamic approach to explore vibrational mode-selective chemistry in single-molecule reactions based on action spectroscopy with STM. Later, we developed an optical STM that combines the STM with light illumination and detection systems to probe molecular energetic processes such as energy transfer, conversion, and dissipation. In this talk, I will discuss some of our long-standing efforts to develop single-molecule spectroscopy using local excitation sources, such as tunneling electrons and localized surface plasmon, generated at the STM junction.

#### 2:40pm SS-WeA-2 Unraveling Orbital Magnetism Contributions to Landau Levels in Moiré Quantum Matter, Joseph Stroscio, NIST INVITED

Flat and narrow band physics in moiré quantum matter (MQM) has proven to be extremely rich with new emergent quantum phases which can be tuned with applied electric and magnetic fields. The topological properties of the eigenstates of the moiré Hamiltonian are critical for establishing the quantum phase of the system. In this talk, we use the quantum ruler of Landau levels to unravel the energy-resolved valley-contrasting orbital magnetism and large magnetic susceptibility that contribute to the energies of Landau levels of twisted double bilayer graphene. These orbital magnetism effects lead to significant deviations from the standard Onsager relation, which manifests as a breakdown in scaling of Landau level orbits. These substantial magnetic responses emerge from the nontrivial quantum geometry of the electronic structure and the large length scale of the moiré lattice potential. We show that this breakdown of the original Onsager

relation is unique in MQM due to the typical superlattice length scales in these systems. Going beyond traditional measurements, STM-based Landau level spectroscopy offers a complete "quantum ruler" resolving the full energy dependence of orbital magnetic properties in moiré quantum matter.

#### 3:00pm SS-WeA-3 Sub-Nanometer Resolved Single-Molecule Optical Imaging, Z. Dong, University of Science and Technology of China; Shaowei Li, University of California, San Diego INVITED

Aspirations for reaching atomic resolution with light have been a major force in shaping nano-optics, whereby a central challenge is to achieve highly localized optical fields. The plasmonic nanocavity defined by the coinage-metal tip and substrate in a scanning tunneling microscope (STM) can provide highly confined and dramatically enhanced electromagnetic fields upon proper plasmonic resonant tuning, which can modify both the excitation and emission of a single molecule inside the nanocavity and produce intriguing new optoelectronic phenomena. In this talk, I shall demonstrate two recent STM-based phenomena related to single-molecule optical spectroscopy. The first is single-molecule Raman scattering closely associated with molecular vibrations. The spatial resolution of tip enhanced Raman spectroscopy (TERS) has been further driven down to the Angstrom scale at the single-bond level. Such a capability not only yields a new methodology called scanning Raman picoscopy for structural reconstruction and tracking bond breaking and forming of surface reactions, but also enables to clarify the chemical enhancement mechanism in TERS through well-controlled local contact environments. The second phenomenon is single-molecule electroluminescence. Through managements over molecular quenching and energy level alignment, we demonstrate clear single-molecule electroluminescence and even single-photon emission. Furthermore, by precisely controlling intermolecular distances, we can not only demonstrate coherent dipole-dipole coupling in homodimers, but also reveal intriguing transitions from incoherent hopping-like Forster energy transfer to coherent wavelike electronic energy transfer in donor-acceptor heterodimers. In addition, the wavelike quantum-coherent transfer channel is found three times more efficient than the incoherent channel in a one-step transfer process, highlighting the advantage of coherent channels in electronic energy transfer processes in large molecular networks. Our results provide new routes to optical imaging, spectroscopy and engineering of light-matter interactions and intermolecular coupling at the sub-nanometer scale.

#### 3:20pm SS-WeA-4 Magnetic Resonance Imaging of Individual Organic Radicals with sub-Molecular Resolution Using a Scanning Tunneling Microscope, Christopher Lutz, G. Czap, IBM Almaden Research Center INVITED

Scanning tunneling microscopy (STM) gives atomic-resolution detection of properties such as the electronic density of states, spin polarization, and spin and vibrational excitations. Electron spin resonance (ESR) of individual atoms and small molecules has extended these capabilities to give very high energy resolution and quantum control, transforming individual adsorbed atoms into sensitive detectors of the local magnetic field. Here we present spin resonance of individual organic radical molecules adsorbed on an ultra-thin MgO film grown on a silver crystal. We find that several nearly-planar fluorenone derivatives become charged to anions upon adsorption on the insulating film. This spontaneous charging quenches the spin of the radicals, and transforms stable molecules into radical anions. These radicals are driven spin-resonantly by the radio-frequency electric field from the tip and sensed locally by magnetoresistance. We found a g-factor of nearly 2 for each species and visualized the delocalized unpaired electron in these molecules by magnetic resonance imaging. We used conventional Fe-terminated tips as well as halogen-functionalized Fe tips in a 1-Kelvin microscope. Potential applications include the investigation of coupled molecular spins and graphene nanoribbon edge states, and the transfer of a spin-resonant molecule to the microscope tip in order to provide a versatile scanning ESR sensor.

#### 4:20pm SS-WeA-7 Revealing the Local Band Structures of Sharp WS<sub>2</sub>/MoS<sub>2</sub> Heterojunction and Graded W<sub>x</sub>Mo<sub>1-x</sub>S<sub>2</sub> Alloy by Near-Field Optical Imaging, Chi Chen, Academia Sinica, Taiwan INVITED

With the development of various chemical vapor deposition (CVD) methods [1], many artificial 2D semiconductors have been synthesized, which increase the chances of forming disrupted interfaces and non-periodic or small-sized systems (defects and grain boundaries). All such systems create local electronic band structures within a finite scale, which cannot be readily explained by solid-state band theory nor be probed easily by confocal microscopes and macroscopic transport.

# Wednesday Afternoon, November 8, 2023

In this study, we investigated abrupt heterojunctions and graded alloys between two transition metal dichalcogenides (TMD), which involve non-periodic band structures and require high spatial resolution. We employed near-field photoluminescence (NF-PL) imaging to study the atomically sharp 1D interfaces between  $WS_2$  and  $MoS_2$ . With an optical resolution of 68 nm, a 105 nm-wide region for quenched PL was confirmed using NF-PL imaging [2]. Our NF-PL imaging resolved the narrowest quenching width and sharpest strain mapping because of the superior spatial resolution and stability of our home-built SNOM [3].

We further developed a near-field broadband absorption (or transmittance, NF-tr) imaging method to overcome the limitations of NF-PL for low-quantum-yield materials. The NF-tr technique provides abbreviation-free and nanoscale-resolution imaging capability of the entire conduction band over highly lateral inhomogeneity. We utilized NF-tr microscopy to investigate the varying bandgap and bowing factor of a single-layered  $W_xMo_{1-x}S_2$  alloy [4]. For the bilayer  $W_xMo_{1-x}S_2$  alloy, the energy contour maps present the bandgap evolution in the alloy and reveal bilayer coupling between the top and bottom layers. We can conclude that the bottom layer has an alloy nature, whereas the top layer is composed of pure  $WS_2$ . High-spatial-resolution spectral capability is essential for analyzing compositional and location-dependent bandgap evolutions.

- [1] K.-C. Chiu and Y.-H. Lee *et al.*, *Adv. Mater.* 30, 1704796 (2018)
- [2] H.-C. Chou and C. Chen *et al.*, *Nanoscale* 14, 6323 (2022)
- [3] J.-R. Yu and C. Chen *et al.*, *Rev. Sci. Instrum.* 91, 073703 (2020)
- [4] P.-W. Tang and C. Chen *et al.*, *ACS Nano*, 16, 5, 7503 (2022)

## 4:40pm SS-WeA-8 On-Surface Chemical Dynamics Probed with Concurrent In Situ STM, Infrared Spectroscopy, and Supersonic Molecular Beams, Steven Sibener, J. Wagner, R. Edel, T. Grabnic, S. Brown, J. Saylor, J. Brown, University of Chicago INVITED

We have developed the capability to elucidate interfacial reaction dynamics using an arguably unique combination of supersonic molecular beams combined with in situ STM and AFM visualization. These capabilities have been implemented in order to reveal the complex spatio-temporal correlations that govern heterogeneous reactions at their most fundamental level spanning atomic, nano, and meso length-scales. For example, time-lapse visualization of reacting interfaces is allowing us to probe the reactivity of specific sites at interfaces and how the presence of a reacted site or local region influences the subsequent reaction probability at proximal sites. Such correlations are important in chemisorption, catalysis, materials oxidation and erosion, and film processing. This capability also opens up a new view for interfacial reaction dynamics where incident beam kinetic energy and angle of incidence can be used for reaction control parameters with outcomes such as site-specific reactivity, changes for overall time-evolving mechanisms, and where the on-surface fate of chemisorbed species can be definitively ascertained. In this work the time-evolving interface can be probed either in real-time or, for reactions occurring under extreme thermal conditions, using time-lapse sequential imagery. This presentation will give illustrative examples from our recent work on the atomic and multiscale oxidative reactivity of HOPG graphite, H reactivity with SAMs, atomic oxygen interactions with single and multilayer graphene including moiré superlattices, and the energy disposal and geometric endpoint for molecular nitrogen chemisorption on Ru. Most recently, the ability to visualize single-molecule nitrogen dissociation events provides a new approach for assessing the importance of adiabatic vs. non-adiabatic interactions in chemisorption by examining the rate of energy disposal and ultimate atomic resting adsorption sites for the dissociatively adsorbed atoms from each individual molecular scattering event. Taken together, these results provide a direct and information-rich complement to traditional gas-surface scattering experiments which monitor volatile products, especially with respect to uncovering the important on-surface chemical events that inform multiscale spatio-temporal correlations that influence interfacial reaction pathways.

5:00pm SS-WeA-9 Unravelling the Mysteries of Water and Ice: A Journey Starting from Single Water Molecule, Ying Jiang, International Center for Quantum Materials, School of Physics, Peking University, China INVITED Despite its ubiquity in nature, water is one of most complicated condensed matters. The understanding of water structure and phase transition is far from satisfactory, and many unusual properties of water remain as puzzles. The main reason arises from the many-body hydrogen (H)-bonding interaction between the water molecules. Moreover, the light H nuclei can exhibit prominent quantum effects, in terms of tunneling and zero-point motion. The so-called nuclear quantum effects (NQE) add additional complexity to water and ice. Therefore, it would be ideal to directly access

the degree of freedom of H in water/ice. To this end, we have steadily continued to improve accuracies of imaging and spectroscopic methods based on scanning probe microscopy (SPM) (tip-enhanced inelastic electron tunneling spectroscopy and higher-order electrostatic force microscopy) [1,2], which acquire unprecedentedly high sensitivity to the H of single water molecule in a nearly non-invasive manner. In this talk, I will showcase the application of those techniques to probe water clusters, ion hydrates, 2D ice and even bulk ice surface [3-6], with increasing complexity. The possibility of combing SPM with quantum sensing technology to perform nanoscale NMR measurement of protons in ambient water will be also briefly discussed [7].

## References:

- [1] Guo *et al.*, *Science* 352, 321 (2016)
- [2] Peng *et al.*, *Nature Communications* 9, 122 (2018)
- [3] Meng *et al.*, *Nature Physics* 11, 235 (2015)
- [4] Peng *et al.*, *Nature* 557, 701 (2018)
- [5] Ma *et al.*, *Nature* 577, 60 (2020)
- [6] Tian *et al.*, *Science* 377, 315 (2022)
- [7] Zheng *et al.*, *Nature Physics* 18, 1317 (2022)

## 5:20pm SS-WeA-10 Probing Chemistry at the Angstrom-Scale via Tip-Enhanced Raman Spectroscopy, Nan Jiang, University of Illinois Chicago INVITED

The chemical interrogation of individual atomic adsorbates on a surface significantly contributes to understanding the atomic-scale processes behind on-surface reactions. However, it remains highly challenging for current imaging or spectroscopic methods to achieve such a high chemical spatial resolution. Tip-enhanced Raman spectroscopy (TERS), which couples scanning tunneling microscopy (STM) and surface-enhanced Raman spectroscopy, provides such a powerful capability to concurrently harvest topographic and chemical information with single-bond sensitivity at the angstrom-scale. Herein, we use ultrahigh vacuum (UHV) TERS to measure the angstrom-scale interfacial interactions of a vertical Van der Waals heterostructure of borophene with tetraphenyldibenzoperiflanthene (DBP) molecules. TERS reveals subtle ripples and compressive strains of the borophene lattice underneath the molecular layer. The induced interfacial strain is demonstrated to extend in borophene by  $\sim 1$  nm beyond the molecular region by virtue of 5 Å chemical spatial resolution. Furthermore, we use our method to probe the local chemical properties of oxidized borophene. The results show that single oxygen adatoms on borophene can be identified and mapped with  $\sim 4.8$  Å spatial resolution and single bond (B-O) sensitivity. In addition to offering atomic-level insights into the above-mentioned systems, our studies demonstrate UHV-TERS as a powerful tool to probe the local chemistry of surface adsorbates and interfacial structures in the atomic regime with widespread utilities in heterogeneous catalysis, on-surface molecular engineering, and low-dimensional materials.

## 5:40pm SS-WeA-11 Single Molecule Characterization of Cobalt Phthalocyanine $CO_2$ Reduction Catalysts, X. Wang, Yale University; P. Zahl, Brookhaven National Laboratory; H. Wang, Eric Altman, U. Schwarz, Yale University

Immobilized cobalt phthalocyanine (CoPc) derivatives have been identified as promising catalysts for  $CO_2$  electroreduction to methanol. The support as well as side chains attached to CoPc have a large effect on the activity and selectivity to methanol. CO adsorption strength is considered a key descriptor for  $CO_2$  reduction activity and selectivity. Therefore, we have begun to study CO interactions with individual supported CoPc molecules using scanning probe methods. This talk focuses on a combined scanning tunneling microscopy, non-contact atomic force microscopy, and Kelvin probe force microscopy characterization of CoPc molecules on Ag(111) with CO functionalized tips. In addition to resolving the atomic structure, the data provides the three-dimensional force field acting between the tethered CO and supported CoPc molecules and the charge distribution across the CoPc that is responsible for it. Analysis of the force field yielded maps of the catalytically relevant equilibrium potential energy between the tethered CO and specific locations within the CoPc molecule. Surprisingly, the maps show that the strongest interaction is not directly above the Co atom, but rather in four nodes surrounding it. The results are being compared with amino-substituted CoPc where the amino groups have been shown to enhance catalytic activity.

# Wednesday Afternoon, November 8, 2023

6:00pm **SS-WeA-12 Switching Chemical Bonds by Mechanical Load at Single Molecule Level via Qplus Atomic Force Microscope**, *A.M. Shashika D. Wijerathna*, *M. Zirnheld*, Old Dominion University; *Z. Win*, City University of Hong Kong, Hong Kong Special Administrative Region of China; *Y. Li*, Center for Nanoscale Materials, Argonne National Laboratory; *R. Zhang*, City University of Hong Kong, Hong Kong Special Administrative Region of China; *S. Hla*, Center for Nanoscale Materials, Argonne National Laboratory; *Y. Zhang*, Old Dominion University

Switching Chemical Bonds by Mechanical Load at Single Molecule Level via Qplus Atomic Force Microscope

A.M. Shashika D. Wijerathna<sup>1</sup>, Markus Zirnheld<sup>1</sup>, Zaw Myo Win<sup>2</sup>, Yang Li<sup>3</sup>, Ruiqin Zhang<sup>2</sup>, Saw Wai Hla<sup>3</sup>, Yuan Zhang<sup>1</sup>

Affiliation: 1. Department of Physics, Old Dominion University, Norfolk, VA, 23529, USA.

2. Department of Physics, City University of Hong Kong, Hong Kong SAR, China.

3. Center for Nanoscale Materials, Argonne National Laboratory, Lemont, IL, 60439, USA.

**Abstract:** Mechanical properties of molecules adsorbed on materials surfaces are increasingly vital for the applications of molecular thin films. Here, we induce molecule conformational change by switching chemical bonds on a single molecule by mechanical load, and quantify the force and energy required for such switch via a low temperature (~ 5K) Scanning Tunneling Microscope (STM) and Qplus Atomic Force Microscope (Q+AFM). Molecule TBrPP-Co (a cobalt porphyrin) deposited on an atomically clean gold substrate typically has two of its pentagon rings tilted upward and the other two downward. An atomically sharp tip of the STM/Q+AFM, which vibrates with a high frequency (~ 30kHz), is employed to run over single TBrPP-Co molecule at different heights with 0.1Å as increment and meanwhile to record tip-molecule interaction strength in the form of tip frequency change. When tip approaches to the threshold distance to the molecule, mechanical load by the tip becomes large enough to switch chemical bonds of the molecule and cause pentagon rings flip their direction. Due to the sensitive nature of tip-molecule interaction, the rings flipping can be directly visualized by STM, as rings tilting upward exhibit two bright protrusions in contrast to rings downward in image. By processing frequency change, we obtain a three-dimensional mechanical potential and force map for the single molecule TBrPP-Co with the resolution of angstrom level in three dimensions. Our preliminary results indicate that an energy barrier of ~67meV for switching between covalent and coordinated bonds to cause rings flipping of TBrPP-Co.

## Applied Surface Science Division

Room B117-119 - Session AS+CA+EL+EM+SE+SS+TF-ThM

### Quantitative Surface Analysis II

**Moderators:** Samantha Rosenberg, Lockheed Martin, Thierry Conard, IMEC, Belgium, Benjamen Reed, National Physical Laboratory, UK

8:00am **AS+CA+EL+EM+SE+SS+TF-ThM-1 OrbiSIMS: Signal, Noise and Transmission Are Three Sides of a Metrology Triangle**, G. Trindade, Y. Zhou, A. Eyres, National Physical Laboratory, UK; M. Keenan, Independent; Ian Gilmore, National Physical Laboratory, UK

In metrology, the science of measurement, a “metrology triangle” approach is used to provide a secure foundation. For example, the Quantum Metrology Triangle links Voltage, Resistance and Current through the Josephson Effect and the Quantum Hall Effect.

The OrbiSIMS<sup>1</sup>, introduced in 2017, has become increasingly popular for biological and material sciences studies owing to its ability to give high confidence in molecular identification (mass resolving power > 240,000 and mass accuracy < 2 ppm) simultaneously with high confidence in localisation (micrometre scale spatially and nanoscale in depth). With a growing number of instruments internationally there is an increased need for metrology for reproducible measurements. We will show how Signal, Noise and Transmission form three sides of a metrology triangle that combine to enable better measurement. In a recent comprehensive study of the noise in an Orbitrap mass spectrometer, a probabilistic model was developed.<sup>2</sup> A region of the intensity scale is described by Poisson statistics allowing the scaling parameter, A, that relates ion current to the number of ions in the trap to be determined. A true signal intensity scale is then established which allows the useful yield of atoms in an implant layer to be measured. Through comparison with time-of-flight and magnetic sector instruments the fractional ion transmission is determined.<sup>3</sup> We will discuss how Signal and Transmission combine to understand matrix effects in biological sample preparation and how understanding Signal and Noise are important for data analytical methods.

1. M. K. Passarelli. et al, I. S. Gilmore, Nat. Methods, 14(2017)12, 1175-1183.
2. M R. Keenan, G. F. Trindade, A. PirkI, C. L. Newell, K. Ayzikov, J. Zhang, L. Matjajic, H. Arlinghaus, A. Eyres, R. Havelund, J. Bunch, A. P. Gould, A. Makarov and Ian S. Gilmore, in preparation.
3. Y. Zhou, A. Franquet, V. Spampinato, G. F. Trindade, P. van der Heide, W. Vandervorst and I S Gilmore, in preparation.

8:20am **AS+CA+EL+EM+SE+SS+TF-ThM-2 Contribution of Imaging X-Ray Photoelectron Spectroscopy to Characterize Chrome Free Passivation Nano-Layer Deposited on Food-Packaging Tinplate: Composition and Chemical Environment**, E. Ros, Vincent Fernandez, CNRS, France; N. Fairley, CASAXPS, UK; B. Humbert, M. Caldes, CNRS, France

To protect metal from corrosion, passivation layer are widely used in food-packaging industry. Those Nano-metric protections create a thin oxide Nano-layer on the metal surface, making it less oxidisable. Common passivation are composed by chromium oxide[1], using hexavalent chromium as a reagent and reducing it. However, because of the toxicity of Cr(VI), European Union is gradually forbidding.Chromium Free Passivation Alternative is based on transitions metal oxides (Sn, Ti, Zr, Mn) and polymers. These samples present some roughness in few micron range observed by Atomic Force Microscopy.XPS Imaging were perform at different binding energy to allow extracting spectrum in each pixel over the eight (Mn 2p, O 1s, Sn 3d, Ti 2p,N 1s, C 1s, P 2s and Zr 3d) XPS core level process. This study show an anti-correlation between atomic concentration of Titanium and Tin Fig(1). We observe a ratio Sn oxide Sn metal homogeneous and independent of the Ti, Sn ratio More over using the vector method [2], [3] concurrently to height XPS core, we could extract two different chemical environments spectrum. The linear Least Square combination of these 2 spectrum allow us to model 131072 regions. To extract information form XPS data on heterogenous sample the combination of XPS imaging energy scan measurement with the vector method is a promising way. These results bring the useful information about different thin layer deposition steps. Imagerie XPS results are in agreement with Raman imagerie analysis

[1]R. Sandenbergh, M. Biermann, and T. von Moltke, ‘Surface Analytical Characterization of Chromium Passivation on Tinplate’, in *Passivation of Metals and Semiconductors, and Properties of Thin Oxide Layers*, P. Marcus and V. Maurice, Eds., Amsterdam: Elsevier Science, 2006, pp. 143–148. doi: 10.1016/B978-0-444-52224-5/50024-X.

[2]J. Baltrusaitis *et al.*, ‘Generalized molybdenum oxide surface chemical state XPS determination via informed amorphous sample model’, *Applied Surface Science*, vol. 326, pp. 151–161, Jan. 2015, doi: 10.1016/j.apsusc.2014.11.077.

[3]M. d’Halluin *et al.*, ‘Graphite-supported ultra-small copper nanoparticles – Preparation, characterization and catalysis applications’, *Carbon*, vol. 93, pp. 974–983, Nov. 2015, doi: 10.1016/j.carbon.2015.06.017.

8:40am **AS+CA+EL+EM+SE+SS+TF-ThM-3 Cryo-Xps for Surface Characterisation of Nanomedicines**, David Cant, National Physical Laboratory,, UK; Y. Pei, National Physical Laboratory, UK; A. Shchukarev, M. Ramstedt, University of Umea, Sweden; S. Marques, M. Segundo, University of Porto, Portugal; J. Parot, A. Molska, S. Borgos, SINTEF, Norway; C. Minelli, A. Shard, National Physical Laboratory, UK

Nanomedicines are an area of great interest for current and future pharmaceutical development. The use of nanoparticles to act as carriers for a therapeutic load has the potential to significantly improve medical outcomes, for example by allowing a therapeutic agent to circulate within the body for longer, or by allowing targeted delivery of a drug to a specific site. Such nanomedicines often rely on specific functional coatings to achieve their desired impact; for example the majority of nanomedicines currently available on the market utilise a poly-ethylene glycol (PEG) surface coating for its ‘stealth’ properties, helping nanomedicines evade the body’s clearance mechanisms. Accurate measurement of the surfaces of such nanomaterials is therefore of great importance, yet direct, quantitative surface chemistry measurements are not commonly available, and vacuum-based analysis methods such as XPS are unlikely to provide a representative measurement of the particles in their hydrated state.

Here we present to the best of our knowledge the first use of Cryo-XPS to provide direct, quantitative measurements of the surface chemistry of nanomedicines in a hydrated state. Two nanomedicine systems were measured: a drug-carrying polymer nanoparticle; and an mRNA loaded lipid nanoparticle. Both systems possessed a supposedly PEG-terminated surface, and were measured using XPS in both aqueous cryogenic state, and dry drop-cast onto a substrate. The results of these measurements clearly demonstrate that while the PEG surface cannot readily be observed in the dry state, the cryogenic measurements exhibit spectra that are consistent with the particle being measured in a hydrated condition.

9:00am **AS+CA+EL+EM+SE+SS+TF-ThM-4 Redox XPS as a Means to Address Some XPS Reproducibility Challenges**, Peter Cumpson, University of New South Wales, Australia

The challenge of better understanding of increasingly-complex specimens in surface analysis has been highlighted recently[1,2,3,4]. Especially at a time of high throughput XPS instruments and broadening of the (non-specialist) user community. An AVS survey conducted in 2018 found that 65% of those responding identified reproducibility as a significant issue [5].

There is an analogy to be made with some radically-different technologies. Machine Learning makes more sense of a moving image than a single snapshot, even if the snapshot were to come from a larger, better calibrated camera. Yet somehow we expect greater calibration precision, reference data and rigorous procedures to be the only route to reliable understanding of single spectra.

Generating a sequence of spectra from a progressively chemically-modified surface can remove many ambiguities that can otherwise cause misinterpretation. Such sequences thereby help with rapid understanding of the unmodified surface. On the theme of “Two is Better than One: Breaking Barriers with Coupled Phenomena” we present results from coupled stepwise oxidation/reduction of the surface and XPS to resolve such ambiguities for a wide range of materials and problems. Gas-phase oxidation agents are used to move through the redox states of a specimen in a controllable way, taking advantage of the logarithmic growth of oxide thickness. What is more, this oxidation is easy to implement in the entry-locks of modern XPS instruments through the use of vacuum ultraviolet light (VUV) and the *in situ* generation of ozone and gas-phase hydroxide free radicals. In the past there have been many studies of how particular materials react to ozone exposure at their surfaces, often employing XPS. Here we reverse this, and use ozone (and VUV) exposure to simplify the

interpretation of spectra from a wide range of unknown materials, we think for the first time.

[1] D R Baer et al, J. Vac. Sci. Technol. A 39, 021601 (2021); <https://doi.org/10.1116/6.0000873>

[2] G. H. Major et al, J. Vac. Sci. Technol. A 38, 061204 (2020); <https://doi.org/10.1116/6.0000685>

[3] G. H. Major et al, J. Vac. Sci. Technol. A 38, 061203 (2020) <https://doi.org/10.1116/6.0000377>

[4] D R Baer and M. H. Engelhard, Journal of Surface Analysis Vol. 26, No.2 (2019) pp. 94-95.

[5] D R Baer, J F Watts, A Herrera-Gomez, K J Gaskell, Surf Interface Anal. 2023; 1- 9. doi:10.1002/sia.7194

9:20am **AS+CA+EL+EM+SE+SS+TF-ThM-5 Sub-Nanometer Depth Profiling of Native Metal Oxide Layers Within Single Lab-XPS Spectra**, *Martin Wortmann*, N. Frese, Bielefeld University, Germany; *K. Viertel*, Bielefeld University of Applied Sciences and Arts, Germany; *D. Graulich*, M. Westphal, T. Kuschel, Bielefeld University, Germany

Many metals form nanometer-thin self-passivating native oxide layers upon exposure to the atmosphere, which affect their interfacial properties and corrosion behavior. Such oxide layers are commonly analyzed by X-ray photoelectron spectroscopy (XPS). Here we propose a simple and accessible depth profiling approach for oxide layers with sub-nanometer depth resolution from single lab-XPS spectra. Metals and their oxides can be distinguished by a binding energy shift to quantify their distinct signal contributions. Analogous to the widely used Hill equation we utilize the known photoelectron's inelastic mean free path to calculate the characteristic oxide layer thickness. However, in contrast to the Hill equation we analyze not only one, but all orbital energies in the XPS spectrum to develop a model that accounts for a depth-resolved concentration profile at the oxide-metal interface. The proposed model not only improves the accuracy and reproducibility of earlier methods but also paves the way for a more holistic understanding of the XPS spectrum.

9:40am **AS+CA+EL+EM+SE+SS+TF-ThM-6 A Tag-and-Count Methodology Based on Atomic Layer Deposition (ALD) and Low Energy Ion Scattering (LEIS) for Quantifying the Number of Silanols on Fused Silica**, *Josh Pinder*, Brigham Young University

The concentration of surface silanols governs many of the properties of glass and fused silica surfaces including surface wetting, surface contamination rates, and thin film adhesion. Indeed, the concentration of surface silanols is impactful for diverse fields such as atomic layer deposition (ALD), chromatography, catalysis, and displays. Accordingly, various analytical and theoretical methods have been employed to determine the number of silanols on surfaces, including density functional theory, FTIR, thermogravimetric analysis, and temperature programmed desorption mass spectrometry. However, many of these methods are better applied to particulate materials than surfaces. In this presentation, we discuss a method for directly

measuring the concentrations of surface silanols on silica-containing surfaces via a tag-and-count methodology. This approach is based on tagging surface silanols by ALD via a single pulse of dimethylzinc or diethylzinc and then quantifying the number of tags (zinc atoms) using high

sensitivity-low energy ion scattering (HS-LEIS). Our method yielded the literature value for both fully hydroxylated fused silica and also fused silica that had been heated to 500, 700, and 900 C. We see this capability as enabling for all who work with glass, fused silica, and silicon wafers,

including for ALD.

11:00am **AS+CA+EL+EM+SE+SS+TF-ThM-10 ASSD Peter M. A. Sherwood Mid-Career Professional Awardee Talk: Providing Fundamental Mechanistic Insights Into Single-Site Catalytic Reactions**, *Jean-Sabin McEwen*<sup>1</sup>, Washington State University

INVITED

The single atom limit achieves the ultimate degree of material efficiency for supported metal catalysts. To this end, the ability to create highly dispersed, single-site catalysts, which are highly efficient and have low cost, is very much desirable. While single atom sites can be created, there is still disagreement over whether the single atom sites are indeed catalytically active or if the observed catalytic activity of single-site catalysts is due to metal nanoparticles either unobserved during initial microscopy studies or formed upon exposure to catalytic conditions. Such disagreements create a crucial need for the development of well-defined single-site catalysts with an accurate theoretical model in order to correctly determine the chemical nature of the catalytically active sites. To this end, we provide new atomistic insights regarding the "44" Cu surface oxide through the integration of synchrotron-based X-ray Photoelectron Spectroscopy (XPS) measurements, Synchrotron X-ray Diffraction measurements (SXRD), Scanning Tunneling Microscopy (STM) and Density Functional Theory (DFT) techniques. We also quantify the low-temperature CO oxidation kinetics on Pt single-site catalysts supported on the "29" Cu surface oxide. The "29" Cu surface oxide is a high coverage chiral structure that arises when we further oxidize the "44" structure. Using STM, CO temperature programmed desorption (TPD), and DFT techniques, we determine that an accurate model for the "29" Cu oxide surface is formed from the growth of a Cu<sub>x</sub>O layer formed from 6 fused hexagonal rings above the Cu (111) surface where 5 oxygen adatoms are added at the center of the Cu<sub>x</sub>O rings. Furthermore, we determine the state of the Pt single atoms before, during, and after reaction through a combination of theoretical and experimental techniques. We also correlate ambient pressure experiments, surface science measurements and first principles-based calculations to demonstrate that Pt/Cu(111) single-atom alloys (SAAs) oxidized with varying degrees of O<sub>2</sub> exposure can be reduced with H<sub>2</sub> with reasonable kinetics (hours). This is in contrast to oxidized pure Cu(111) where such reduction is very slow (days). We further contrast the catalytic properties of Rh/Cu(111) SAAs with varying degrees of O<sub>2</sub> exposure to the those of Pt/Cu(111) SAAs. Finally, we report the effects of a copper oxide thin film toward the segregation of noble metal single-atoms on Cu (111) using DFT.

11:40am **AS+CA+EL+EM+SE+SS+TF-ThM-12 Beyond the Physical Origin of the Shirley Background in Photoemission Spectra: Other Predictions of the Interchannel Coupling with Valence Band Losses Mechanism**, *Alberto Herrera-Gomez*, CINVESTAV-Unidad Queretaro, Mexico

The physical mechanism proposed in our 2017 paper about the origin of the Shirley background in photoemission spectra<sup>1</sup> es based on interchannel coupling<sup>2</sup> but with the important addition of energy losses in the valence band.<sup>3</sup> Besides the Shirley background, it is possible to derive other predictions of the interchannel Coupling with Valence Band Losses mechanism (ICLM). Two of them are discussed in this paper: 1) the quantitative relation between Auger peaks and the Shirley background and 2) the conduction-band-like structure of the extended region of the Shirley background.

<sup>1</sup> A. Herrera-Gomez et al. Surface and Interface Analysis 50(2), 246–252 (2018).

<sup>2</sup> E.W.B. Dias et al. Phys Rev B 78(2), 4553–4556 (1997).

<sup>3</sup>

<http://www.qro.cinvestav.mx/~aherrera/reportesInternos/unknownOriginShirley.pdf>

12:00pm **AS+CA+EL+EM+SE+SS+TF-ThM-13 Aging of Hydrophilicity in a Nano-Textured SS316 Thin Film Fabricated by Magnetron Sputtering**, *Pakman Yiu*, Ming Chi University of Technology, Taiwan; *J. Chu*, *J. You*, National Taiwan University of Science and Technology, Taiwan

According to the structural zone model by J.A. Thronton[1], we may manipulate the surface morphology of a thin film by altering the deposition temperature and vacuum. Therefore in this study, we prepared a series of SS316 thin film by magnetron sputtering under different Argon working pressure. Resultant thin film possessed a pressure dependent nano-textured surface which was dependent on working pressure. Furthermore, we discovered that the textured surface was highly hydrophilic (water

<sup>1</sup> ASSD Peter Sherwood Award



contact angle <15 degrees). The hydrophilicity could be attributed to the combinatorial contribution of surface roughness and capillary effect. However, we also discovered that the hydrophilicity aged with time, where after 21 days the surface turned hydrophobic with water contact angle >90 degrees. XPS studies on both as-deposited and 21-days stored sample films revealed that there was a Carbon-rich surface layer on the surface which grew with time. Interestingly when we tried to clean the surface with Argon atmospheric plasma, the hydrophilicity was almost fully restored. Results revealed that the aging of hydrophilicity may due to the fact that nano-surface texture gathers hydrocarbons in the atmosphere, which eventually formed an extra film that altered the surface wetting property. Understanding the aging mechanism and method of recovery may contribute to the development of a long-lasting hydrophilic surface, which is very useful in applications such as self-cleaning surface and medical apparatus[2,3]

[1] J.A. Thornton, Ann. Rev. Mater. Sci. 7 (1977) 239–260.

[2] A. Syafiq, B. Vengadaesvaran, A.K. Pandey, Nasrudin Abd. Rahim, J. Nanomater. 2018 (2018) 6412601.

[3] M. Xiao, Y.M. Chen, M.N. Biao, X.D. Zhang, B.C. Yang, Mater. Biol. Appl. 70 (2017) 1057–1070.

## Fundamental Discoveries in Heterogeneous Catalysis Focus Topic

### Room B113 - Session HC+SS-ThM

#### Dynamics and Mechanisms in Heterogeneously Catalyzed Reactions

**Moderators:** Arthur Utz, Tufts University, Jason Weaver, University of Florida

8:00am **HC+SS-ThM-1 Dehydration and Dehydrogenation of Formate on Fe<sub>3</sub>O<sub>4</sub>(001)**, Marcus Sharp, Pacific Northwest National Laboratory / Washington State University; C. Lee, S. Smith, B. Kay, Z. Dohnálek, Pacific Northwest National Laboratory

Interest in improving the activity and selectivity of catalysts has been persistent due to their importance in numerous chemical industries. Yet the mechanistic understanding of the active site structure, coordination environment, and stability is often lacking. Using a combination of temperature programmed reaction spectroscopy (TPRS), molecular beam scattering (MBS), and X-ray photoelectron spectroscopy (XPS) we investigate the reactivity of formic acid on the Fe<sub>3</sub>O<sub>4</sub>(001) that serves as a model reducible oxide support for single-atom catalysts. XPS shows that formic acid deprotonates at low temperature (~80 K), forming a formate intermediate and a protonated lattice oxygen (hydroxyl). At higher temperatures (400–600 K), the formate undergoes dehydration to CO and H<sub>2</sub>O via two desorption channels, while dehydrogenation to CO<sub>2</sub> is a minor channel. Angle-resolved TPRS and MBS experiments show that CO leaves the surface with excess kinetic energy closely focused along the surface normal. Surprisingly, not all formate species can react through the low-temperature channel. XPS, however, does not indicate a change in surface species throughout reaction temperatures. The addition of isotopically labeled formic acid (DCOOD) after the depletion of the low-temperature reaction channel show a complete mixing of all surface formate species. Similarly, the addition of atomic hydrogen after the depletion of the low-temperature reaction shows that surface hydroxyls are important in guiding the decomposition reaction to various reaction channels. Fe deposition on top of Fe<sub>3</sub>O<sub>4</sub>(001) reveals that Fe based-structures also act as the active sites for the high-temperature desorption of CO. This study illustrates the complexity of reaction intermediates at catalyst surfaces where changes in surface morphology can lead to differences in product selectivity and activity.

8:20am **HC+SS-ThM-2 The Effect of No and Co on the Rh(100) Surface at Atmospheric Pressure**, D. Boden, J. Meyer, Irene Groot, Leiden University, Netherlands

Rhodium is used in automotive catalysis to reduce NO and CO emissions in the exhaust by catalyzing the reduction of NO to N<sub>2</sub> and the oxidation of CO to CO<sub>2</sub>. This means the rhodium nanoparticles in the catalyst are exposed to high pressures of NO and CO, both known to be highly corrosive gases, which leads to disintegration and sintering of the rhodium catalyst. It is important to understand the effect high pressures of NO and CO have on the rhodium surface at the nano scale, in order to design strategies to impede catalyst deactivation. Here, one of the most active rhodium facets,

Rh(100), is studied at atmospheric pressures of NO and CO with scanning tunnelling microscopy (STM), in order to observe the roughening of the surface in situ. Additionally, atomistic thermodynamics, based on density functional theory (DFT) calculations, is used in combination with ex situ ultrahigh vacuum techniques (low-energy electron diffraction and Auger electron spectroscopy) to understand the behavior of adsorbates on the surface during the STM experiments, at the atomic scale. The formation of rhodium islands on the (100) terraces is observed at high CO pressures, in conjunction with roughening of the step edges. Interestingly, roughening does not occur at the same pressures of NO. The surface roughening is also less severe when co-dosing NO and CO, even at identical CO partial pressures. The results from atomistic thermodynamics show that NO likely inhibits CO adsorption by blocking the CO adsorption sites, thereby preventing carbonyl formation and decreasing surface roughening.

8:40am **HC+SS-ThM-3 Sustainable Production of Aromatics via Methane Dehydroaromatization: Role of Dynamic Carbon Accumulation**, M. Hossain, Virginia Tech; M. Rahman, Southwest Research Institute, San Antonio Texas; D. Maiti, E. Sobchinsky, M. Kunz, R. Fushimi, Idaho National Laboratory; **Sheima Khatib**, Virginia Tech

**INVITED**

Natural gas, mainly composed of methane, constitutes an available and cheap resource that can be used as a building block to produce chemicals. Methane dehydroaromatization (MDA) is a reaction capable of directly converting methane to value-added aromatics, without an intermediate syngas step. The reaction happens in non-oxidative conditions, producing mainly benzene and hydrogen,  $6 \text{CH}_4(\text{g}) \rightarrow \text{C}_6\text{H}_6(\text{g}) + 9\text{H}_2(\text{g})$ . Zeolite-supported Mo catalysts have so far been the most widely studied catalysts in MDA, but they do not fulfill the conversion and stability requirements for commercialization. During the reaction induction period, Mo oxide species gradually reduce to Mo carbides, which are responsible for methane activation and subsequent conversion to aromatics. We have developed a strategy to improve benzene yield and catalyst stability by controlling the activation of the Mo species to optimize their reduction and dispersion before exposure to reaction conditions. Our results indicate that when activation of catalysts is performed by reduction in pure hydrogen under temperature-controlled conditions, the carbides formed (ex situ) lead to more selective catalysts that deactivate more slowly compared to carbides formed during reaction (in situ). To explain this difference, we studied the dynamic carbon accumulation kinetics on varying redox states of MoOx/HZSM-5 catalyst via strategic molecular probe experiments in the Temporal Analysis of Products (TAP) reactor. Incremental pulse-by-pulse TAP investigation helps to distinguish different surface reactions and paves the way for elucidating the role of catalyst state towards preferential soft coke formation, as opposed to hard coke that results in catalyst deactivation. These intrinsic kinetic fingerprints of the catalyst will provide guidance towards better MDA reaction protocols for sustained high aromatics production from waste greenhouse gas, methane.

9:20am **HC+SS-ThM-5 Mechanistic Understanding of Methanol Synthesis on an In<sub>2</sub>O<sub>3</sub> Catalyst**, Yong Yang, ShanghaiTech University, China

Indium oxide (In<sub>2</sub>O<sub>3</sub>) became a very promising catalyst in recent years for its high selectivity of CO<sub>2</sub> hydrogenation to methanol, an ideal fuel for green energy. The reaction normally requires elevated temperature from 220 to 330°C and relative high pressure around 50 bar. Deep mechanistic insight with experimental evidence is still in demand for effective development in catalyst rational design. The widely applied direct kinetics investigation by *in situ* IR of this reaction is difficult due the formation of In<sub>2</sub>O<sub>3</sub> black under H<sub>2</sub> reduction condition.

Here based on a recent optimized c-In<sub>2</sub>O<sub>3</sub> catalyst, we investigate methanol synthesis reactivity correlated spectroscopic and kinetics properties at up to 16 bar and 270°C by online MS isotope kinetics measurements, *in situ* time resolved FT-IR and XPS (ThermoFisher ESCALab250Xi), in both in steady-states and transients. In all kinetics experiments reported here, the input total flow rate is controlled around 15 sccm with H<sub>2</sub>/D<sub>2</sub>:CO<sub>2</sub>:Ar ratio at 10.5 sccm:3.5 sccm:1.4 sccm and the resulted gas hour space velocity is around 17 L/g/Hr.

Both steady-states and transients isotope input results clearly indicate a normal kinetic isotope effect (KIE). In addition pressure dependence study indicates that the reaction rate is nearly proportional to the input pressure and Arrhenius plot yield activation energies with both inputs remain almost constant at different pressures, with a higher activation energy (E<sub>a</sub>) for D<sub>2</sub>/CO<sub>2</sub> than H<sub>2</sub>/CO<sub>2</sub> (120 vs. 100 kJ/mol). The KIE and pressure dependence behaviors are essentially different from Cu based catalyst in the same reaction, although E<sub>a</sub> values are close. A universal reaction rate equation with parameters of pressure and temperature is thus provided. Based on

# Thursday Morning, November 9, 2023

results from two series of isotope switching transients experiments from  $D_2/CO_2$  to  $H_2/CO_2$ , quantitative transient products analysis of exchanged D/H isotopic species reveals that there are up to 2.5 monolayers of dissociated deuterium involved in the D isotopomer methanol products. This indicates that the active surface is highly reduced with a high efficiency of surface hydrogenation to methanol. The surface species characterization by *in situ* FT-IR and XPS investigate sample *in situ* prepared as pre-oxidized, pre-reduced and further exposed with water vapor or  $CO_2$ . The combined results provide key evidence for main XPS features assignments.

These results help elucidating the kinetics and spectroscopic fundamentals in this reaction and hopefully will provide useful information toward the rational design of active and stable catalysts based on  $In_2O_3$  for  $CO_2$  hydrogenation to methanol.

**9:40am HC+SS-ThM-6 The Strong Metal-Support Interaction Under Reactive Conditions and Its Influence on the Hydrogen Evolution Reaction Over Pt/TiO<sub>2</sub>(110), Philip Petzoldt**, Technical University of Munich, Germany; *M. Eder*, TU Wien, Austria; *M. Blum*, Lawrence Berkeley National Laboratory (LBNL); *T. Kratky*, Technical University of Munich, Germany; *S. Günther*, Technical University Munich, Germany; *M. Tschurl*, *B. Lechner*, *U. Heiz*, Technical University of Munich, Germany

Covering reactive nanoparticles with thin metal oxide films is a promising strategy to improve their stability and catalytic selectivity. Reductive heating of noble metal particles supported on reducible oxides initiates their encapsulation due to the strong metal-support interaction (SMSI). This phenomenon has been studied under well-defined UHV conditions on single crystals and on more applied, structurally inhomogeneous catalysts. However, only few studies provide insight at the atomic scale under reactive conditions which is crucial for the systematic optimization of catalytic systems.

In this contribution, we investigate the dynamic behavior of the SMSI state on Pt-loaded  $TiO_2(110)$  under reactive conditions and its influence on the catalyst's activity in the photocatalytic hydrogen evolution reaction. Employing near ambient pressure XPS, we show that the SMSI kinetics may be tuned by choosing the oxygen pressure. Monitoring the hydrogen evolution reaction by mass spectrometry, we further demonstrate that the impact of the noble metal encapsulation on the catalyst's chemistry depends on the complex interplay of reaction conditions and catalyst preparation.

Our results provide new mechanistic insights into the interaction of noble metal particles with the support and may foster the development of catalysts with improved stability and selectivity.

**11:00am HC+SS-ThM-10 Rotational Orientation Effects in Hydrogen-Surface Scattering, Helen Chadwick**, *Y. Alkoby*, *G. Alexandrowicz*, Swansea University, UK

INVITED

The interaction of hydrogen with surfaces plays an important role in many heterogeneously catalysed reactions, for example converting ortho-hydrogen to para-hydrogen for the safe storage of liquid  $H_2$  fuel, in the Haber Process for making ammonia and in the Fischer-Tropsch synthesis for making longer chain hydrocarbons. Carefully controlled, quantum state resolved experiments play a pivotal role in providing benchmarks which can be used to help develop accurate, predictive theoretical models of these important interactions. The influence of the rotational orientation projection quantum state of the molecule ( $m_l$ ), which can be considered classically to describe whether the hydrogen is rotating like a helicopter or cartwheel when it collides with the surface, has been less well characterised due to the challenges associated with preparing these quantum states, particularly in closed shell, ground state molecules. Here I will present a unique magnetic manipulation interferometry technique [1] that allows us to control and manipulate the rotational orientation and nuclear spin projection ( $m_l$ ) quantum states of small molecules both before and after they collide with a surface. Using the elastic scattering of  $H_2$  from LiF as an example [2], I will demonstrate that we can extract empirical scattering matrices from the data which can be compared directly to those from theoretical calculations. I will also show new results for  $H_2$  scattering from the stepped Cu(511) surface, where signals for several different diffraction channels have been measured which exhibit different dependencies on the rotational orientation states, as well as observations which suggest that  $H_2$  can dissociate when it collides with the surface. All of these results combined, provide very stringent experimental benchmarks which will help develop accurate theoretical models.

**Acknowledgments:** This work was supported by the Horizon 2020 Research and Innovation Programme Grant Number 772228 and an EPSRC New Horizons Grant Number EP/V048589/1.

Thursday Morning, November 9, 2023

## References

- [1] O. Godsi et al., Nat. Comm. 8, 15357 (2017).
- [2] Y. Alkoby et al., Nat. Comm. 11, 3110 (2020).

**11:40am HC+SS-ThM-12 Studies of Pt-Sn Catalysts for Methylcyclohexane Dehydrogenation to Toluene, Donna Chen**, University Of South Carolina; *M. Qiao*, *A. Ahsen*, *A. Heyden*, *J. Monnier*, University of South Carolina

The use of  $H_2$  as an energy carrier has emerged as an attractive alternative to fossil fuels, but a major challenge for the  $H_2$ -based economy lies in the efficiency of storage and transportation. The use of liquid organic hydrogen carriers (LOHC) would allow for the reversible storage of  $H_2$  through hydrogenation-dehydrogenation reactions. The toluene-methylcyclohexane (MCH) pair is ideal for this purpose because MCH has a relatively high gravimetric storage density, and both compounds are widely available, low-toxicity liquids at ambient temperature. While catalytic hydrogenation of LOHCs is exothermic and facile, a major problem with using LOHCs for hydrogen storage is that catalytic dehydrogenation is endothermic and not always reversible due to side reactions. Pt catalysts are active for dehydrogenation of MCH to toluene, but undesirable C-C bond breaking reactions also lead to coking and deactivation. In this work, model Pt-Sn bimetallic surfaces are studied for MCH dehydrogenation in order to understand the role of Sn in preventing the deactivation of Pt surfaces. Pt-Sn alloy surfaces were prepared by depositing Sn on Pt(111) and annealing to various temperatures to form ordered overlayers, which were characterized by low energy electron diffraction, scanning tunneling microscopy (STM), and X-ray photoelectron spectroscopy (XPS) in an ultrahigh vacuum (UHV) chamber. The model surfaces were then transferred into a flow reactor coupled directly to the UHV chamber for kinetic studies under realistic pressure conditions; after MCH reaction, the surfaces were transferred back to the UHV chamber for characterization by XPS and STM. The activity of the model single-crystal surfaces are also compared with the conventional catalysts consisting of supported Pt-Sn particles. Computational work will help identify the role of the various active sites and determine reaction mechanisms, as well as the rate and selectivity controlling steps at the active sites.

**12:00pm HC+SS-ThM-13 Platinum@Hexaniobate Nanopeapods: A Directed Photocatalytic Architecture for Dye-Sensitized Semiconductor  $H_2$  Production Under Visible Light Irradiation, Clare Davis-Wheeler Chin**, Sandia National Laboratories, USA; *P. Fontenot*, Tulane University; *T. Rostamzadeh*, University of New Orleans; *L. Treadwell*, Sandia National Laboratories, USA; *R. Schmehl*, Tulane University; *J. Wiley*, University of New Orleans

Platinum@hexaniobate nanopeapods (Pt@HNB NPPs) are a nanocomposite heterogeneous photocatalyst that was selectively engineered to increase the efficiency of hydrogen production from visible light photolysis. Pt@HNB NPPs consist of linear arrays of high surface area Pt nanocubes encapsulated within scrolled sheets of the semiconductor  $H_xK_{4-x}Nb_6O_{17}$ , and were synthesized in high yield via facile one-pot microwave heating method that is fast, reproducible, and more easily scalable than multi-step approaches required by many other state-of-the-art catalysts. The Pt@HNB NPPs unique 3D architecture enables physical separation of the Pt catalysts from competing surface reactions, promoting electron efficient delivery to the isolated reduction environment along directed charge transport pathways that kinetically prohibit recombination reactions. Pt@HNB NPPs catalytic activity was assessed in direct comparison to representative state-of-the-art Pt/semiconductor nanocomposites (extPt-HNB NSCs) and unsupported Pt nanocubes. Photolysis under identical conditions exhibited superior  $H_2$  production by the Pt@HNB NPPs, which exceeded other catalyst  $H_2$  yields ( $\mu\text{mol}$ ) by a factor of 10. Turnover number (TON) and apparent quantum yield (AQY) values showed similar dramatic increases over the other catalysts. Overall, the results clearly demonstrate that Pt@HNB NPPs represent a unique, intricate nanoarchitecture among state-of-the-art heterogeneous catalysts, offering obvious benefits as a new architectural pathway towards efficient, versatile, and scalable hydrogen energy production. Potential factors behind the Pt@HNB NPPs superior performance are discussed below, as are the impacts of systematic variation of photolysis parameters and the use of a non-aqueous reductive quenching photosystem.

## Funding Statement

This material is based upon work supported by the National Science Foundation under grants CHE-1412670 (C.D.-W.C., T.R., J.B.W) and CHE-2004178 (J.B.W). Work is also supported by the Laboratory Directed Research and Development program at Sandia National Laboratories (C.D.-W.C., L.J.T.), a multimission laboratory managed and operated by National

# Thursday Morning, November 9, 2023

Technology and Engineering Solutions of Sandia LLC, a wholly owned subsidiary of Honeywell International Inc. for the U.S. Department of Energy's National Nuclear Security Administration under contract DE-NA0003525. (This paper describes objective technical results and analysis. Any subjective views or opinions that might be expressed in the paper do not necessarily represent the views of the U.S. Department of Energy of the United States Government).

## Plasma Science and Technology Division Room A106 - Session PS2+AS+SS-ThM

### Plasma-Surface Interactions I

**Moderators:** Lei Liu, Lam Research Corporation, Pingshan Luan, TEL Technology Center America

11:00am **PS2+AS+SS-ThM-10 Remote Plasma-Activated and Electron Beam-Induced Etching of Ruthenium and Its Comparison to Tantalum, Yudong Li<sup>1</sup>**, University of Maryland College Park; *C. Preischl, M. Budach, H. Marbach, D. Rhinow*, Carl Zeiss SMT, Germany; *G. Oehrlein*, University of Maryland College Park

Refractory metals are of importance in microfabrication, which necessitates patterning of these materials. One issue is to reduce near-surface modifications of materials during processing, which is often due to ion bombardment and atomic mixing. Recently, we have developed a novel technique of combining electron beam (ebeam) and remote plasma (RP) for materials processing [1, 2]. Material damage is significantly reduced since energetic ion bombardment is prevented. The RP generates reactive neutral precursors and the ebeam provides energy deposition to enable further precursor-materials interactions.

Here we investigate the effects of ebeam and RP on Ru and Ta with the goal of selective etching. The simultaneous irradiation of ebeam and RP with Ar and O<sub>2</sub> as the feed gas induces Ru etching. The Ru ER increases with emission current, electron energy, and O<sub>2</sub> flow rate, while it shows less dependence on RP power. A pretreatment step by ebeam/RP or RP only with Ar/O<sub>2</sub>/CF<sub>4</sub> significantly enhances the subsequent Ru ER induced by ebeam/RP with Ar/O<sub>2</sub>. This effect is likely associated with the reactor wall passivation by the introduction of CF<sub>4</sub> through RP, which reduces recombination of O atoms on reactor surfaces. For Ta, RP with fluorine-rich Ar/O<sub>2</sub>/CF<sub>4</sub> induces Ta etching at a high rate. If instead an O<sub>2</sub>-rich gas mixture is used, we observe Ta oxidation. The RP sustains the spontaneous Ta etching by generating F which interacts with Ta and forms volatile tantalum fluoride. Contrary to the Ru metal, where the ebeam induces etching, the ebeam is found to promote oxidation of Ta. The opposite roles of ebeam on Ru and Ta and the sensitive dependence on CF<sub>4</sub> flow rate of Ta etching provides the opportunity to achieve Ru over Ta etching selectivity.

We gratefully acknowledge the financial support of this work by Carl Zeiss SMT GmbH

References:

1. Lin, K.-Y., et al., SiO<sub>2</sub> etching and surface evolution using combined exposure to CF<sub>4</sub>/O<sub>2</sub> remote plasma and electron beam. *Journal of Vacuum Science & Technology A*, 2022. 40(6).
2. Lin, K.-Y., et al., *Electron beam-induced etching of SiO<sub>2</sub>, Si<sub>3</sub>N<sub>4</sub>, and poly-Si assisted by CF<sub>4</sub>/O<sub>2</sub> remote plasma*. *Journal of Vacuum Science & Technology A*, 2022. 41(1).

11:20am **PS2+AS+SS-ThM-11 Plasma Surface Ionization Wave Interaction with Single Channel Structures, Joshua Morsell, S. Shannon**, North Carolina State University

The interaction of atmospheric pressure plasma jets (APPJ) with materials has found promising applications in the fields of plasma medicine, catalysis, and material treatment. One area of interest is the surface ionization waves (SIW) present in these plasmas. SIWs interactions with complex interfaces is critical to these applications and require further study. A complex interface is any target with non-uniform electrical properties and/or non-planar surface morphology. The focus of this work is to study how surface ionization waves interact with single channel structures in dielectric media. The results show that the fraction of the SIW that escapes the channel is dependent on both driving voltage and channel width.

The plasma source in this study is an APPJ powered by a nanosecond DC pulse of positive polarity with helium as the working gas as used in [J. Morsell et al., *J. Phys D: Appl. Phys.* 56 (2023), 145201]. Voltage and current

data are collected via integrated current and high voltage probes at the source head. Time resolved ICCD imaging is used to image SIW propagation. The single channel targets consist of a 25 x 50 mm glass slide which has had a single channel etched across its minor axis. There are six total channel samples with different widths and depths. These samples are mounted to a target stage, which has another glass slide with an optically transparent conductor acting as a ground plane allowing imaging through the substrate.

SIW velocities in the system have been measured. The first is the SIW velocity within the channel, the second is the radial velocity of the portion of the SIW that escapes the channel. Both velocities increase with increasing voltage but show no significant trends with channel geometry. Velocity magnitudes for radial surface waves are 40-70 km/s and in-channel velocities are determined to be 60-130 km/s. Total light emission from the discharge is used to determine the fraction of the SIW escaping the channel. There exists a strong dependence of SIW portioning with channel geometry and driving voltage. As voltage increases the SIW is less confined and the fraction of the SIW escaping the channel increases. As channel width increases less of the SIW is allowed to escape the channel. No conclusive trends are observed with respect to channel depth. Observation also reveals that the fraction of the escaping SIW relates to the sample area exposed to the discharge. A smaller area of the substrate is exposed to the SIW for low voltages and large geometry channels.

This work is supported by the U.S. Department of Energy, Office of Science, Office of Fusion Energy Sciences under Award Number DE-SC0020232.

11:40am **PS2+AS+SS-ThM-12 Plasma-wall Interactions: Implications for Advanced Chamber Materials Requirements, John Daugherty**, Lam Research Corporation **INVITED**

In semiconductor device fabrication, plasma-assisted processes dominate both the deposition and etching of materials. Over 50 years of successive technology nodes have motivated innovations and continuous improvements in plasma reactor technology, and the semiconductor industry now employs a sophisticated portfolio of plasma reactors that use a wide variety of chemistry and operating approaches. Today, many aspects of the fabrication process must achieve process variations of ~1% and often must contribute particle contamination of less than one particle per wafer pass. Despite dramatic improvement in reactor design and in chamber materials, it remains challenging to achieve current variation requirements because plasma reactors still suffer from process drift, molecular contamination, and particulate contamination that originate from plasma-modification of the chamber materials. The first consideration in choosing a chamber material is the expected maximum ion bombardment energy. The plasma conditions within a single chamber are quite nonuniform, and the ion energy may fall into several ranges. Some parts experience <20 eV ions, and while these parts can be engineered for very long lifetime, challenges remain in meeting performance requirements. Other parts experience ion energies >100 eV (sometimes >1 keV in etch processes). These parts are almost always cost-sensitive consumables. There is an intermediate range of ~50 to 100 eV where there is considerable materials design complexity because of the desire to maintain process stability for thousands of wafers while operating very near the energy thresholds for ion-enhanced chemical modification of the wall material. Another design consideration is that the chamber materials must withstand a repeating sequence of multiple chemistries and plasma conditions followed by *in situ* plasma cleans using still different chemistry. The variety of chemically reactive molecules and free radicals include mixtures containing multiple halogens, hydrogen, oxygen, and depositing species from fluorocarbons, hydrocarbons, complex deposition precursors, and etch products. Recently we have adapted sophisticated materials metrology to examine the materials modifications that occur throughout the lifecycle of real production parts. We have also performed control experiments that allow us to infer the dominant plasma processes that cause the materials modifications we observe on production parts used in various applications. The implications for what types of materials are suitable for different parts of a plasma reactor are explored in this presentation.

<sup>1</sup> PSTD Coburn & Winters Student Award Finalist

## Surface Science Division

Room D136 - Session SS1+AS-ThM

### Molecular Organization at Surfaces

Moderators: Eric Altman, Yale University, Zdenek Jakub, CEITEC

#### 8:00am SS1+AS-ThM-1 Supramolecular Self-assembly and Metal-Ligand Redox Assembly at Surfaces, Steven Tait, Indiana University INVITED

The selection and positioning of specific functional groups will direct packing and stacking of organic building blocks, which determine the electronic and chemical properties of molecular thin films and semiconductors. Design of molecular ligands for metal-organic complexation at surfaces can address the long-standing grand challenge of high selectivity in heterogeneous catalysis. Our group is working to develop principles of on-surface molecular self-assembly<sup>1</sup> and of metal-organic complexation<sup>2</sup> to gain new insight into molecular layers and new chemical activity at metal single-site catalysts.<sup>3</sup> This work involves close collaboration with multiple research groups to synergistically combine talent in design, synthesis, sample preparation, characterization, analysis, theory, and computational modeling. We use a range of surface characterization tools to interrogate these systems under well-controlled environments, including scanning probe microscopy, photoelectron spectroscopy, vibrational spectroscopy, and mass spectrometry. We investigate systems under a variety of conditions: solution/solid interface, ultra-high vacuum, and flow reactor conditions at high temperature and high pressure. Here, I will report on recent results in several aspects of this work. We have demonstrated the impact of conformational entropy in impeding self-assembly, but that this can be overcome with appropriate selection of co-solutes. Metal-organic complexes at surfaces can be designed to achieve single-site metal centers in which we can observe redox isomerism, control of metal oxidation state, transmetallation, and chemical spillover to the support. We have transferred this design concept for single-site catalysts to high-surface-area powder oxide supports and shown that these can operate as effective catalysts in solution and under gas flow conditions. Ongoing work will seek to extend understanding of these systems to achieve molecular thin films and single-site catalysts of greater complexity.

#### References

- [1] D. L. Wisman, H. Kim, C. Kim, T. W. Morris, D. Lee, and S. L. Tait, *Chemistry – a European Journal* **27**, 13887-13893 (2021). DOI: 10.1002/chem.202101611 [https://doi.org/10.1002/chem.202101611]
- [2] T. W. Morris, D. L. Wisman, N. Ud Din, D. Le, T. S. Rahman, S. L. Tait, *Surface Science* **712**, 121888 (2021). DOI: 10.1016/j.susc.2021.121888 [https://doi.org/10.1016/j.susc.2021.121888]
- [3] E. Wasim, N. Ud Din, D. Le, X. Zhou, M. S. Pape, G. E. Sterbinsky, T. S. Rahman, S. L. Tait, *Journal of Catalysis* **413**, 81-92 (2022). DOI: 10.1016/j.jcat.2022.06.010 [https://doi.org/10.1016/j.jcat.2022.06.010]

#### 8:40am SS1+AS-ThM-3 Self-Assembly Controlled at the Level of Individual Functional Groups, Benjamin Heiner, A. Pittsford, S. Kandel, University of Notre Dame

Molecular self-assembly is a process that occurs when component molecules spontaneously organize into a specific arrangement due to the intermolecular interactions between them. These interactions are influenced by the functional groups present on the component molecules. By understanding the effects that different functional groups have on the self-assembly process, we can predict and control it. To do this, we study "families" of molecules that have a common backbone but differ in the functional groups they possess. We use a combination of experimental techniques, such as pulse deposition for scanning tunneling microscopy (STM), and a variety of computational methods to investigate the changes in self-assembly behavior that result from small modifications to the functional groups. In this talk/poster, I will present our work on a family of molecules with an indole backbone, including indol carboxylic acids, multiple isatin derivatives, and proline. By studying these molecules, we are able to gain a deeper understanding of the various intermolecular interactions that drive self-assembly in these systems.

#### 9:00am SS1+AS-ThM-4 Atomically-Defined, Air-Stable 2D Metal-Organic Frameworks on Graphene: How the Support Defines the System Properties, Zdenek Jakub, A. Kurowska, J. Planer, A. Shahsavari, P. Prochazka, J. Cechal, CEITEC - Central European Institute of Technology, Czechia

The functionality of 2D metal-organic frameworks (MOFs), crucially depends on the local environment of the embedded metal, and such details

are best ascertained on 2D MOFs supported on atomically flat surfaces. Here, we present three systems which are well-defined at the atomic-scale, decoupled from the metal support and stable both in ultrahigh vacuum and in ambient conditions: M-TCNQ (M = Ni, Fe, Mn) supported on epitaxial graphene/Ir(111). We show that these systems are monophasic with M<sub>2</sub>(TCNQ)<sub>2</sub> stoichiometry, and we demonstrate their remarkable chemical and thermal stability. Furthermore, by a combined experimental and computational approach we study the differences between 2D MOF systems supported on graphene and on Au(111), the prototypical surface for on-surface synthesis. We show that the Fe-TCNQ on graphene is non-planar with iron in quasi-tetrahedral sites, but on Au(111) it is planarized by stronger van-der-Waals interaction. Combined with the distinct energy level alignment with the supports, this results in significant differences in the 2D MOF properties on these two surfaces. Our results outline the limitations of common on-surface approaches using metal supports and show that the intrinsic 2D MOF properties can be partially retained on graphene. The modular M-TCNQ/graphene system combines the atomic-scale definition required for fundamental studies with the robustness and stability needed for applications, thus we consider it an ideal model for research in single atom catalysis or spintronics.

#### 9:20am SS1+AS-ThM-5 Using 2D COFs to Stabilize Single-Atom Catalysts on Model Surfaces: From Ultra-High Vacuum System to Ambient Conditions, Yufei Bai, Indiana University; D. Wisman, NAVSEA Crane; S. Tait, Indiana University

Single-atom catalysts (SACs) combine the advantages of homogeneous and heterogeneous catalysts by limiting the reaction sites to isolated single metal atoms with well-defined chemical characters. Our group has developed a metal-ligand coordination method to stabilize SACs using 1,10-phenanthroline-5,6-dione (PDO) to coordinate with metal atoms such as Pt, Fe, and Cr. In order to further improve the stability of SACs and increase metal loading, we have synthesized single-layered covalent organic frameworks (SCOFs) on model surfaces under ultra-high vacuum (UHV) conditions or under ambient conditions. These two-dimensional (2D) networks with high thermal and chemical stability were used to confine single Pt atoms coordinated with ligands into SCOF pores. Under UHV conditions, the successful formation of the SCOF with regular hexagonal pores on the Au(111) surface was achieved by surface-mediated Ullmann radical coupling of 1,3,5-tris-(4-bromophenyl)benzene (TBB) and characterized by scanning tunneling microscopy (STM). Further sequential deposition of PDO ligand and Pt on the TBB-SCOF surface allowed the formation of single-site Pt catalysts by coordination interaction. STM images have proved the confinement of PDO in the SCOF pores, while X-ray photoelectron spectroscopy (XPS) has proven the oxidation state of Pt, which is an indication of the single atom character. Under ambient conditions, a 2D imine-linked SCOF was formed on the highly oriented pyrolytic graphite (HOPG) surface by a solid-vapor interface mechanism, which allows for a high quality SCOF with long-range order. STM characterization has shown that regular SCOF networks with negligible defects were formed on the HOPG surface with domain sizes greater than 1 μm × 1 μm. These systems which combine the COF and metal-ligand coordination strategy to stabilize SACs offer the possibility to achieve higher stability and greater loading in SACs.

#### 9:40am SS1+AS-ThM-6 Protein Adsorption on Mixed Self-Assembled Monolayers: Influence of Chain Length and Terminal Group, Rebecca Thompson, St. Edward's University

Mixed self-assembled monolayers (SAMs) are often used as highly tunable substrates for biomedical and biosensing applications. It is well documented, however, that mixed SAMs can be highly disordered at the molecular level and do not pack as closely or homogeneously, particularly when the chain lengths and head groups of the SAM thiol components are significantly different. In the current study, we explore the impact of SAM structure and mixing ratio on the weak physisorption behavior of bovine serum albumin (BSA), which adsorbs more readily to hydrophobic, methyl-terminated SAMs. Our results suggest that once the mixture includes 50% or more of the methyl terminus, mixing ratio alone is a relatively good predictor of adsorption, regardless of the relative chain lengths of the thiols used in the mixture. This trend persists at any mixing ratio for SAMs where methyl- and hydroxyl-terminated groups are the same length or where the hydroxyl-terminated thiol is longer. The only variance observed is at low mixing ratios (<50% methyl-terminated) for a mixed SAM where the methyl-terminated component has a longer chain length. Relative protein adsorption increases on these mixtures, perhaps due to the disordered exposure of the excess alkane backbone. Taken together, however, we do not find significant evidence that varying chain lengths for mixed SAMs

# Thursday Morning, November 9, 2023

prepared on polycrystalline substrates and analyzed in air have an outsized influence on nanoscopic adsorption behavior, despite molecular-level disorder in the SAM itself.

## Surface Science Division

### Room D136 - Session SS2+AS+TF-ThM

#### Thin Film Surface Chemistry

Moderators: Eric Altman, Yale University, Zdenek Jakub, CEITEC

11:00am **SS2+AS+TF-ThM-10 Ultrafast Exciton Dynamics of Phthalocyanine Films with Different Molecular Orientations, Hui Ung Hwang, S. Kim, J. Kim**, Korea Research Institute of Standards and Science (KRIS), Republic of Korea

Organic semiconductors (OSCs) have enormous potential in advanced optoelectronic devices, such as organic light-emitting diodes and organic solar cells. To achieve higher performance and functional versatility for these applications, a deeper understanding of the generation and relaxation mechanism of photoexcited excitons in molecular films is essential. In this study, we investigate the ultrafast dynamics of excitons in planar-shape molecules of phthalocyanines (Pc), which can adopt a lying-down or standing-up orientation depending on the substrate used, as shown in Fig. 1.<sup>1</sup> The distinct ionization-energy difference of more than 0.5 eV measured by photoelectron spectroscopy confirms that the Pc thin film on HOPG substrate grows in the lying-down direction and the Pc on ITO grows in the standing-up direction. Exciton energy and population from the molecules with these two different orientations are measured by time-resolved two-photon photoemission (tr-2PPE) with time resolution of 85 fs. In this measurement, we first pump a singlet exciton population in the Pc with a femtosecond pulse and probe its evolution as a function of delay time with an ultraviolet pulse. Singlet excitons have a variety of relaxation pathways, including diffusion between molecules, intersystem crossing to triplet states, and dissociation at the interface with metals. The tr-2PPE experiments show that the exciton relaxation in Pc molecules with the standing-up geometry is dominated by exciton diffusion in the direction perpendicular to the substrate, resulting in relatively slow exciton relaxation. However, for Pc molecules in the lying-down geometry, the excitons undergo faster transfer to the metal interface due to aligned  $\pi$ -orbital overlap with neighboring molecules toward the substrate. These results imply that OSCs exhibit different exciton relaxation dynamics depending on their orientation and suggest that for planar molecules like Pc, the lying-down geometry is more favorable for exciton transfer and dissociation to the metal interface.

11:20am **SS2+AS+TF-ThM-11 Understanding the Surface Chemistry of Oxide Thin Films by Isotope Labeling, Yingge Du**, Pacific Northwest National Laboratory **INVITED**

Isotopic engineering is developing into a key approach to study the nucleation, diffusion, phase transition, and reaction of materials at an atomic level to reveal transport pathways, kinetics, and working/failure mechanisms of functional materials and devices. Understanding these phenomena leads to deeper insights into relevant physical processes, such as the transport and intercalation of ions in energy conversion and storage devices, and the role of active sites and supports during heterogeneous catalytic reactions. Likewise, isotopic engineering is being pursued as a means of modifying functionality to enable future technological applications. In this talk, I will present our work employing isotope labeling (e.g., <sup>18</sup>O and <sup>2</sup>H) during complex oxide thin films' (e.g., WO<sub>3</sub>, SrFeO<sub>2.5</sub>, and La<sub>1-x</sub>Sr<sub>x</sub>FeO<sub>3</sub>) synthesis and post-growth processing to track the distribution and redistribution of the isotope tracers. Isotope-resolved analysis techniques with high spatial resolution, such as time-of-flight secondary ion mass spectrometry and atom probe tomography, facilitate the accurate quantification of isotopic placement and concentration in well-defined heterostructures with precisely positioned, isotope-enriched layers. These studies allow us to better understand the growth mechanisms, surface chemistry, and elemental diffusion under working and extreme conditions.

12:00pm **SS2+AS+TF-ThM-13 Interaction of Self-Assembled Monolayers with Atomic Oxygen During Area-Selective Atomic Layer Deposition, Silvia Armini**, IMEC Belgium; A. Brady Boyd, School of Physical Sciences, Dublin City University, Ireland

Utilising self-assembled monolayers (SAMs) to achieve area-selective atomic layer deposition (AS-ALD) as an approach to bottom-up nanofabrication has recently gained significant attention from the nanoelectronics industry.

With the continued downscaling of feature sizes, top-down processing can no longer reach the challenging demands of the industry which requires conformal coating of high aspect ratio vias and a reduction in misalignment errors in multi-layered devices. In this work we attempt to imitate the effects of the ALD oxidation pulse experienced by the SAMs during the AS-ALD process by exposing two SAMs of different chain lengths and different functional groups, (3-trimethoxysilylpropyl)diethylenetriamine (DETA) and octadecyltrimethoxysilane (OTMS), to numerous controlled in-vacuo atomic oxygen exposures with subsequent characterisation by X-ray photoelectron spectroscopy (XPS). We monitor the sequential removal of the deposited monolayers with each successive atomic oxygen exposure for both SAMs. The etch rate is observed to be distinct for the different SAMs, the amino-terminated short chain DETA SAM reveals a linear etch rate while the longer chain OTMS SAM reveals an exponential etch rate. The results presented provide some insights into what characteristics are important for choosing the correct SAM for AS-ALD applications.

## Fundamental Discoveries in Heterogeneous Catalysis Focus Topic

Room B113 - Session HC+SS-ThA

### Closing in on Reality & HC Discovery Reception

**Moderators:** Liney Arnadottir, Oregon State University, Ashleigh Baber, James Madison University, Dan Killelea, Loyola University Chicago

2:20pm **HC+SS-ThA-1 Ion Imaging applied to Heterogeneous Catalysis on Metals**, *Theofanis Kitsopoulos*, University of Southern Mississippi **INVITED**  
I will discuss how to impalement ion imaging methods to measure the kinetics and dynamics of elementary reaction on metal surfaces. I will discuss the recombination of H atoms on Pt and Pd, followed by a discussion on the kinetics of formic acid adsorption on Pt and Pd

3:00pm **HC+SS-ThA-3 Structure-Sensitive Metal-Support Interactions – Applications to Selective Hydrogenation Reactions**, *Helena Hagelin Weaver, H. Zhao, M. Lapak, L. Hsiao, D. Choi, C. Bowers*, University of Florida **INVITED**

Producing hyperpolarized molecules is important for increasing signal intensities in nuclear magnetic resonance (NMR) or magnetic resonance imaging (MRI) applications, and one efficient strategy is to add a parahydrogen molecule, where the nuclei have antiparallel spins, to an unsaturated substrate. The requirements for the production of a hyperpolarized molecule are that the added hydrogens must come from the same hydrogen molecule, i.e. a pairwise addition, the spins must be preserved, and the hydrogens in the generated product must be inequivalent. While this is efficient over homogeneous organometallic catalysts, heterogeneous catalysts would be preferred to facilitate separation of hyperpolarized product from the catalyst and allow continuous operation. However, over typical heterogeneous catalysts, i.e. oxide-supported metal nanoparticles, the pairwise addition of parahydrogen is challenging due to facile and reversible dissociation of dihydrogen, rapid diffusion of hydrogen atoms across the metal surface, step-wise addition of hydrogen atoms to the unsaturated molecule, and spillover of hydrogen from the active metal to the oxide support, as these are all mechanisms that can lead to a rapid loss in the singlet spin-correlation of the original parahydrogen molecule. Therefore, the pairwise selectivity in hydrogenation reactions over supported metal catalysts is often very low (< 1%).

To limit diffusion of hydrogen across the metal surface and improve the pairwise selectivity in the hydrogenation of propene, the metal particle size was first reduced to the limit, i.e. single atoms on the support. Single atoms on an oxide support are indeed more selective to pairwise addition of parahydrogen than larger nanoparticles of the same metal, but the activity is low and stability is an issue during reaction conditions. Another approach is to limit diffusion by blocking metal sites with an oxide overlayer. This was done by inducing strong metal-support interactions via a high-temperature reduction of titania-supported catalysts. The structure of the titania support, anatase versus rutile, influenced the metal-support interactions, and active metals, such as Rh and Ir, exhibited different behavior in the pairwise selective addition of parahydrogen to propene. However, in all cases, the high temperature reduction increased the pairwise selectivity regardless of whether geometric (migration of titania over metal) or electronic metal-support interactions were induced. Preliminary data reveal that oxide layers deposited by ALD can also improve the pairwise selectivity in hydrogenation reactions.

3:40pm **HC+SS-ThA-5 High Activity and Selectivity of Dilute Ti-Cu(111) Alloys Toward the Deoxygenation of Ethanol to Ethylene**, *J. Shi*, University of Florida; *H. Ngan, P. Sautet*, University of California at Los Angeles; *Jason Weaver*, University of Florida

Alloys comprised of an early transition metal dispersed in a coinage metal can provide opportunities for effecting selective chemical transformations of organic oxygenates and other compounds. In this talk, I will discuss our recent work to synthesize dilute Ti-Cu(111) surface alloys in ultrahigh vacuum and characterize their structural and chemical properties using experiments and DFT. We find that Cu-capped, Ti-containing islands are preferentially generated on step edges of Cu(111) during Ti deposition below ~500 K, whereas Ti atoms alloy into the step edges during deposition above 500 K. These dilute Ti-Cu(111) surfaces are highly selective for the deoxygenation of ethanol, resulting in the production of only C<sub>2</sub>H<sub>4</sub> and H<sub>2</sub> near 400 K during temperature programmed reaction spectroscopy. DFT

calculations corroborate the high selectivity of metallic Ti-Cu(111) surfaces toward ethanol deoxygenation and predict that C<sub>2</sub>H<sub>4</sub> production becomes significantly favored as the Ti ensemble size is increased from monomer to trimer, and that the O released to Ti during C-O bond cleavage promotes desorption of the C<sub>2</sub>H<sub>4</sub> product by destabilizing its adsorbed state.

## Surface Science Division

Room D136 - Session SS+HC-ThA

### Alloys and Complex Surfaces

**Moderators:** Arthur Utz, Tufts University, Zhenrong Zhang, Baylor University

2:20pm **SS+HC-ThA-1 Single-Atom Alloy Catalysts: Born in a Vacuum, Tested in Reactors, and Understood In Silico**, *E Charles Sykes*, Tufts University **INVITED**

In this talk I will discuss a new class of heterogeneous catalysts called *Single-Atom Alloys* in which precious, reactive metals are utilized at the ultimate limit of efficiency. These catalysts were discovered by combining atomic-scale scanning probes with more traditional approaches to study surface-catalyzed chemical reactions. This research provided links between atomic-scale surface structure and reactivity which are key to understanding and ultimately controlling important catalytic processes. In collaboration with Maria Flytzani-Stephanopoulos these concepts derived from our surface science and theoretical calculations have been used to design *Single-Atom Alloy* nanoparticle catalysts that are shown to perform industrially relevant reactions at realistic reaction conditions. For example, alloying elements like platinum and palladium with cheaper, less reactive host metals like copper enables 1) dramatic cost savings in catalyst manufacture, 2) more selective hydrogenation and dehydrogenation reactions, 3) reduced susceptibility to CO poisoning, and 4) higher resistance to deactivation by coking. I go on to describe very recent theory work by collaborators Stamatakis (UCL) and Michaelides (Cambridge University) that predicts reactivity trends for a wide range of *Single-Atom Alloy* combinations for important reaction steps like H-H, C-H, N-H, O-H, and CO<sub>2</sub> activation. Overall, I hope to highlight that this combined surface science, theoretical, and catalyst synthesis and testing approach provides a new and somewhat general method for the a priori design of new heterogeneous catalysts.

3:00pm **SS+HC-ThA-3 Heterogeneities in Early Oxide Evolution on Ni-Cr Alloys Studied with a Combination of XPEEM and Data Analytics Methods**, *Keithen Orson*, University of Virginia; *W. Blades*, University of Arizona; *Y. Niu, A. Zakharov*, Max IV Laboratory, Sweden; *P. Reinke*, University of Virginia

The Ni-Cr alloy system is coveted for its mechanical properties and its resistance to degradation in high-temperature, corrosive environments. This resistance comes primarily from a chemically complex passive film composed of nanometers-thin layer of oxides and hydroxides, but many questions remain about the early stages of passive film growth. Studying this early regime gives insights into how surface orientation and features like grain boundary influence oxide nucleation and growth. The early regime is also where competition between Ni and Cr oxidation occurs on the surface. We studied oxide growth on Ni<sub>22</sub>wt%Cr using the XPEEM techniques  $\mu$ -XAS and  $\mu$ -XPS, giving chemical specificity with a pixel size of 50 nm. We conducted a controlled oxidation on a clean surface with up to 65 L of oxygen at 773 K which records oxide evolution with video rate focused on a region with (212) and (104) surfaces and the corresponding grain boundary. To address the size and complexity of the hyperspectral images we use Principal Component Analysis (PCA) and Non-Negative Matrix Analysis (NNMA) to identify the various spectral components and thus bonding states in the image with spatial and temporal resolution. The Ni L-edge spectra change little over the oxidation process and are characteristic for Ni(O) in line with the known preponderance of Cr oxidation under these conditions. All XAS images include image artifacts mostly seen as modulation of background intensity and slope. Valence band spectra (h $\nu$ =95 eV) reveal grain-dependent work function shifts and appear characteristic of the bonding state for O<sub>ads</sub>. The Cr L-edge shows strong spatial heterogeneities, with NNMA revealing the emergence of chromia nuclei. PCA, while less directly interpretable, gives good qualitative agreement with the NNMA. NNMA analysis informs segmentation of movies taken at a single energy in the Cr-L edge characteristic of oxide. Island nucleation begins between 5 and 20 L of exposure and a logistic growth behavior up to 65L of exposure consistent with Avrami-type nucleation. Chromium oxide particle density and distribution varies widely

across the two grains, while particle size remains nearly constant. 21% of the (212) grain is covered evenly by oxide particles, while particle density on (104) is only 11% at the endpoint of the oxidation experiment. A region in the vicinity of the grain boundary on (212) is nearly devoid of chromia particles. In summary, early-stage Ni-Cr oxidation is grain- and texture-specific with chromia island growth dominating in the 0-65 L oxidation regime. Work function shifts and O adsorbates possibly play a role in these heterogeneities behavior.

3:20pm **SS+HC-ThA-4 The Impact of Crystallographic Orientation on the Oxidation of Ni-Cr Alloys**, *Petra Reinke*, University of Virginia, USA; *W. Blades*, Arizona State University; *D. Jessup*, *J. St.Martin*, *K. Orson*, University of Virginia, USA

Ni-Cr alloys in the FCC random solid solution structure are coveted for their mechanical properties combined with a superb corrosion resistance and thermal stability. The corrosion resistance in aqueous solution, specifically pitting resistance, can be further improved by addition of a third alloying element such as Mo or W. [1] The role of alloy composition and temperature is well studied but significant knowledge gaps exist in our understanding of the initial oxidation steps until complete oxide layers have formed and Cabrera-Mott type growth models can be applied. The competition between Ni and Cr oxidation plays out at < 873 K of relevance for many energy applications. This regime is highly sensitive to the specifics of surface reactions but also impacted by alloy microstructure. The crystallographic orientation of the surface varies significantly between adjacent grains, and reaches deep into the crystallographic triangle with complex terrace and kink structures. Ni-Cr(100) and Ni-Cr(111) surfaces show highly distinct oxidation pathways modulated by the interfacial epitaxy between NiO and the alloy surface. [2,3] Recent work demonstrated that the pitting resistance in acidic solution is strongly grain orientation dependent. [4] It can be assumed that the orientation of oxide grains in the protective layer leads to contact potentials which influence reactant and vacancy diffusion across the oxide layer as the growth continues.

We will present combined STM, in-situ and operando XPS studies which resolve the oxidation process as a function of crystallographic orientation. We will introduce our approach to identify, and study individual grains with wide variability in surface (h k l) through a combination of metallurgical processing, EBSD, and SEM. The oxidation of individual grains is then be studied and significant variation in oxidation rate and oxide composition are isolated. Thermally induced faceting adds to the complexity of orientation dependent oxidation. It is generally assumed that the epitaxial relation between Ni-Cr and NiO drives its rapid nucleation and layered growth mode. We are extending this assessment beyond the well-studied singular surfaces and calculate structural interfacial models which will also include several chromia surfaces albeit chromia tends to nucleate as sub-oxide surface clusters. [2] The role of interfacial energies in the initial oxidation steps will be assessed for the singular and higher index surfaces.

[1] C. Volders *et al.* *npj Materials Degradation* **6**, 52 (2022).

[2] W. H. Blades *et al.* *ACS Applied Materials & Interfaces* **10**, 43219-43229 (2018).

[3] W. H. Blades *et al.* *Corrosion Science* **209**, 110755 (2022).

[4] K. Gusieva *et al.* *The Journal of Physical Chemistry C* **122**, 19499-19513 (2018).

3:40pm **SS+HC-ThA-5 Structure of Electrochemical Electrode/Electrolyte Interfaces from First Principles**, *Axel Groß*, University of Ulm, Germany

Our knowledge about structures and processes at electrochemical electrode-electrolyte interfaces is still rather limited, in spite of its technological relevance in energy conversion and storage. First-principles simulations can help to elucidate these structures in spite of the fact that these simulations are hampered by the complexity of these interfaces together with the fact that the dependence of these interfaces on the electrode potential needs to be properly taken into account. In this contribution, I will first show which insights first-principles calculations can provide with respect to halide and sulfate adsorbate structures at electrochemical interfaces [1,2] using grand-canonical approaches yielding reliable Pourbaix diagrams of the stable adsorbate phases. Furthermore I will demonstrate how ab initio molecular dynamics simulations can contribute to a better understanding of the structure of electric double layers at metal electrodes [3,4]. The presentation will conclude with some general remarks about remaining challenges in our understanding of electrochemical electrolyte/electrode interfaces [5].

## References

- [1] F. Gossenberger, F. Juarez, and A. Groß, *Front. Chem.* **8**, 634 (2020).
- [2] A. Groß, *J. Phys. Chem. C* **126**, 11439 (2022).
- [3] S. Sakong and Axel Groß, *Phys. Chem. Chem. Phys.* **22**, 10431 (2020).
- [4] A. Groß and S. Sakong, *Chem. Rev.* **122**, 10746-10776 (2022).
- [5] A. Groß, *Curr. Opin. Electrochem.* **40**, 101345 (2023).

4:00pm **SS+HC-ThA-6 Surface Characteristics of Flexible Carbon-Doped Oxide Thin Films Under Reactive Ion Etching Process Using Fluorocarbon-Based Plasma**, *Seonhee Jang*, *T. Poche*, *R. Chowdhury*, University of Louisiana at Lafayette

The microelectronics industry is increasing research on flexible electronics. Instead of the traditional rigid Si-based electronics, flexible electronics utilize polymer substrates that allow stretching, bending, and folding of the device, which drastically expand its applications. A wide variety of inorganic materials, semiconductors, dielectrics, and metals have been integrated for the fabrication of flexible electronic devices. One of the dielectric materials employed in semiconductor devices is carbon-doped silicon oxide (SiCOH). In this study, flexible low-k SiCOH films were produced by plasma-enhanced chemical vapor deposition (PECVD) of tetrakis(trimethylsilyloxy)silane (C<sub>12</sub>H<sub>36</sub>O<sub>4</sub>Si<sub>5</sub>) precursor onto flexible indium tin oxide/polyethylene naphthalate (ITO/PEN) substrates using a set of different plasma powers, yielding the films with varying material properties. The physical properties including refractive index, extinction coefficient, surface morphology and roughness, and surface wettability were determined. The surface structures were analyzed by Fourier transform infrared (FTIR) and X-ray photoelectron (XPS) spectra. Four prominent peaks of Si-O-Si stretching, Si-CH<sub>3</sub> bending, Si-(CH<sub>3</sub>)<sub>x</sub> stretching, and CH<sub>x</sub> stretching modes were observed in the FTIR spectra. High-resolution XPS spectra of Si2p, C1s, and F1s were analyzed for the chemical bond structure and elemental composition. Mechanical properties including elastic modulus and hardness were measured using nanoindentation. The pristine SiCOH films were then subjected to an inductively coupled plasma-reactive ion etching (ICP-RIE) process. The etching properties of the flexible SiCOH films were characterized under a set of fluorocarbon (CF<sub>4</sub>)-based plasmas such as CF<sub>4</sub>, CF<sub>4</sub>+O<sub>2</sub>, and CF<sub>4</sub>+Ar. The CF<sub>4</sub> flow rate was maintained at 35 sccm while the O<sub>2</sub> and Ar flow rates were both at 24 sccm. The RF plasma at 13.56 MHz was maintained at 200 W and the ICP power at 40 W. The operating pressure and temperature were 10.0 Pa and ambient temperature, respectively. The duration for etching process was 30 s. Using deconvolution of FTIR and XPS spectra, the surface structures of the SiCOH films after etching process were compared with those of the pristine film. The fraction ratios of the deconvoluted peaks in each prominent peak in the FTIR spectra depended on the deposition plasma power and RIE etching gas composition. In the XPS spectra analysis, each Si2p and C1s peak showed a depressed peak intensity after etching process. With additional etchants of O<sub>2</sub> and Ar, the F1s peak shifted to higher binding energy for lower deposition plasma power and lower binding energy for higher deposition plasma power. Surface properties of flexible SiCOH films after etching were changed according to composition of etchants.

## Surface Science Division

### Room Oregon Ballroom 203-204 - Session SS-ThP

#### Surface Science Poster Session

**SS-ThP-1 ESI Investigations of Melamine and Cyanuric Acid Clusters and Their Relationship to STM Experiments, Alex Walter, K. Handy, J. Soucek, S. Kandel, University of Notre Dame**

Pulse deposition, a novel sample deposition technique for scanning tunneling microscopy (STM), sprays molecules onto a surface through a process that forces non-equilibrium, high-energy structures. Electrospray ionization mass spectrometry (ESI-MS) is a “soft” ionization method; molecules of interest do not fully fragment, but instead can be observed whole, as can dimers, trimers, and other supramolecular structures, which is often seen as a limitation. However, this clustering of molecules allows for a “screening” of sorts for pulse-deposited STM experiments, which are significantly more time-intensive. ESI-MS and pulse deposition have similar sample delivery methods, and thus can be compared to each other and used to study molecules in tandem. For example, melamine and cyanuric acid together form highly toxic complexes in the body, but the precise crystallization and intermolecular forces that drive the creation of the toxic clusters is unknown. Using the ESI-MS as a precursor to investigation with pulse deposited STM imaging, we observed several stable noncovalent clusters of melamine and cyanuric acid, ranging from mixed dimers to mixed nonamers (four melamines and five cyanuric acids). In this presentation, I will discuss the results of our ESI-MS experiments on melamine and cyanuric acid as well as comment on STM experiments of different solution ratios and how ESI-MS and STM results can be jointly interpreted.

**SS-ThP-2 Scanning Tunneling Microscopy Study of the H<sub>2</sub>O-CO Co-Adsorbed Fe<sub>3</sub>O<sub>4</sub>(111) Surface for Understanding the Water-Gas Shift Reaction Mechanism, Asa Kiuchi, Y. Eda, T. Hirai, T. Shimizu, Keio University, Japan**

Magnetite (Fe<sub>3</sub>O<sub>4</sub>) is an attractive catalyst for the water-gas shift reaction (WGSR), owing to its low cost and minimal environmental impact. However, the reaction path remains unclear despite extensive experimental and theoretical studies. This is partly due to the difficulty in conducting experiments and the complexity of analyzing data on co-adsorbed systems, which has resulted in a lack of clarity in the overall picture.

To clarify the mechanism of the WGSR on magnetite, we performed scanning tunneling microscopy (STM) to observe CO exposed, H<sub>2</sub>O adsorbed, and H<sub>2</sub>O-CO co-adsorbed Fe<sub>3</sub>O<sub>4</sub>(111) surfaces. Our results confirmed that CO molecules do not adsorb on the bare surface at room temperature, agreeing with the previous study based on temperature programmed desorption[1]. Two types of adsorbate species appeared on the surface after the exposure to H<sub>2</sub>O, which we attribute to dissociated species, OH, and molecular water. We also found a larger adsorbate on the H<sub>2</sub>O-CO co-adsorbed surface, although it is unclear if this species is an intermediate of the WGSR due to the complexity of the STM image. We are currently developing image analysis methods to identify and classify the adsorbed species. Our study provides a new insight into the atomistic mechanism of the WGSR on Fe<sub>3</sub>O<sub>4</sub>(111).

[1]C. Lemire *et al.*, *Surf. Sci.* **572**, 103(2004).

**SS-ThP-3 Growth of Metal Nanoclusters on Thin Layer Moiré Pattern of Graphene and Feo on Single Crystal, Shilpa Choyal, D. Liu, N. Jiang, UIC**  
Graphene, a two-dimensional (2D) carbon crystal with sp<sup>2</sup> hybridization, has attracted much attention in recent years due to its novel chemical, electrical, and mechanical properties. Even materials that do not form cluster superlattices upon room temperature deposition may be grown into such by low-temperature deposition. A graphene monolayer was prepared on an Ir (111) single crystal, ethylene (C<sub>2</sub>H<sub>4</sub>) is pyrolytically cleaved on the surface. The resulting superstructure is examined using scanning tunneling microscopy (STM) and was identified as a well-aligned, incommensurate pattern known as moiré. This moiré pattern arises from overlapping the graphene lattice and the Ir (111) lattice, resulting in alternating bright and dark regions.

The moiré patterns in graphene act as nucleation sites for the growth of plasmonic metal nanoclusters. When Ag/Au metal is deposited on graphene, it nucleates at these sites to form nanoclusters on the surface. Through STM, we have examined the nucleation and growth of these nanoclusters, studying their shape, organization, and structural evolution.

Additionally, we have also investigated the stability of these nanoclusters at different temperatures.

Moiré patterns are also found at iron oxide (FeO) thin layers on Au (111) surfaces. The FeO nanoislands are mostly truncated triangular and exhibit clear moiré superlattices. These superlattices result from the lattice mismatch between FeO and Au (111). In contrast to graphene, FeO demonstrates a preference for wetting by different metals, which imparts unique surface properties. FeO islands have two different growth sites one from Fe-edges and the other from O-edges. In addition to being located on top of FeO islands, different metal prefers to nucleate on the edge of FeO islands, where they selectively grow on the Fe-edges and O-edges.

**SS-ThP-4 Post-Synthesis Isotopic Purification of Oxygen in TiO<sub>2</sub> via Controllable Surface Injection of Interstitial Atoms, H. Jeong, Nabil Hilmy Abuyazid, E. Seebauer, University of Illinois at Urbana Champaign**

Isotopically pure semiconductors have important applications for cooling electronic devices and for quantum computing and sensing. Raw materials of sufficiently high isotopic purity are rare and expensive, thereby creating special opportunities for post-synthesis methods that remove isotopic impurities. Through isotopic self-diffusion measurements of oxygen in rutile TiO<sub>2</sub> single crystals immersed in water, we demonstrate fractionation of <sup>18</sup>O by a factor of three below natural abundance in a near-surface region of 10 nm or more. The specially prepared and submerged surface injects large fluxes of O interstitials, which displace lattice <sup>18</sup>O deeper into the solid due to the statistics of interstitial-mediated diffusion combined with steep interstitial gradients. Multiscale modeling offers quantitative insights into how these physical effects work together and how they might be optimized. Both ultraviolet illumination and solution pH affect the experimental injection rate, and demonstrate that adjustments to the chemistry between the surface and fluid can be used to control chemistry between the surface and defects in the bulk. The benefits of such control extend beyond isotopic fractionation to defect engineering, as the injected O interstitials also remove O vacancies and compensate donor H impurities. Importantly, all these effects occur near room temperature. This accesses a regime wherein equilibrium concentrations of native defects become vanishingly small, and where kinetic effects dominate defect behavior. It thereby becomes possible to create materials whose properties circumvent thermodynamic constraints.

**SS-ThP-5 Analyses of Surface Structure and Chemical States of Carbon Black Nano Particles, Mari Isagoda<sup>1</sup>, Keio University, Japan; T. Aoki, Asahi Carbon Co., Ltd., Japan; T. Shimizu, Keio University, Japan**

Carbon black (CB) is widely used as pigment and reinforcement material in tire production and is also expected to work as conductive auxiliaries of Lithium-ion batteries. To improve properties for these applications, precise control of the surface structure and chemical states of CB particles is critical. The crystallite model — particles made of small flakes of layered graphene — has been proposed based on transmission electron microscopy (TEM), and the edges of these graphene flakes are expected to be terminated with several types of functional groups [1]. However, the validity of the model and the exact types and locations of functional groups are still in debate. In this study, we employed atomic force microscopy (AFM), scanning tunneling microscopy (STM), Raman spectroscopy, and x-ray photoelectron spectroscopy (XPS) to provide a comprehensive characterization of the surface structure and chemical states of CB particles.

In AFM and STM measurements of samples prepared by the drop-drying method, we observed that carbon black exists as aggregates of particles with a variety of sizes, ranging from approximately 10 nm to 300 nm. Our STM images of small-size particles less than 10 nm in diameter cannot be adequately explained by the crystallite model. Raman spectra of powdered samples showed two peaks centered at 1340 cm<sup>-1</sup> and 1590 cm<sup>-1</sup>, which correspond to D-band and G-band[2], respectively. By comparing the spectra with those of other carbon-based materials, we concluded that the carbon black consists of graphene sheets, as in the crystallite model, but it is rather close to amorphous. XPS suggests the existence of oxygen-containing species.

[1] S. Khodabakhshi, P. F. Fulvio, and E. Andreoli, *Carbon* **162**, 604-649 (2020).

[2] M. A. Pimenta, et al., *Phys. Chem. Chem. Phys.* **9**, 1276-1291 (2007)."

<sup>1</sup> SSD Morton S. Traum Award Finalist



**SS-ThP-6 Surface Chemistry of Zirconium Borohydride on Zirconium Diboride (0001), Ayoyele Ologun, M. Trenary, University of Illinois - Chicago**  
Zirconium diboride  $ZrB_2$  is an extremely hard material with a high melting point of 3246 °C; given these properties,  $ZrB_2$  can be used for various applications, such as high-resistant coatings for body armors and tanks. In addition, it has also been explored as a diffusion barrier in microelectronics. Industrially, highly conformal thin films of  $ZrB_2$  are grown via chemical vapor deposition (CVD), using zirconium borohydride  $Zr(BH_4)_4$  as a precursor. While surface chemistry plays a central role in the CVD of  $ZrB_2$  from the  $Zr(BH_4)_4$  precursor, the surface mechanism is yet to be explored. In this study, we investigated the surface mechanism of  $Zr(BH_4)_4$  decomposition on a  $ZrB_2(0001)$  surface with reflection absorption infrared spectroscopy (RAIRS), temperature-programmed desorption (TPD), and X-ray photoelectron spectroscopy (XPS). The RAIRS spectra obtained on exposing the  $ZrB_2(0001)$  surface at 90K to  $Zr(BH_4)_4(g)$  closely matched that of the pure compound, indicating adsorption of  $Zr(BH_4)_4$  without decomposition. However, new surface intermediates were formed upon heating to 280 K, as shown by the retention of the  $\nu B-H$  stretch ( $2569\text{ cm}^{-1}$ ) and  $\delta H-B-H$  bend ( $1228$  &  $1057\text{ cm}^{-1}$ ) in the RAIRS spectra. These surface intermediates were tentatively identified as either  $BH_4$  or  $BH_3$  and were found stable up to 330 K. Temperature-programmed desorption studies revealed the desorption of  $B_2H_6$  and  $H_2$  at around 470 K.

**SS-ThP-7 An Annotated Compendium of X-Ray Photoelectron Spectroscopy (XPS) Spectra, Samira Jafari, M. Linford, A. Dean, B. Kulbacki, S. Ko, Brigham Young University**

X-Ray photoelectron spectroscopy (XPS) is a powerful tool for studying surfaces, where, in its conventional embodiment, it is sensitive to the upper 5 – 10 nm of materials. XPS is widely used throughout science and technology. In XPS, photoemission of core electrons is a result of X-rays striking a surface. Two types of XPS spectra are collected: survey spectra and narrow scans. Survey spectra reveal the elements at surfaces. Narrow scans provide chemical/oxidation state information about those elements. XPS spectra are sometimes inappropriately acquired because of (a) contamination on the surface, (b) contamination in the instrument, e.g., due to a previously-analyzed fluorine-containing sample, and (c) poor method development, e.g., a failure to take a sufficient number of scans. For these reasons, it is important for analysts to have comparison spectra in their work. We intend to collect a number of XPS spectra of different materials and compile them into an annotated compendium that can help other XPS users. Spectral processing will largely be with CasaXPS. Data acquisition of narrow scans will be undertaken at low pass energies that will minimize peak FWHM values, while still providing good

statistics for the spectra. We hope this compendium will be a good resource for other researchers and scientists in their interpretation of their XPS spectra.

**SS-ThP-8 Determination of Band Alignment in Semiconductor Heterojunctions by X-Ray Photoelectron Spectroscopy (XPS), Mohamed Nejib Hedhili, T. Ng, K. Lee, B. Ooi, KAUST, Saudi Arabia; O. Bakr, Kaust, Saudi Arabia**

Heterojunctions are widely used as an essential building block in advanced semiconductor devices because of their multiple functionalities. The electrical and optical properties of heterojunctions are strongly governed by their electronic band alignment.

High-resolution X-ray photoemission spectroscopy (HR-XPS) is proven to be a powerful way of measuring the valence band offsets in semiconductor heterojunctions. This study aims to determine the band alignment to different semiconductor heterojunctions by direct X-ray photoelectron spectroscopy (XPS) measurements. Type-I and Type-II band alignment were obtained.

Design of heterojunction based electronic/photonic devices requires an accurate determination of the band offset. This parameter is crucial to tailor heterojunction based devices as per the operating requirement.

**SS-ThP-9 Localized Plasmon-Controlled Chemistry at and Beyond the Nanoscale, Chamath Siribaddana, S. Rajak, S. Choyal, D. Liu, S. Mahapatra, L. Li, N. Jiang, University of Illinois Chicago**

Probing the effect of the local chemical environment of surface nanostructures is a challenge because the spatial resolution of conventional spectroscopic techniques is limited by the diffraction limit of light. Coupling

light with plasmonic nano-objects creates highly localized surface plasmons (LSPs), which allows us to break this limit. Tip-enhanced Raman spectroscopy (TERS) is one such surface spectroscopic technique that uses the apex of the tip of a scanning tunneling microscope made from a plasmonic metal as a nano object to couple light to the near field. The Raman modes of the nanostructure underneath this tip are greatly enhanced which allows us to obtain chemical information with Angstrom scale spatial resolution. Thus, TERS can probe intermolecular interactions, molecule-substrate interactions, organic-2D material heterostructures, and the reactivity of 2-D materials to reveal how the local chemical environment affects the chemical and physical interactions of a molecule or a nanostructure on a surface. Apart from probing the local environment, the highly localized nature of LSPs can be used to drive energy-intensive and unselective thermally activated chemical reactions using light with a lower energy input and a site-selective manner. The controllability of LSPRs was demonstrated by dissociating a single bond inside a molecule in the presence of multiple equivalent bonds. The insights obtained into the local environment enable precise control of self-assemblies, on-surface reactions, and LSPRs and expand the ability to synthesize nanostructures with tailored electronic, optical, and magnetic properties required for next-generation nanodevices.

**SS-ThP-10 Heterostructured Nanomaterials Fabrication Using a Modular MBE Research Platform, Lukasz Walczak, Research and Development Division, PREVAC sp. z o.o., Raciborska 61, 44-362 Rogow, Poland; M. Florek, Research and Development Division, PREVAC sp. z o.o, Poland; M. Kwoka, Department of Microelectronics, Silesian University of Technology, Poland**

Many important processes such as energy conversion, electrochemical, corrosion, and biological processes take place at solid-gas and solid-liquid interfaces [1-3]. The molecular beam epitaxy (MBE) method is the one of powerful techniques for creating new nanomaterials and it is the key to improving the performance of novel battery generation or renewable energy sources such as solar, wind, or hydropower energy conversion devices. We would like to promote an original, modular ultra-high vacuum system for the fabrication of heterostructured nanomaterials by the molecular beam epitaxy (MBE) method. Its basic element is a vacuum installation, which consists of a sample loading chamber, a substrate preparation (cleaning) chamber, and a proper MBE chamber for the deposition of selected nanomaterials. All vacuum chambers are connected by appropriate vacuum locks and magnetic sample transfers between the above-mentioned chambers, which enables the implementation of all technological and research works without contact of deposited nanomaterials with the atmospheric environment. Vacuum conditions in all of the above-mentioned vacuum chambers are created using independent systems of various types of vacuum pumps. For the control of the substrate cleaning process, the deposition of nano-layers of selected electronic materials, and their initial characterization, the above-mentioned vacuum installation is equipped with electronic control systems and measurement data acquisition systems. Correct operation of the designed and the completed installation has been verified on the example of the deposition of Mg nano-layers on the Si substrate. The conducted technological works and preliminary research works as well as the obtained results confirmed that the designed and assembled modular vacuum system can be very useful for the deposition of nanolayers of selected electronic materials using the MBE method, on the one hand on terms of their potential research applications, and on the other - in terms of their potential industrial applications, incl. for the production of photovoltaic renewable energy sources.

#### References:

- [1]S. Choudhury et al. C 2021, 7, 28.
- [2]A. Asyuda et al. Phys. Chem. Chem. Phys., 2020,22, 10957-10967.
- [3]H. Aldahhak et al. . J. Phys. Chem. C 2020, 124, 11, 6090–6102.

**SS-ThP-12 Angular and Velocity Distributions of  $NO_2$  and  $O_2$  Desorption from an Oxidized  $Ag(111)$  Surface, Arved Cedric Dorst, Georg-August Universität, Göttingen, Germany; R. Dissanayake, Max Planck Institute for Multidisciplinary Sciences, Germany; D. Schauer mann, Georg-August Universität, Göttingen, Germany; D. Killelea, Loyola University Chicago; T. Schäfer, Georg-August Universität, Göttingen, Germany**  
Transition group metals are used as catalysts in various oxidation reactions. A common example is silver which found industrial usage in the epoxidation of ethylene to the ethylene oxide. To optimize such processes it is required to understand the dynamics and microscopic details. In this talk, the velocity and angular distribution of  $NO_2$  and

recombinatively-desorbing oxygen from Ag(111) will be presented. Experimentally, we combined velocity-map imaging (VMI) and temperature-programmed desorption (TPD). NO<sub>2</sub> decomposes into NO and O after adsorption on silver. At 510 K, a clean p(4 × 4)-O reconstruction with a maximum oxygen coverage of  $\theta_0 = 0.375$  ML forms on Ag(111).<sup>1</sup> The reaction probability *S* of NO<sub>2</sub> decomposition was studied at this temperature as a function oxygen coverage  $\theta_0$ . *S* is coverage-independent up to  $\theta_0 = 0.3$  ML which is a clear indication for a precursor-mediated mechanism.

In TPD spectra, the recombinative desorption of O atoms occurs as a defined O<sub>2</sub> desorption feature around 600 K. In contrast to NO<sub>2</sub> whose desorption appears thermal, these oxygen molecules exhibit a clearly hyper-thermal velocity distribution; (*v*) is >200 m · s<sup>-1</sup> above a flux-weighted, thermal velocity distribution. Compared to Rh(111),<sup>2</sup> we observe a significantly narrower cos<sup>8</sup>( $\theta$ ) angular distribution for the flux density of O<sub>2</sub> and the velocity distribution differs stronger from a thermal one. Finally, first results for the epoxidation of styrene to styrene oxide will be shown. We observe that the epoxide forms only at high oxygen coverage.

[1] A. Michaelides, K. Reuter, and M. Scheffler, *J. Vac. Sci. Technol.* **A23**, 1487 (2005).

[2] A.C. Dorst, F. Güthoff, D. Schauermaun, A.M. Wodtke, D.R. Killelea, and T. Schäfer, *Phys. Chem. Chem. Phys.* **24**, 26421 (2022).

## SS-ThP-14 Growth and Characterization of Bimetallic NiCo Particles on CeO<sub>2</sub>(111) Thin Film Surfaces, *T. Ara, Nishan Paudyal, J. Zhou*, University of Wyoming

Ceria-supported Ni and Co have been of great interest as economical and promising catalysts for chemical reactions including CO oxidation, CO<sub>2</sub> hydrogenation, ethanol reforming, and dry reforming of methane. They can exhibit promising reactivity owing to the strong metal-support interaction. Bimetallic NiCo could provide interesting properties compared to individual metal counterparts due to the synergistic effects between two metals as well as the interaction between the metal and ceria. To elucidate the nature of the activity, we investigated the nucleation, growth, and sintering of metal particles of Ni, Co, and NiCo over well-ordered CeO<sub>2</sub>(111) thin films using scanning tunneling microscopy and x-ray photoelectron spectroscopy under ultrahigh vacuum conditions. Our results indicate that oxidation of the metal (Co, Ni) occurs at the cost of Ce<sup>4+</sup> reduction to Ce<sup>3+</sup> upon deposition of low coverages (< 0.2 ML) of Co or Ni over CeO<sub>2</sub>(111) at room temperature. Both Ni and Co form small particles that are less than two-atomic layer high with no clear preferential nucleation at step edges, suggesting a strong metal-support interaction. Compared to Ni, Co forms relatively smaller particles with a higher particle density on CeO<sub>2</sub>(111) at 300 K that experiences less sintering with heating up to 800 K. Our studies show that bimetallic NiCo particles can be prepared by deposition of Ni followed by Co on CeO<sub>2</sub>. As demonstrated by scanning tunneling microscopy data, Co primarily deposits onto the pre-dosed Ni particles on CeO<sub>2</sub> at 300 K to produce NiCo bimetallic particles and addition of Co can inhibit the sintering of Ni and enhance its thermal stability on ceria with heating.

## SS-ThP-15 DFT Calculations of Cyanuric Acid and Melamine from ESI-MS, *Kaitlyn Handy, A. Walter, J. Soucek, S. Kandel, S. Corcelli*, University of Notre Dame

With the use of electrospray ionization mass spectroscopy (ESI-MS) we are able to observe clusters of cyanuric acid and melamine in solution. The clusters consist of homogenous and heterogenous mixtures with varying ratios of molecules. Several of these clusters are observed forming in high concentrations. Using density functional theory (DFT), calculations are run to model possible cluster structures. Both homogenous and heterogenous clusters arrange in a lattice structure. When there are clusters with disproportionality more cyanuric acid or melamine the molecular structure has variations leading to the molecule not lying flat. Larger clusters show increased stability when compared to smaller clusters.

## SS-ThP-17 Scanning Tunneling Microscopy Studies of Diarylethene Monolayer and Cluster Formation on Noble Metal Surfaces, *Tomoko K. Shimizu, T. Kaneko*, Keio University, Japan; *K. Sagisaka*, National Institute for Materials Science, Japan

The supramolecular assembly on metal surfaces is governed by a subtle balance between intermolecular interaction and molecule-substrate interaction. Even on chemically similar metals, such as Cu, Ag, and Au, the deposition of the same molecule under the same condition may result in different types of assembled structures. We have observed such a case with

a molecule called diarylethene, famous for its photochromism and expected to work as single molecule switching device.

After depositing molecular powder of the open-form isomer on metal surfaces at room temperature, scanning tunneling microscopy (STM) was performed in ultra-high vacuum at liquid helium temperature. Our STM images revealed the presence of both the open-form and closed-form isomers on all three metals. This is due to a stability reversal on metals compared to the gas phase, arising from charge transfer between molecules and metallic substrates[1]. Isolated adsorption was predominant on Cu(111) even after annealing. Co-deposition of NaCl was necessary to form a homogeneous monolayer, which was achieved via ion-dipole interaction[2]. On Au(111), closed-form isomers formed small clusters, such as trimers and tetramers, while the open-form remained isolated. In contrast, larger clusters made of both the open- and closed-form isomers were found on Ag(111), including chain-type clusters and three-fold symmetric chiral clusters. Mild annealing transformed all the open-form isomers to the closed-form isomers, and only three-fold symmetric clusters made of nine or more closed-form isomers were observed. The clusters found on Ag(111) have three-dimensional structures, suggesting local and weak intermolecular interaction. Theoretical analysis is underway to clarify the exact structures and interactions involved.

## References

[1] T. K. Shimizu, et al., *Chem. Commun.* **49**, 8710-8712 (2013).

[2] T. K. Shimizu, et al., *Angew. Chem. Int. Ed.* **53**, 13729-13733 (2014).

## SS-ThP-18 Distinguishing Elements at the sub-Nanometer Scale on the Surface of a High Entropy Alloy, *Lauren Kim, W. Scougale*, University of Wyoming; *P. Sharma*, Lehigh University; *N. Shirato, S. Wiegold*, Argonne National Laboratory; *W. Chen*, Northwestern University; *V. Rose*, Argonne National Laboratory; *G. Balasubramanian*, Lehigh University; *T. Chien*, University of Wyoming

High entropy materials, including high entropy alloys (HEAs), high entropy Van der Waals materials (HEX), and high entropy oxides (HEOs), have drawn the attention of scientists and engineers for their various functionalities and properties. While a wide variety of properties are being studied in these materials, a microscopic understanding is still missing. In this work, the spatial resolving power of scanning tunneling microscopy (STM) is combined with the elemental resolving X-ray absorption spectroscopy (XAS) to achieve this goal. With the unique X-ray assisted tunneling effect, the elemental distributions on the surface of a HEA at the sub-nm scale were revealed by a synchrotron X-ray scanning tunneling microscope (SX-STM). The elemental distribution at sub-nm scale was revealed by maximizing the correlation coefficient between the collected XAS mappings and the atomic scale elemental modeling. The results shown here demonstrate that SX-STM is a promising tool to reveal elements at the sub-nm scale, even for high entropy materials.

## SS-ThP-19 Soft X-Ray Spectro-Microscopy for Electrochemical Interfaces, *Xiao Zhao, E. Carlson, T. Mefford, W. Chueh*, Stanford University

Most electrochemical reactions occur at interfaces. In response to applied voltage, electron and energy transfer between the first few atomic layers of electrochemical active materials and absorbates. Electrochemical reactions are also highly heterogeneous, as most electrochemical processes preferentially take place around active sites with certain facets, coordination structure and chemical environment. Characterizing these reactions requires a spectroscopic imaging platform with interfacial sensitivity and chemical sensitivity. **Direct characterization of electrochemical interfaces** is further complicated by the presence of liquid electrolyte, which requires the measurement performed *in-situ/operando*.

Here we are presenting the recent development of Scanning Total Electron Yield X-ray Microscopy (STEYXM) based on the Scanning Transmission X-ray Microscopy (STXM), which enables *in-situ* X-ray spectroscopic imaging of various electrochemical interfaces with **25nm spatial resolution and ~5nm surface sensitivity**. A custom electrochemical flow cell is used with three electrodes setup. The traditional transmission mode could provide complimentary bulk information of electrodes, while the electron yield mode maps the surface structure and oxidation state of electrodes, as well as the local electrochemical double layer structure. We anticipate that the development of STEYXM will enable the investigation of surface electrochemistry and advance our fundamental understanding of electrochemical reactions.

# Thursday Evening, November 9, 2023

**SS-ThP-20 Effect of Heat Treatment on Silicon Carbide Reinforced Aluminum Matrix Composite Fabricated Through an Optimized Stir Casting Process, Conner Neely, D. Madiraju, M. Rabea, California State Polytechnic University, Pomona**

The purpose of this study is to determine the additional effect of heat treating on the hardness, corrosion resistance, and mechanical strength of cast aluminum matrix composites reinforced with SiC. The effects of heat treatment will be compared to an identical but untreated cast aluminum matrix composite reinforced by SiC, and additionally to pure aluminum. Accordingly, both composite samples were created from the same batch of matrix alloy in combination with SiC, melted and homogenized in an induction furnace to ensure stability and consistency of crystal structure. Microstructure and morphology analyses were conducted, the hardness was measured by the Micro Vickers hardness Tester (HM-200), corrosion of the samples was tested using salt spray chamber, and the tensile strength by a universal test machine. It was found that the heat treatment increased the hardness in the way of wear resistance of the Al-SiC composite, improved the corrosion resistance, the tensile strength, and showed more favorable material properties than the unaltered test sample of the Al-SiC composite.

**SS-ThP-22 Atomic-Scale Hydration Structures Visualized by Three-Dimensional Atomic Force Microscopy (3D-AFM), Keisuke Miyazawa, Kanazawa University, Japan**

Water molecules on a surface influence the chemical reactivity and molecular adsorption behavior of a surface. Given that these interfacial properties are influenced by local interactions between the material surface and water molecules, a deep understanding of the atomic-scale surface structures and their hydration structures is crucial for the design of surface functions. Recently, three-dimensional atomic force microscopy (3D-AFM) was developed as a method for investigating Subnanometer-scale hydration and flexible molecular structures on various surfaces. In 3D-AFM, an interaction force applied to an AFM tip is measured during the AFM tip 3D scanning at a solid-liquid interface to generate a 3D force image with atomic-scale local contrasts reflecting the local density distributions of molecules on a surface. Recent studies revealed the hydration structures of calcite (Fukuma et al., PRB 92 (2015) 155412), fluorite (Miyazawa et al., Nanoscale 8 (2016) 7334), sapphire and quartz (Nagai et al., Nanoscale 15 (2023) 13262). In this presentation, we present the recent studies of atomic-scale hydration structures investigations, and future prospects of 3D visualization of various solid-liquid interfacial phenomena using 3D-AFM.

## Applied Surface Science Division

Room **B117-119** - Session

**AS+2D+CA+EM+MS+NS+SE+SS+TF-FrM**

## Industrial Applications

**Moderators:** Marko Sturm, University of Twente, Netherlands, Alan Spool, Western Digital Corporation, Yundong Zhou, National Physical Laboratory, UK

8:20am **AS+2D+CA+EM+MS+NS+SE+SS+TF-FrM-1 Correlative Analysis Using Time-of-flight Secondary Ion Mass Spectrometry for Beam Sensitive Samples**, Jean-Paul Barnes, C. Guyot, P. Hirchenhahn, A. De Carvalho, N. Gauthier, T. Maindron, B. Gilquin, D. Ratel, C. Gaude, O. Renault, Univ. Grenoble Alpes, CEA, Leti, France; A. Galtayries, Chimie ParisTech, PSL University, CNRS, Institut de Recherche de Chimie Paris, France; G. Fisher, Physical Electronics USA; C. Seydoux, P. Jouneau, Univ. Grenoble Alpes, CEA, IRIG-MEM, France

**INVITED**

Time-of-flight Secondary Ion Mass Spectrometry (TOF-SIMS) is now widely used for materials analysis in domains such as semiconductor and energy applications. These challenging applications also provide access to well-controlled, custom made samples that have allowed the limits of TOF-SIMS analysis to be identified and helped in the development of correlative analysis approaches. Recent examples include combining AFM measurements with TOF-SIMS depth profiling to correct for sputter rate differences [1] or to measure mechanical or electrical properties and performing X-ray tomography prior to FIB-TOF-SIMS analysis to allow morphological and compositional data from the same volume to be visualized [2]. Currently we are working on two aspects. Firstly improving the quantification and chemical sensitivity of the technique by combining TOF-SIMS with photoemission techniques (XPS or XPEEM), and secondly trying to improve the lateral resolution by correlation with SEM and AFM measurements. Recent examples will be shown for the analysis of beam sensitive organic samples such as OLED devices, brain tissue samples after medical device implantation [3] and symbiotic microorganisms [4]. As well as the correlative aspects between techniques, we will show how tandem mass spectrometry can help in analyzing complex organic samples. In all cases the importance of sample preparation is paramount, especially for biological samples. For example, for the correlation between TOF-SIMS and XPS on OLED samples, a wedge crater protocol has been developed to allow analysis on exactly the same area of the sample whilst minimizing beam damage to the sample. Wedge crater preparation and transfer between instruments is performed under a protected environment (vacuum or inert gas) to avoid unwanted surface modifications.

Part of this work, carried out on the Platform for Nanocharacterisation (PFNC), was supported by the "Recherches Technologiques de Base" and the "CARNOT" program of the French National Research Agency (ANR).

[1] M. A. Moreno *et al.* *JVST B*, vol. 36, MAY 2018.

[2] A. Priebe *et al.* *ULTRAMICROSCOPY*, vol. 173, pp. 10-13, FEB 2017.

[3] A. G. De Carvalho *et al.* *Biointerphases*, vol. 15, 2020.

[4] C. Uwizeye *et al.* *PNAS*. Vol 118, e2025252118, 2021.

9:00am **AS+2D+CA+EM+MS+NS+SE+SS+TF-FrM-3 Secondary Ion Mass Spectroscopy of Battery Surface and Interface Chemistry – Metrology and Applications**, Yundong Zhou, S. Marchesini, X. Yao, Y. Zhao, I. Gilmore, National Physical Laboratory, UK

Batteries are very important to achieve carbon net zero. Understanding battery materials change, electrode surfaces, solid electrolyte interphase (SEI) evolution and novel solid-state electrolyte structures is very helpful for developing better batteries. Surface chemical analysis techniques such as X-ray photoelectron spectroscopy (XPS) and Raman spectroscopy are often used but they have their limitations. XPS analysis cannot always resolve overlapping binding energies for some key SEI elements. The SEI often has poor Raman signal intensity. These are all hurdles for battery applications.

Secondary ion mass spectrometry has great potential to study interfacial chemistry in batteries owing to high sensitivity and high-resolution imaging in 2D and 3D. In this study, we use an OrbiSIMS instrument which is equipped with two complementary mass spectrometers (MS). A time-of-flight (ToF) MS has the capability for 2D and 3D imaging using a Bi<sub>3</sub><sup>+</sup> liquid metal ion gun with a spatial resolution of up to 200 nm but with modest mass resolving power. The Orbitrap MS offers high mass resolution and mass accuracy (> 240,000 at m/z 200 and < 2 ppm, respectively). The instrument is equipped with low energy Cs and O<sub>2</sub> sputter beams for high

resolution depth profiling of inorganic materials. It also has a Leica docking station enabling samples to be transferred using a vacuum sample transfer chamber from an argon glove box without atmospheric exposure. To improve the quality of measurements on battery materials, we have used ion implanted materials to determine relative sensitivity factors for relevant elements. We have also conducted a systematic study to optimise the OrbiSIMS depth profiling capability. These findings along with recommendations to reduce effects of signal saturation will be discussed and examples of the application to batteries will be provided. We will provide examples of the application of ToF MS and Orbitrap MS. (1,2)

1. X. Yao *et al.*, *Energy Environ. Sci.*, 2023, DOI: 10.1039/D2EE04006A.
2. S. Marchesini *et al.*, *ACS Appl. Mater. Interfaces*, 14(2022)52779-52793.

9:20am **AS+2D+CA+EM+MS+NS+SE+SS+TF-FrM-4 Characterizing Ion Distribution at the Solid-Electrolyte Interface in Solid-State Lithium Ion Batteries with ToF-SIMS**, Teodora Zagorac, University of Illinois - Chicago; M. Counihan, J. Lee, Y. Zhang, Argonne National Laboratory, USA; L. Hanley, University of Illinois - Chicago; S. Tepavcevic, Argonne National Laboratory, USA

Interest in solid state lithium-ion batteries as the next generation of energy storage devices has led to intense study of the chemistry, structure, and manufacturing processes for polymer electrolytes. Lithium bis(trifluoromethanesulfonyl) imide (LiTFSI) salt is often used to introduce Li ions into the solid-state electrolyte. Lithium bis(fluorosulfonyl)imide salt (LiFSI) and lithium nitrate (LiNO<sub>3</sub>) are less expensive salts with the potential to improve performance characteristics over pure LiTFSI in certain electrolyte formulations. The differences in distribution and reactivity of these different salts are still unknown but are critical to battery performance. Time-of-flight secondary ion mass spectrometry (ToF-SIMS) imaging and depth profiling was performed to compare the distributions of Li<sup>+</sup> cations and TFSI<sup>-</sup>, FSI<sup>-</sup>, and NO<sub>3</sub><sup>-</sup> anions across the solid-electrolyte interface (SEI) formed between the polymer electrolyte and thin lithium metal electrode. Experiments were performed on ~600 nm salt-rich poly(ethylene oxide) electrolytes with ~10 nm overlayers of vapor-deposited Li metal. Samples were probed with 30 keV Bi<sub>3</sub><sup>+</sup> from a liquid metal ion gun while depth profiling with 10 keV Ar<sub>1400</sub> gas cluster ion beam to collect both positive and negative ion mass spectra. Ion distributions from the three salts and their 3D images will be presented and discussed in terms of the relative composition of their SEI layers. Chemical differences from ToF-SIMS analysis help explain the differences in electrochemical SEI formation and half cell cycling: LiTFSI and LiFSI are similar, but LiNO<sub>3</sub> presents much different electrochemical properties.

9:40am **AS+2D+CA+EM+MS+NS+SE+SS+TF-FrM-5 A Perspective on X-ray Photoelectron Spectroscopy (XPS) Peak Fitting, and Reporting of XPS Data Acquisition and Peak Fitting Parameters in the Literature**, Matthew Linford, G. Major, J. Pinder, Brigham Young University

We recently reported that a rather large fraction (ca. 40 %) of the XPS peak fitting in the literature is at best suspect. In a recent Perspective article (doi: 10.1116/6.0002437) we argue that the various stakeholders of the problem can act together to improve the current situation. This Perspective begins with representative examples of poor XPS peak fitting. The purpose of showing these examples is to demonstrate to the reader that we are not quibbling or arguing over subtle interpretations of the data. Increasingly, we see errors that might be classified as egregious. We argue that science is in a state of 'pre-crisis' more than in a state of 'crisis'. We suggest that if too much incorrect data analysis enters the literature it may cease to be self-correcting. We note the very large number of surface and material characterization techniques available today and how this presents a challenge for scientists. Consequently, it is likely that many manuscripts are incompletely reviewed today. Graduate students and post-docs at research institutions are often given minimal training on acquiring and analyzing XPS data. High fees for instruments can limit access to them and student training. Prisoner's dilemmas may help explain situations in science that lead to suboptimal outcomes for the community. Authors are primarily responsible for the quality of the research in their papers, not reviewers or editors. We question the wisdom of placing the names of reviewers and editors on papers. In some cases, staff scientists are not adequately recognized for their intellectual contributions to projects. Selective reviewing may allow more reviews to be performed without overtaxing the community. Reviewing at some open access journals may be inadequate.

# Friday Morning, November 10, 2023

Collaboration needs to be encouraged to a greater extent at some institutions.

10:00am **AS+2D+CA+EM+MS+NS+SE+SS+TF-FrM-6 Unsupervised and Supervised Machine Learning Applied to ToF-SIMS of an Organic Matter-Rich Mudstone with Molecular Biomarker**, *M. Pasterski*, University of Illinois Chicago; *M. Lorenz*, Oak Ridge National Laboratory; *A. Ievlev*, Oak Ridge National Laboratory; *R. Wickramasinghe*, *Luke Hanley*, *F. Kenig*, University of Illinois Chicago

Time-of-flight secondary ion mass spectrometry (ToF-SIMS) imaging has been used to detect organic compounds including molecular biosignatures (biomarkers) in geologic samples (R.C. Wickramasinghe, *et al.*, *Anal. Chem.*, 2021, 93, 15949). The spatial distribution of these biomarkers can help determine when and how these organics were incorporated into the host rock. ToF-SIMS imaging can rapidly collect a large amount of data, but molecular and fragment ions of different species are mixed together in complex mass spectra that are difficult to interpret. Here, we apply unsupervised and supervised machine learning (ML) to help interpret the mass spectra obtained by ToF-SIMS of an organic-carbon-rich mudstone from the Middle Jurassic of England (UK). It was previously shown that the presence of sterane molecular biomarkers in this sample can be detected via ToF-SIMS (M.J. Pasterski, *et al.*, *Astrobiol.*, in press). We use unsupervised ML on field emission scanning electron microscopy – electron dispersive spectroscopy (SEM-EDS) measurements to define compositional categories based on differences in elemental abundances. We then test the ability of four ML algorithms - k-nearest neighbors (KNN), recursive partitioning and regressive trees (RPART), eXtreme gradient boost (XGBoost), and random forest (RF) - to classify the ToF-SIMS spectra using the categories assigned via SEM-EDS, using organic and inorganic labels, as well as using presence or absence of detectable steranes. KNN provided the highest predictive accuracy and balanced accuracy. The feature importance, or the specific features of the ToF-SIMS data used by the KNN model to make classifications could not be determined, preventing post-hoc model interpretation. However, the feature importance extracted from the other three models was useful for interpreting spectra. We determined that some of the organic ions used to classify biomarker containing spectra may be fragment ions derived from kerogen.

10:40am **AS+2D+CA+EM+MS+NS+SE+SS+TF-FrM-8 Probing Thin Film Interfaces at the Nanoscale by Low Energy Ion Scattering**, *Marko Sturm*, *A. Chandrasekaran*, *A. Valpreda*, *A. Zameshin*, *R. Van de Kruijs*, *A. Yakshin*, *F. Bijkerk*, *M. Ackermann*, University of Twente, Netherlands **INVITED**

The growth of thin films with nanometer range thickness is of great importance for application topics as nanoelectronics, oxidation protection of thin films and optical coatings for X-ray applications. The performance of these coatings often critically depends on the sharpness of the interfaces between different layers. In this talk I will outline how we use Low-energy ion scattering (LEIS) to study interface formation between layers of different transition metals (TMs) and between TMs and Si.

LEIS with noble gas ions as projectiles yields surface peaks that indicate the composition of the outermost atomic layer of a sample. This makes the technique excellently suited to study whether deposition of a thin film leads to a closed layer. However, deposition of an overlayer on top of an underlayer may result in surface segregation of underlayer atoms (driven by surface energy differences or stress), such that the surface composition is not directly representative for the in-depth concentration profile. We analyzed the evolution of surface coverage versus deposited thickness for a large set of TM/TM film combinations, deposited by magnetron sputtering in a system that allows LEIS analysis without vacuum break after deposition. By applying a model that takes into account surface segregation, the interface profiles were derived from these layer growth profiles, which we call deposition depth profile. In addition, we demonstrated that the sharpness of interfaces in TM/TM film systems can be predicted by a phenomenological model with the crystal structure and surface energy of the materials as input parameter. This model in principle predicts the sharpness of the interface in any TM/TM thin film combination! [1]

Apart from surface peaks, LEIS spectra typically also contain so-called tails, caused by projectiles that, after sub-surface scattering, are reionized when leaving the sample. It was demonstrated before that LEIS tails can be used to determine thickness of various thin film systems, when the stopping power of the projectiles is known. Here, we show that LEIS tails can also be used to determine the sharpness of interfaces of few nm Si-on-W and Si-on-Mo films, by comparing LEIS measurements with Monte Carlo simulations with the TRBS code, which takes into account multiple scattering and stopping in the target. This approach allows interface

characterization from a single sample, without the need to make a deposition depth profile.

References:

[1] A. Chandrasekaran, R.W.E. van de Kruijs, J.M. Sturm, A.A. Zameshin and F. Bijkerk, *ACS Applied Materials & Interfaces* **11**, 46311 (2019)

11:20am **AS+2D+CA+EM+MS+NS+SE+SS+TF-FrM-10 The Effect of Instrument Settings, Sample Distance, and Tilt on TofsimsSecondary Ion Intensities**, *Alan Spool*, *L. Finney*, Western Digital

Experiments were performed to explore the effects of various instrument settings and sample placements on secondary ion intensities to better understand what factors have the greatest effect on repeatability and replicability in TOF-SIMS. A batch of magnetic recording disks used in hard disk drive manufacture, natively flat and homogeneous, were used as test samples for the purpose. As expected, by far the largest variable altering raw intensities was the LMIG tip stability. LMIG tips can have stable emission currents while still producing variable pulsed LMIG beam currents with resultant variable secondary ion counts. This variability sometimes is seen in slow current drift, but is sometimes so rapid that measurements taken directly before each measurement are not close enough in time to properly scale the measurement results. In these cases, normalization is the only solution. Secondary ion intensities were remarkably insensitive to small variations in sample height (position relative to the extractor). Far more interesting were the changes to the secondary ion intensities that resulted from tilting the sample. These effects varied amongst the secondary ions detected such that normalization did not remove them. Secondary ion emission as a function of emission angle has long been understood to be like a cosine function and to vary somewhat from ion to ion. These different angular profiles explain the differences seen in ion detection as a function of tilt. Some of these differences proved to be asymmetrical, varying depending on whether the sample was tilted toward or away from the primary ion source, an indication that in some situations some residual momentum from the initial primary ion impact onto the surface is carried into the secondary ion emission. These results have implications for attempts to do quantitative analysis on any sample that is not completely flat.

11:40am **AS+2D+CA+EM+MS+NS+SE+SS+TF-FrM-11 Evaluation of Unaltered and Irradiated Nuclear Graphite Surfaces through Integrated Traditional XPS and HAXPES Techniques**, *Jonathan Counsell*, *L. Soomary*, *K. Zahra*, Kratos Analytical Limited, UK; *B. Spencer*, *A. Theodosiou*, University of Manchester, UK

Graphite-moderated reactors have been operational worldwide for several decades. There exists a substantial body of research in this domain, with particular emphasis on investigating the impact of irradiation damage on the graphite matrix. In order to satisfy the design and regulatory requisites of these advanced reactors, it becomes imperative to gain a deeper comprehension of the retention and transportation mechanisms of fission products within graphite.

This study outlines a technique for the precise assessment of the surface chemistry of highly-oriented pyrolytic graphite (HOPG), serving as a representative model akin to the current graphite grades utilized in the nuclear sector. We delve into the process of surface etching aimed at eliminating surface adsorbates and contaminants. This process involves the utilization of both monatomic and cluster ions, the former inadvertently causing undesirable damage to the graphite structure. Such damage is evidenced by a significant reduction in the sp<sup>2</sup> component of C 1s. We introduce the use of UPS analysis as a straightforward means of determining the presence of sp<sup>2</sup> characteristics in the uppermost atomic layers.

Moreover, we examine the consequences of high-energy ion implantation (Cs<sup>+</sup>) and the ensuing damage to the HOPG surface. This examination is carried out using XPS (1486eV) and HAXPES (2984eV), thereby showcasing the capability to characterize the resulting surface damage and the associated alterations within the probed depths.

## Fundamental Discoveries in Heterogeneous Catalysis Focus Topic

### Room B113 - Session HC+SS-FrM

#### Greatest Hits in Heterogeneous Catalysis

**Moderators:** Liney Arnadottir, Oregon State University, Ashleigh Baber, James Madison University, Dan Killelea, Loyola University Chicago

#### 8:20am HC+SS-FrM-1 CO Characterized Pt/Cu(111) Single Atom Alloy (SAA) for the Hydrogenation of Unsaturated Aldehydes, David Molina, M. Trenary, University of Illinois - Chicago

The use of heterogeneous catalysts is of high importance in a vast number of industrial processes. A promising new type of heterogeneous catalyst known as single atom alloys (SAAs) greatly reduce the amount of precious metal (e.g. Pt, Pd, Rh, Ru) used and have shown enhancements in selectivity, when compared to their pure counterparts, in various types of reactions, including hydrogenation reactions. Hence, it is important to be able to quantify the amount of precious metal on the surface of these catalysts and understand their properties. We have used reflection absorption infrared spectroscopy (RAIRS) and temperature programmed desorption (TPD) of adsorbed CO were used to probe the properties of Pt/Cu(111) surfaces, ranging from a multilayer film of Pt on Cu(111) to 2% Pt/Cu(111). For Pt deposition on Cu(111) at room temperature, the Pt coverage was varied from a multilayer film to 0.23 monolayer (ML). As the Pt coverage decreased, a RAIR C–O stretch peak in the range of 2041–2050  $\text{cm}^{-1}$  showed isolated Pt atoms embedded in the Cu(111) surface. Pt islands were identified by a C–O stretch peak in the range of 2058–2067  $\text{cm}^{-1}$ , showing CO on top of Pt atoms. These islands also allowed for CO to bind at bridge sites between two Pt atoms and this was supported by the observed C–O stretch peak at 1852  $\text{cm}^{-1}$ . Deposition of low coverages of Pt at 380, 450 and 550 K formed SAAs in which surface Pt is only present as isolated atoms that had replaced Cu atoms in the topmost atomic layer, in agreement with previous studies with scanning tunneling microscopy. Adsorption of CO on top of the Pt atoms of the SAAs leads to a C–O stretch in the range of 2041–2046  $\text{cm}^{-1}$ . Compared to the SAA formed by Pt deposition at 380 K, deposition at 450 and 550 K led to more dispersed Pt atoms as indicated by the lack of a shift of the C–O stretch peaks, indicating that the distance between CO molecules was not low enough for dipole-dipole coupling shifts to occur. In all cases, the C–O stretch of CO on the Pt atoms of Pt/Cu(111) was significantly redshifted relative to its value on Pt(111), which is a manifestation of how nearby Cu atoms alter the Pt–CO bonding. The well characterized Pt/Cu(111) SAA is currently being used to study the hydrogenation of model unsaturated aldehydes.

#### 8:40am HC+SS-FrM-2 Efficient Catalyst and Protection Layer of Ni/ $\alpha$ -Al<sub>2</sub>O<sub>3</sub> Catalysts for Improved H<sub>2</sub>O/CO<sub>2</sub> Reforming Reaction of CH<sub>4</sub> via Atomic Layer Deposition, Dae Woong Kim, H. Jeong, W. Hong, J. Park, S. Oh, J. Jang, Hyundai Motor Company, Republic of Korea

Recently, production of synthetic gas by combined steam and CO<sub>2</sub> reforming reaction of CH<sub>4</sub> (CSCR) is proposed for dealing with the energy problem. In the CSCR process as methane reforming reaction, the synthesis of steam (H<sub>2</sub>O), CH<sub>4</sub>, and CO<sub>2</sub> occurs at high temperatures and pressures in the presence of metal catalysts. [1] In general, Ni-based catalysts are attractive materials because of their relatively high activity and low cost as compared to noble metal catalysts. [2] As a support structure, a thermally stable, acid-free and inert  $\alpha$ -Al<sub>2</sub>O<sub>3</sub> is a well-known material. [3] However, catalytic pellets through mixed powder sintering have low structural strength as well as poor catalytic utilization due to dead nickel volume. Therefore, atomic layer deposition (ALD) is proposed as a reliable and atomic scale-adjustable process for conformally growing NiO on  $\alpha$ -Al<sub>2</sub>O<sub>3</sub> surface with an exact thickness. In the case of ALD-based catalyst growth, the reaction efficiency can be maximized without a catalyst dead area because the catalyst is formed only on the active surface where the reforming reaction can occur.

In this work, ALD NiO film was grown on  $\alpha$ -Al<sub>2</sub>O<sub>3</sub> pellet supporter which is followed by reduction annealing for highly active CSCR reforming catalyst with a low Ni concentration. Furthermore, an ultra-thin Al<sub>2</sub>O<sub>3</sub> protection layer was proposed to enhance stability and coking resistant of Ni/ $\alpha$ -Al<sub>2</sub>O<sub>3</sub> catalyst during reforming reaction. Detailed experimental results will be presented.

[1] Energy Fuels 2015, 29, 1055–1065

[2] RSC Advanced 2015, 5, 7539–7546

[3] Journal of Energy Chemistry 22(2013)919–927

[4] Catalysis Science & Technology 2020, 10, 8283

9:00am HC+SS-FrM-3 Complementary Outer Atomic Layer Analysis of Catalyst Materials Using LEIS, P. Br uner, IONTOF GmbH, Germany; J. J arvilehto, Department of Chemical and Metallurgical Engineering, Aalto University School of Chemical Engineering, Finland; S. Saedy, Chemical Engineering Department, Delft University of Technology, Netherlands; Thomas Grehl, IONTOF GmbH, Germany

Performance of material in heterogeneous catalysis is dominated by the composition and chemical state of the outer atomic layer. A number of techniques successfully characterize the material at and close to the surface (e.g. XPS) or directly the interaction of the gas phase with the surface (operando techniques, e.g. IR). Also, physical properties like specific surface area are determined. However, Low Energy Ion Scattering (LEIS) is the only technique capable of determining specifically the elemental composition of the outer atomic layer. This opens a range of possibilities to learn about the materials and especially the preparation of catalysts. Due to the high sensitivity of LEIS, this can be performed on both model as well as industrial catalysts.

In this contribution, we will highlight a range of catalysis applications of LEIS on very different materials. This includes nanoparticles and their catalytically active phase on the surface of these particles, and how this surface changes depending on the environment, e.g. a calcination procedure. This can be a dispersed Pt phase and the prevention of sintering by ALD coating. Also industrial particles used for low cost catalysts are shown, specifically the behavior of the active Fe phase and reorganization of the surface under calcination. Another example is demonstrating the Pt deposition inside porous Al<sub>2</sub>O<sub>3</sub> beads using ALD [1], and how LEIS analysis can help to optimize the process.

Common to all examples is the specific view that LEIS allows due to its single atomic layer information depth, complementing the information gathered from the many other (surface) analytical techniques applied to catalyst materials.

[1] J. J arvilehto, Thesis, Aalto University, <https://aaltdoc.aalto.fi/handle/123456789/119352>

#### 9:20am HC+SS-FrM-4 Size-Selected Pt<sub>n</sub> Cluster Electrocatalysts for Alcohol Oxidation, Zihan Wang, University of Utah, China; T. Masubuchi, University of Utah, Japan; M. O'Brien, S. Anderson, University of Utah

Alcohol oxidation is catalyzed by size-selected Pt<sub>n</sub> clusters deposited on indium tin oxide (ITO) and highly oriented pyrolytic graphite (HOPG) electrodes is being investigated. Clusters are generated in the gas phase, mass selected, then deposited on the electrode supports under controlled conditions, in UHV. Electrocatalysis is studied using a unique *in situ* system that allows aqueous electrochemistry to be studied in an antechamber on the UHV system, without exposure to air. Based on cyclic voltammetry (CV), the activity and selectivity for oxidation of 1- and 2-propanol are strongly dependent on cluster size, for Pt<sub>n</sub>/ITO, and the activity is correlated with Pt core level binding energies measured by XPS. For HOPG, high activity has been observed for both soft- and hard-landed clusters, and the challenge is to understand the nature of the Pt-HOPG binding for cluster prepared under different conditions. Preliminary data shows that even HOPG, which has weak bonding with Pt, can preserve the deposited cluster size long enough to give size-dependent electrocatalysis, if the clusters are deposited under conditions that pin them to the support. The results for propanol oxidation are expected to provide insight into primary vs. secondary alcohol oxidation in glycerol, which is important for upgrading biobased glycerol into commercial products.

#### 9:40am HC+SS-FrM-5 Calorimetric Energies of Metal Atoms within Nanoparticles on Oxide and Carbon Supports: Improved Size Dependencies, Adhesion Energies and Trends versus Metal Element with the Spherical Cap Model, Kun Zhao, University of Washington; D. Auerbach, Max Planck Institute for Multidisciplinary Sciences, Germany; C. Campbell, University of Washington

The chemical potential of metal atoms in supported nanoparticles is an important descriptor of their catalytic performance that captures the effects of particle size and support. Previously, we used the hemispherical cap model (HCM), which assumes 90 degree contact angle of nanoparticles, to model the chemical potential versus size of the nanoparticles. The HCM has been successful in predicting the chemical potential increase with the decreasing of particle size and gives linear trends of adhesion energy with the metal oxophilicity or carbophilicity per unit area for the metal nanoparticles on oxide or carbon supports, respectively. However, the assumption of 90 degree contact angle in the HCM creates errors in the contact angle, particle size and adhesion energy when compared to the expectation of equilibrium shape.

# Friday Morning, November 10, 2023

Here, we will relax the assumption of hemispherical shape, and treat the more general case of spherical caps with any contact angle. We show that by simultaneously analyzing the data from metal vapor adsorption calorimetry (metal chemical potential versus coverage) and the data from He<sup>+</sup> low-energy ion scattering spectroscopy or LEIS (signal versus coverage) within this new spherical cap model (SCM), we can determine the only contact angle that is consistent with both these sets of data. We then apply that approach to reanalyze all the metal / support systems which we had previously analyzed using the HCM to determine this self-consistent contact angle and the corresponding adhesion energy. These analyses rely on our recently developed SCM model for analyzing LEIS signals versus coverage which accounts for blocking of ion trajectories by particle material for any contact angle.<sup>1</sup> The resulting adhesion energies and contact angles are more accurate in predicting chemical potential versus size for all the metal / support systems. The trends of adhesion energy versus metal oxophilicity (for each oxide support) and carbophilicity (for carbon support) per unit area are also improved compared to earlier reports, and now better explain the support effect on the adhesion of metal nanoparticles.

## Reference

1. Zhao, K.; Auerbach, D.; Campbell, C. T. Low Energy Ion Scattering Intensities from Supported Nanoparticles: The Spherical Cap Model. *J. Phys. Chem. C* 2023. <https://doi.org/10.1021/acs.jpcc.3c01175>

10:00am **HC+SS-FrM-6 Insights Into Adsorbate-Driven Surface Restructuring Using Size-Selected Pt/SiO<sub>2</sub> Nanoparticle Catalysts, Christopher O'Connor, T. Kim, C. Owen, Harvard University; N. Marcella, University of Illinois; A. Frenkel, Stony Brook University/Brookhaven National Laboratory; B. Kozinsky, C. Reece, Harvard University**

Heterogeneous catalysts are complex, dynamic materials that can undergo restructuring under reaction conditions. A key aspiration in the rationale design of catalysts is to tune performance (activity, selectivity, and stability) by using reactant conditions (composition, pressure, and temperature) and materials architecture to modify surface structure and composition. Herein, we investigate size-dependent catalyst restructuring under reactions conditions using a series of well controlled size-selected (1 – 8 nm) platinum nanoparticles supported on SiO<sub>2</sub> (Pt/SiO<sub>2</sub>) as a model system. Diffuse Reflectance Infrared Fourier Transform Spectroscopy (DRIFTS) measurements on 2 nm Pt/SiO<sub>2</sub> show that ~35% of CO adsorption sites are undercoordinated Pt under 1 mbar CO at 25 °C which is consistent with a regular truncated octahedral nanoparticle model. Under a CO environment, an incremental increase in temperature up to 350 °C induces restructuring to form a more undercoordinated surface indicated by a ~ 14% increase in total Pt sites for CO adsorption and ~ 75% undercoordinated surface sites. A thermal treatment at 350 °C under an inert atmosphere can reverse the catalyst structure to a well-coordinated surface, while cooling under a CO atmosphere can partially trap the surface in an undercoordinated structure. In contrast, 8 nm Pt/SiO<sub>2</sub> does not undergo significant restructuring from 25 to 350 °C under 1 mbar CO as evidenced by DRIFTS measurements. The experimental results are compared to theoretical calculations and molecular dynamics simulations to provide atomistic insight into the experimentally observed nanoparticle restructuring. This study clearly demonstrates that the adsorbate-driven surface restructuring of supported nanoparticle catalysts is strongly dependent on the reaction conditions (gas composition and temperature) and nanoparticle size, having broad implications for the structure of catalytically active surfaces under reaction conditions.

**Bold page numbers indicate presenter**

— A —

A. Castro, F.: NS1+2D+BI+SS-MoM-1, **3**  
 Abbondanza, G.: SS1+HC-MoM-6, 6  
 Abuyazid, N.: SS-ThP-4, **48**  
 Ackermann, M.:  
 AS+2D+CA+EM+MS+NS+SE+SS+TF-FrM-8, 53  
 Adams, D.:  
 AS+2D+CA+EL+EM+MS+NS+SE+SS+TF-WeM-6, **26**  
 Addamane, S.:  
 AS+2D+CA+EL+EM+MS+NS+SE+SS+TF-WeM-6, 26  
 Adesope, Q.: SS+2D+AS+HC-WeM-2, **28**  
 Adriaensens, P.: SS+HC-TuA-11, 23  
 Ahmad, M.: LX+AS+HC+SS-MoM-8, 3  
 Ahsen, A.: HC+SS-ThM-12, 42  
 Ai, Q.: CA+AS+LS+NS+SS+VT-MoA-3, 8  
 Alemansour, H.: NS1+2D+BI+SS-MoM-4, 4  
 Alexandrowicz, G.: HC+SS-ThM-10, 42  
 Alfonso, D.: SS1+HC-MoM-5, 6  
 Alhowity, S.: SS+2D+AS+HC-WeM-2, 28  
 Alipour, A.: NS1+2D+BI+SS-MoM-4, 4  
 Alkoby, Y.: HC+SS-ThM-10, 42  
 Altman, E.: SS-WeA-11, **37**  
 Amann, A.: NS1+2D+BI+SS-MoM-4, 4  
 Amann, P.: LX+AS+HC+SS-MoM-3, **2**  
 An, R.: SS+HC-TuA-11, 23  
 Andany, S.: NS1+2D+BI+SS-MoM-5, 4  
 Anderson, S.: HC+SS-FrM-4, 54; HC+SS-WeA-11, **35**  
 Andersson, J.: BI2+AS+HC+SS-MoM-8, 1  
 Angrick, C.: SS+AS+TF-MoA-8, **11**  
 Aoki, T.: SS-ThP-5, 48  
 Ara, T.: HC+SS-WeA-4, 34; SS-ThP-14, 50  
 Arat, K.: NS1+2D+BI+SS-MoM-4, 4  
 Arias, S.: NS+2D+EM+MN+SS-TuM-11, 16  
 Armini, S.: SS2+AS+TF-ThM-13, **45**  
 Árnadóttir, L.: LX+AS+BI+HC+SS+TH-MoA-1, **9**  
 Artyushkova, K.:  
 AS+2D+CA+EL+EM+MS+NS+SE+SS+TF-WeM-5, 25; AS+CA+EL+EM+SE+SS+TF-WeA-9, 33; CA1+AS+LS+NS+SS+VT-MoM-3, **1**  
 Asmari, N.: NS1+2D+BI+SS-MoM-5, 4  
 Atoyebi, O.: BI2+AS+HC+SS-MoM-9, 1  
 Auerbach, D.: HC+SS-FrM-5, 54  
 — B —  
 Baer, D.: AS+CA+EL+EM+SE+SS+TF-WeA-1, **32**  
 Baert, K.: SS+AS+TF-MoA-9, 12; SS+HC-TuA-11, 23  
 Bagus, P.: TH1+AS+SS-TuM-6, 19;  
 TH2+AS+SS-TuM-12, 20  
 Bai, Y.: SS1+AS-ThM-5, **44**  
 Bakr, O.: SS-ThP-8, 49  
 Balajka, J.: SS+2D+AS+HC-TuM-13, **18**  
 Balakrishnan, G.: QS+SS-TuA-4, 21  
 Balasubramanian, G.: SS-ThP-18, 50  
 Ballard, J.: QS+SS-TuA-11, **22**  
 Balogun, K.: SS+2D+AS+HC-WeM-2, 28  
 Bamford, S.: CA1+AS+LS+NS+SS+VT-MoM-5, 2  
 Barnes, J.:  
 AS+2D+CA+EM+MS+NS+SE+SS+TF-FrM-1, **52**  
 Barnum, A.:  
 AS+2D+CA+EL+EM+MS+NS+SE+SS+TF-WeM-5, 25  
 Batista, V.: SS+HC-TuA-1, **22**  
 Beasley, M.: BI2+AS+HC+SS-MoM-9, 1  
 Beaudoin, F.: QS+SS-TuA-11, 22  
 Bediako, D.: SS+2D+AS+HC-WeM-3, **29**  
 Bégin, T.: TF2+AP+SE+SS-WeM-12, 30

Benayad, A.:  
 AS+2D+CA+EL+EM+MS+NS+SE+SS+TF-WeM-4, 25  
 Benesova, M.: TH1+AS+SS-TuM-5, 19  
 Berg, R.: SS+HC-TuA-10, **23**  
 Biderman, N.: AS+CA+EL+EM+SE+SS+TF-WeA-9, **33**  
 Bijkerk, F.:  
 AS+2D+CA+EM+MS+NS+SE+SS+TF-FrM-8, 53  
 Biswas, P.: TF2+AP+SE+SS-WeM-13, **31**  
 Blades, W.: SS+HC-ThA-3, 46; SS+HC-ThA-4, 47  
 Blockhuys, F.: SS+HC-TuA-11, 23  
 Blomfield, C.: AS+CA+EL+EM+SE+SS+TF-WeA-4, 33  
 Blum, M.: HC+SS-ThM-6, 42  
 Boden, D.: HC+SS-ThM-2, 41  
 Borgos, S.: AS+CA+EL+EM+SE+SS+TF-ThM-3, 39  
 Boscoboinik, J.: LX+AS+HC+SS-MoM-8, **3**  
 Bowden, M.: TF2+AP+SE+SS-WeM-13, 31  
 Bowers, C.: HC+SS-ThA-3, 46  
 Boyce, B.:  
 AS+2D+CA+EL+EM+MS+NS+SE+SS+TF-WeM-6, 26  
 Boyen, H.: AS+CA+EL+EM+SE+SS+TF-WeA-3, 32  
 Brady Boyd, A.: SS2+AS+TF-ThM-13, 45  
 Braun, J.: SS+AS+TF-MoA-8, 11  
 Brontvein, O.: NS1+2D+BI+SS-MoM-6, 4  
 Brown, J.: SS-WeA-8, 37  
 Brown, S.: SS-WeA-8, 37  
 Brown-Tseng, E.: SS+AS+TF-MoA-9, 12  
 Brugger-Hatzl, M.: NS+2D+EM+MN+SS-TuM-5, 15  
 Brundle, C.: TH2+AS+SS-TuM-12, **20**  
 Brüner, P.: HC+SS-FrM-3, 54  
 Buchine, I.: NS+2D+EM+MN+SS-TuM-4, 15  
 Budach, M.: PS2+AS+SS-ThM-10, 43  
 Burnham, N.: NS+2D+EM+MN+SS-TuM-10, **16**  
 — C —  
 Cabrera German, D.:  
 AS+CA+EL+EM+SE+SS+TF-WeA-2, 32  
 Cahen, D.: NS+2D+EM+MN+SS-TuM-4, 15  
 Caldes, M.: AS+CA+EL+EM+SE+SS+TF-ThM-2, 39  
 Calegari Andrade, M.: SS+HC-TuA-7, **23**  
 Campbell, C.: HC+SS-FrM-5, 54; HC+SS-WeA-3, **34**  
 Cant, D.: AS+CA+EL+EM+SE+SS+TF-ThM-3, **39**  
 Caouette, M.: CA1+AS+LS+NS+SS+VT-MoM-3, 1  
 Cardwell, N.: CA+AS+LS+LX+MN+SE+SS-TuM-4, 13  
 Carlson, E.: SS-ThP-19, 50  
 Caron, A.: SS2-MoM-9, 7  
 Carpena-Nuñez, J.: LX+AS+HC+SS-MoM-4, 2  
 Castanheira, N.: AS+CA+EL+EM+SE+SS+TF-WeA-7, 33  
 Cechal, J.: SS1+AS-ThM-4, 44  
 Celebi, A.: SS2-MoM-10, 7  
 Ceratti, D.: NS+2D+EM+MN+SS-TuM-4, 15  
 Chadwick, H.: HC+SS-ThM-10, **42**  
 Chandrasekaran, A.:  
 AS+2D+CA+EM+MS+NS+SE+SS+TF-FrM-8, 53  
 Charvier, R.:  
 AS+2D+CA+EL+EM+MS+NS+SE+SS+TF-WeM-4, 25; CA+AS+LS+NS+SS+VT-MoA-10, 9  
 Chen, C.: SS-WeA-7, **36**

Chen, D.: HC+SS-ThM-12, **42**  
 Chen, J.:  
 AS+2D+CA+EL+EM+MS+NS+SE+SS+TF-WeM-5, 25  
 Chen, W.: SS-ThP-18, 50  
 Cheng, S.: SS+2D+AS+HC-WeM-6, 29  
 Chien, T.: SS-ThP-18, 50  
 Choi, D.: HC+SS-ThA-3, 46  
 Choi, H.: NS1+2D+BI+SS-MoM-3, 4  
 Choi, M.: SS+AS+TF-MoA-11, 12;  
 TF2+AP+SE+SS-WeM-13, 31  
 Chowdhury, R.: SS+HC-ThA-6, 47  
 Choyal, S.: SS-ThP-3, **48**; SS-ThP-9, 49  
 Christ, B.: TH2+AS+SS-TuM-12, 20  
 Chu, J.: AS+CA+EL+EM+SE+SS+TF-ThM-13, 40  
 Chu, T.: NS1+2D+BI+SS-MoM-3, 4  
 Chuckwu, K.: LX+AS+BI+HC+SS+TH-MoA-1, 9  
 Chueh, W.: SS-ThP-19, 50  
 Chukwunenye, P.: SS+2D+AS+HC-WeM-2, 28  
 Cinar, V.: SS+AS+TF-MoA-3, 10  
 Ciobanu, C.: NS+2D+EM+MN+SS-TuM-3, 15  
 Clark, A.: CA1+AS+LS+NS+SS+VT-MoM-1, **1**  
 Clark, B.: CA+AS+LS+NS+SS+VT-MoA-6, 8  
 Clingerman, D.: SS+AS+TF-MoA-9, 12  
 Coaletzi, G.: SS+2D+AS+HC-WeM-12, 30  
 Cohen, S.: NS+2D+EM+MN+SS-TuM-4, **15**;  
 NS1+2D+BI+SS-MoM-6, **4**  
 Colburn, T.:  
 AS+2D+CA+EL+EM+MS+NS+SE+SS+TF-WeM-5, 25  
 Conard, T.: AS+CA+EL+EM+SE+SS+TF-WeA-3, **32**  
 Conti, A.: SS+2D+AS+HC-TuM-13, 18  
 Corcelli, S.: SS-ThP-15, 50  
 Cortazar Martinez, O.:  
 AS+CA+EL+EM+SE+SS+TF-WeA-2, 32  
 Counihan, M.:  
 AS+2D+CA+EM+MS+NS+SE+SS+TF-FrM-4, 52  
 Counsell, J.:  
 AS+2D+CA+EM+MS+NS+SE+SS+TF-FrM-11, **53**; AS+CA+EL+EM+SE+SS+TF-WeA-4, 33  
 Crist, B.: SS+HC-TuA-12, **24**  
 Cristaudo, V.: SS+AS+TF-MoA-9, **12**  
 Cumpson, P.: AS+CA+EL+EM+SE+SS+TF-ThM-4, **39**  
 Cundari, T.: SS+2D+AS+HC-WeM-2, 28  
 Custer, J.:  
 AS+2D+CA+EL+EM+MS+NS+SE+SS+TF-WeM-6, 26  
 Czap, G.: SS-WeA-4, 36  
 — D —  
 Danilov, A.: NS2+2D+BI+EL+SS-MoM-10, **5**  
 Danner, A.: SS+AS+TF-MoA-3, **10**  
 Daugherty, J.: PS2+AS+SS-ThM-12, **43**  
 Dauskardt, R.:  
 AS+2D+CA+EL+EM+MS+NS+SE+SS+TF-WeM-5, 25  
 Davis-Wheeler Chin, C.: HC+SS-ThM-13, **42**  
 De Carvalho, A.:  
 AS+2D+CA+EM+MS+NS+SE+SS+TF-FrM-1, 52  
 de Siervo, A.: HC+SS-WeA-7, **35**  
 Dean, A.: SS-ThP-7, 49  
 DelRio, F.:  
 AS+2D+CA+EL+EM+MS+NS+SE+SS+TF-WeM-6, 26  
 Deng, X.: SS1+HC-MoM-5, 6  
 Desta, D.: AS+CA+EL+EM+SE+SS+TF-WeA-3, 32  
 Dhas, J.: SS+AS+TF-MoA-11, 12  
 Diebold, A.:  
 AS+2D+CA+EL+EM+MS+NS+SE+SS+TF-WeM-10, **26**



## Author Index

- Diebold, U.: HC+SS-WeM-2, 27;  
SS+2D+AS+HC-TuM-1, 16; SS+2D+AS+HC-TuM-10, 18; SS+2D+AS+HC-TuM-13, 18;  
SS+2D+AS+HC-TuM-2, 17; SS+2D+AS+HC-WeM-1, 28
- Dietrich, P.: CA+AS+LS+LX+MN+SE+SS-TuM-10, **14**; LX+AS+HC+SS-MoM-5, 3
- Dimitrakellis, P.: LX+AS+HC+SS-MoM-8, 3
- Dingreville, R.:  
AS+2D+CA+EL+EM+MS+NS+SE+SS+TF-WeM-6, 26
- Dissanayake, R.: SS-ThP-12, 49
- Dohnalek, Z.: HC+SS-WeM-12, **28**
- Dohnálek, Z.: HC+SS-ThM-1, 41
- Domenichini, B.: CA+AS+LS+NS+SS+VT-MoA-10, 9
- Donath, M.: SS+AS+TF-MoA-8, 11
- Dong, W.: SS+HC-TuA-1, 22
- Dong, Z.: SS-WeA-3, 36
- Dorneles de Mello, M.: LX+AS+HC+SS-MoM-8, 3
- Dorst, A.: SS-ThP-12, **49**
- D'Souza, F.: SS+2D+AS+HC-WeM-2, 28
- Du, Y.: SS+AS+TF-MoA-11, 12; SS2+AS+TF-ThM-11, **45**; TF2+AP+SE+SS-WeM-13, 31
- Duchon, T.: SS1+HC-MoM-1, 5
- Dunkelberger, A.: BI2+AS+HC+SS-MoM-9, 1
- Dziadkowiec, J.: SS2-MoM-10, 7
- E —
- Eda, Y.: SS-ThP-2, 48
- Edel, R.: SS-WeA-8, 37
- Eder, M.: HC+SS-ThM-6, 42;  
LX+AS+BI+HC+SS+TH-MoA-5, 10;  
SS+2D+AS+HC-WeM-1, **28**
- Eller, M.: CA+AS+LS+LX+MN+SE+SS-TuM-1, 13
- Émond, N.: TF2+AP+SE+SS-WeM-12, 30
- Endo, Y.: HC+SS-WeM-1, 27
- Engbrecht, K.: CA+AS+LS+NS+SS+VT-MoA-11, 9
- Eparvier, F.: SS+HC-TuA-10, 23
- Erickson, T.: SS+2D+AS+HC-WeM-11, **30**;  
SS+2D+AS+HC-WeM-12, 30
- Esch, F.: LX+AS+BI+HC+SS+TH-MoA-5, 10;  
SS+2D+AS+HC-WeM-5, 29
- Eyres, A.:  
AS+2D+CA+EL+EM+MS+NS+SE+SS+TF-WeM-13, 26; AS+CA+EL+EM+SE+SS+TF-ThM-1, 39
- F —
- F. Trindade, G.:  
AS+2D+CA+EL+EM+MS+NS+SE+SS+TF-WeM-13, **26**
- Fairley, N.: AS+CA+EL+EM+SE+SS+TF-ThM-2, 39
- Fantner, G.: NS1+2D+BI+SS-MoM-5, 4
- Farber, R.: QS+SS-TuA-9, 21
- Fears, K.: BI2+AS+HC+SS-MoM-9, 1
- Fernandez Velasco, L.: SS+HC-TuA-11, 23
- Fernandez, V.: AS+CA+EL+EM+SE+SS+TF-ThM-2, **39**
- Finj, E.: NS+2D+EM+MN+SS-TuM-10, 16
- Finney, L.:  
AS+2D+CA+EM+MS+NS+SE+SS+TF-FrM-10, 53
- Finzel, J.: SS+AS+TF-MoA-3, 10
- Fisher, G.:  
AS+2D+CA+EM+MS+NS+SE+SS+TF-FrM-1, 52
- Flavell, W.: LX+AS+HC+SS-MoM-10, 3
- Florek, M.: SS-ThP-10, 49
- Fontenot, P.: HC+SS-ThM-13, 42
- Fowler, E.:  
AS+2D+CA+EL+EM+MS+NS+SE+SS+TF-WeM-6, 26
- Franceschi, G.: SS+2D+AS+HC-TuM-2, 17
- Franchini, C.: HC+SS-WeM-2, 27
- Frenkel, A.: HC+SS-FrM-6, 55
- Frerichs, H.: NS1+2D+BI+SS-MoM-4, 4
- Frese, N.: AS+CA+EL+EM+SE+SS+TF-ThM-5, 40
- Freund, H.: TH1+AS+SS-TuM-1, **18**
- Frye, M.: TF2+AP+SE+SS-WeM-10, 30
- Fuchs, E.: QS+SS-TuA-11, 22
- Fuller, E.: SS+AS+TF-MoA-10, 12
- Furukawa, M.: HC+SS-WeM-1, 27
- Fushimi, R.: HC+SS-ThM-3, 41
- G —
- Gajdek, D.: SS1+HC-MoM-6, 6
- Galtayries, A.:  
AS+2D+CA+EM+MS+NS+SE+SS+TF-FrM-1, 52
- Ganesan, A.: SS+2D+AS+HC-WeM-2, 28
- Garcia Michel, E.: SS+AS+TF-MoA-10, 12
- Gardiner, J.: NS1+2D+BI+SS-MoM-4, 4
- Gardner, W.: CA1+AS+LS+NS+SS+VT-MoM-5, 2
- Garten, L.: TF2+AP+SE+SS-WeM-10, **30**
- Gaude, C.:  
AS+2D+CA+EM+MS+NS+SE+SS+TF-FrM-1, 52
- Gauthier, N.:  
AS+2D+CA+EL+EM+MS+NS+SE+SS+TF-WeM-4, 25;  
AS+2D+CA+EM+MS+NS+SE+SS+TF-FrM-1, 52
- Gelb, L.: AS+CA+EL+EM+SE+SS+TF-WeA-7, **33**
- Gericke, S.: HC+SS-WeA-9, 35
- Gewirth, A.: SS1+HC-MoM-3, **6**
- Gharaee, M.: SS+2D+AS+HC-WeM-2, 28
- Giesen, M.: SS1+HC-MoM-1, 5
- Gillum, M.: SS+AS+TF-MoA-6, **11**
- Gilmore, I.:  
AS+2D+CA+EL+EM+MS+NS+SE+SS+TF-WeM-13, 26;  
AS+2D+CA+EM+MS+NS+SE+SS+TF-FrM-3, 52; AS+CA+EL+EM+SE+SS+TF-ThM-1, **39**
- Gilquin, B.:  
AS+2D+CA+EM+MS+NS+SE+SS+TF-FrM-1, 52
- Golding, M.:  
AS+2D+CA+EL+EM+MS+NS+SE+SS+TF-WeM-5, 25
- Goldstein, B.: QS+SS-TuA-12, 22
- Gofuński, M.: CA+AS+LS+LX+MN+SE+SS-TuM-1, 13
- González-Barrio, M.: SS+AS+TF-MoA-10, 12
- Good, K.: AS+CA+EL+EM+SE+SS+TF-WeA-4, **33**
- Göttlicher, J.: TH1+AS+SS-TuM-5, 19
- Gould, I.: CA+AS+LS+LX+MN+SE+SS-TuM-3, 13
- Grabnic, T.: SS-WeA-8, 37
- Graulich, D.: AS+CA+EL+EM+SE+SS+TF-ThM-5, 40
- Grehl, T.: HC+SS-FrM-3, **54**
- Grespi, A.: HC+SS-WeA-9, 35; SS1+HC-MoM-6, 6
- Groot, I.: HC+SS-ThM-2, **41**
- Groß, A.: SS+HC-ThA-5, **47**
- Guiheux, D.: CA+AS+LS+NS+SS+VT-MoA-10, 9
- Günther, S.: HC+SS-ThM-6, 42;  
LX+AS+BI+HC+SS+TH-MoA-5, 10
- Guyot, C.:  
AS+2D+CA+EM+MS+NS+SE+SS+TF-FrM-1, 52
- Guzman Bucio, D.: AS+CA+EL+EM+SE+SS+TF-WeA-2, **32**
- Gys, N.: SS+HC-TuA-11, **23**
- H —
- Hagelin Weaver, H.: HC+SS-ThA-3, **46**
- Hahn, M.: LX+AS+BI+HC+SS+TH-MoA-10, **10**
- Hall, H.: SS+2D+AS+HC-WeM-11, 30;  
SS+2D+AS+HC-WeM-12, 30
- Hammer, L.: SS+2D+AS+HC-TuM-1, 16
- Han, S.: QS+SS-TuA-4, 21
- Handy, K.: SS-ThP-1, 48; SS-ThP-15, **50**
- Hanley, L.:  
AS+2D+CA+EM+MS+NS+SE+SS+TF-FrM-4, 52; AS+2D+CA+EM+MS+NS+SE+SS+TF-FrM-6, **53**
- Harlow, G.: SS1+HC-MoM-6, 6
- Harvey, S.: CA+AS+LS+LX+MN+SE+SS-TuM-3, **13**
- Hauffman, T.: SS+AS+TF-MoA-9, 12; SS+HC-TuA-11, 23; SS1+HC-MoM-2, 6
- Haverkort, M.: TH1+AS+SS-TuM-5, 19
- Hayashida, K.: HC+SS-WeM-1, 27
- Head, A.: LX+AS+HC+SS-MoM-4, **2**
- Hedhili, M.: SS-ThP-8, **49**
- Heiner, B.: SS1+AS-ThM-3, **44**
- Heiz, U.: HC+SS-ThM-6, 42;  
LX+AS+BI+HC+SS+TH-MoA-5, 10;  
SS+2D+AS+HC-WeM-1, 28
- Heldebrant, D.: CA+AS+LS+NS+SS+VT-MoA-8, 8
- Hendricks, J.: QS+SS-TuA-12, **22**
- Henry, M.: QS+SS-TuA-4, 21
- Hernandez, J.: SS+2D+AS+HC-WeM-12, 30
- Herrera Gomez, A.:  
AS+CA+EL+EM+SE+SS+TF-WeA-2, 32
- Herrera-Gomez, A.:  
AS+CA+EL+EM+SE+SS+TF-ThM-12, **40**
- Heyden, A.: HC+SS-ThM-12, 42
- Hirai, T.: SS-ThP-2, 48
- Hirchenhahn, P.:  
AS+2D+CA+EM+MS+NS+SE+SS+TF-FrM-1, 52
- Hla, S.: SS-WeA-12, 38
- Homma, K.: HC+SS-WeM-1, 27
- Hong, W.: HC+SS-FrM-2, 54
- Hossain, M.: HC+SS-ThM-3, 41
- Hosseini, N.: NS1+2D+BI+SS-MoM-5, 4
- Hrabar, S.: CA+AS+LS+LX+MN+SE+SS-TuM-1, 13
- Hsiao, L.: HC+SS-ThA-3, 46
- Hubin, A.: SS1+HC-MoM-2, 6
- Humbert, B.: AS+CA+EL+EM+SE+SS+TF-ThM-2, 39
- Hütner, J.: SS+2D+AS+HC-TuM-13, 18
- Hwang, H.: SS2+AS+TF-ThM-10, **45**
- I —
- Ievlev, A.: AS+2D+CA+EM+MS+NS+SE+SS+TF-FrM-6, 53
- Imre, A.: SS+2D+AS+HC-TuM-1, **16**
- Ingram, D.: SS+2D+AS+HC-WeM-11, 30
- Isagoda, M.: SS-ThP-5, **48**
- Ito, S.: HC+SS-WeM-1, 27
- Itzhak, N.: NS1+2D+BI+SS-MoM-6, 4
- J —
- Jafari, S.: SS-ThP-7, **49**
- Jain, M.:  
AS+2D+CA+EL+EM+MS+NS+SE+SS+TF-WeM-6, 26
- Jakub, Z.: HC+SS-WeM-2, 27; SS1+AS-ThM-4, **44**
- Jamka, E.: SS+AS+TF-MoA-6, 11
- Jang, J.: HC+SS-FrM-2, 54
- Jang, S.: SS+HC-ThA-6, **47**
- Janulaitis, N.: HC+SS-WeA-3, 34
- Järvillehto, J.: HC+SS-FrM-3, 54
- Jelezko, F.: QS+SS-TuA-1, **21**
- Jensen, E.: SS+HC-TuA-9, **23**
- Jeong, H.: HC+SS-FrM-2, 54; SS-ThP-4, 48

## Author Index

- Jernigan, G.: AS+2D+CA+EL+EM+MS+NS+SE+SS+TF-WeM-1, **25**
- Jessup, D.: SS+HC-ThA-4, 47
- Jiang, N.: SS+2D+AS+HC-TuM-3, 17; SS-ThP-3, 48; SS-ThP-9, 49; SS-WeA-10, **37**
- Jiang, Y.: SS-WeA-9, **37**
- Johns, J.: CA+AS+LS+LX+MN+SE+SS-TuM-13, **14**
- Johnson, D.: SS2-MoM-9, 7
- Johnson, G.: CA+AS+LS+NS+SS+VT-MoA-8, 8
- Jones, A.: SS+HC-TuA-10, 23
- Jones, J.: CA1+AS+LS+NS+SS+VT-MoM-3, 1
- Joselevich, E.: NS1+2D+BI+SS-MoM-6, 4
- Joseph, L.: HC+SS-WeM-13, **28**
- Jouneau, P.: AS+2D+CA+EM+MS+NS+SE+SS+TF-FrM-1, 52
- Jugovac, M.: SS+AS+TF-MoA-10, 12
- Juhel, M.: CA+AS+LS+NS+SS+VT-MoA-10, 9
- Jung, J.: SS+AS+TF-MoA-5, 11
- K —
- Kaiser, S.: LX+AS+BI+HC+SS+TH-MoA-5, 10
- Kalasad, M.: AS+2D+CA+EL+EM+MS+NS+SE+SS+TF-WeM-6, 26
- Kalinin, S.: NS+2D+EM+MN+SS-TuM-1, **15**; NS+2D+EM+MN+SS-TuM-12, 16
- Kandel, S.: SS1+AS-ThM-3, 44; SS-ThP-1, 48; SS-ThP-15, 50
- Kaneko, T.: SS-ThP-17, 50
- Kangül, M.: NS1+2D+BI+SS-MoM-5, 4
- Karagoz, B.: LX+AS+HC+SS-MoM-4, 2
- Kas, J.: TH2+AS+SS-TuM-10, 20
- Kaspar, T.: TF2+AP+SE+SS-WeM-13, 31
- Kauffman, D.: SS1+HC-MoM-5, 6
- Kay, B.: HC+SS-ThM-1, 41
- Kaya, S.: SS+2D+AS+HC-WeM-11, 30
- Kazuma, E.: SS+AS+TF-MoA-5, 11
- Keenan, M.: AS+CA+EL+EM+SE+SS+TF-ThM-1, 39
- Kelber, J.: SS+2D+AS+HC-WeM-2, 28
- Kenig, F.: AS+2D+CA+EM+MS+NS+SE+SS+TF-FrM-6, 53
- Khatib, S.: HC+SS-ThM-3, **41**
- Killelea, D.: SS+AS+TF-MoA-6, 11; SS-ThP-12, 49
- Kim, D.: HC+SS-FrM-2, **54**
- Kim, J.: NS1+2D+BI+SS-MoM-3, 4; SS2+AS+TF-ThM-10, 45
- Kim, L.: SS-ThP-18, **50**
- Kim, S.: SS2+AS+TF-ThM-10, 45
- Kim, T.: HC+SS-FrM-6, 55; HC+SS-WeA-10, 35
- Kim, Y.: SS+AS+TF-MoA-5, 11; SS-WeA-1, **36**
- Kiðlinger, T.: SS+2D+AS+HC-TuM-1, 16
- Kitsopoulos, T.: HC+SS-ThA-1, **46**
- Kiuchi, A.: SS-ThP-2, **48**
- Ko, S.: SS-ThP-7, 49
- Ko, W.: QS+SS-TuA-10, **22**; QS+SS-TuA-3, 21
- Kogler, M.: AS+CA+EL+EM+SE+SS+TF-WeA-11, **34**
- Koirala, K.: TF2+AP+SE+SS-WeM-13, 31
- Kolel-Veetil, M.: BI2+AS+HC+SS-MoM-9, 1
- Kolmakov, A.: CA+AS+LS+LX+MN+SE+SS-TuM-1, 13; LX+AS+HC+SS-MoM-1, **2**
- Kothari, R.: AS+2D+CA+EL+EM+MS+NS+SE+SS+TF-WeM-6, 26
- Kovac, A.: TH1+AS+SS-TuM-5, 19
- Kozinsky, B.: HC+SS-FrM-6, 55
- Kratky, T.: HC+SS-ThM-6, 42; LX+AS+BI+HC+SS+TH-MoA-5, 10
- Kraushofer, F.: LX+AS+BI+HC+SS+TH-MoA-5, 10; SS+2D+AS+HC-TuM-1, 16; SS+2D+AS+HC-WeM-5, 29
- Krinninger, M.: LX+AS+BI+HC+SS+TH-MoA-5, 10; SS+2D+AS+HC-WeM-5, **29**
- Kugler, D.: SS+2D+AS+HC-TuM-13, 18
- Kulbacki, B.: SS-ThP-7, 49
- Kumar, S.: NS+2D+EM+MN+SS-TuM-4, 15
- Kunz, M.: HC+SS-ThM-3, 41
- Kunze, K.: LX+AS+HC+SS-MoM-5, 3
- Kurahashi, M.: SS+AS+TF-MoA-1, **10**
- Kurowska, A.: SS1+AS-ThM-4, 44
- Kuschel, T.: AS+CA+EL+EM+SE+SS+TF-ThM-5, 40
- Kwoka, M.: SS-ThP-10, 49
- L —
- Lado, J.: QS+SS-TuA-10, 22; QS+SS-TuA-3, 21
- Laha, P.: SS+AS+TF-MoA-9, 12
- Lambeets, S.: CA+AS+LS+LX+MN+SE+SS-TuM-4, **13**
- Lane, C.: QS+SS-TuA-3, 21
- Lapak, M.: HC+SS-ThA-3, 46
- Larsson, A.: HC+SS-WeA-9, 35; SS1+HC-MoM-6, 6
- Lauhon, L.: NS1+2D+BI+SS-MoM-3, **4**
- Lechner, B.: HC+SS-ThM-6, 42; LX+AS+BI+HC+SS+TH-MoA-5, **10**; SS+2D+AS+HC-WeM-5, 29
- Lee, C.: HC+SS-ThM-1, 41
- Lee, D.: LX+AS+HC+SS-MoM-8, 3
- Lee, J.: AS+2D+CA+EM+MS+NS+SE+SS+TF-FrM-4, 52
- Lee, K.: SS-ThP-8, 49
- Lee, M.: SS+AS+TF-MoA-5, **11**
- Lee, S.: CA+AS+LS+LX+MN+SE+SS-TuM-1, 13; SS+2D+AS+HC-TuM-4, **17**
- Leggett, G.: BI2+AS+HC+SS-MoM-10, **1**
- Lewandowski, M.: SS+2D+AS+HC-TuM-5, **17**
- Lewis, F.: SS+AS+TF-MoA-6, 11
- Lezuo, L.: SS+2D+AS+HC-TuM-2, 17
- Li, A.: QS+SS-TuA-4, 21
- Li, C.: NS2+2D+BI+EL+SS-MoM-11, 5
- Li, D.: TF2+AP+SE+SS-WeM-13, 31
- Li, L.: SS-ThP-9, 49
- Li, S.: SS-WeA-3, **36**
- Li, Y.: PS2+AS+SS-ThM-10, **43**; SS-WeA-12, 38
- Lim, M.: SS+AS+TF-MoA-9, 12
- Linford, M.: AS+2D+CA+EM+MS+NS+SE+SS+TF-FrM-5, **52**; CA+AS+LS+NS+SS+VT-MoA-6, 8; SS-ThP-7, 49
- Lisenfeld, J.: QS+SS-TuA-7, **21**
- Liu, B.: SS+2D+AS+HC-WeM-6, **29**
- Liu, D.: SS+2D+AS+HC-TuM-3, **17**; SS-ThP-3, 48; SS-ThP-9, 49
- Liu, Y.: NS+2D+EM+MN+SS-TuM-12, **16**
- Lizarbe, A.: CA+AS+LS+NS+SS+VT-MoA-6, **8**
- Lorenz, M.: AS+2D+CA+EM+MS+NS+SE+SS+TF-FrM-6, 53
- Lou, J.: CA+AS+LS+NS+SS+VT-MoA-3, 8
- Lu, W.: SS+HC-TuA-3, 22
- Lucatorto, T.: SS+HC-TuA-10, 23
- Lundgren, L.: SS+HC-TuA-11, 23
- Lungföglar, E.: HC+SS-WeA-9, **35**; SS1+HC-MoM-6, 6
- Lutz, C.: SS-WeA-4, **36**
- Lyu, L.: NS+2D+EM+MN+SS-TuM-10, 16
- M —
- Macak, K.: AS+CA+EL+EM+SE+SS+TF-WeA-4, 33
- Mack, P.: AS+2D+CA+EL+EM+MS+NS+SE+SS+TF-WeM-12, **26**
- Madelat, N.: SS1+HC-MoM-2, 6
- Madiraju, D.: SS-ThP-20, 51
- Mahapatra, S.: SS-ThP-9, 49
- Maindron, T.: AS+2D+CA+EM+MS+NS+SE+SS+TF-FrM-1, 52
- Maiti, D.: HC+SS-ThM-3, 41
- Major, G.: AS+2D+CA+EM+MS+NS+SE+SS+TF-FrM-5, 52; CA+AS+LS+NS+SS+VT-MoA-6, 8
- Maksymovych, P.: QS+SS-TuA-10, 22; QS+SS-TuA-3, **21**
- Mansouri, S.: TF2+AP+SE+SS-WeM-12, 30
- Marbach, H.: PS2+AS+SS-ThM-10, 43
- Marcella, N.: HC+SS-FrM-6, 55
- Marchesini, S.: AS+2D+CA+EM+MS+NS+SE+SS+TF-FrM-3, 52
- Marcoen, K.: SS+HC-TuA-11, 23
- Margot, J.: TF2+AP+SE+SS-WeM-12, 30
- Marković, D.: AS+2D+CA+EL+EM+MS+NS+SE+SS+TF-WeM-3, 25
- Marques, S.: AS+CA+EL+EM+SE+SS+TF-ThM-3, 39
- Martinez, E.: AS+2D+CA+EL+EM+MS+NS+SE+SS+TF-WeM-4, 25
- Maruyama, B.: LX+AS+HC+SS-MoM-4, 2
- Mascaraque, A.: SS+AS+TF-MoA-10, 12
- Masubuchi, T.: HC+SS-FrM-4, 54
- Maza, W.: BI2+AS+HC+SS-MoM-9, 1
- McEwen, J.: AS+CA+EL+EM+SE+SS+TF-ThM-10, **40**; CA+AS+LS+LX+MN+SE+SS-TuM-4, 13
- McGehee, M.: CA+AS+LS+LX+MN+SE+SS-TuM-3, 13
- McGillivray, S.: SS2-MoM-9, 7
- McHenry, T.: SS2-MoM-9, 7
- Mears, L.: SS2-MoM-10, 7
- Mefford, T.: SS-ThP-19, 50
- Meier, M.: HC+SS-WeM-2, 27
- Merte, L.: SS1+HC-MoM-6, 6
- Meyer, J.: HC+SS-ThM-2, 41
- Meynen, V.: SS+HC-TuA-11, 23
- Mi, Z.: SS+HC-TuA-1, 22
- Miao, Y.: LX+AS+HC+SS-MoM-8, 3
- Michielsen, B.: SS+HC-TuA-11, 23
- Minelli, C.: AS+CA+EL+EM+SE+SS+TF-ThM-3, 39
- Mirabella, F.: CA+AS+LS+LX+MN+SE+SS-TuM-10, 14; LX+AS+HC+SS-MoM-5, 3
- Miroshnik, L.: QS+SS-TuA-4, **21**
- Mittendorfer, F.: SS+2D+AS+HC-TuM-13, 18
- Miyazawa, K.: SS-ThP-22, **51**
- Mobberley, J.: CA+AS+LS+NS+SS+VT-MoA-11, 9
- Moffitt, C.: AS+CA+EL+EM+SE+SS+TF-WeA-4, 33
- Mohamed, C.: TF2+AP+SE+SS-WeM-12, 30
- Mohgouk Zouknak, L.: CA+AS+LS+NS+SS+VT-MoA-10, 9
- Mohite, A.: CA+AS+LS+NS+SS+VT-MoA-3, 8
- Molina, D.: HC+SS-FrM-1, **54**
- Molska, A.: AS+CA+EL+EM+SE+SS+TF-ThM-3, 39
- Monnier, J.: HC+SS-ThM-12, 42
- Montes, L.: NS1+2D+BI+SS-MoM-4, 4
- Moody, M.: NS1+2D+BI+SS-MoM-3, 4
- Morales, D.: CA+AS+LS+LX+MN+SE+SS-TuM-3, 13
- Moras, P.: SS+AS+TF-MoA-10, 12
- Morgan, D.: AS+CA+EL+EM+SE+SS+TF-WeA-10, **34**; CA+AS+LS+NS+SS+VT-MoA-6, 8
- Mori, T.: HC+SS-WeM-1, 27
- Morinaga, T.: HC+SS-WeM-1, 27
- Morsell, J.: PS2+AS+SS-ThM-11, **43**
- Mueller, D.: SS1+HC-MoM-1, **5**

## Author Index

- Muir, B.: CA1+AS+LS+NS+SS+VT-MoM-5, 2  
Mullens, S.: SS+HC-TuA-11, 23  
— N —  
Nakamura, J.: HC+SS-WeM-1, 27; SS+AS+TF-MoA-4, 11  
Navid, I.: SS+HC-TuA-1, 22  
Nawaz, A.: SS+HC-TuA-4, 23  
Neely, C.: SS-ThP-20, 51  
Nemsak, S.: CA+AS+LS+LX+MN+SE+SS-TuM-12, 14  
Ng, T.: SS-ThP-8, 49  
Ngan, H.: HC+SS-ThA-5, 46  
Nguyen, H.: LX+AS+BI+HC+SS+TH-MoA-1, 9  
Nguyen, M.: CA+AS+LS+NS+SS+VT-MoA-8, 8  
Nguyen-Phan, T.: SS1+HC-MoM-5, 6  
Niu, Y.: SS+HC-ThA-3, 46  
Nunney, T.:  
AS+2D+CA+EL+EM+MS+NS+SE+SS+TF-WeM-3, 25  
Nykypanchuk, D.: LX+AS+HC+SS-MoM-8, 3  
— O —  
O'Brien, M.: HC+SS-FrM-4, 54  
O'Connor, C.: HC+SS-WeA-10, 35  
O'Connor, C.: HC+SS-FrM-6, 55  
Oehrlein, G.: PS2+AS+SS-ThM-10, 43  
Ogasawara, H.: HC+SS-WeM-1, 27  
Oh, S.: HC+SS-FrM-2, 54  
Olgiate, M.: SS2-MoM-10, 7  
Ologun, A.: SS-ThP-6, 49  
Omolere, O.: SS+2D+AS+HC-WeM-2, 28  
Onyango, I.: CA+AS+LS+LX+MN+SE+SS-TuM-4, 13  
Ooi, B.: SS-ThP-8, 49  
Orson, K.: SS+HC-ThA-3, 46; SS+HC-ThA-4, 47  
Owen, C.: HC+SS-FrM-6, 55  
Owen, J.: QS+SS-TuA-11, 22  
— P —  
Pacchioni, G.: HC+SS-WeM-3, 27  
Palmstrom, A.: CA+AS+LS+LX+MN+SE+SS-TuM-3, 13  
Park, J.: HC+SS-FrM-2, 54  
Park, K.: SS+HC-TuA-3, 22  
Parkinson, G.: HC+SS-WeM-2, 27; HC+SS-WeM-5, 27; SS+2D+AS+HC-TuM-10, 18; SS+2D+AS+HC-WeM-1, 28  
Parot, J.: AS+CA+EL+EM+SE+SS+TF-ThM-3, 39  
Pasterski, M.:  
AS+2D+CA+EM+MS+NS+SE+SS+TF-FrM-6, 53  
Patriotis, M.: QS+SS-TuA-4, 21  
Paudel, B.: SS+AS+TF-MoA-11, 12  
Paudyal, N.: SS-ThP-14, 50  
Pavelec, J.: HC+SS-WeM-2, 27;  
SS+2D+AS+HC-TuM-10, 18; SS+2D+AS+HC-WeM-1, 28  
Pawlak, B.: SS+HC-TuA-11, 23  
Pearson, J.: SS+AS+TF-MoA-10, 12  
Pei, J.: NS+2D+EM+MN+SS-TuM-10, 16  
Pei, Y.: AS+CA+EL+EM+SE+SS+TF-ThM-3, 39  
Penedo, M.: NS1+2D+BI+SS-MoM-5, 4  
Perea, D.: CA+AS+LS+LX+MN+SE+SS-TuM-4, 13  
Petzoldt, P.: HC+SS-ThM-6, 42;  
LX+AS+BI+HC+SS+TH-MoA-5, 10;  
SS+2D+AS+HC-WeM-1, 28  
Pfaff, S.: HC+SS-WeA-9, 35  
Pham, T.: LX+AS+BI+HC+SS+TH-MoA-3, 9  
Phillips, C.: NS2+2D+BI+EL+SS-MoM-11, 5  
Pichler, C.: AS+CA+EL+EM+SE+SS+TF-WeA-11, 34  
Pigram, P.: CA1+AS+LS+NS+SS+VT-MoM-5, 2  
Pinder, J.: AS+2D+CA+EM+MS+NS+SE+SS+TF-FrM-5, 52; AS+CA+EL+EM+SE+SS+TF-ThM-6, 40  
Piras, A.: SS+HC-TuA-11, 23  
Pittsford, A.: SS1+AS-ThM-3, 44  
Planer, J.: SS1+AS-ThM-4, 44  
Plank, H.: NS+2D+EM+MN+SS-TuM-5, 15  
Planksy, J.: LX+AS+BI+HC+SS+TH-MoA-5, 10  
Poche, T.: SS+HC-ThA-6, 47  
Polly, R.: TH1+AS+SS-TuM-6, 19  
Postawa, Z.: CA+AS+LS+LX+MN+SE+SS-TuM-1, 13  
Potma, E.: NS2+2D+BI+EL+SS-MoM-8, 5  
Potyrailo, R.: CA+AS+LS+LX+MN+SE+SS-TuM-5, 14  
Poulikakos, L.: NS+2D+EM+MN+SS-TuM-10, 16  
Powers, M.: HC+SS-WeM-13, 28  
Prabhakaran, V.: CA+AS+LS+NS+SS+VT-MoA-8, 8  
Prathibha Jasti, N.: NS+2D+EM+MN+SS-TuM-4, 15  
Preischi, C.: PS2+AS+SS-ThM-10, 43  
Prochazka, P.: SS1+AS-ThM-4, 44  
Puntscher, L.: HC+SS-WeM-2, 27; HC+SS-WeM-5, 27  
— Q —  
Qiao, M.: HC+SS-ThM-12, 42  
— R —  
Rabea, M.: SS-ThP-20, 51  
Raboño Borbolla, J.:  
AS+CA+EL+EM+SE+SS+TF-WeA-2, 32  
Radetić, M.:  
AS+2D+CA+EL+EM+MS+NS+SE+SS+TF-WeM-3, 25  
Radnik, J.: AS+CA+EL+EM+SE+SS+TF-WeA-8, 33  
Rahman, M.: HC+SS-ThM-3, 41; HC+SS-WeA-4, 34  
Rajak, S.: SS-ThP-9, 49  
Ramach, U.: BI2+AS+HC+SS-MoM-8, 1  
Raman, A.: SS+HC-TuA-7, 23  
Ramanantoanina, H.: TH1+AS+SS-TuM-5, 19  
Ramisch, L.: HC+SS-WeA-9, 35  
Ramstedt, M.: AS+CA+EL+EM+SE+SS+TF-ThM-3, 39  
Randall, J.: QS+SS-TuA-11, 22  
Ratel, D.: AS+2D+CA+EM+MS+NS+SE+SS+TF-FrM-1, 52  
Rath, D.: SS+2D+AS+HC-TuM-10, 18  
Reece, C.: HC+SS-FrM-6, 55; HC+SS-WeA-10, 35  
Reed, B.: AS+CA+EL+EM+SE+SS+TF-WeA-8, 33  
Reekmans, G.: SS+HC-TuA-11, 23  
Reeks, J.: SS2-MoM-9, 7  
Refvik, N.: SS+2D+AS+HC-WeM-5, 29  
Rehr, J.: TH2+AS+SS-TuM-10, 20  
Reimann, A.: SS+AS+TF-MoA-8, 11  
Reinke, P.: SS+HC-ThA-3, 46; SS+HC-ThA-4, 47  
Renault, O.:  
AS+2D+CA+EL+EM+MS+NS+SE+SS+TF-WeM-4, 25;  
AS+2D+CA+EM+MS+NS+SE+SS+TF-FrM-1, 52;  
CA+AS+LS+NS+SS+VT-MoA-10, 9  
Revzin, A.: CA+AS+LS+LX+MN+SE+SS-TuM-1, 13  
Rheinfrank, E.: SS+2D+AS+HC-TuM-2, 17  
Rhinow, D.: PS2+AS+SS-ThM-10, 43  
Risner-Jamgaard, J.:  
AS+2D+CA+EL+EM+MS+NS+SE+SS+TF-WeM-5, 25  
Riva, M.: SS+2D+AS+HC-TuM-1, 16;  
SS+2D+AS+HC-TuM-2, 17  
Roberts, A.: AS+CA+EL+EM+SE+SS+TF-WeA-4, 33  
Rodriguez, M.:  
AS+2D+CA+EL+EM+MS+NS+SE+SS+TF-WeM-6, 26  
Roldan Cuenya, B.: SS+2D+AS+HC-TuM-4, 17  
Ros, E.: AS+CA+EL+EM+SE+SS+TF-ThM-2, 39  
Rose, V.: SS-ThP-18, 50  
Rosenhek-Goldian, I.: NS+2D+EM+MN+SS-TuM-4, 15; NS1+2D+BI+SS-MoM-6, 4  
Rosenstein, J.: HC+SS-WeM-13, 28  
Rostamzadeh, T.: HC+SS-ThM-13, 42  
Rummel, B.: QS+SS-TuA-4, 21  
— S —  
Saedy, S.: HC+SS-FrM-3, 54  
Sagisaka, K.: SS-ThP-17, 50  
Salagre, E.: SS+AS+TF-MoA-10, 12  
Sautet, P.: HC+SS-ThA-5, 46  
Sayler, J.: SS-WeA-8, 37  
Schacherl, B.: TH1+AS+SS-TuM-3, 19;  
TH1+AS+SS-TuM-5, 19  
Schäfer, T.: SS-ThP-12, 49  
Schaff, O.: LX+AS+HC+SS-MoM-5, 3  
Schauerer, D.: SS-ThP-12, 49  
Schmehl, R.: HC+SS-ThM-13, 42  
Schmid, M.: HC+SS-WeM-2, 27;  
SS+2D+AS+HC-TuM-1, 16; SS+2D+AS+HC-TuM-10, 18; SS+2D+AS+HC-TuM-13, 18; SS+2D+AS+HC-TuM-2, 17; SS+2D+AS+HC-WeM-1, 28  
Schmidt, J.: HC+SS-WeA-1, 34  
Schneider, C.: SS1+HC-MoM-1, 5  
Schreier, M.: HC+SS-WeM-10, 28  
Schroeder, S.: LX+AS+BI+HC+SS+TH-MoA-8, 10  
Schwalb, C.: NS1+2D+BI+SS-MoM-4, 4  
Schwarz, U.: SS-WeA-11, 37  
Schweikert, E.: CA+AS+LS+LX+MN+SE+SS-TuM-1, 13  
Scougale, W.: SS-ThP-18, 50  
Seebauer, E.: SS-ThP-4, 48  
Seewald, L.: NS+2D+EM+MN+SS-TuM-5, 15  
Segovia, P.: SS+AS+TF-MoA-10, 12  
Segundo, M.: AS+CA+EL+EM+SE+SS+TF-ThM-3, 39  
Seibert, S.: NS1+2D+BI+SS-MoM-4, 4  
Selloni, A.: SS+HC-TuA-7, 23  
Seydoux, C.:  
AS+2D+CA+EM+MS+NS+SE+SS+TF-FrM-1, 52  
Shahsavari, A.: SS1+AS-ThM-4, 44  
Shaikhutdinov, S.: SS+2D+AS+HC-TuM-4, 17  
Shannon, S.: PS2+AS+SS-ThM-11, 43  
Shard, A.: AS+CA+EL+EM+SE+SS+TF-ThM-3, 39; AS+CA+EL+EM+SE+SS+TF-WeA-8, 33  
Sharma, P.: SS-ThP-18, 50  
Sharp, M.: HC+SS-ThM-1, 41  
Shchukarev, A.: AS+CA+EL+EM+SE+SS+TF-ThM-3, 39  
Shi, J.: HC+SS-ThA-5, 46  
Shimizu, T.: SS-ThP-17, 50; SS-ThP-2, 48; SS-ThP-5, 48  
Shirato, N.: SS-ThP-18, 50  
Sibener, S.: QS+SS-TuA-9, 21; SS-WeA-8, 37  
Sidhik, S.: CA+AS+LS+NS+SS+VT-MoA-3, 8  
Siemons, L.: SS+HC-TuA-11, 23  
Sigillito, A.: QS+SS-TuA-11, 22  
Singh, S.: HC+SS-WeM-1, 27  
Sinno, T.: QS+SS-TuA-4, 21  
Siribaddana, C.: SS-ThP-9, 49  
Smit, M.: SS2-MoM-9, 7  
Smith, A.: SS+2D+AS+HC-WeM-10, 29;  
SS+2D+AS+HC-WeM-11, 30; SS+2D+AS+HC-WeM-12, 30  
Smith, S.: HC+SS-ThM-1, 41  
Sobchinsky, E.: HC+SS-ThM-3, 41

## Author Index

- Sobczak, C.: AS+2D+CA+EL+EM+MS+NS+SE+SS+TF-WeM-6, 26
- Sombut, P.: HC+SS-WeM-2, **27**; HC+SS-WeM-5, 27
- Son, J.: CA+AS+LS+NS+SS+VT-MoA-11, **9**
- Song, S.: QS+SS-TuA-10, 22; QS+SS-TuA-3, 21
- Soomary, L.: AS+2D+CA+EM+MS+NS+SE+SS+TF-FrM-11, 53
- Soucek, J.: SS-ThP-1, 48; SS-ThP-15, 50
- Spagna, S.: NS1+2D+BI+SS-MoM-4, 4
- Spencer, B.: AS+2D+CA+EM+MS+NS+SE+SS+TF-FrM-11, 53
- Spool, A.: AS+2D+CA+EM+MS+NS+SE+SS+TF-FrM-10, **53**
- St.Martin, J.: SS+HC-ThA-4, 47
- Stacchiola, D.: LX+AS+HC+SS-MoM-4, 2; SS+2D+AS+HC-TuM-12, **18**
- Stan, G.: NS+2D+EM+MN+SS-TuM-3, **15**
- Steely, L.: SS+AS+TF-MoA-9, 12
- Steininger, R.: TH1+AS+SS-TuM-5, 19
- Strange, L.: TF2+AP+SE+SS-WeM-13, 31
- Strocio, J.: SS-WeA-2, **36**
- Strzhemechny, Y.: SS2-MoM-9, 7
- Stuehn, L.: NS1+2D+BI+SS-MoM-4, 4
- Sturm, M.: AS+2D+CA+EM+MS+NS+SE+SS+TF-FrM-8, **53**
- Suleiman, A.: TF2+AP+SE+SS-WeM-12, **30**
- Sumiyoshi, A.: SS+AS+TF-MoA-4, **11**
- Sun, K.: SS+2D+AS+HC-WeM-12, 30
- Sun, R.: CA1+AS+LS+NS+SS+VT-MoM-5, 2
- Sushko, P.: TF2+AP+SE+SS-WeM-13, 31
- Suzer, S.: SS2-MoM-8, **6**
- Swain, P.: NS1+2D+BI+SS-MoM-5, **4**
- Sykes, E.: SS+AS+TF-MoA-3, 10; SS+HC-ThA-1, **46**
- T —
- Tait, S.: SS1+AS-ThM-1, **44**; SS1+AS-ThM-5, 44
- Takeuchi, I.: SS+AS+TF-MoA-10, 12
- Takeuchi, N.: SS+2D+AS+HC-WeM-12, 30
- Takeya, J.: SS+AS+TF-MoA-5, 11
- Takeyasu, K.: HC+SS-WeM-1, **27**
- Talin, A.: SS+AS+TF-MoA-10, 12
- Tarrio, C.: SS+HC-TuA-10, 23
- Tate, J.: TF2+AP+SE+SS-WeM-13, 31
- Tepavcevic, S.: AS+2D+CA+EM+MS+NS+SE+SS+TF-FrM-4, 52
- Terlier, T.: CA+AS+LS+NS+SS+VT-MoA-3, **8**
- Terryn, H.: SS+AS+TF-MoA-9, 12; SS1+HC-MoM-2, 6
- Theodosiou, A.: AS+2D+CA+EM+MS+NS+SE+SS+TF-FrM-11, 53
- Thissen, A.: CA+AS+LS+LX+MN+SE+SS-TuM-10, 14; LX+AS+HC+SS-MoM-5, **3**
- Thompson, R.: SS1+AS-ThM-6, **44**
- Tong, X.: SS+2D+AS+HC-TuM-11, **18**
- Treadwell, L.: HC+SS-ThM-13, 42
- Trenary, M.: HC+SS-FrM-1, 54; SS+AS+TF-MoA-5, 11; SS-ThP-6, 49
- Trindade, G.: AS+CA+EL+EM+SE+SS+TF-ThM-1, 39
- Tsapatsis, M.: LX+AS+HC+SS-MoM-8, 3
- Tschurl, M.: HC+SS-ThM-6, 42; LX+AS+BI+HC+SS+TH-MoA-5, 10; SS+2D+AS+HC-WeM-1, 28
- Tseng, H.: AS+2D+CA+EL+EM+MS+NS+SE+SS+TF-WeM-3, 25
- U —
- Upadhyay, S.: SS+2D+AS+HC-WeM-11, 30; SS+2D+AS+HC-WeM-12, **30**
- Utz, A.: HC+SS-WeM-13, 28
- V —
- Vailionis, A.: AS+2D+CA+EL+EM+MS+NS+SE+SS+TF-WeM-5, 25
- Valery, A.: CA+AS+LS+NS+SS+VT-MoA-10, 9
- Valpreda, A.: AS+2D+CA+EM+MS+NS+SE+SS+TF-FrM-8, 53
- Valtiner, M.: AS+CA+EL+EM+SE+SS+TF-WeA-11, 34; BI2+AS+HC+SS-MoM-8, 1; SS2-MoM-10, 7
- Van de Kruijs, R.: AS+2D+CA+EM+MS+NS+SE+SS+TF-FrM-8, 53
- Van Doorslaer, S.: SS+HC-TuA-11, 23
- Vanleenhove, A.: AS+CA+EL+EM+SE+SS+TF-WeA-3, 32
- Vasudevan, R.: NS+2D+EM+MN+SS-TuM-12, 16
- Vazquez Lepe, M.: AS+CA+EL+EM+SE+SS+TF-WeA-2, 32
- Verkhoturov, D.: CA+AS+LS+LX+MN+SE+SS-TuM-1, **13**
- Verkhoturov, S.: CA+AS+LS+LX+MN+SE+SS-TuM-1, 13
- Viertel, K.: AS+CA+EL+EM+SE+SS+TF-ThM-5, 40
- Visart de Bocarmé, T.: CA+AS+LS+LX+MN+SE+SS-TuM-4, 13
- Vitova, T.: TH1+AS+SS-TuM-5, **19**
- Vlachos, D.: LX+AS+HC+SS-MoM-8, 3
- Vorng, J.: AS+2D+CA+EL+EM+MS+NS+SE+SS+TF-WeM-13, 26
- W —
- Wagner, J.: SS-WeA-8, 37
- Wagner, M.: NS2+2D+BI+EL+SS-MoM-11, **5**
- Walczak, L.: SS-ThP-10, **49**
- Walker, A.: AS+CA+EL+EM+SE+SS+TF-WeA-7, 33
- Wallander, H.: SS1+HC-MoM-6, 6
- Walter, A.: SS-ThP-1, **48**; SS-ThP-15, 50
- Wang, C.: CA+AS+LS+NS+SS+VT-MoA-5, **8**; HC+SS-WeM-2, 27; HC+SS-WeM-5, 27
- Wang, F.: CA+AS+LS+NS+SS+VT-MoA-1, **8**
- Wang, H.: SS-WeA-11, 37
- Wang, X.: SS-WeA-11, 37
- Wang, Z.: HC+SS-FrM-4, **54**
- Watson, D.: AS+CA+EL+EM+SE+SS+TF-WeA-9, 33
- Weaver, J.: HC+SS-ThA-5, **46**
- Weiland, C.: AS+CA+EL+EM+SE+SS+TF-WeA-2, 32
- Wen, B.: SS+HC-TuA-7, 23
- Westphal, M.: AS+CA+EL+EM+SE+SS+TF-ThM-5, 40
- Wickramasinghe, R.: AS+2D+CA+EM+MS+NS+SE+SS+TF-FrM-6, 53
- Wieghold, S.: SS-ThP-18, 50
- Wijerathna, A.: SS-WeA-12, **38**
- Wiley, J.: HC+SS-ThM-13, 42
- Willson, S.: QS+SS-TuA-9, **21**
- Winn, Z.: SS-WeA-12, 38
- Winkler, D.: CA1+AS+LS+NS+SS+VT-MoM-5, 2
- Winkler, R.: NS+2D+EM+MN+SS-TuM-5, 15
- Wisman, D.: SS1+AS-ThM-5, 44
- Woicik, J.: AS+CA+EL+EM+SE+SS+TF-WeA-2, 32
- Wong, S.: CA1+AS+LS+NS+SS+VT-MoM-5, 2
- Wood, B.: LX+AS+BI+HC+SS+TH-MoA-3, 9
- Wortmann, M.: AS+CA+EL+EM+SE+SS+TF-ThM-5, **40**
- Wouters, B.: SS1+HC-MoM-2, 6
- Wyns, K.: SS+HC-TuA-11, 23
- X —
- Xiao, Y.: SS+HC-TuA-1, 22
- Xu, Y.: HC+SS-WeA-4, **34**
- Y —
- Yakshin, A.: AS+2D+CA+EM+MS+NS+SE+SS+TF-FrM-8, 53
- Yan, J.: QS+SS-TuA-10, 22; QS+SS-TuA-3, 21
- Yang, K.: SS+HC-TuA-1, 22
- Yang, Y.: HC+SS-ThM-5, **41**
- Yao, X.: AS+2D+CA+EM+MS+NS+SE+SS+TF-FrM-3, 52
- Ye, Z.: SS+HC-TuA-1, 22
- Yiu, P.: AS+CA+EL+EM+SE+SS+TF-ThM-13, **40**
- You, J.: AS+CA+EL+EM+SE+SS+TF-ThM-13, 40
- Z —
- Zaera, F.: HC+SS-WeM-6, **27**
- Zagorac, T.: AS+2D+CA+EM+MS+NS+SE+SS+TF-FrM-4, **52**
- Zahl, P.: NS+2D+EM+MN+SS-TuM-11, **16**; SS-WeA-11, 37
- Zahra, K.: AS+2D+CA+EM+MS+NS+SE+SS+TF-FrM-11, 53
- Zakharov, A.: SS+HC-ThA-3, 46
- Zakharov, D.: LX+AS+HC+SS-MoM-4, 2
- Zameshin, A.: AS+2D+CA+EM+MS+NS+SE+SS+TF-FrM-8, 53
- Zetterberg, J.: HC+SS-WeA-9, 35
- Zhang, C.: SS+AS+TF-MoA-5, 11
- Zhang, K.: SS+HC-TuA-11, 23
- Zhang, R.: SS-WeA-12, 38
- Zhang, Y.: AS+2D+CA+EM+MS+NS+SE+SS+TF-FrM-4, 52; NS+2D+EM+MN+SS-TuM-11, 16; SS-WeA-12, 38
- Zhang, Z.: SS+HC-TuA-3, **22**
- Zhao, H.: HC+SS-ThA-3, 46
- Zhao, K.: HC+SS-FrM-5, **54**; HC+SS-WeA-3, 34
- Zhao, X.: SS-ThP-19, **50**
- Zhao, Y.: AS+2D+CA+EM+MS+NS+SE+SS+TF-FrM-3, 52
- Zheng, W.: LX+AS+HC+SS-MoM-8, 3
- Zhou, H.: TF2+AP+SE+SS-WeM-13, 31
- Zhou, J.: HC+SS-WeA-4, 34; SS-ThP-14, 50
- Zhou, P.: SS+HC-TuA-1, 22
- Zhou, Y.: AS+2D+CA+EM+MS+NS+SE+SS+TF-FrM-3, **52**; AS+CA+EL+EM+SE+SS+TF-ThM-1, 39
- Zhu, H.: SS+HC-TuA-3, 22
- Zhu, Z.: NS1+2D+BI+SS-MoM-3, 4; SS+AS+TF-MoA-11, **12**
- Ziatdinov, M.: NS+2D+EM+MN+SS-TuM-12, 16
- Zirnheld, M.: SS-WeA-12, 38